

MAGNETIC MEASUREMENT ON
LHC PROTOTYPE QUADRUPOLE
AT ROOM TEMPÉRATURE

CEA-SACLAY DAPNIA/STCM

SIMON Fabrice

● **Large Hadron Collider:**

- ❖ European laboratory for particle physics (CERN).
- ❖ Proton-proton collider, 7 TeV per beam.
- ❖ 27 km circumference ring.

● **STCM is in charge of the Short Straight Section**

↔ **main quadrupole magnet :**

- ❖ Design.
- ❖ Prototype construction.
- ❖ Magnetic measurements at cold and room temperature.
- ❖ To follow through the industrial manufacture.

Collaboration

CERN : J.Billan, V.Remondino

5 radial coils mole

Data acquisition and analysis

CEA : Y.Le Noa (SIG), D.Leboeuf(SGPI),
F.Simon(STCM)

Automated bench

Summary

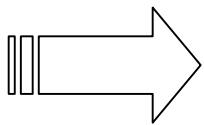
- Mole and data acquisition
- Bench Why an automated bench?
 Description
- Tests of the system
- Results On the collared coils
 On the cold mass
 Multipole coefficients evolution
- Conclusion

Mole and data acquisition

- Rotating array of 5 radial coils.
- Coils parameters :
 - 750mm long
 - 400 turns (20x20)
 - 2 m² area
- Mean radius of the external coils : 17mm.
- Precisely machined mandrel.
- Calibrated in a dipole and a quadrupole .
- Only 2 signals are send to 2 VFC :
 - Absolute output from the external coil E1,
 - Hardware bucked output E1-M1-M2+C.
- Included in the mole :
 - angle encoder
 - brake
 - electrolytic level
- 256 data recorded in 1 second and processed by a SUN station with Labview.

Why an automated bench

- Room temperature magnetic measurement will be carried out in the industry for the mass production.
- After the collared coil assembly and after the cold mass.
- To detect as early as possible assembly imperfections or drifts of the tooling.



Magnetic measurement must fulfil :

- Minimum handling,
- Be usable by anybody,
- Security for the operator, equipment and magnets,
- Be as fast as possible.

DESCRIPTION

- A support and its cover with windows.
- A group of motors for the rotation and levelling of the mole.
- A long bore tube including shaft spacers for the transmission of the rotation.
- 8 tables among which 2 are motorised for transverse displacements to go from an aperture to the other.
- A 8m-linear module with a driving belt for the longitudinal movements along each aperture :
 - One safety, 5 measuring and an outer position
- Switches and optical sensors to control the positioning.
- An automated system to drive the displacements.
- Many sensors to insure the security.

TEST OF THE SYSTEM

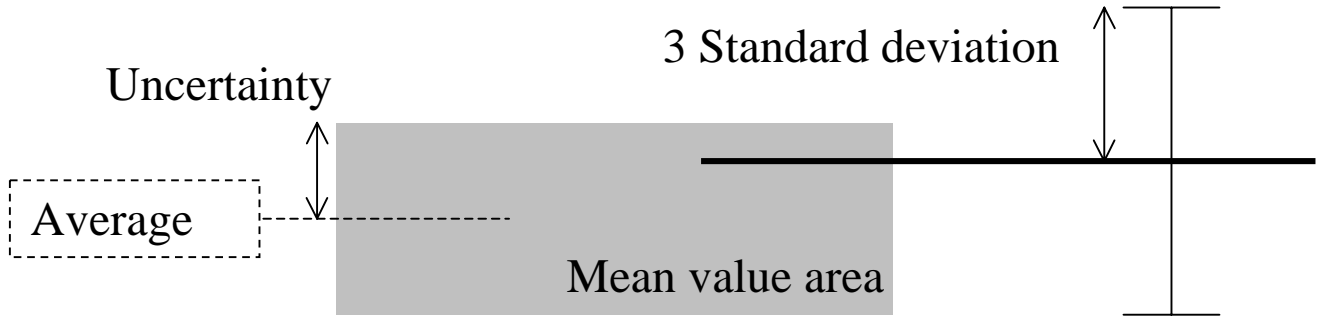
- In spite of the elasticity of the 16m-belt, the accuracy of the measuring position is 0.1mm between 2 different positions.
- The 3.1m-long magnet is then measured over $3.75\text{m} \pm 0.1\text{mm}$.
- The reproducibility is about $5 \cdot 10^{-2}$ unit.
- The setting/dismantling of the mole and the vibrations have no effect .
- Mobile phones can provide up to 0.3unit.
- Comparison on a copper-coils quadrupole at room temperature with the cold magnetic measurement system :

	'Cold' system	'room' system
Gradient (T/m)	3.72	3.73
C_3 (unit)	1.03	0.97

- Bucking about 900 for C_1 and 400 for C_2 .

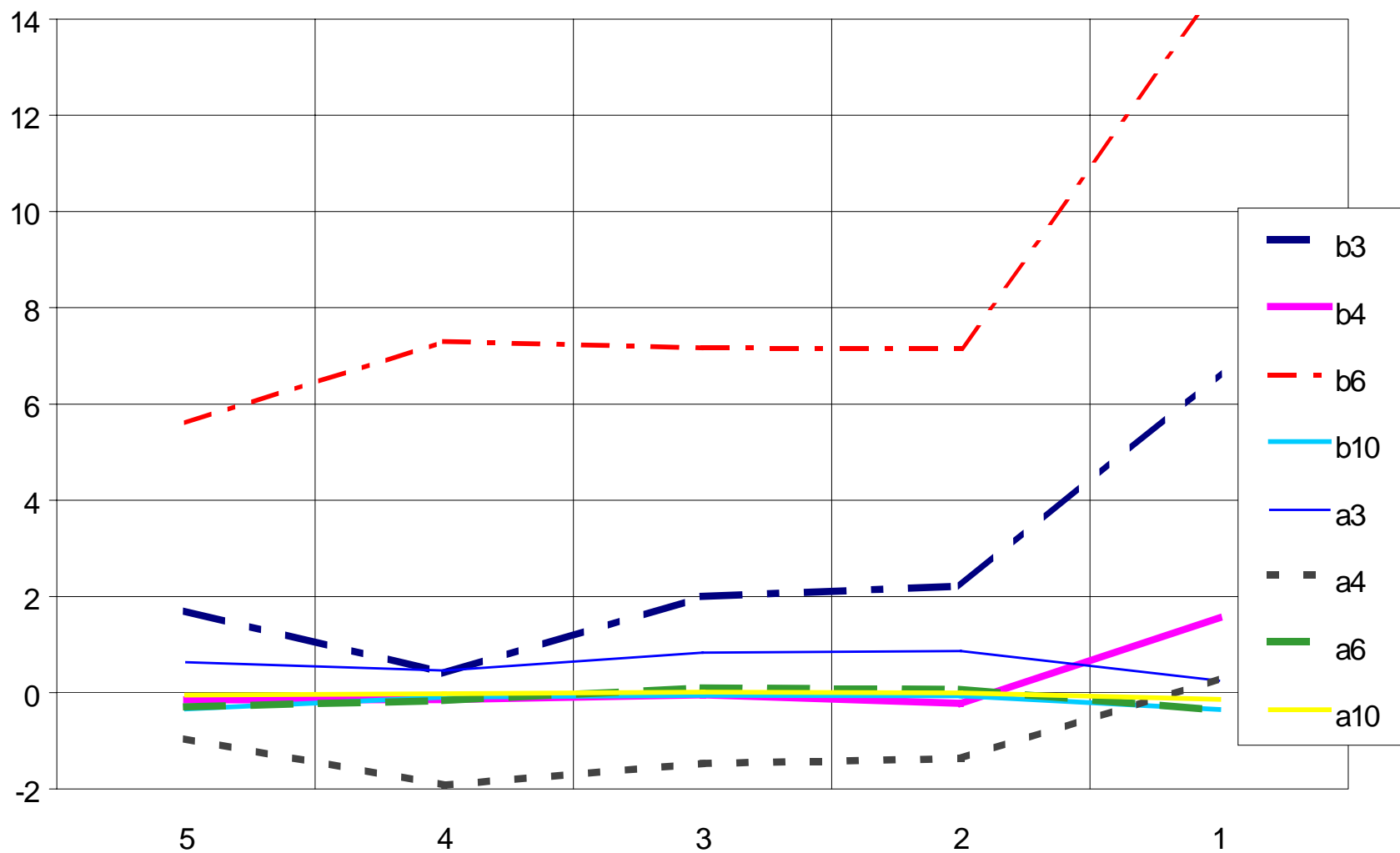
COLLARED COILS

CERN SPECIFIED VALUES.



RESULTS AT THE CENTER OF THE COILS.

	coil q1	coil q2	CERN values	
			min	max
b_3	2.01	3.58	-3.04	3.08
b_4	-0.05	0.01	-1.45	1.45
b_6	7.17	6.24	2.42	5.44
a_3	-0.83	-4.36	-3.06	3.06
a_4	1.48	3.12	-1.45	1.45
a_6	-0.09	-0.17	-1.51	1.51



Multipole coefficients over the q1-coil length

COLD MASS

◆ The gradient is 221.6 T/m at the nominal current with the yoke and the magnetic length 3114mm when 223.05 T/m and 3112 mm are expected.

◆ The given values are integrated over the length of the apertures as :

$$\text{Integrated value}(C_n) = \frac{3}{5} \cdot \frac{\sum_{\text{positions}=1 \text{ to } 5} C_n^{\text{pos}}}{\sum_{\text{positions}=2 \text{ to } 4} B_2^{\text{pos}}}$$

(Collared coil integrated value differ from those at the center)

◆ Difference with the collared coil :

- The magnetic yoke increases the quadrupole field,
- It changes the coefficients at the ends,
- The mole has been recalibrated.

COLD MASS

- ◆ Yoked values are smaller but collared values give a good and first information on what the cold mass will be.

		b_3	b_4	b_6	b_{10}
External aperture (q2)	collared	3.86	-0.09	5.99	-0.12
	yoked	3.20	-0.18	5.59	-0.12
Internal aperture (q1)	collared	1.89	0.08	6.67	-0.12
	yoked	1.88	0.06	6.25	-0.12

Integrated multipole coefficients in unit at room temperature (17mm)

- ◆ Variations on coefficients over the length are hold.

CONCLUSION

Magnets

- ❖ Analysis is running :
 - midplane shifts are out of the question,
 - Radial displacements are suspected.
- ❖ q1 and q2 coils are not significant samples because of problems during their fabrication.
- ❖ More coils are needed to detect a trend and correct possible imperfections.

Bench

- ❖ Operator handlings reduce to the minimum : connecting the mole and put in place the magnets.
- ❖ Less than 3 hours for a complete measurement (magnet installation included).
- ❖ Corrector magnets could be also measured in a next time.

SLIDE 4

The mole includes a rotating array of 5 radial coils, 2 externals (E), 2 medium (M) and a central one (C). One of the external is not used. The mean radius of the external coil is 17mm. The main parameters are a coil length of 750 mm and a surface of 2m² for the 400 turns coils. The coils are wound with 20 turns of a flat cable made of 20 parallel wires connected in series.

Because the mandrels are precisely machined and calibrated in a dipole and a quadrupole to know respectively the surface and radii of each coil, one can create a hardware bucking signal. It means that the 4 coils E1, M1, M2 and C are wired together and the total output is directly sent to a VFC. A second VFC is used for the absolute signal from E1.

SLIDE 5

Obviously a bench supports and moves the mole in front and inside the 2 apertures of the cold mass. The measuring system is designed to allow room temperature measurements in the industry for the mass production of the quadrupole at two stages of the production. After the collaring to control their quality before mounting the yoke and after the cold mass assembly as part of the final acceptance tests.

The aims of the 2 tests are above all to detect as early as possible any assembly imperfection or drifts in the tooling so as to correct them before rejection of the magnets may occur. Hence magnetic measurement in the industry must fulfil :

- Minimum handlings for the operator
- Be usable by anybody and especially by a non -specialist of magnetic measurement.
- Carry out the security for the operator, equipment and magnets
- Require a minimum time to be integrated in an industrial process.

For this purpose, the bench is automated.

SLIDE 6

It consists of a support, a group of motors for the rotation of the mole and a long bore tube to transmit this rotation. 8 tables among which 2 are motorised puts the mole in front of one of the 2 apertures of the cold mass. Obviously this displacement is inhibited when testing the collared coil. A 8-meter linear module with a driving belt moves the mole from the safety position to 1 of the 5 measuring ones and to an outer position for connecting the mole and the acquisition cable at the end of the magnets. Switches and an electronic device control the movements.

SLIDE 7

Before measuring our magnets, we have tested the system and trained ourselves on a dummy copper-coil. Our main worry was the elasticity of the 16 meters driving belt, which could have made impossible a correct placing. But, thanks to our choices of conception, the accuracy is 0.1mm between any 2 different positions. It means that the 3m-long magnets are measured over $3.75\text{m} \pm 0.1\text{ mm}$. The mechanical part on the uncertainty of the magnetic length is 0.1mm.

The reproducibility on the multipole coefficients is about 0.05 unit and is free from biasing effects caused by setting or disconnecting the mole from the transmission tube and also from vibrations. The bucking is about 900 for dipole field and 400 for quadrupole terms.

Because of the mobile phone fashion, we tested it and remarked that they can induce up to 0.3 unit if someone calls closely next to the magnet.

At least, we looked after the uncertainty and validity of the measured values. Therefore we compare this system with the one developed by CEA for the cold magnetic measurement campaign in 1995. This cold system will also run for cold measurements on the current prototypes. The results are identical.

At the end of the training period, we are confident with our room temperature system.

SLIDE 8

On the scheme, one can see the 5 measuring positions (1 for the lead side, 3 for the magnet centre and 5 for the second end). We measured a quadrupole field at 12.5 Amperes that gives at nominal current a gradient of 210.5 T/m, less by 0.2 % than the design value.

The magnetic length, calculated with the formula, is different by 0.1% from the design value.

The $B_2^{pos n}$ are the absolute quadrupole field in Tesla measured by the E1 coil at the position n.

SLIDE 9

The CERN specifications give 3 values, the average, uncertainty and standard deviation. The mean value of a set of magnets can be between the average specified value more or less the uncertainty. And each magnet measurement of the set can vary by 3 time the standard deviation around this mean value. By consequence, we can calculate the min and max value for a single magnet. You can see on the table that some multipole coefficients are out, especially the dodecapole term. Even if we have not tested magnets enough, it seems to be a systematic error. The next magnets under construction will have the same design than this one in order to confirm the trend.

SLIDE 10

Looking at the details of the measurements as a function of position, there appears to be little variations over the length in the central part. On position 1, you can see the influence of the connection end. This effect increases the magnetic length but is reduced when yoking the magnets into the cold mass.

SLIDE 11

The yoke grows the gradient by 5.4% up to 221.6 T/m, 0.7% less than the design value. The magnetic length is now 3114mm, 2mm higher than the expected one.

The given values on the slide 12 are integrated over the length with the formula. C_n^{pos} is the multipole coefficient n (skew or normal) at one of the 5 positions. It is expressed in Tesla, that means non normalised with the quadrupole local field.

The differences that can be observed are due to the upper quadrupole field, the reduced coefficients at the ends because the yoke closes the flux, and also to the fact that the mole has been recalibrated between the collared and yoked tests. The really first tests we made on the new mole do not show significant variations with the old one. But some changes can not be excluded.

SLIDE13

It has to be noticed that the analysis is still running. Presently radial and midplane shifts seem to be out of the question. We suspect azimuthal over compression. No final conclusions can be made on this first magnet because the collared coils q1 and q2 are not significant samples since we have some problems during their construction. We need more coils to have a valid statistic.

Concerning the bench itself, it is already operating and we reach our goals. Handlings are reduced to the minimum. The operator only has to put the magnets on his support, to enter the name of the magnet in the software and to connect the mole.

Consequently a complete measurement for the 2 apertures of a cold mass requires less than 3 hours. At least it is foreseen to measure the corrector magnets. These magnets are in the cold mass at each end of the quadrupole. But we have to test it before.



US LHC ACCELERATOR PROJECT

*brookhaven - **fermilab** - berkeley*

Fermilab Plans for Magnetic Measurements of MQX Magnets

P. Schlabach

22 April 1999

- Overview of Plan for Testing MQX Magnets at Fermilab
- Magnetic Measurement Apparatus
- Status



US LHC ACCELERATOR PROJECT

brookhaven - fermilab - berkeley

Summary of Tests

- Prototype (2)
 - cold mass fully instrumented with voltage taps; quench localization with taps and quench antenna
 - some additional instrumentation to characterize behavior of cryostat and cold mass during cool down
- FNAL quads (9)
 - minimal instrumentation
 - protection only
 - quench training
 - quench localization with antenna
 - field measurement with rotating coil **warm** and **cold**
 - alignment with SSW **warm** and **cold**



US LHC ACCELERATOR PROJECT

brookhaven - fermilab - berkeley

Summary of Tests (2)

- FNAL quads
 - we assume separate powering of the Q2a/b for field measurement and alignment
 - schedule allows extra time during measurements of the first two production magnets for special studies
- KEK quads (18)
 - we assume quench training and field measurements done at KEK
 - 2 KEK quads will be tested cold
 - full set of production tests as performed on FNAL quads
 - The remainder will be tested warm
 - minimal set of tests
 - validate assembly
 - warm measurements of field
 - field alignment with respect to cryostat fiducials



US LHC ACCELERATOR PROJECT

*brookhaven - **fermilab** - berkeley*

Summary of Tests (3)

- corrector elements
 - we assume quench training and field measurements are done elsewhere and that relative alignment of the different corrector layers is also determined elsewhere
 - provide whatever tests are necessary to validate assembly
 - no field measurements
 - measure field alignment with respect to fiducials
 - we believe we can do this with the magnet warm



US LHC ACCELERATOR PROJECT

brookhaven - fermilab - berkeley

MQX Magnetic Measurements

- fabrication measurements
 - axial scans of field with with rotating coil ± 10 A current
 - after collaring
 - after yoking
 - requirement is a quality check not an assembly aid
 - no field quality tuning shims
- magnetic field measurement
 - integral magnetic field measurement of cryostated cold mass/corrector assemblies
- alignment
 - determination of magnetic field axis and roll angle both warm and cold for quadrupole and any corrector package



US LHC ACCELERATOR PROJECT

brookhaven - fermilab - berkeley

Magnet lengths

approximate lengths (m)		# cold masses	# corrector(s)	total length	
Q1	6.5	1	0	6.5	
Q2	6.5	1	2	7.5	
Q2	5.5	2	1	11.5	
corrector	0.5				



US LHC ACCELERATOR PROJECT

brookhaven - fermilab - berkeley

Apparatus

- A rotating coil field measurement system for quality assurance tests during fabrication
 - short (~1m) probe
 - axial scanning system to measure field locally
 - requires supports which open and close as the system moves
 - required stroke > 6.5 m
 - belt drive system (lead screw in long lengths expensive)
 - accuracy of position not so great
 - perhaps augmented by auxiliary measurement of position
 - what is the requirement for accuracy?
 - integral field measurement available from integration of local measurements if desired
 - presumably not as accurate as integral probe but adequate



US LHC ACCELERATOR PROJECT

brookhaven - fermilab - berkeley

Apparatus (2)

- A rotating coil field measurement system for measurement of production magnets
 - total length of system > 16 m

Test Stand Length	
Q2a/b+corrector	11.5
feed can	3
end can	1
total	15.5



US LHC ACCELERATOR PROJECT

brookhaven - fermilab - berkeley

Apparatus (3)

- A rotating coil field measurement system
 - total length of system > 16 m
 - integral, multi-section probe
 - axial drive system similar to that of fabrication measurement system
 - stroke $> 15.5 - 1 = 14.5$ m
 - perhaps can be reduced by approximately the length of one cold mass
 - insert and remove drive-shaft when moving from one cold mass to the other
 - cold masses are tested sequentially so not so painful
 - need to design in protection against failure modes
 - close when power fails, only small section can open at one time, no damage by misalignments



US LHC ACCELERATOR PROJECT

brookhaven - fermilab - berkeley

Apparatus (4)

- A rotating coil field measurement system
 - do we want to attempt an absolute measure of the field angle or simply normalize to the quadrupole angle?
 - requires (for example)
 - calibration dipole at entry to feed can
 - gravity sensor(s) in probe used to maintain alignment when drive shaft is inserted
 - do we need it?



US LHC ACCELERATOR PROJECT

brookhaven - fermilab - berkeley

Apparatus (5)

- SSW system for alignment of magnets
 - relative to cryostat fiducials
 - average field angle (100 μ rad)
 - magnetic field center (50 μ)
 - true magnetic axis (150 μ)
- transfer function measurement
- cross check on rotating coil measurements for low order harmonics
- absolute calibration of rotating coil(s)



US LHC ACCELERATOR PROJECT

brookhaven - fermilab - berkeley

Apparatus (6)

- **SSW system, challenges**
 - Wire lengths up to 20m for Q2a/b
 - two ~5.5 m cold masses in a single cryostat separated by corrector
 - Asymmetric geometry
 - Warm (10A) measurements in addition to cold (>10kA) measurements
 - alignment of KEK magnets in FNAL cryostats
 - Determine relative alignment of Q2a/b cold masses
 - determine true quad axes, not just average centers



US LHC ACCELERATOR PROJECT

brookhaven - fermilab - berkeley

Apparatus (7)

- A quench antenna for quench localization will be implemented in the anti-cryostat vacuum space



US LHC ACCELERATOR PROJECT

brookhaven - fermilab - berkeley

Apparatus (8)

- Anti-cryostat
 - 63 mm available bore
 - 38 mm available for measurement probe
 - instrumentation installed in the vacuum space
 - quench antenna panels
 - copper on kapton
 - some number of RTD/heater winding pairs
 - monitor temperature inside warm bore
 - heaters allow thawing of system if necessary
- design similar to that used in VMTF anti-cryostat
 - G10 spiders, super-insulation
 - instrumentation in vacuum space is different, wires come through vacuum seal



US LHC ACCELERATOR PROJECT

brookhaven - fermilab - berkeley

Readout

- Rotating Coil
 - Warm system based on METROLAB integrator (VME)
 - 1/winding
 - DVM for current readout
 - triggered simultaneously by angular encoder
 - Cold measurement
 - bandwidth an issue for PDI-based system
 - tests indicate limitation at 1-2 Hz probe rotation speed
 - in principle not an issue for LHC quads
 - we're exploring other options



US LHC ACCELERATOR PROJECT

brookhaven - fermilab - berkeley

Readout

- SSW
 - Existing systems use METROLAB integrator
 - Upgrade (clean up) motion control system
 - considering 6 axis controller fully integrated with stages
 - product of Newport (stage manufacturer)



US LHC ACCELERATOR PROJECT

brookhaven - fermilab - berkeley

Readout

- Quench Antenna
 - Using commercial VME ADC module(s)
 - (Pentek mother/daughter board)
 - Used for Vtap readout in vertical dewar
 - Some issues with channel count/configuration mismatches
 - mismatches between optimal configuration for Vtap and Q.A.



US LHC ACCELERATOR PROJECT

brookhaven - fermilab - berkeley

A Few Words about Software

- Building a new system
 - Similar look as existing SSC system
 - Platform portability
 - JAVA
 - Extremely flexible GUI-based user configurability
 - Integrated measurement control



US LHC ACCELERATOR PROJECT

brookhaven - fermilab - berkeley

Status

- Warm measurement system
 - Probe body being slotted
 - Drive system being procured
 - Readout prototype tested
- Cold measurement system
 - Procuring stock for probe body
 - Work out final details (radius, # of sections), start machining next month
 - Drive system: wait as long as possible to see how warm system goes (?)
- SSW
 - Systems operational (3)
 - Stagger upgrade of motion control so one system is always operational
 - Motion control upgrade probably linked to new measurement system software



US LHC ACCELERATOR PROJECT

brookhaven - fermilab - berkeley

Status (2)

- Anti-cryostat
 - Finalize layout in next month or two
- Quench antenna
 - Finalize panel design, # this month
 - Delivery next spring/summer
- Long probe, software set the schedule
 - Goals
 - probe ready for calibration next summer
 - software: full system with minimal functionality by spring
 - I.e. structure would be there but not all the pieces that plug into the structure
 - start with SSW, add rotating coil measurements (?)



US LHC ACCELERATOR PROJECT

brookhaven - fermilab - berkeley

Status (3)

- Measurement of first full length prototype set for Oct, 2000

Recent Tests with the Fermilab SSW System

9/23/1999

P. Schlabach

- LHC HGQ Alignment
 - Measurement requirements
 - average quad center to $50\mu\text{m}(x, y)$
 - roll to $100\mu\text{rad}$
 - integral strength to few units
 - includes transfer of alignment parameters to cryostat
 - Wire lengths up to 20m for Q2a/b
 - two $\sim 5.5\text{m}$ HGQ magnets in a single cryostat separated by corrector
 - Asymmetric geometry
 - Warm(10A) measurements in addition to cold (10kA) measurements
 - alignment of KEK magnets in FNAL cryostats
 - Determine relative alignment of Q2a/b cold masses
 - determine true quad axes, not just average centers

- Recent measurement program was proof of principle
 - Warm measurements on ~1.8m model HGQ magnet
 - Alignment measurements for various wire length
 - Verify that the following are manageable issues
 - signal strength
 - wire length
 - measurement technique
 - Need to stretch a long wire, mimic the asymmetric geometry (reduced range of wire motion) that will occur with a Q2a/b and measure the field with 10 A current
 - Measurements of other magnets were also done



SSW3 set-up in MTF
for tests with long wires (using
permanent quadrupole magnet)

- Standard Measurements
 - Single 100 μ m CuBe wire stretched between two sets of precision stages (return of wire loop lies fixed on bottom of beam pipe or outside magnet).
 - Change in flux from wire motions - which depends only on wire start and stop points, not on path - is measured by integrator; when wire is on average at center, positive and negative motions of the wire result in the same size change in flux. Controlling wire motion to high accuracy using precision positioning stages yields high sensitivity in the determination of magnetic center.
 - Center is determined with respect to wire endpoints; position of these endpoints can then be transferred to fiducials on the cryostat.
 - Make measurements at various tensions and extrapolate to infinite tension to remove wire sag effects.

Measurement Techniques

New tests

- What's new
 - Use vibration of wire in magnetic field to **determine frequency**; wire sag is inversely proportional to frequency squared (try to obtain 0.5% *accuracy* of tension or frequency in order to get intercept deviation of fit to measurements at various tensions to be less than 10 μ m). The concern is that friction, torque on tension gauge, change in wire density during stretching may affect the tension reported by the gauge.
 - Power magnet with **AC current**, use FFT to extract flux measurement (try to improve on basic measurement of change in flux (typically 1 μ Vs because of non-linear changes in offset which occur during movement of the wire from start to end positions)).

Measurement Techniques

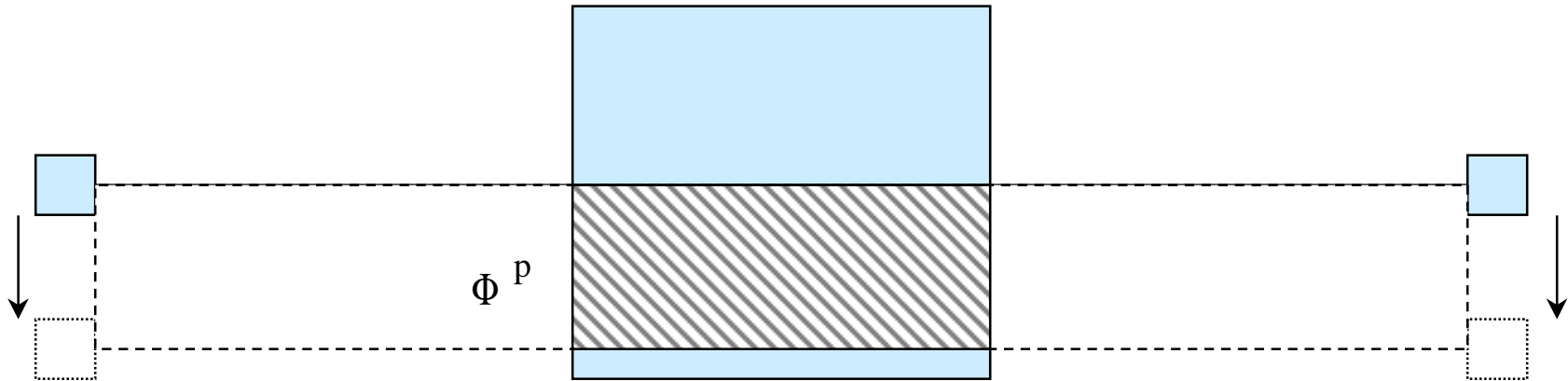
New tests

- Measure with the stages at either end of the magnet moving co-directionally and **counter-directionally** to determine true magnetic axis (not just average axis). Can move wire to this location and confirm that it is at center
- Measure stage and magnet location with **laser tracker system**, compare axis location as measured in external fixed coordinate system as a function of wire length.

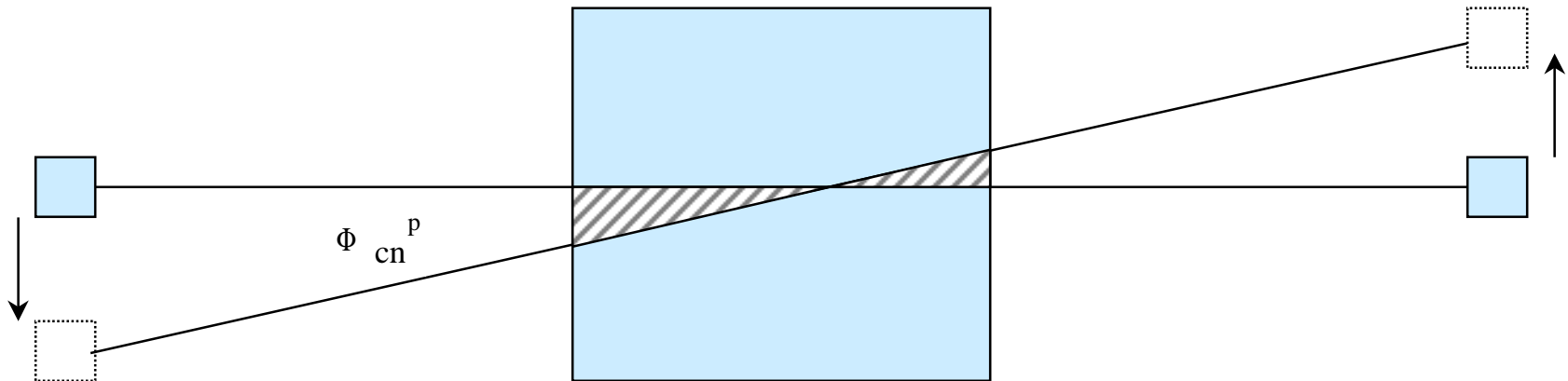
Measurement Techniques

Counter-directional measurements

Co-directional motion (standard)



Counter-directional motion (to find true axis)



Measurement Techniques y-direction

For y-direction, have to account for wire sagitta

$$y_0(z) = \left(y_a - \frac{y_b - y_a}{L_m} \cdot a + \frac{y_b - y_a}{L_m} \cdot z \right) + \frac{1}{k} \left[\cosh \left[k \cdot \left(z - \frac{L_w}{2} \right) \right] - \cosh \left(k \cdot \frac{L_w}{2} \right) \right]$$

where k is the parameter of the catenary given by $k = \frac{w}{T}$
(T is tension, w is weight/length)

Can measure as a function of $1/T$ and extrapolate to infinite tension - the term caused by wire sag then drops out.

Measurement Techniques Using wire vibration freq.

Extrapolation technique may be limited by tension gauge accuracy, frictional effects, torque effects on gauge (linear/non-linear), changes in w (e.g. stretching).

Instead can measure the fundamental frequency of the wire vibration

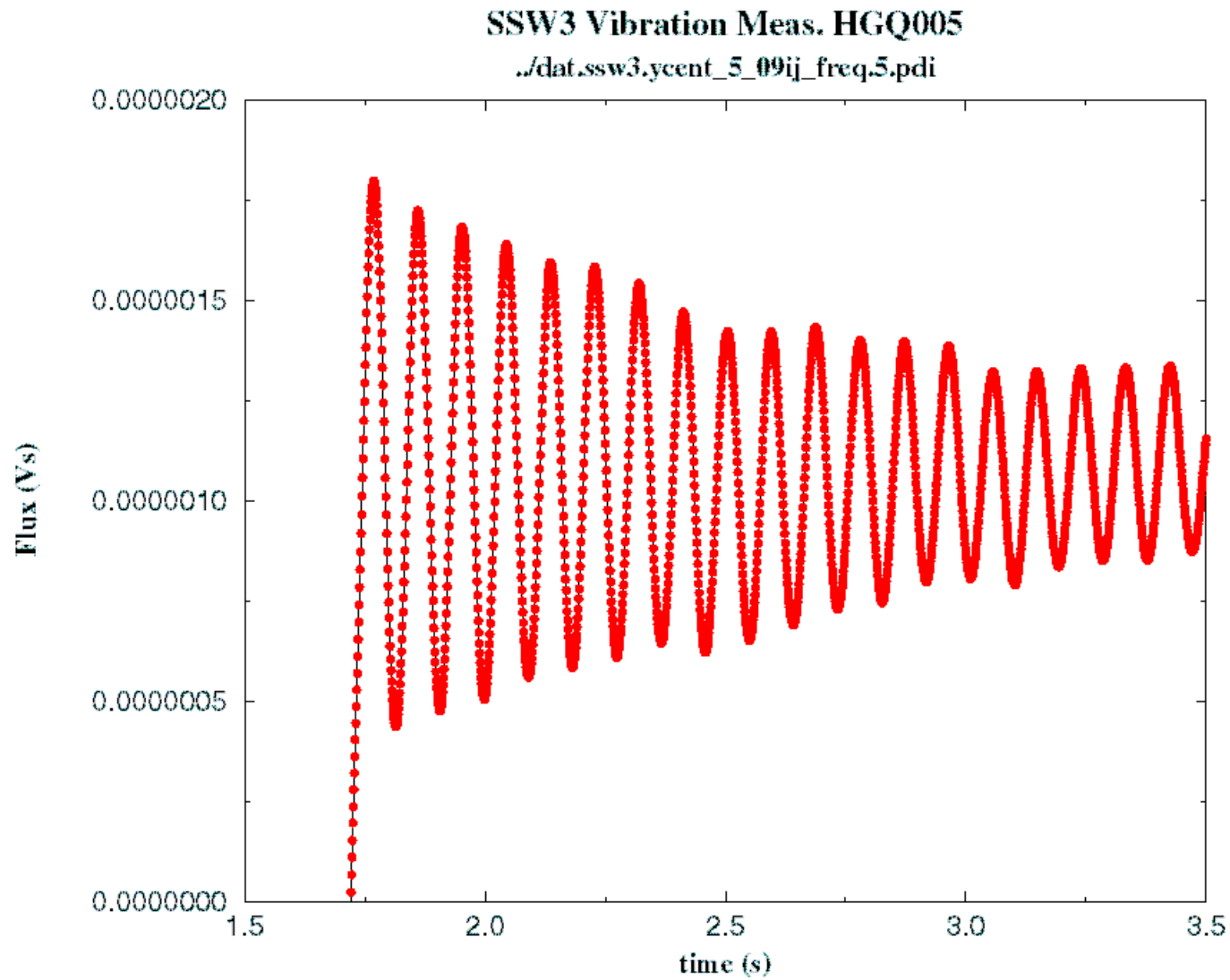
$$f = \frac{1}{2 \cdot L_w} \cdot \sqrt{T \cdot \frac{g}{w}} \qquad k = \frac{w}{T} = \frac{g}{4 \cdot f^2 \cdot L_w^2}$$

to avoid these effects. Need $\sim 0.3\%$ frequency accuracy to achieve $\sim 10\text{-}20\mu\text{m}$ error for 20m wire.

Measure as a function of $1/f^2$ to eliminate sag.

Measurement Techniques

Vibration frequency

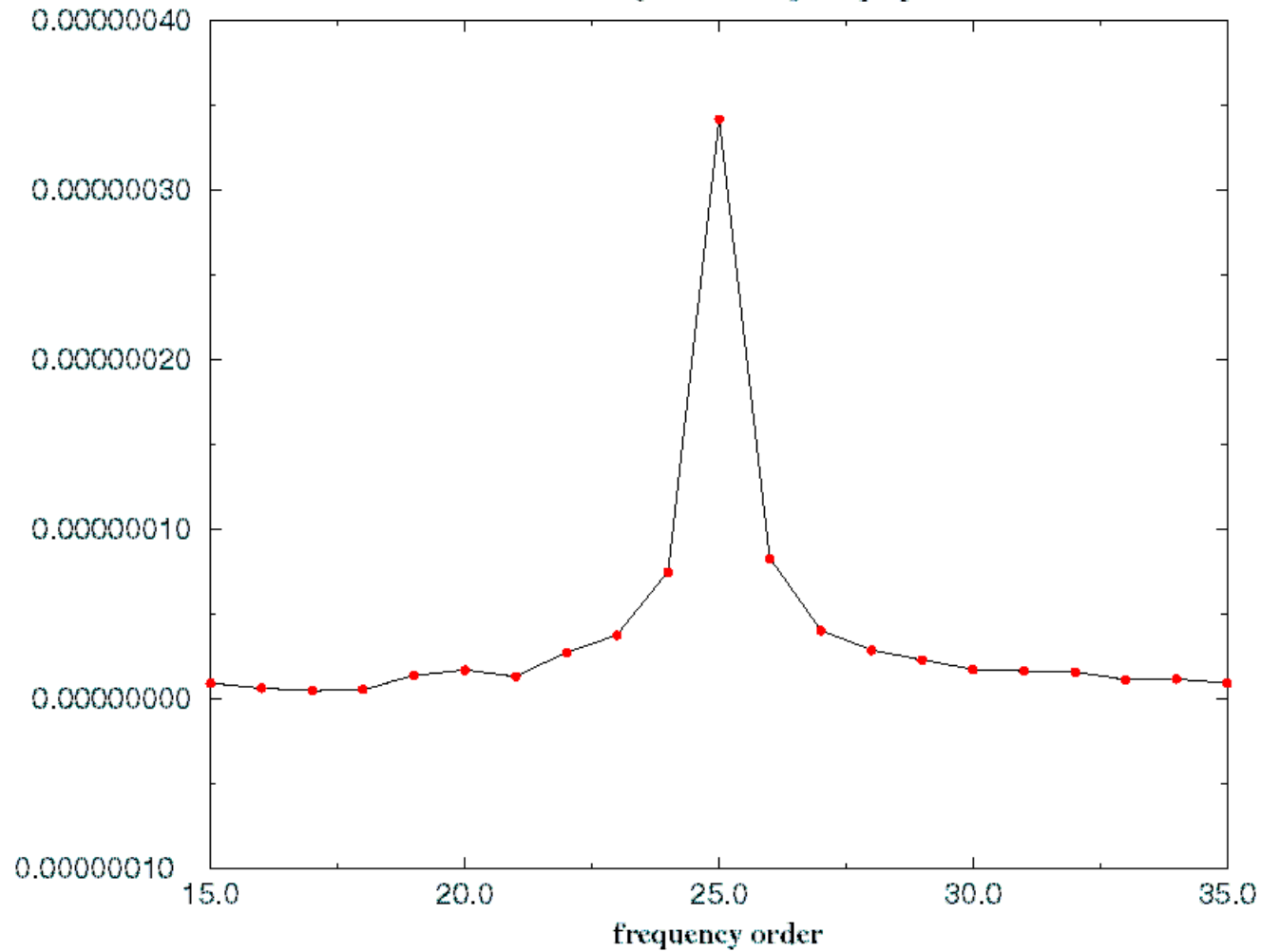


Measurement Techniques

Vibration frequency

SSW3 Vibration Meas. HGQ005

./dat.ssw3.ycent_5_09ij_freq.5.pdi



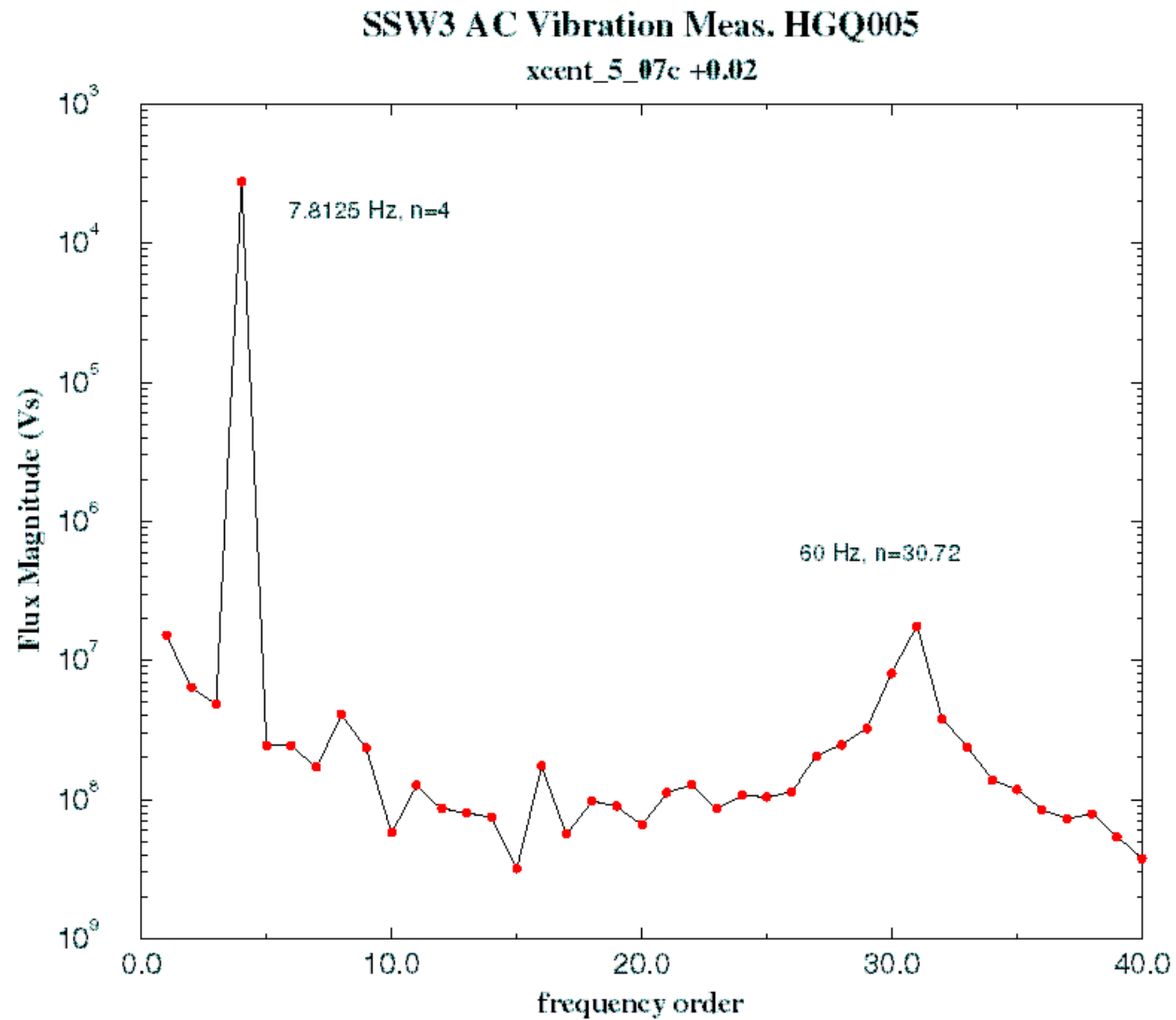
Measurement Techniques

AC current

- AC magnet current
 - Find flux at fixed wire position using change in magnet current (rather than finding flux during change in wire position)
 - Exclude noise at frequencies other than that exciting the magnet

Measurement Techniques

AC current



Measurements Jan-May, 1999

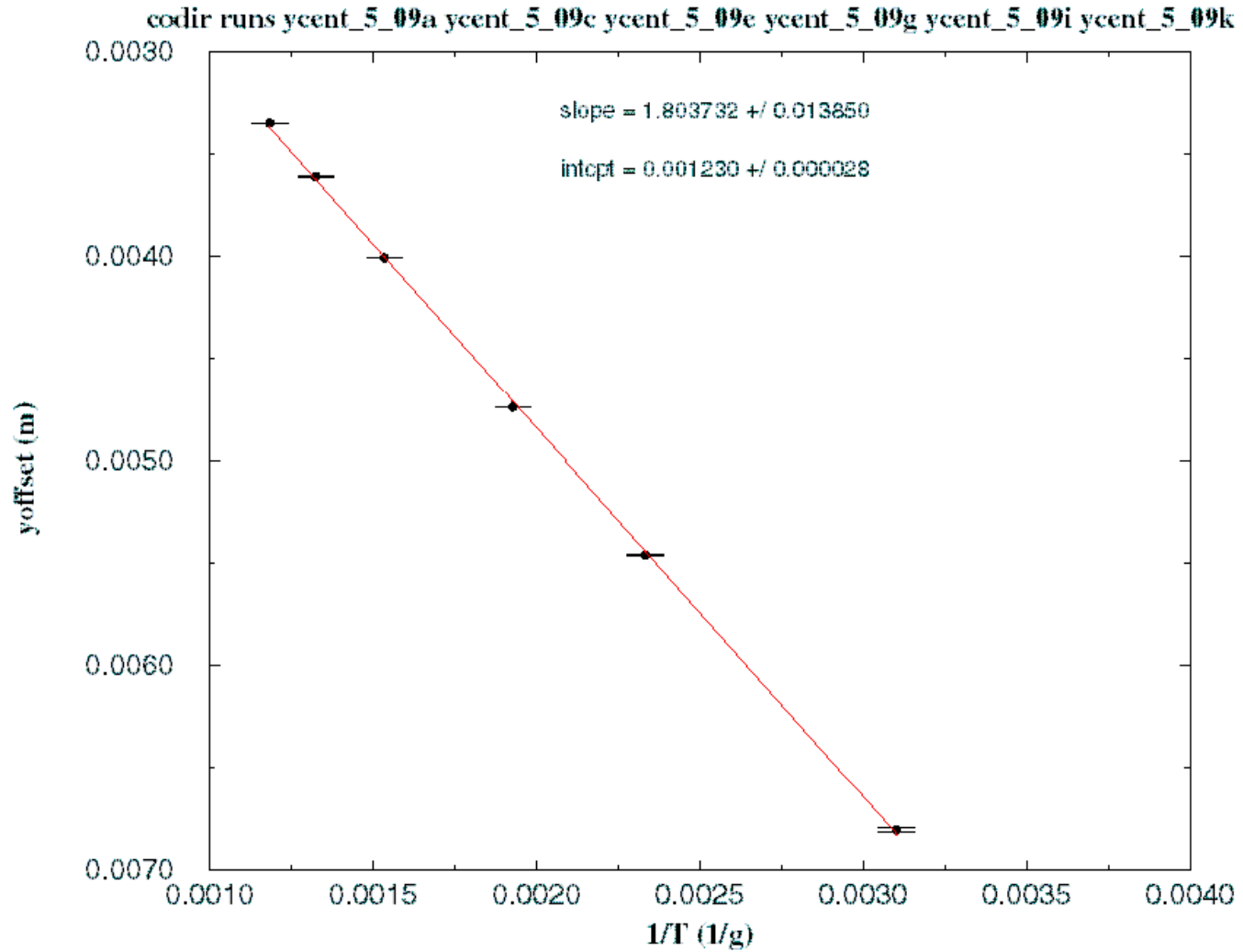
Measurements summary

Magnet	Test dates	Type	Int. g dl	I	DC	AC	Wire L	1/T	1/f^2	Harm
PQP003	Jan-Feb '99	Recy. Perm.	1.6 T	-	X		1.5m, 13m		X	
MQT003	Mar '99	Trim	0.053 T	2A		X	1m			X
TSF357	Apr '99	Spool	0.027 T	0.2A		X	2m	X		
HGQ005	Apr-May '99	LBQ proto.	0.38 T	11A		X	2.5m, 11m, 16m	X	X	X

Sample Measurements

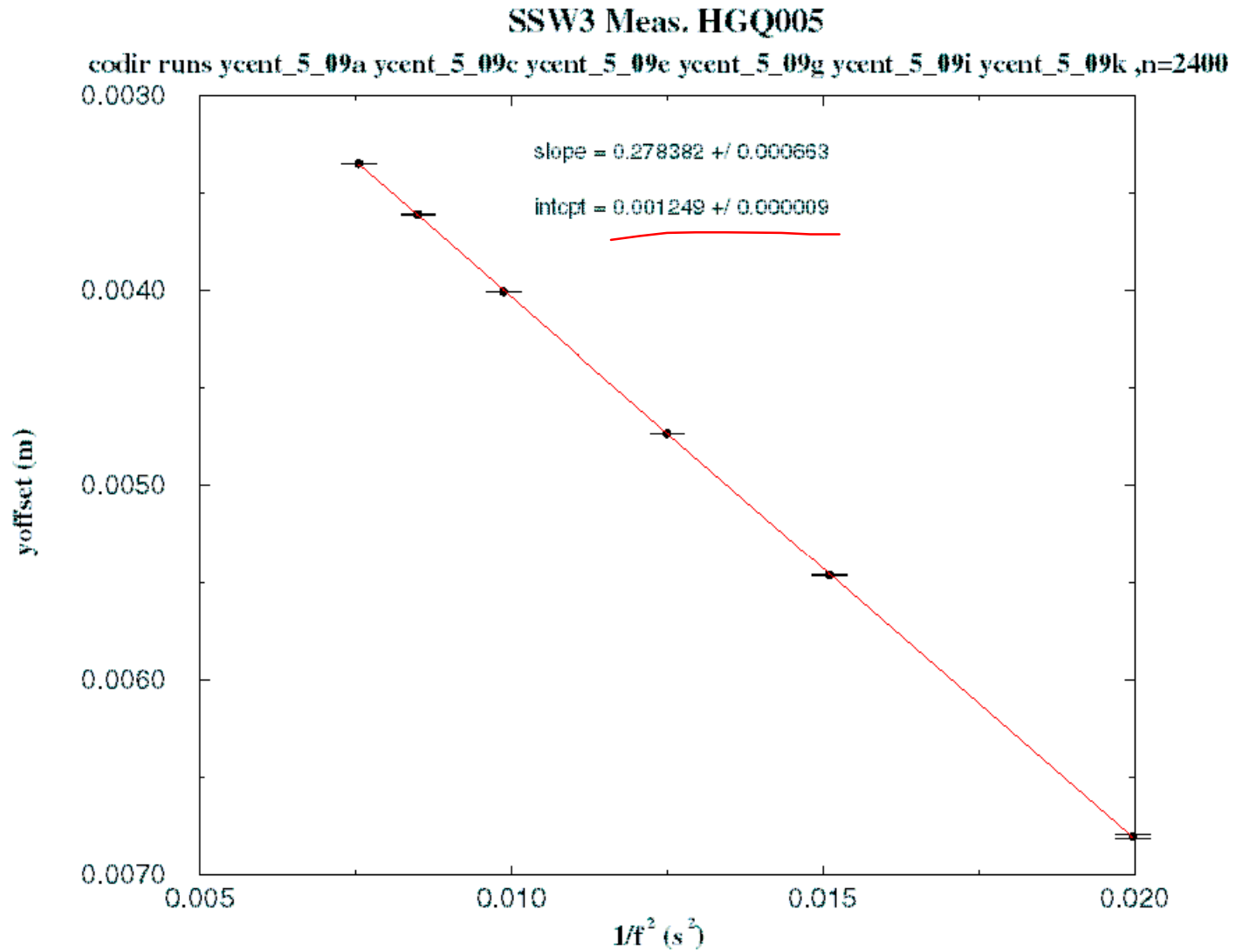
y_0 vs $1/T$, $L_w=16m$, Co-dir.

SSW3 Meas. HGQ005



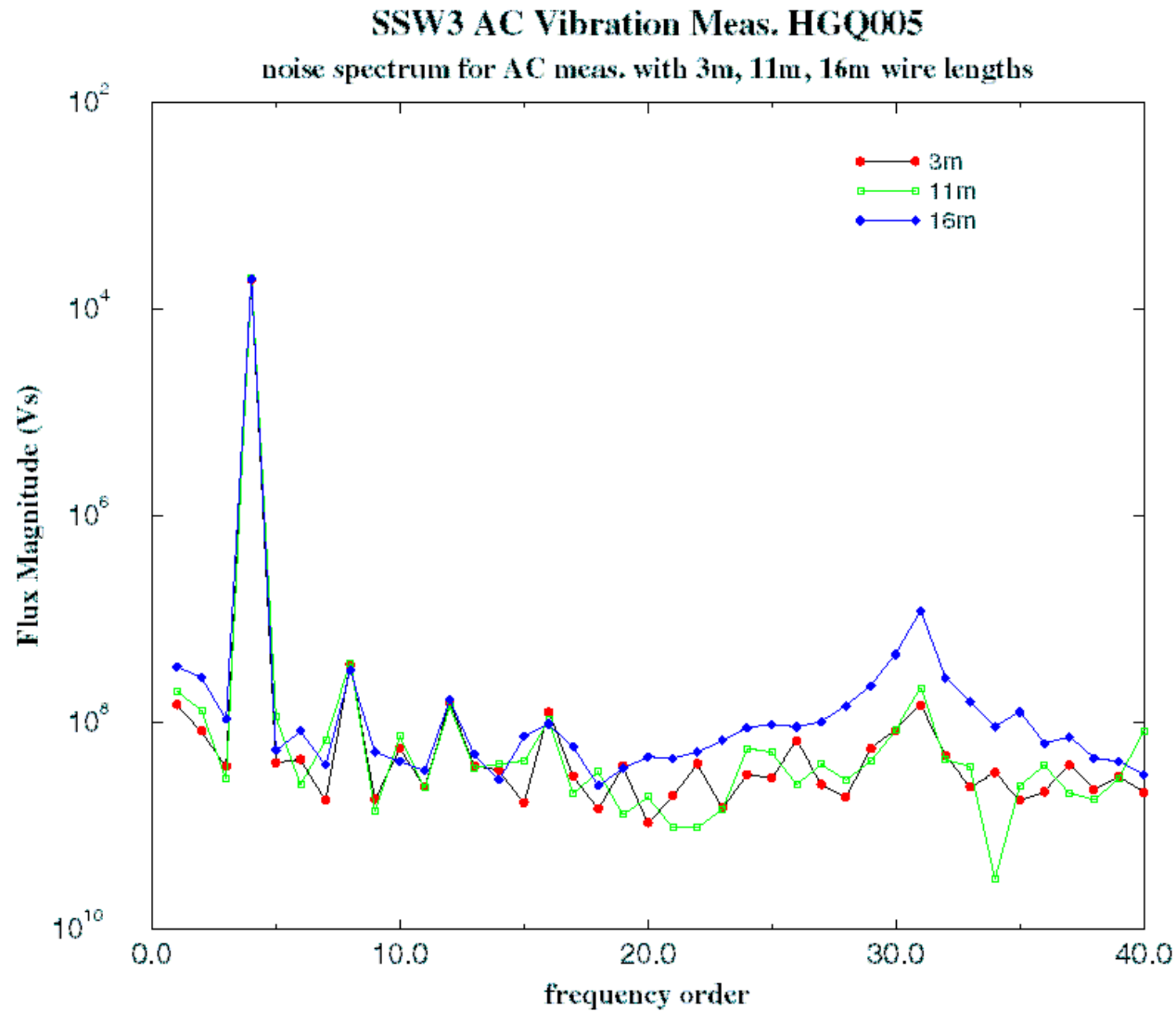
Sample Measurements

y_0 vs $1/f^2$, $L_w=16m$, Co-dir.



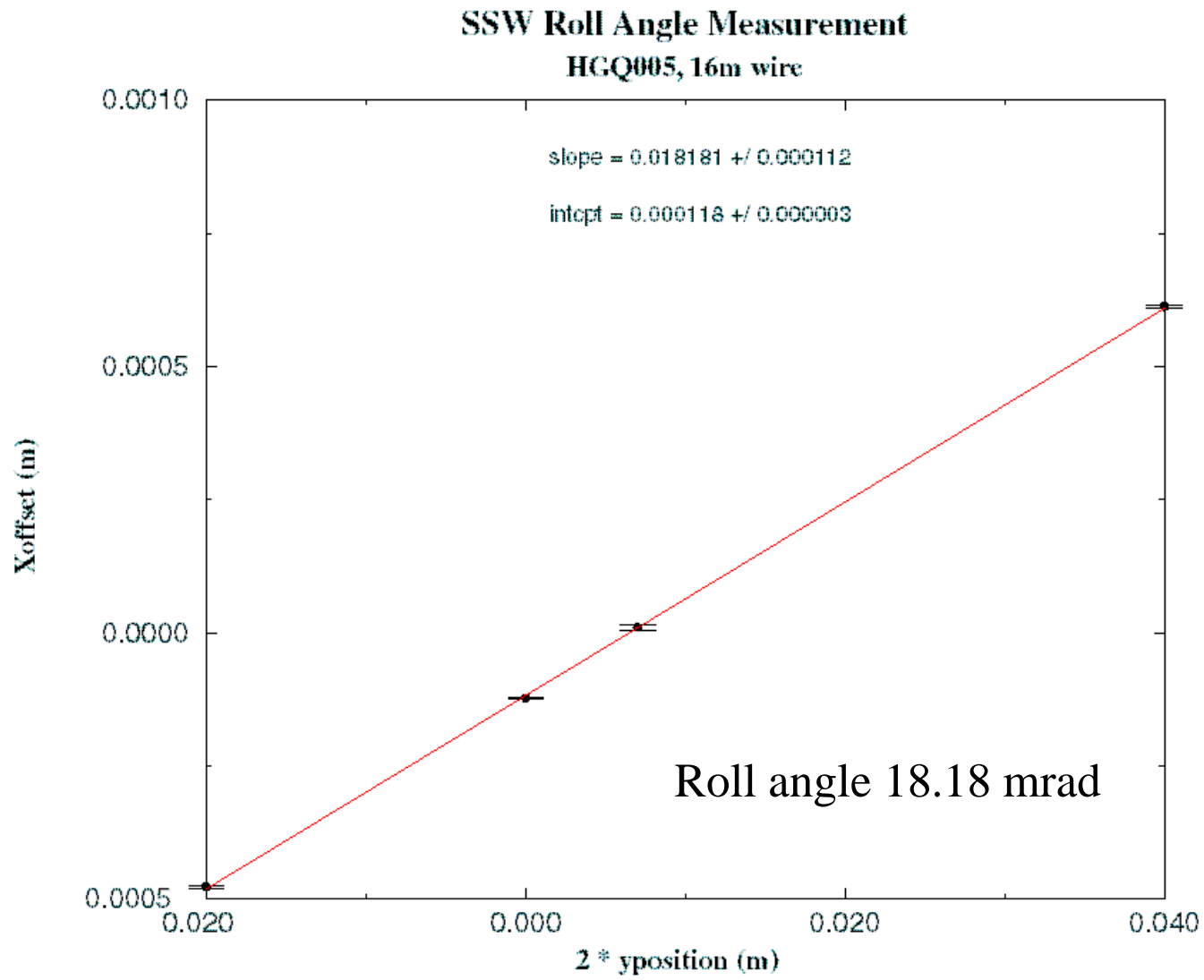
Sample Measurements

AC noise spectrum vs wire length



Results

Roll Angle



Results

Axis Location Comparison

Comparison of Changes in SSW and LT at 3m, 11m, 16m Wire Lengths

	11m - 3m			16m - 11m			16m -3m		
	SSW	survey	surv-SSW	SSW	survey	surv-SSW	SSW	survey	surv-SSW
y@mag_a	0.002224	0.002343	0.000119	-0.001447	-0.001474	-0.000027	0.000777	0.000869	0.000092
y@mag_b	0.002357	0.002201	-0.000156	-0.001022	-0.001008	0.000014	0.001335	0.001193	-0.000142
y@mag_center	0.002291	0.002272	-0.000019	-0.001235	-0.001241	-0.000006	0.001056	0.001031	-0.000025

	11m - 3m			16m - 11m			16m -3m		
	SSW	survey	surv-SSW	SSW	survey	surv-SSW	SSW	survey	surv-SSW
x@mag_a	0.000023	0.000012	-0.000011	-0.000048	0.000062	0.000111	-0.000026	0.000074	0.000100
x@mag_b	-0.000006	-0.000065	-0.000059	-0.000006	-0.000057	-0.000051	-0.000012	-0.000123	-0.000111
x@mag_center	0.000008	-0.000025	-0.000033	-0.000027	0.000006	0.000033	-0.000019	-0.000019	0.000000

Results

Axis Location Reproducibility

16m wire length

Axis	Meas #	SSW ave. offset	Comment	ID
x	1	-0.000088	5_10a,c,e are after y offset measurement	5_10a
	2	-0.000092		5_10c
	3	-0.000101		5_10e
y	1	-0.001270	3 tensions (drop 200g tension), 2 freq/tens.	5_06a-h
	2	-0.001225	4 tensions (drop 200g tension), 2 freq/tens.	5_06m-p
	3	-0.001283	3 tensions (btw 425 and 625g), 2 freq/tens.	5_07a-f
	4	-0.001249	6 tensions (btw 325 and 825g), 5 freq/tens.	5_09a-l

11m wire length

Axis	Meas #	SSW ave. offset	Comment	ID
x	1	0.000097	5_04e, g, i are after y offset measurement	5_04e
	2	0.000106		5_04g
	3	0.000000		after adjusting stages based on previous 2 runs
y	1	0.000019	4 tensions, 2 freq/tens.	4_30m-t
	2	-0.000001	5 tensions, 2 freq/tens.	5_02a-l
	3	-0.000014	5 tensions, 2 freq/tens.	5_04a-j

Results

Harmonics

HGQ005 integrated harmonics magnitude at $R=0.017\text{m}$ compared to VMTF rotating coil warm measurement ($z=0.05, 0.75, 1.5\text{m}$ positions average weighted by TF)

n	SSW	VMTF probe
1	0.033	0.000
2	10000.465	10000.000
3	1.583	1.284
4	1.490	1.458
5	0.229	0.331
6	0.768	1.822
7	0.230	0.078
8	0.068	0.064
9	0.046	0.018
10	0.042	0.078

What next?

- Wire improvement ?
 - Mg wire (1.6 times better strength to weight than BeCu) (on order)
 - Kevlar (conductive coating?, twist with Mg wire?)
 - Carbon fiber (conductivity good enough?, flexibility?)

	properties		available wire		
	Tensile strength (kpsi)	Density (g/cm ³)	size(um)	w (g/m)	breaking tension (g)
BeCu	190	8.26	100	0.067	1100
Mg (AZ61a)	69	1.8	150	0.033	900
Kevlar (200 Denier)	~200	1.8	~250	0.022	~3000
Carbon fiber (M46J-1k)	611	1.84	160	0.037	8600

Summary

- AC technique - 2 orders of magnitude noise improvement. Made good measurements at room temperature with model magnet.
- Wire vibration frequency - better than 0.5% - should be enough for 20m wire sag removal to 25-50 μ m.
- Counter-directional measurements found true axis to better than 150 μ m. For longer magnets, signal size (and therefore resolution) should improve with magnet length squared.
- Obtained same results for different wire lengths 3-16m. Average axis the same to better than 50 μ m including laser tracker measurement uncertainties.
- Results are consistent with calculations

**Trajectory Straightening, Fiducialization and
Alignment of the Strong-Focusing VISA Undulator,
using Pulsed Wire and Interferometric Techniques:
Part I (presented by G. Rakowsky)**

George Rakowsky, BNL and Robert Ruland, SLAC

ABSTRACT

Brief description of the VISA FEL experiment. Design of the in-vacuum undulator and its vacuum vessel. Alignment tolerance and error budget. Magnet sorting and matching. Pulsed wire measurements. Trajectory shimming. Determining the magnetic axis.

The contents of this talk were not available for inclusion in the proceedings.

Fiducialization and Alignment of the VISA Undulator[♦]

R. Ruland, D. Arnett, G. Bowden, R. Carr, B. Dix, B. Fuss, C. Le Cocq, Z. Wolf

SLAC, Stanford, CA

J. Aspenleiter, G. Rakowsky, J. Skaritka

BNL, Upton, NY

Abstract

The Visible-Infrared SASE Amplifier (VISA) undulator [1] will be installed at Brookhaven National Laboratory by the end of the year. Each undulator segment is set up on a pulsed-wire bench to characterize the magnetic properties and to locate the magnetic axis of the FODO array [2]. Subsequently, the location of the magnetic axis, as defined by the wire, is referenced to tooling balls on each magnet segment by means of a straightness interferometer. After installation in the vacuum chamber, the four magnet segments are aligned with respect to themselves. Finally the beam line reference laser [3] is pointed and positioned to be collinear to the undulator axis. The goal of these procedures is to keep the combined rms trajectory error, due to magnetic and alignment errors, below 50 μm .

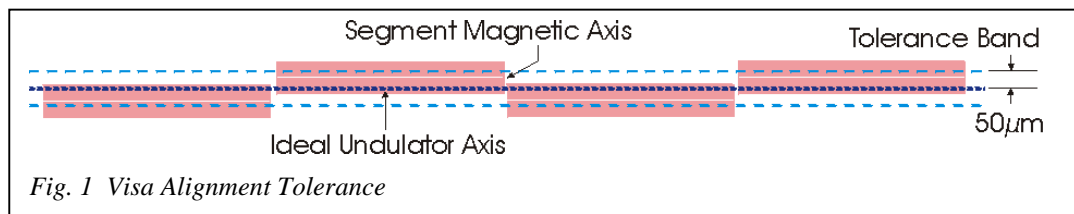
1 Introduction

The four-meter long undulator consisting of four 99 cm long segments is supported on a strongback and mounted inside a vacuum vessel. The undulator segments need to be aligned to 50 μm with respect to each other so that maximum **Self-Amplified Spontaneous Emission (SASE)** gain can be attained.

To accomplish successful alignment three tasks need to be completed. Firstly, the undulator segments need to be fiducialized. Secondly, the segments will be aligned, at first conventionally with respect to the global beam line coordinate system and then interferometrically with respect to their common axis. As a final task, the beam of a laser (**Reference Laser Beam - RLB**), which will provide the reference for the diagnostic pop-in monitors, has to be pointed such that it becomes collinear to the undulator axis.

2 Error Budget

The fiducialization and alignment residuals have to be kept to less than 50 μm (see fig. 1). The first two entries in the total budget come from the fiducialization process, positioning and RLB alignment being the remaining contributions. Their



[♦] Work supported by the United States Department of Energy, Office of Basic Energy Sciences under contract No. DE-AC03-76SF00515

To be presented at the XI Magnetic Measurement Workshop at Brookhaven National Laboratory, NY, Sept. 21-24, 1999

associated projected errors are shown in the table 1 and, added in quadrature, come very close to the desired final residual of 50 μm .

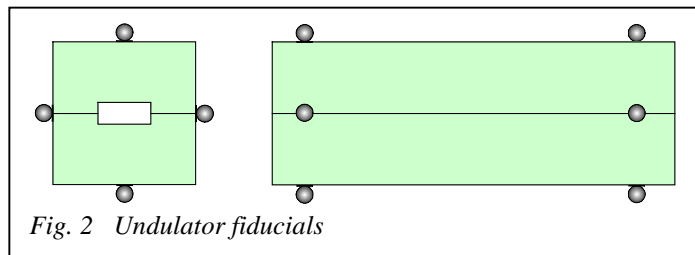
Table 1: Tolerance Budget

<i>Alignment Error Budget</i>	<i>projected</i> [μm]	<i>achieved</i> [μm]
<i>Magnetic Centerline Determination</i>	20	10
<i>Transfer onto Fiducials</i>	23	8
<i>Positioning</i>	28	
<i>Setup RLB with respect to Undulators</i>	29	
<i>Total (added in quadrature)</i>	51	42

3 General Approach

3.1 Fiducials

Fiducials are measured independently and are considered as such for both horizontal and vertical coordinates. The single dimensionality does not, however, represent a limitation. To obtain micron type results, great care must be taken to avoid any kind of first order errors. Hence, in high precision industrial metrology, measurements are always taken in the principal plane, i.e. horizontal measurements are carried out in the horizontal plane and vertical measurements in the vertical plane, respectively. Consequently, the undulator is designed to have the horizontal fiducials on the side and the vertical fiducials on the top. For redundancy reasons tooling balls are also placed on the other sides (see fig. 2).



3.2 Straightness Measurements

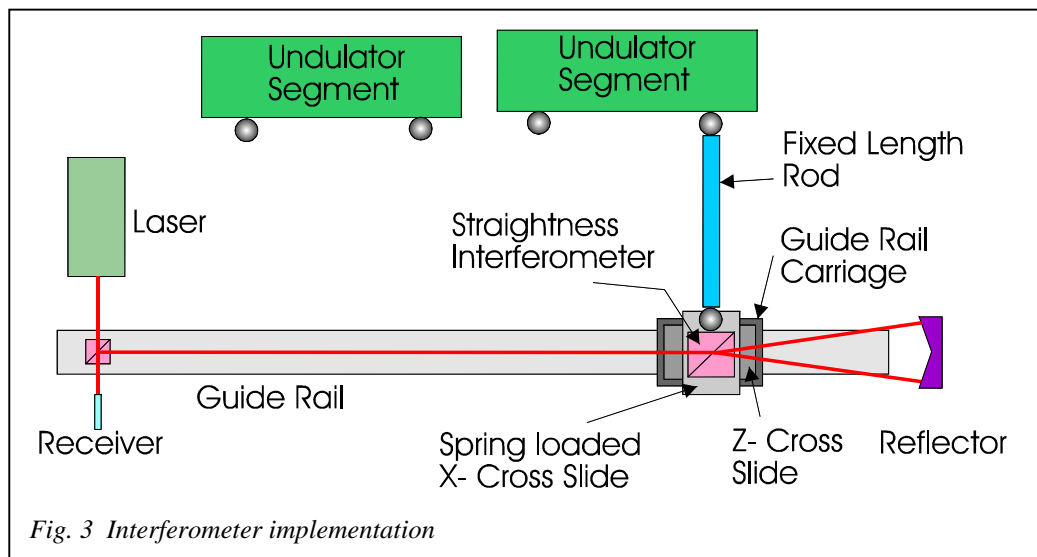
The extremely tight alignment tolerance precludes the application of traditional high precision optical alignment methods, including laser tracker based procedures. However, because of the straight-line geometry and the relatively short length, interferometric straightness measurement techniques can be used. A standard HP straightness interferometer in "long distance" mode (0.5m - 30m) will provide a straightness resolution of 0.8 μm with 5 μm accuracy over the length of the undulator, and a straightness measurement range of ± 1.5 mm. This method is one dimensional, i.e. horizontal and vertical positioning are accomplished using two independent straightness interferometer systems.

4 Instrumentation

4.1 Measuring Straightness Offsets

Straightness Interferometer

A straightness interferometer is not much different from a typical distance measurement interferometer. The Michelson interferometer is replaced by a Wollaston prism and the retro reflector by a straightness reflector. To measure straightness, however, the reflector is held fixed, and the Wollaston prism moves along the object being measured. Since the interferometer counts fringes, the beam signal must never be interrupted, e.g. due to a deviation of the Wollaston prism from the beam or by blocking off the beam transport, since this would cause the interferometer to lose count. To prevent a possible deviation of the Wollaston prism from the beam path and to also maintain maximum measurement range to both sides, i.e. to keep the prism centered on the beam, the Wollaston prism is usually mounted to a carriage riding on a precision guide rail. Because the guide rail moves the Wollaston prism parallel to the measurement object, an interface between the prism and the fiducials is needed. A constant distance rod



can realize such an interface. Whenever the prism is in the longitudinal vicinity of a fiducial, the rod is inserted between the Wollaston prism and the fiducial. To facilitate the insertion of the rod and to provide constant measurement conditions, the Wollaston prism is mounted on a cross slide. In addition, to ease the placement of the rod, both ends have a sleeve, which fits loosely over the tooling ball on the undulator as well as the one on the prism (see fig. 3, sleeves are not shown). However, this implementation does not provide any indication of when the rod is truly perpendicular to the measurement interferometer beam. Fortunately, this is not a new and unique problem, being also a condition typical to optical tooling measurements.

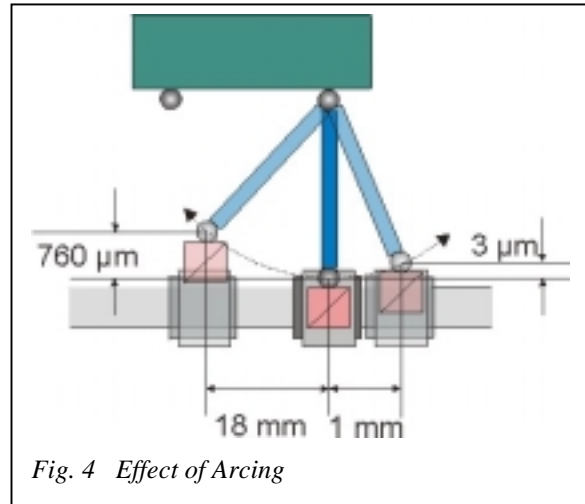
Arcing

To overcome the problem, the instrument operator instructs the rod man to arc the scale while he is constantly reading the scale. He knows that when he observes the smallest scale value, the scale must be perpendicular to the line of sight. This arcing can be implemented in this set up by slowly moving the Wollaston prism in the Z direction while watching the straightness interferometer read-out (see fig. 4). Since it proved less accurate to manually move the carriage at a constant speed across a measurement point, an additional motor driven stage was added between the carriage and the X cross slide. In this configuration, the carriage is moved by hand to a position of about an inch before a measurement point. Then the Z stage drive is engaged, which moves the Wollaston prism across the unknown measurement point. A computer interfaced to the drive read-out and the interferometer readout records coordinate pairs (z, x) over this distance. Subsequently, a simple circle fit not only solves for the true measurement point and thus for the shortest distance, but also improves the significance of the solution by fitting many readings.

4.2 Finding the Wire

Wire Finder Design

A “pulsed-wire” bench is used to determine the magnetic centerline [2]. The wire position on either side of an undulator pair will be detected with Wire Finders (see fig. 5). The position measurement is carried out in one plane at a time with one device on either side of the undulator. Each wire finder is mounted on a frame, which sits perpendicular to beam direction on the undulator support plate during magnetic measurements. Each frame carries two tooling balls in



the measurement plane in the same geometry as the tooling balls on the undulator. A laser-based design allows detecting the wire position without touching it. The device consists of a laser emitter mounted so that the emerging beam will pass through a slit across the wire to a receiver on the other side. After measuring the intensity of the signal received, a computation based on the signal profile will provide an accurate determination of the wire position.

Wire Finder Calibration

The wire position measurements need to be related to the reference tooling ball on the wire finder frame. Since the device measures only in one dimension at a time, a calibration can be simply achieved by determining the lateral offset of the wire finder's coordinate system with respect to one of the tooling balls. This is accomplished by performing the wire measurement a second time, this time however with the fixture yawed by 180° (fig. 6, 7). To retain the fixture in the same transverse position during both measurements, a calibration mount is required where the fixture rests on its tooling balls in a kinematic mount. The kinematic mount can be realized by a combination of the standard cone, V-groove, and flat mounts. One tooling ball sits in a cone shaped mount, the second one sits in a V-groove with the V-groove oriented perpendicular to beam direction. The remaining degree of freedom restraint consists just of a dowel pin stopping the plate from flipping around its pitch axis. To complete the calibration, the distance between the tooling balls needs to be measured accurately. Hence, the wire position with respect to one tooling ball in the first position will be half of the tooling ball distance plus the lateral offset plus the micrometer reading. This value is referred to as the wire offset and is vital in completing the fiducialization of the magnets.



Fig. 6 Wire Finder in Calibration Stand, zero° yaw position



Fig. 7 Wire Finder in Calibration Stand, 180° yaw position

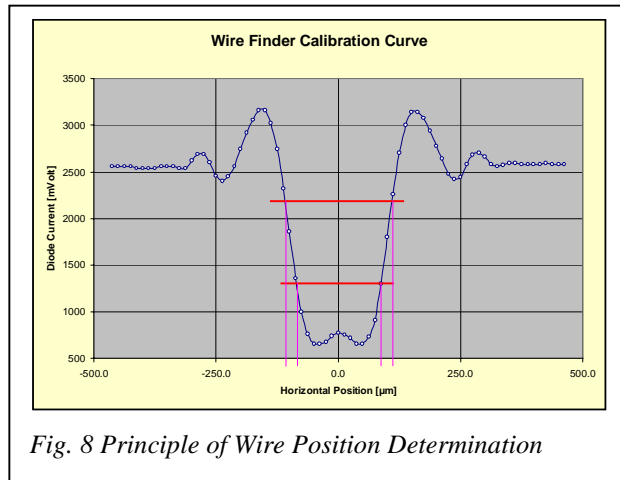


Fig. 8 Principle of Wire Position Determination

Wire position measurement

The actual wire position measurement is carried out by driving the detector assembly across the wire profile. The micrometer readings are recorded at two defined detector voltage output levels on either side of the wire. The mean of the micrometer readings yields the wire center position (see fig. 8).

4.3 RLB Laser Finder

A laser beam cannot be picked up accurately by standard mechanical alignment instrumentation. Therefore, a tool was needed that would reference an optical beam to mechanical fiducials.

Detector Fixture Design

The Laser Finder (LF) consists of a frame, which carries four tooling balls in the same geometry and dimensions as they are when mounted to the end of an undulator. A quadrant detector is mounted to the center of the frame within a few hundred microns (see fig. 9). The quadrant detector will give a read-out of the beam position in the quadrant detector's coordinate system.

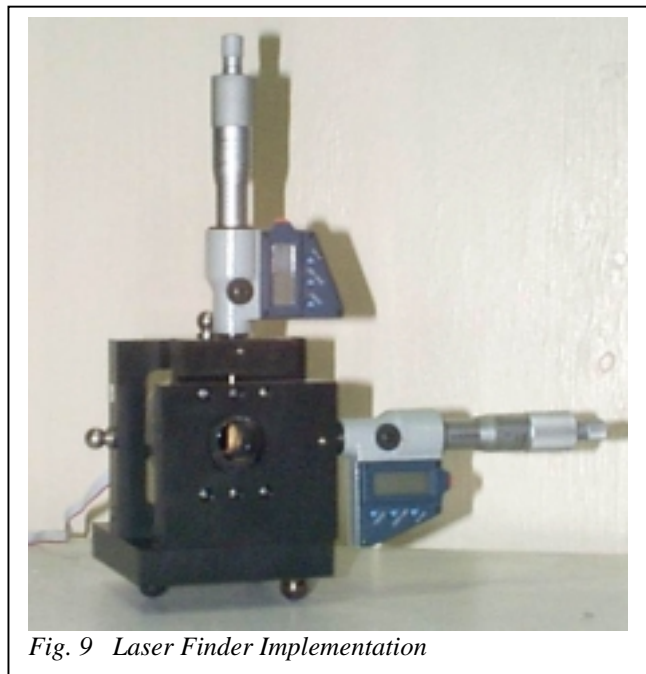
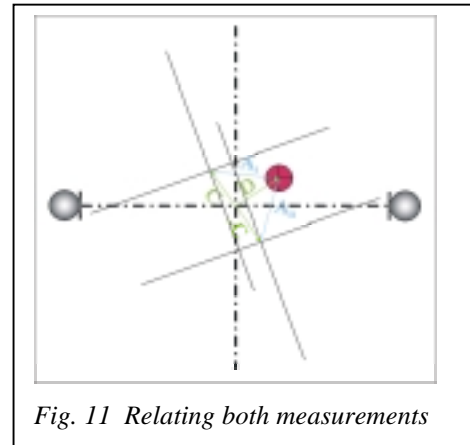
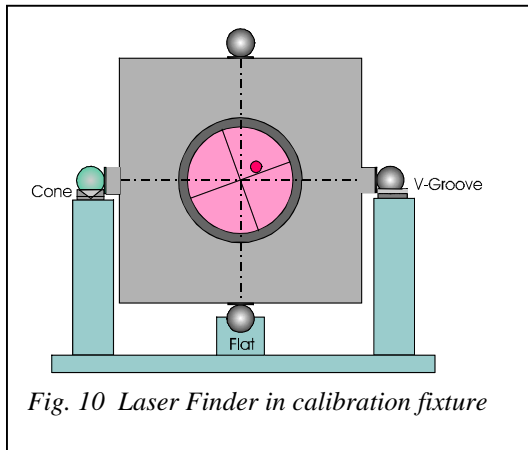


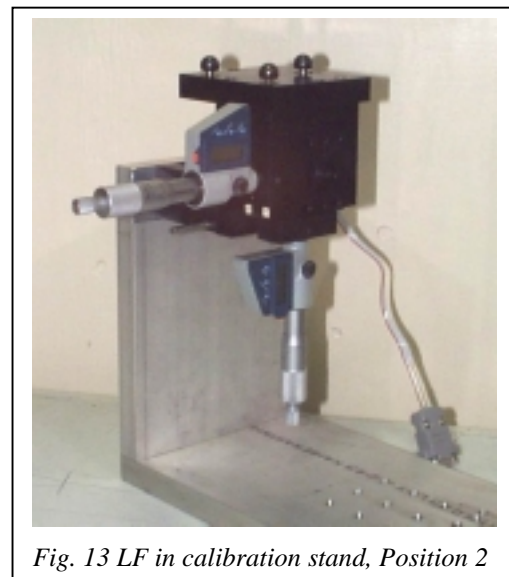
Fig. 9 Laser Finder Implementation

The Laser Finder is built as a nulling device. The quadrant detector is mounted on a two-dimensional cross slide. The position of the quadrant detector can be adjusted by micrometers horizontally and vertically. The quadrant detector sums the laser intensity readings on each of the two halves of the sensitive surface and then compares the two. This arrangement is subsequently electronically rotated 90° to measure the other dimension. The detector's coordinate system needs to be related to the tooling ball coordinate system through calibration measurements.



Laser Finder Calibration

Firstly, the positions of the four tooling balls are measured accurately on a coordinate measurement machine. Secondly, the frame is set up on a calibration stand similar to the Wire finder (see fig. 10). An X, Y reading of the beam spot is taken. Subsequently, the frame is rolled by 180° and a second reading is taken. The depiction in fig. 11 combines the geometric relationship from both readings. Figures 12 and 13 show the Laser Finder during calibration. A simple vector algebra operation will produce the unknown calibration offsets D and, C, both



expressed in a Cartesian coordinate system with its datum located with respect to the symmetry axes of the two horizontal tooling balls.

It should be pointed out that this procedure does not solve for a parameter representing the rotation between the tooling ball coordinate system and the quadrant detector coordinate system. While the procedure could be expanded to include this parameter, it is believed not to be required as long as the quadrant detector is carefully aligned with respect to the tooling balls.

5 Fiducialization Concept

The fiducialization measurements are carried out in one dimension (plus length) at a time (fig. 14). It consists of six-steps, which are subsequently repeated for the other dimension and additionally for closure checks in the 180° and 270° roll positions:

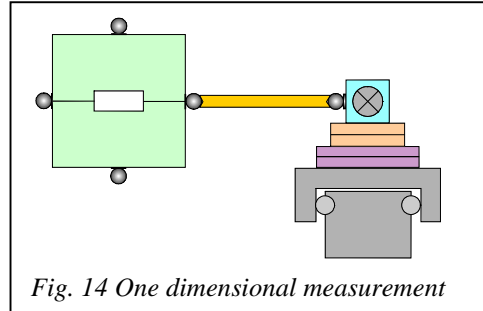


Fig. 14 One dimensional measurement

5.1 Find Magnetic Centerline

The first step in the fiducialization of the undulator magnets involves determining the magnetic centerline. This step will yield a wire that is physically positioned along the magnetic centerline of an undulator pair [4].

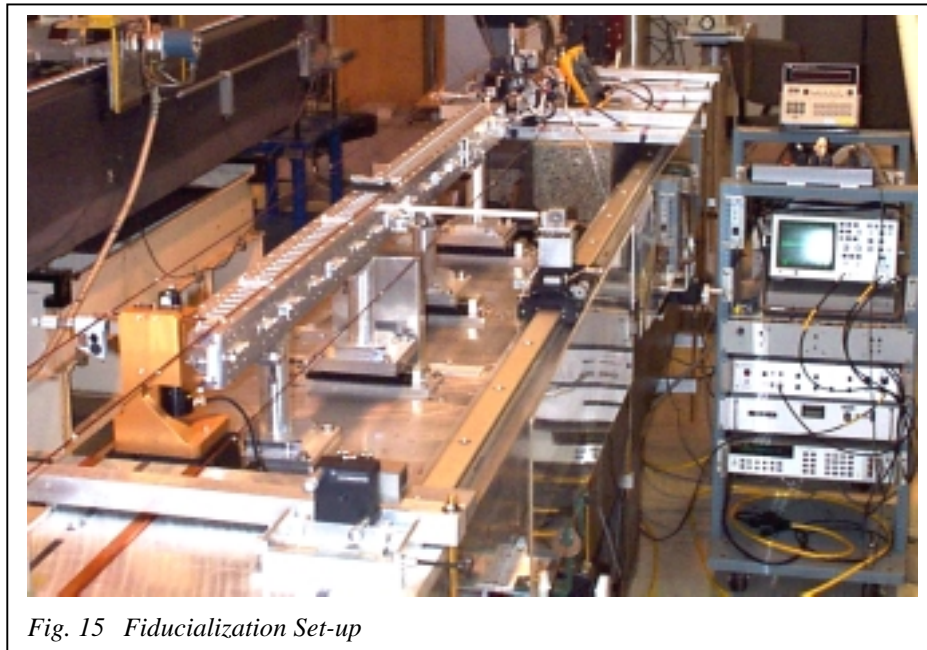


Fig. 15 Fiducialization Set-up

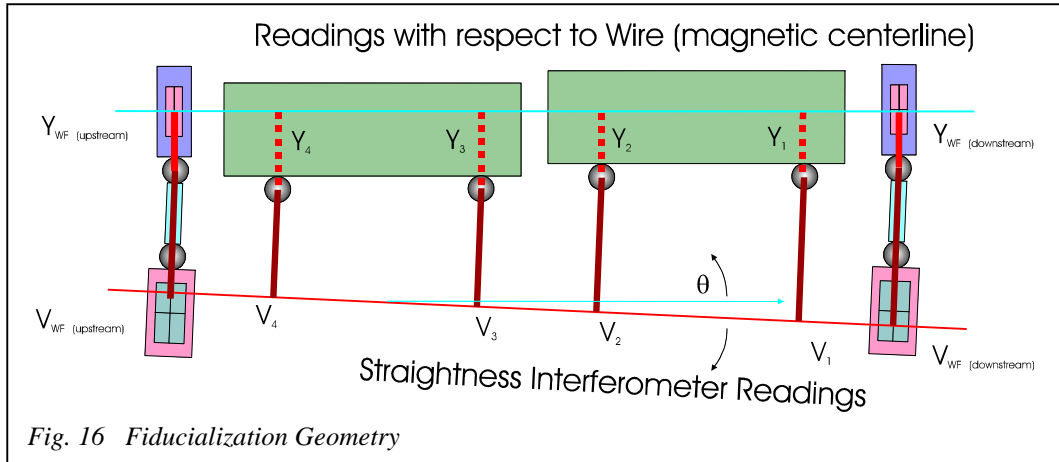
5.2 Detect Wire Position

Two Wire Finders, one positioned on each the upstream and downstream sides of a pair of undulator segments (see fig. 15), are used to detect the wire position and relate it to the Wire Finders' reference tooling balls. By combining the wire position information and the relationship of the detector zero to the reference

tooling ball which is known from calibration, the position of the Wire Finder reference tooling ball is known with respect to the magnetic axis.

5.3 Map Fiducial Positions with Respect to a Straight Line

Next a straightness interferometer setup is used to measure the position of the undulator tooling balls relative to the Wire Finder reference tooling balls.



5.4 Calculate Fiducial Offsets

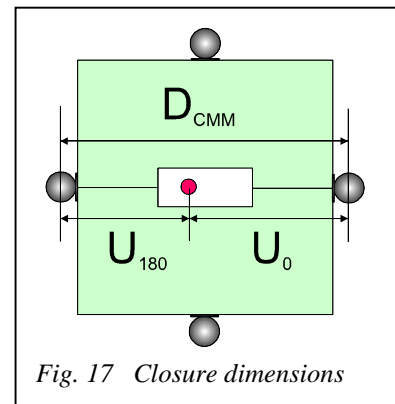
After correcting for the non-parallelity effect between the wire and the interferometer axes, the perpendicular distance of the tooling balls from the magnetic axis is obtained (fig. 16).

5.5 Repeat for Other Dimensions

To avoid wire sag effects that would bias the vertical position measurements and to carry out all measurements in the principle plane of each tooling ball, the fiducialization process is designed to be one-dimensional (plus z distance) only. The vertical positioning will be accomplished by rolling the undulator segment by 90° thus creating another horizontal measurement.

5.6 Closure Check

The above steps are all repeated by rolling the undulator segment into the 180° and 270° positions. Adding the fiducialization values of two opposite tooling balls in both the horizontal and vertical plane yields the spatial distance between the respective two tooling balls. Comparing this value against a previous measurement on a high accuracy Coordinate Measurement Machine (CMM) provides a valuable check against measurement and systematic errors (fig. 17).



6 Alignment

A six step process was designed to accomplish the alignment goal.

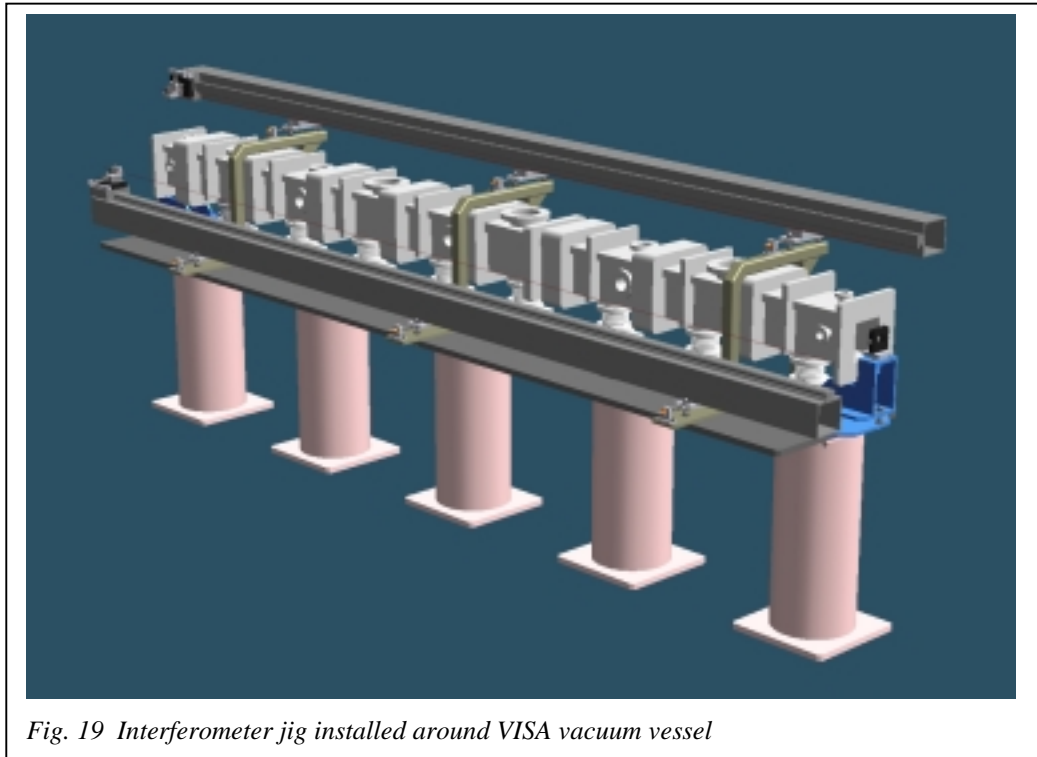
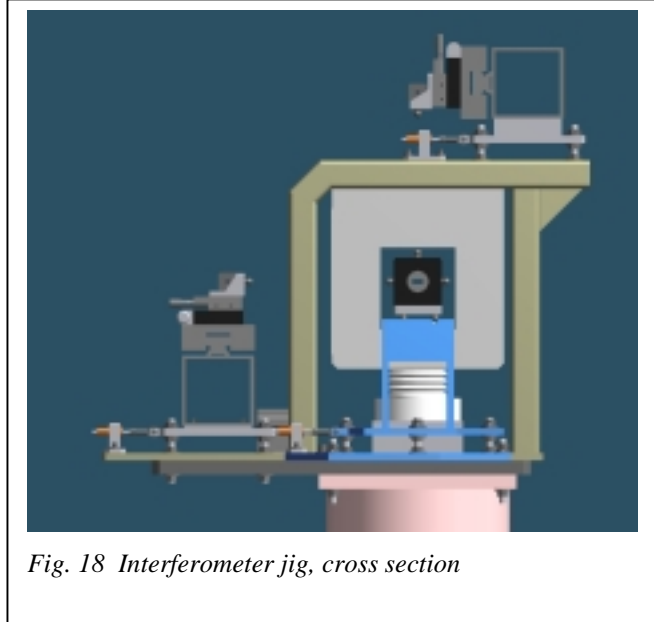
6.1 Installation Alignment

Conventional alignment methods will be used to support mechanical installation. This step will align the undulator with respect to the global beam line coordinate system and with respect to the common axis with an accuracy of about 150 – 200 μm .

6.2 Map Undulator Fiducials

The technique underlying the fine alignment is analogous to the fiducialization process as it is based on the use of straightness interferometry. A dual straightness interferometer setup is used to measure the position of the undulator tooling balls relative to the arbitrary straightness interferometer reference line.

Since test measurements had shown that it was necessary to control the alignment process



in both the vertical and horizontal plane simultaneously, two straightness interferometers are set up, one in the horizontal plane and one in the vertical plane. A special alignment jig was designed to facilitate the setup and alignment of both straightness interferometers (see fig. 18-22). Figures 23-25 show details of the arcing and interface rod implementation. To minimize the number of necessary iterations, the straightness interferometer reference line should be set-up fairly parallel to the initial axis of the undulator segments.



Fig. 20 VISA test installation with jig

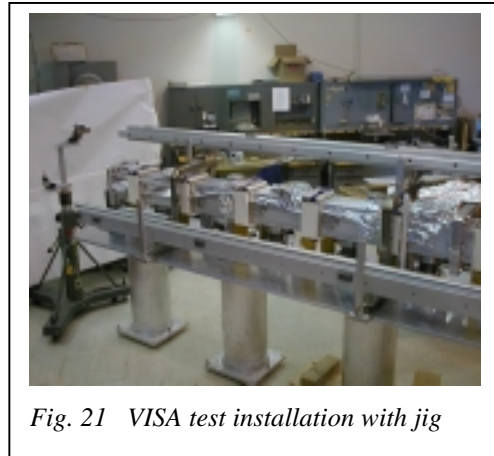


Fig. 21 VISA test installation with jig

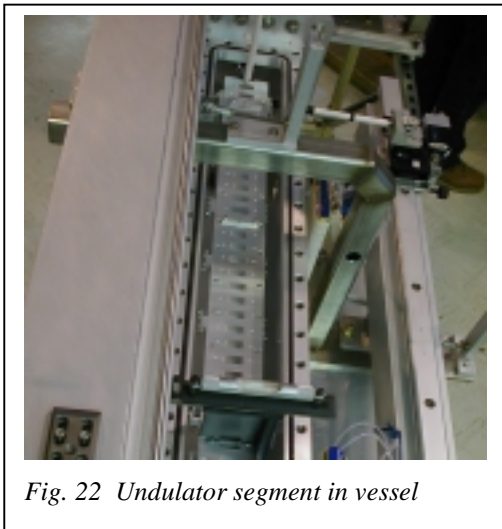


Fig. 22 Undulator segment in vessel

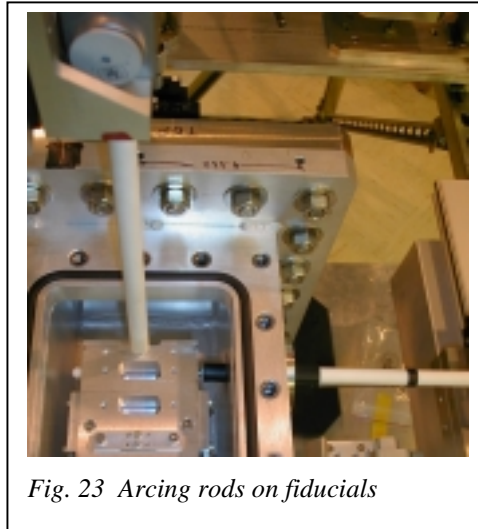


Fig. 23 Arcing rods on fiducials



Fig. 24 Arcing drive and stop

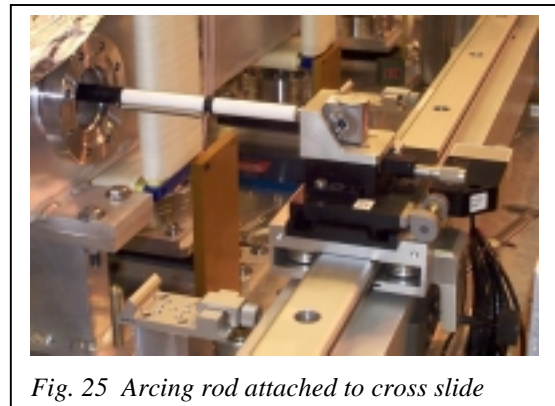


Fig. 25 Arcing rod attached to cross slide

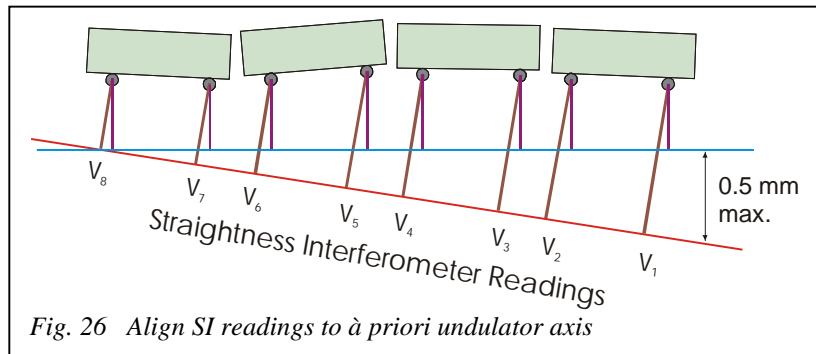
To create an accurate snap shot of an undulator segment's position, the horizontal and vertical straightness interferometer readings are taken simultaneously. It should be stressed again that the straightness interferometer is only a relative measurement tool. The capability to align the undulators to an absolute position is only provided through conventional alignment.

6.3 Mathematically Align Coordinate Systems

The raw measurements are taken in different coordinate systems, which have different datums: the SI coordinate system, the undulator segment fiducialization coordinate system, and the undulator common axis coordinate system.

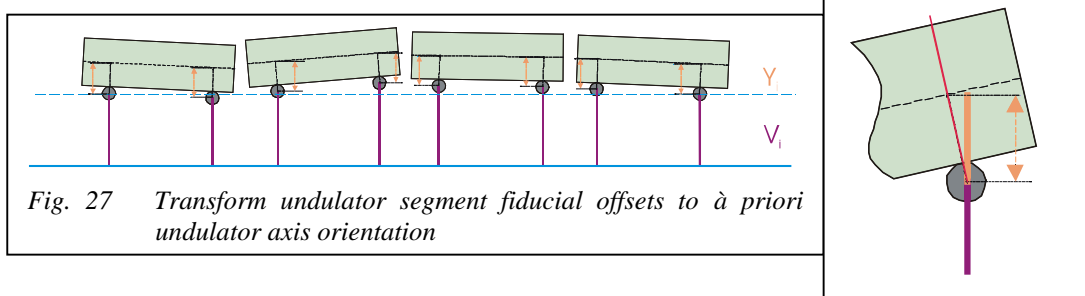
Align SI Readings to À Priori Undulator Axis

In a first step the straightness interferometer readings need to be corrected for the non-parallelity of the à priori undulator axis and straightness interferometer coordinate systems. A similarity transformation is used to compute the corrected straightness interferometer readings (see fig. 26).



Transform Undulator Segment Fiducialization Offsets Into À Priori Axis System

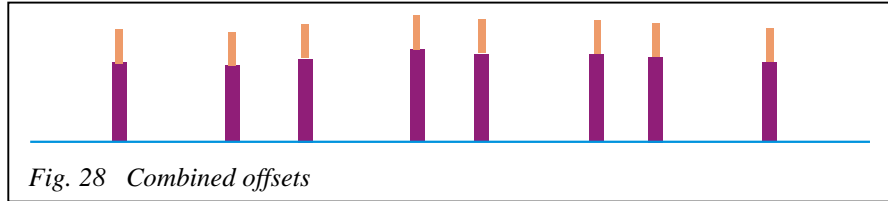
The fiducialization offsets were determined in a coordinate system whose axis is aligned to the individual segment's centerline. Since at this stage the individual segments are potentially yawed and pitched with respect to each other, the nominal fiducial offsets need to be transformed into the à priori axis system (see fig. 27).



Combine transformed offsets and readings

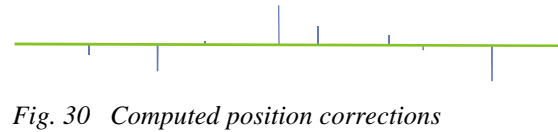
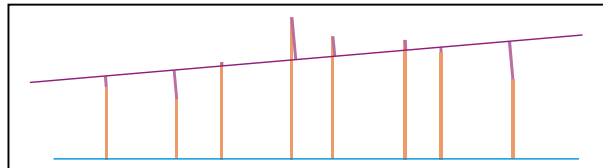
After transformation of the SI readings and the nominal fiducialization offsets into a common coordinate system, the two values can be combined and represent

the actual offset from the undulator segment's magnetic centerline at the tooling balls position with respect to the à priori common undulator axis (fig. 28).



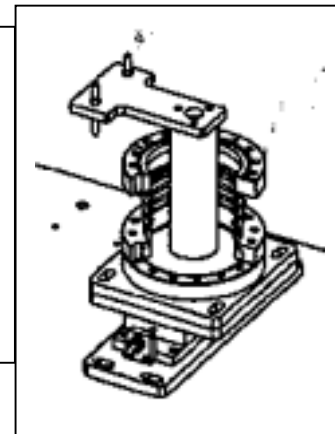
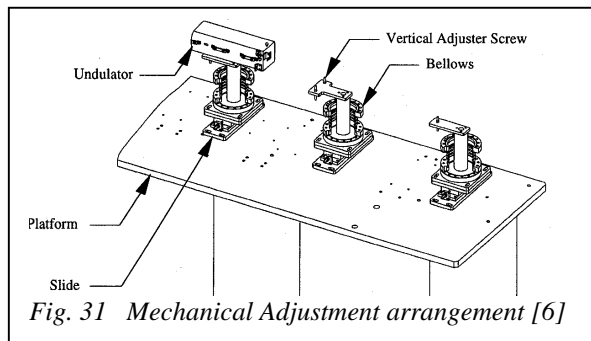
6.4 Fit Straight Line to Data

From these measurements position corrections for the undulator magnets can be calculated. To minimize necessary movements a line fit is applied to the data (fig. 29). The resulting offsets from the fitted line (fig. 30) represent the corrections, which need to be applied to align the undulator segments to a common straight line.



6.5 Apply position corrections

The above computed position corrections are applied under the control of the dual axis straightness interferometer system. For ease of operation, the corrections are translated into fractions of rotation of the respective screws controlling the positioning device (fig. 31).



6.6 Quality Control Map

After all adjustments are applied, the undulator fiducial positions are again recorded. Due to the geometry and construction of the supports, a slight coupling between the adjustment axes is to be expected. This might require iterating the last two steps. After the positioning goal is achieved, a final map including the fiducials of the Laser Finder in both the upstream and downstream position is recorded and processed.

7 Measurement Results

7.1 Wire Finder Calibration

The results of a repeatability test of the Wire Finder calibration are shown in fig. 32. The calibration was carried out before the Wire finder was used on the fiducialization bench and afterwards at the end of the day. Both calibration sets consisted of four individual measurements. The small differences between individual measurements and between the two sets demonstrate the accuracy and reliability of the device. The calculated Standard Deviation projects that the contribution of the Wire Finders to the total error budget will be negligible.

Laser Finder Calibration Comparison							
Golden Fixture				Black Fixture			
before	Δ	after	Δ	before	Δ	after	Δ
43.2745	-0.003	43.2742	0.000	43.4017	0.000	43.4038	0.000
43.2698	0.002	43.2752	-0.001	43.4035	-0.002	43.4057	-0.002
43.2713	0.001	43.2729	0.002	43.4006	0.001	43.4025	0.001
43.2724	0.000	43.2758	-0.001	43.4016	0.000	43.4038	0.000
43.272		43.275		43.402		43.404	
	-0.003				-0.002		
StD.	1.5	μm		StD.	1.2	μm	

Fig. 32 Laser finder Calibration Comparison

7.2 Fiducialization Repeatability

Four sets of measurements were taken which began with centering the pulsed wire on the magnetic axis, measuring the wire position, and then taking interferometer readings of the tooling balls (see fig. 33, 34). After each set, the magnets as well as the interferometer were moved to guarantee independent measurements. The measurements of each set were first reduced by taking out the skewness between the reference lines and then used to project the perpendicular offset of the tooling balls from the magnetic center line. The measurement data is presented in figure 35. Fig. 36 shows the results of the data reduction. All but two of the independent measurements agree to within two μm , the worst data point is 6 μm off. The standard deviation of all measurements is 2.3 μm .

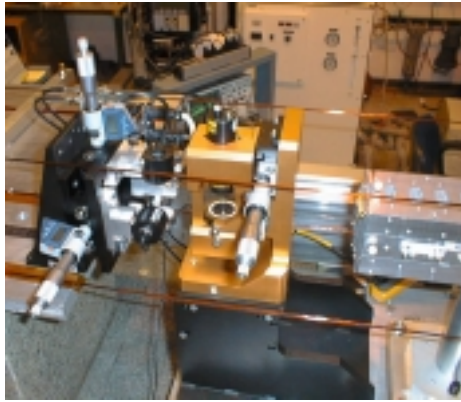


Fig. 33 Pulsed wire detector and Wire Finder



Fig. 34 Bench with undulator magnet and interferometer set-up

		Wire (Magnetic Axis)		Interferometer Readings		
		z	y	u	v	
Measurement Set 1	WF_G	0	50.533	0	0.298	
	WF_B	2223	50.503	2223	0.9293	
	M1_TB4			169	0.351	
	M1_TB8			1134	0.7418	
	M2_TB4			1162	0.6367	
	M2_TB8			2129	0.9225	
Measurement Set 2	WF_G	0	50.532	0	-0.3343	
	WF_B	2223	50.501	2223	0.2683	
	M1_TB4			169	-0.281	
	M1_TB8			1134	0.0551	
	M2_TB4			1162	-0.0073	
	M2_TB8			2129	0.2639	
Measurement Set 3	WF_G	0	50.534	0	1.9019	
	WF_B	2223	50.504	2223	2.5144	
	M1_TB4			169	1.9518	
	M1_TB8			1134	2.3371	
	M2_TB4			1162	2.2279	
	M2_TB8			2129	2.5051	
Measurement Set 4	WF_G	0	50.532	0	-0.0784	
	WF_B	2223	50.501	2223	0.5409	
	M1_TB4			169	-0.0226	
	M1_TB8			1134	0.3654	
	M2_TB4			1162	0.2553	
	M2_TB8			2129	0.5368	

Fig. 35 Fiducialization Rpeatability

	Measurement 1	Measurement 2	Measurement 3	Measurement 4	Average
M1_TB4	50.536	50.537	50.535	50.538	50.537
M1_TB8	50.639	50.650	50.641	50.644	50.644
M2_TB4	50.526	50.528	50.524	50.526	50.526
M2_TB8	50.524	50.523	50.522	50.524	50.523
	Δ	Δ	Δ	Δ	
M1_TB4	0.84	-0.56	1.51	-1.79	
M1_TB8	4.29	-6.26	2.30	-0.33	
M2_TB4	-0.09	-1.87	1.79	0.16	
M2_TB8	-0.71	0.06	1.59	-0.94	

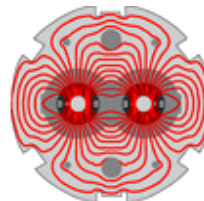
Fig. 36 Fiducialization test analysis

8 Conclusion

Initial fiducialization measurements confirm that the “Magnetic Centerline Determination” and “Transfer onto Fiducials” tolerances cannot only be met, but at least cut in half. The alignment jig has been assembled in the “test assembly” area and successfully tested. Presently, the fine alignment is scheduled for the end of the year [5].

References

- [1] R. Carr et al.: *The VISA FEL Undulator*, Proceedings of the 20th International FEL Conference (FEL98), Williamsburg, VA, August 1998.
- [2] G. Rakowsky et al.: *Measurement and Optimization of the VISA Undulator*, Proceedings of the 1999 Particle Accelerator Conference (PAC99), New York City, NY, March/April 1999.
- [3] R. Ruland et al.: *Alignment of the VISA Undulator*, Proceedings of the 1999 Particle Accelerator Conference (PAC99), New York City, NY, March/April 1999, SLAC Pub. 8086
- [4] G. Rakowsky, *ibid.*
- [5] A. Tremaine et al.: "*Status and Initial Commissioning of a High Gain 800 nm SASE FEL*," Proceedings of the 21st International FEL Conference (FEL99), Hamburg, Germany, August 1999.
- [6] M. Libkind et al.: *Mechanical Design of the VISA Undulator*, Proceedings of the 1999 Particle Accelerator Conference (PAC99), New York City, NY, March/April 1999.



Finding magnetic axis of LHC superconducting magnets in warm conditions

Laurent Deniau, CERN-LHC/MTA

September 1999

Laurent.Deniau@cern.ch



Field measurement in warm conditions with rotating coils system

Advantages

- ☞ Superconducting magnet in warm conditions
 - ⇒ no cool down
 - ⇒ big save of time

Disadvantages

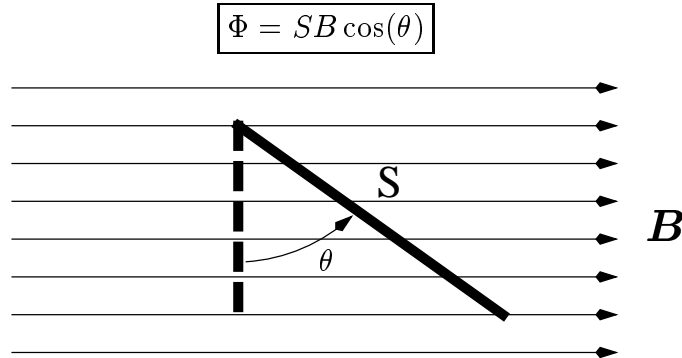
- ☞ Superconducting magnet in warm conditions
 - ⇒ low current (⇒ low field)
 - ⇒ low emf (⇒ high voltage amplifier gains)
 - ⇒ bad SNR (Signal-Noise Ratio)
 - ⇒ bad harmonics accuracy
 - ⇒ unable to find the field axis of dipole magnet

Improvements for better SNR

- ☞ Increase the coil rotation speed
 - ⇒ vibrations, speed variations
- ☞ Increase the coil surface (winding turns)
 - ⇒ very difficult to make (small aperture size)
- ☞ Increase the flux variation (200A/s ramp rate)
 - ⇒ very high current at the end of the measurement
- ☞ Use AC power supply with high frequency
 - ⇒ Eddy currents, magnet bandwidth, AC stability.

Magnetic flux

- ☞ The magnetic flux Φ through a flat surface in a uniform magnetic field depends on the PROJECTION of the area perpendicular to the magnetic field lines.

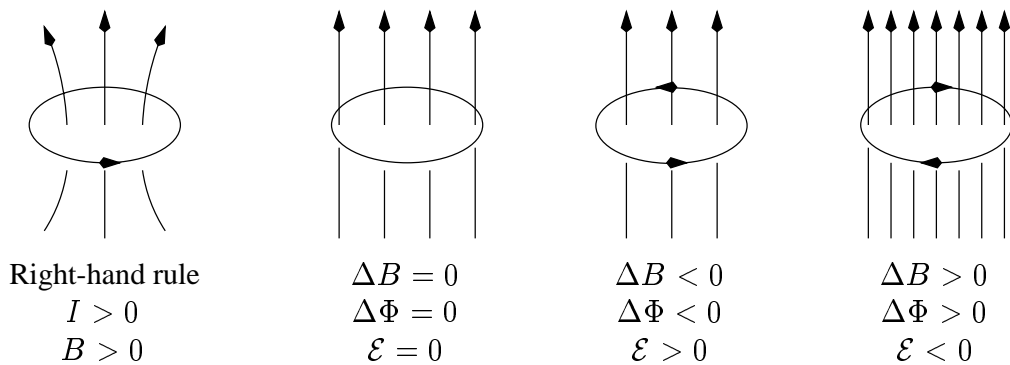


- ☞ The SI unit of magnetic flux is the weber ($\text{Wb} \equiv \text{V}\cdot\text{s} \equiv \text{T}\cdot\text{m}^2$).

Induced electromotive force

- ☞ The induced *emf* along any closed path is proportional to the RATE OF CHANGE of magnetic flux through the area bounded by the path (Faraday's Law, 1821)
- ☞ The effect of the induced *emf* is such as to OPPOSE THE CHANGE in flux that produce it (Lenz's Law, 1834). This is a consequence of the conservation of energy.

$$\mathcal{E} = -\frac{d\Phi}{dt}$$



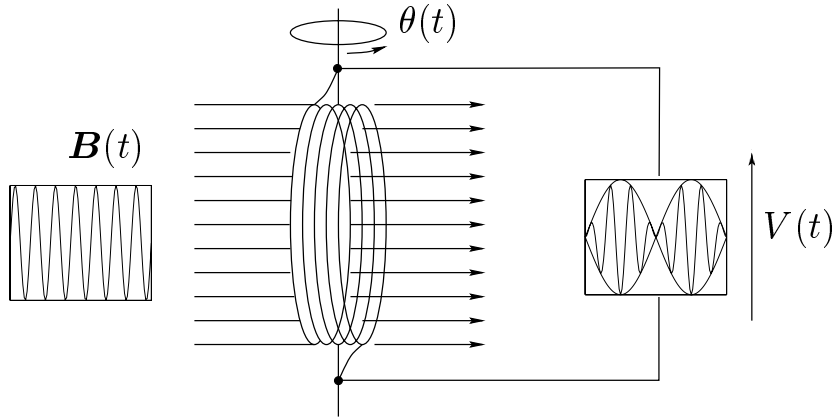
(Lorentz's force) (Faraday's law)

$$\mathbf{F} = q(\mathbf{E} + \mathbf{v} \times \mathbf{B}) \quad ; \quad \mathcal{E} = \oint_C (\mathbf{E} + \mathbf{v} \times \mathbf{B}) \cdot d\mathbf{l}$$

Motion in a pure $2n$ -poles time-dependent magnetic field

(Amplitude Modulation without carrier)

$$\theta(t) = \omega t \quad ; \quad \mathbf{B}(t) = B_n \cos(\omega_0 t + \phi_0)$$



$$\Phi(t) = SB_n \cos(\omega_0 t + \phi_0) \cos(n\omega t)$$

$$\mathcal{E}(t) = -2\pi SB_n [f_0 \sin(\omega_0 t + \phi_0) \cos(n\omega t) + n f \cos(\omega_0 t + \phi_0) \sin(n\omega t)]$$

For $f_0 \gg nf$, we have:

$$\mathcal{E}(t) \approx -\omega_0 SB_n \sin(\omega_0 t + \phi_0) \cos(n\omega t)$$

where $n = 1, 2, 3, \dots$ for dipole, quadrupole, sextupole, ...

⇒ Since $B_n \propto I$ and $V \propto \mathcal{E}$, the measured voltage amplitude ranges are proportional to the AC frequency. Thus we can use the frequency f_0 as a voltage AMPLIFIER.

$$V(t) \propto f_0 I(t)$$

⇒ The flux and the field amplitude ranges remain INDEPENDENT of the AC frequency (f_0 -invariant).

2n-poles field, harmonics form

$$\Phi(t) = \text{Re} \left[\sum_{n=1}^{\infty} \frac{\kappa_n}{R_{ref}^{n-1}} C_n(t) e^{in\theta(t)} \right]$$

where $C_n(t)$ are the AC field harmonics with $C_n(t) \propto I(t) = I_0 \cos(\omega_0 t + \phi_0)$
 κ_n are the rotating coil sensitivity factors (FIXED)
 $\theta(t)$ is the coil angular position (KNOWN)
 R_{ref} is the reference radius (FIXED, 17mm for LHC)

Flux in term of DC harmonics

$$\begin{aligned} \Phi(t) &= \text{Re} \left[\sum_{n=1}^{\infty} \frac{\kappa_n}{R_{ref}^{n-1}} C_n e^{in\omega t} \cos(\omega_0 t + \phi_0) \right] \\ &= \text{Re} \left[\sum_{n=1}^{\infty} \frac{\kappa_n}{R_{ref}^{n-1}} \frac{C_n}{2} \underbrace{\left[e^{i[(n\omega+\omega_0)t+\phi_0]} + e^{-i[(n\omega-\omega_0)t+\phi_0]} \right]}_{\text{frequency shifts}} \right] \\ &= \hat{\Phi}(t) \cos(\omega_0 t + \phi_0) \end{aligned}$$

where C_n are the DC field harmonics with $C_n \propto I_0$

- ⇒ The modulated DC flux gets a frequency shift to ω_0 and a phase shift by ϕ_0 .
- ⇒ All phenomena external to the magnet (i.e. earth magnetic field, electrical networks) with frequencies outside of the bandwidth $f_0 \pm nf$ can be easily REMOVED from the AC flux with a pass-band filter. In fact, the demodulation process will automatically remove them !

Recovering the DC field harmonics

(isochronous amplitude demodulation)

☞ We modulate (again) the flux $\Phi(t)$ with a sinusoid and with a cosinusoid, both with the same frequency as the AC source:

$$\begin{aligned}\Phi_0(t) &= \hat{\Phi}(t) \cos(\omega_0 t + \phi_0) \sin(\omega_0 t) \\ &= \frac{1}{2} \hat{\Phi}(t) [\sin(2\omega_0 t + \phi_0) - \sin(\phi_0)] \\ \Phi_1(t) &= \hat{\Phi}(t) \cos(\omega_0 t + \phi_0) \cos(\omega_0 t) \\ &= \frac{1}{2} \hat{\Phi}(t) [\cos(2\omega_0 t + \phi_0) + \cos(\phi_0)]\end{aligned}$$

☞ We apply a low-pass filter to these signals with $B_h < f_c < 2f_0 - B_h$ where B_h is the bandwidth of the magnet harmonics we want to study. Then we get:

$$\hat{\Phi}_0(t) = -\frac{1}{2} \hat{\Phi}(t) \sin(\phi_0) \quad ; \quad \hat{\Phi}_1(t) = \frac{1}{2} \hat{\Phi}(t) \cos(\phi_0)$$

☞ Therefore, we can recover the phase of the AC source:

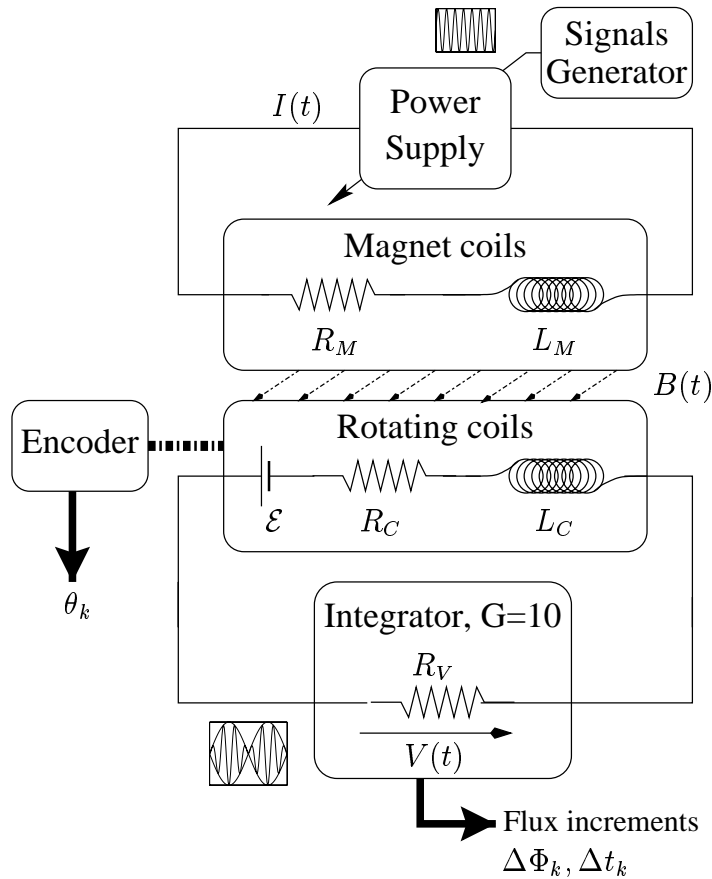
$$\phi_0(t) = \arctan \left(-\frac{\hat{\Phi}_0(t)}{\hat{\Phi}_1(t)} \right)$$

☞ And rebuild the DC field components

$$\hat{\Phi}(t) = 2 \operatorname{sign}(\phi_0(t)) \sqrt{\hat{\Phi}_0(t)^2 + \hat{\Phi}_1(t)^2}$$

☞ We can now go on with the standard way of computing the magnet field harmonics !

Experiment



Parameters

☞ AC stability:

- $I_0 = 1.4\text{A}$ ($\epsilon < 10^{-2}\text{A}$, GOOD)
- $f_0 \in (40, 250)\text{Hz}$ ($\epsilon \gg 10^{-2}\text{Hz}$, BAD)

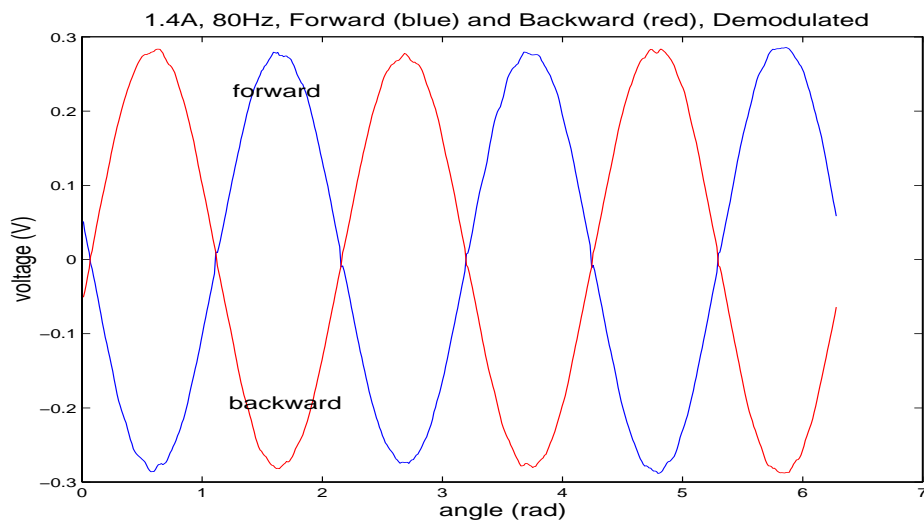
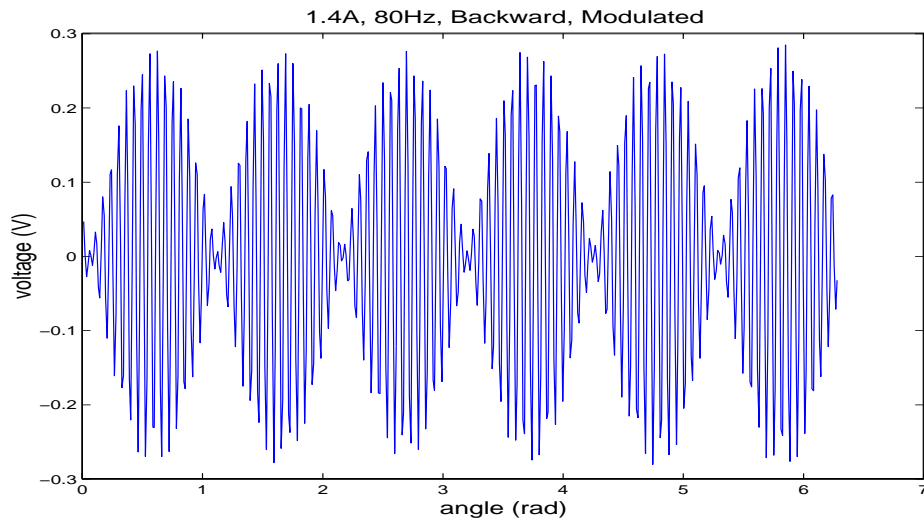
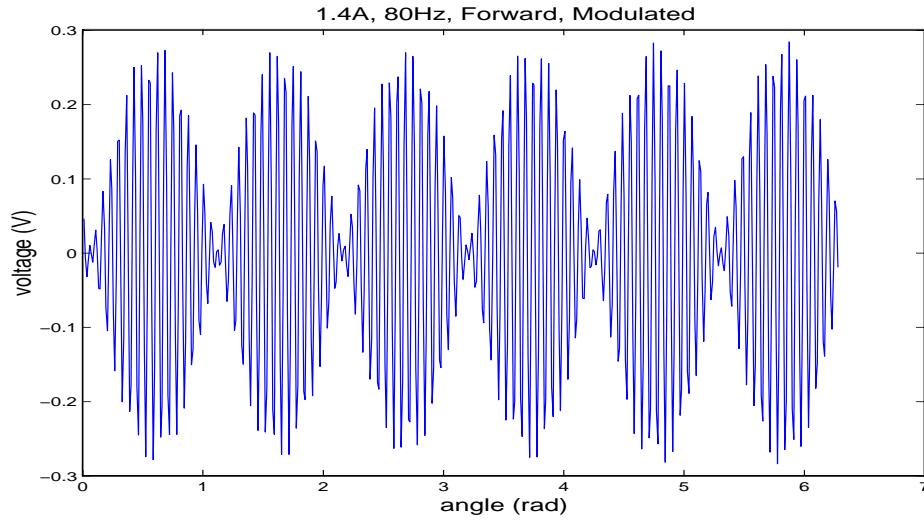
☞ Coil rotation stability:

- $\omega \approx 5.25\text{rad/s}$ ($\epsilon < 0.1\%$ for 1m shaft, $\epsilon < 3\%$ for 15m shaft)
- $\phi = 0$ (trigger)

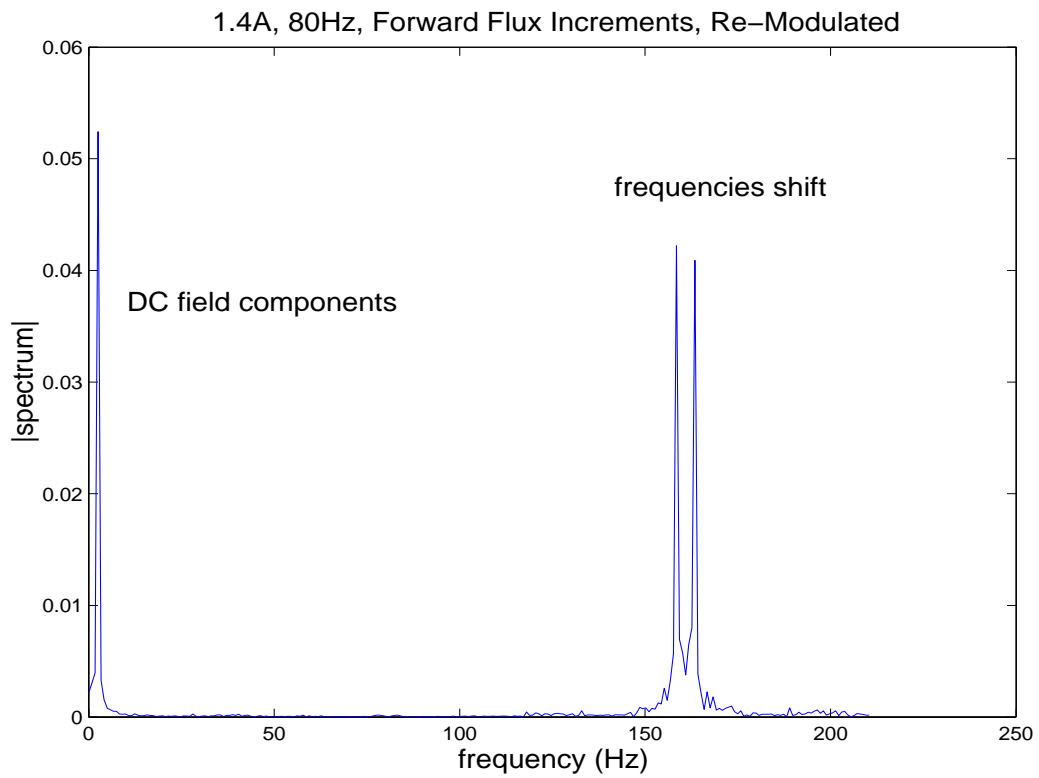
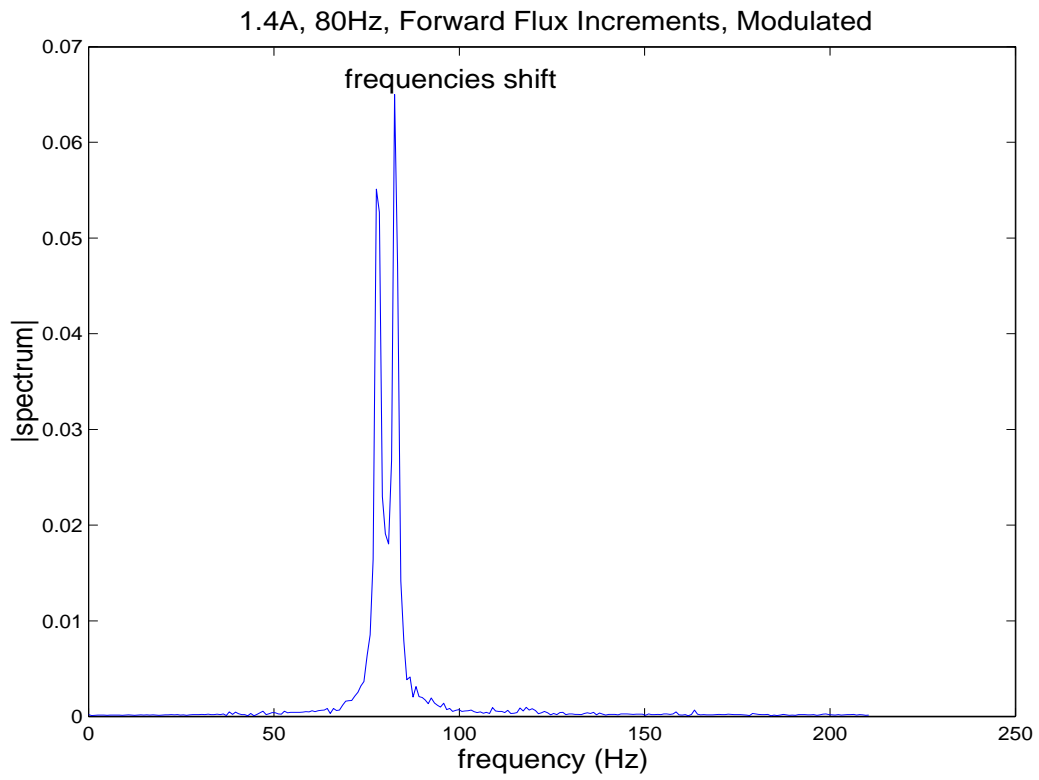
☞ Acquisition:

- Sampling rate $\approx 426\text{Hz}$ (512 points/turn, TO BE IMPROVED)
- Sampling accuracy $\approx 10^{-2}\text{V}$ for range 0 – 10V (GOOD ENOUGH)
- In tegrator output $\Delta\Phi_k = \underbrace{-\Delta t_k}_{\propto f} \underbrace{V_k}_{\propto f_0}$ makes $\Phi_k \propto f_0$!

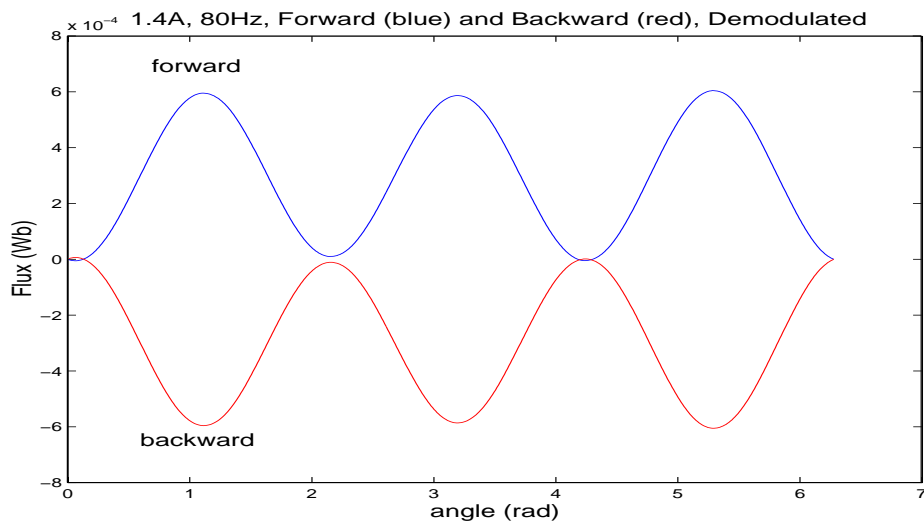
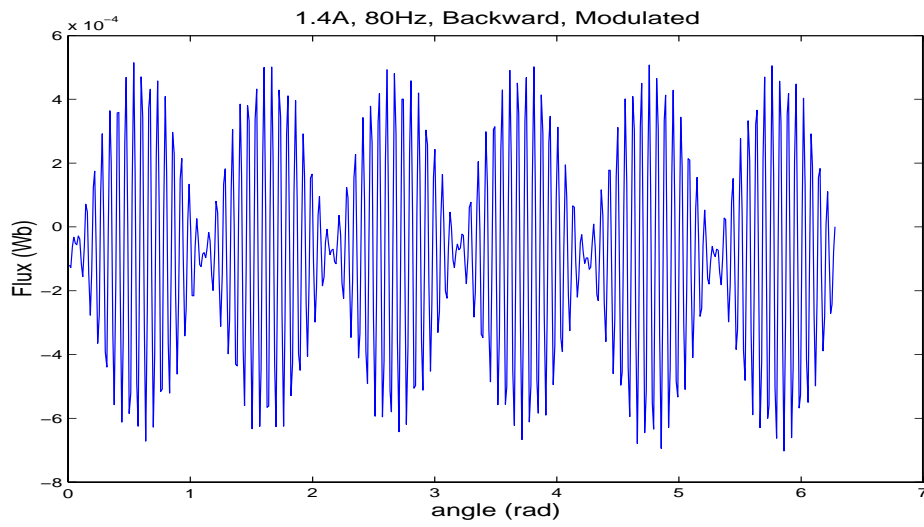
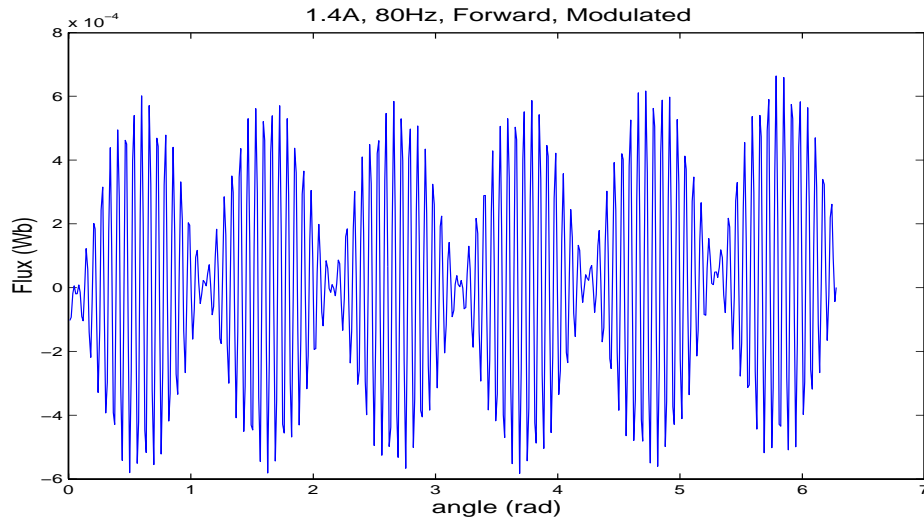
Voltage, 80Hz, 1.4A



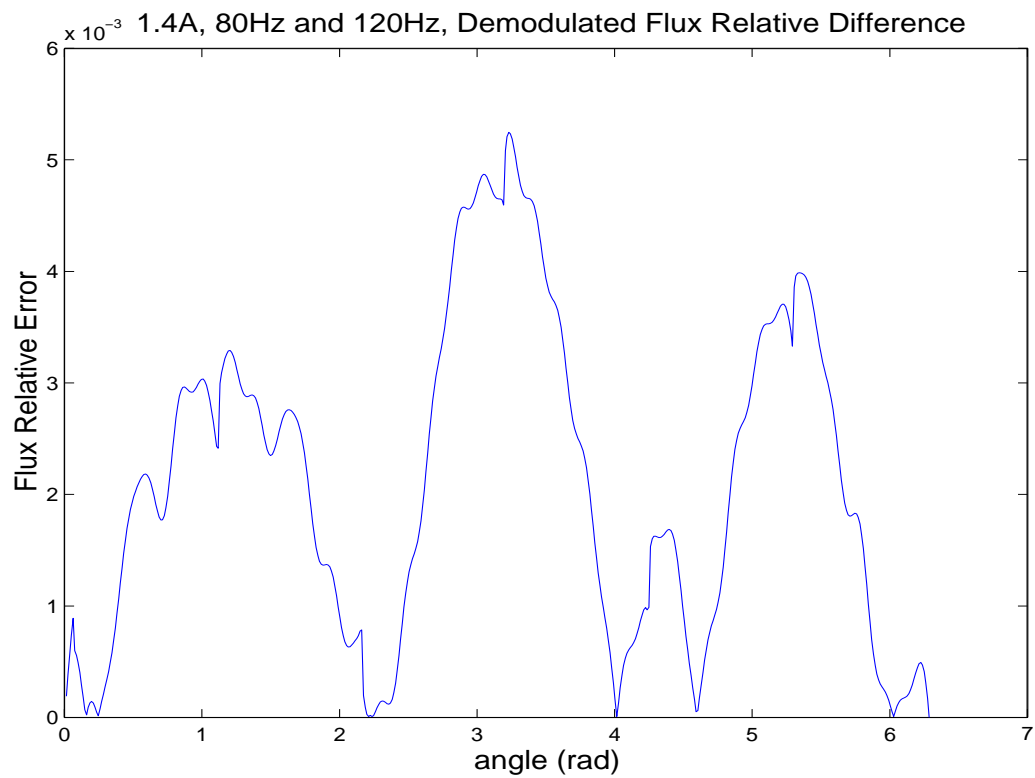
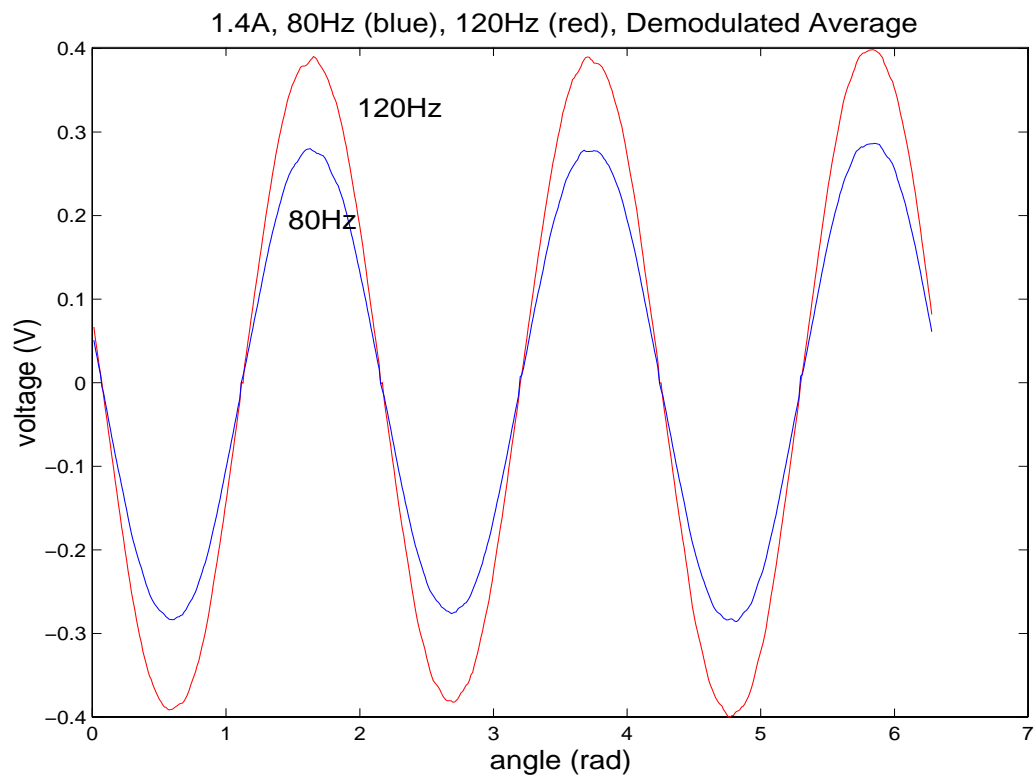
Spectrum, 80Hz, 1.4A



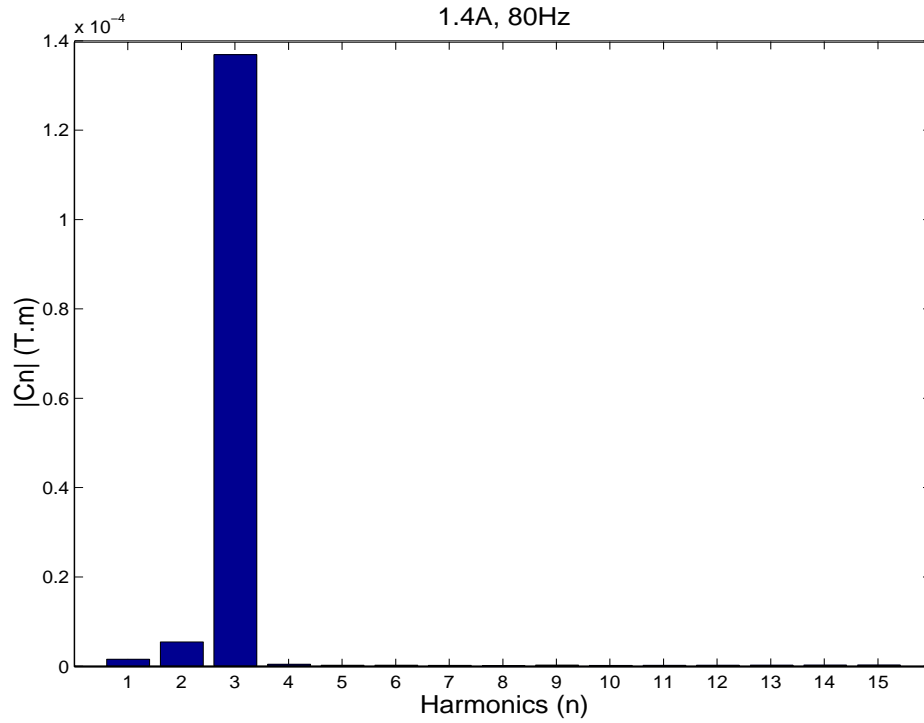
Flux, 80Hz, 1.4A



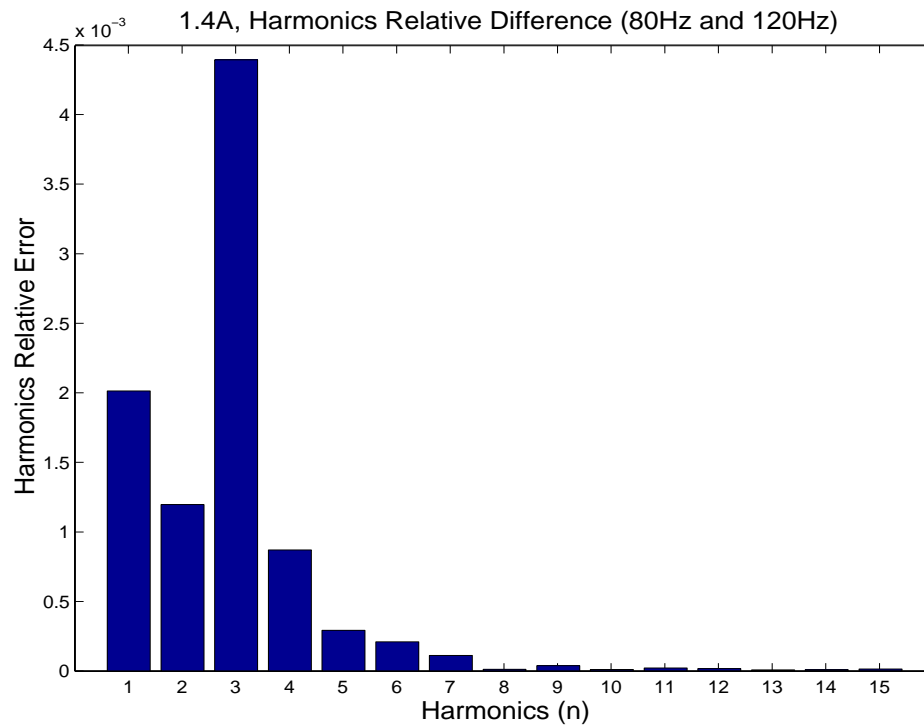
Voltage and Flux, 80Hz and 120Hz, 1.4A



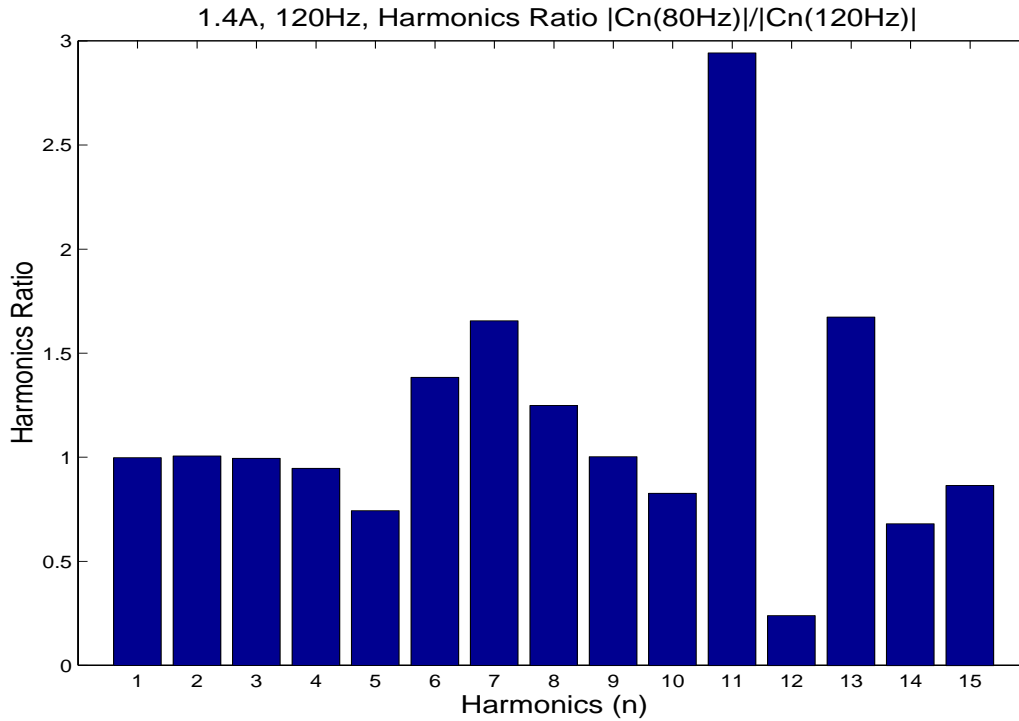
Harmonics, 80Hz, 1.4A



Frequency Invariance 80Hz and 120Hz, 1.4A



Harmonics Relative Errors 80Hz and 120Hz, 1.4A



Harmonics Relative Errors 80Hz and 120Hz, 1.4A

n	$\frac{ C_n _{80\text{Hz}}}{ C_n _{120\text{Hz}}}$
1	0.9978
2	1.0070
3	0.9956
4	0.9477
5	0.7435
6	1.3845
7	1.6568
8	1.2493
9	1.0039
10	0.8282
11	2.9433
12	0.2406
13	1.6749
14	0.6818
15	0.8653

Conclusions

- ☞ Need a HIGHER AC FREQUENCY in order to get a better modulation (nicer envelope).
- ☞ Need a BETTER SAMPLING RATE. We plan to use in parallel of the actual system, another fast acquisition system with a sampling rate of 10KHz.
- ☞ Bad stability in AC frequency is NOT a problem with high sampling rate and high AC frequency ($f_0 \geq 500\text{Hz}$). Otherwise we need a better stability or a better instantaneous knowledge of $f_0(t)$ for good measurement accuracy/reproducibility at low sampling rate.
- ☞ Bad stability of the rotation speed ω is NOT a problem with high sampling rate.
- ☞ For 15m dipole, medium current ($I_0 \approx 1\text{A}$) and high AC frequency ($f_0 \approx 500\text{Hz}$), we have to take care of Eddy currents produced by copper.

OPTIONAL SLIDES

Potential difference

- ☞ The potential difference is defined as the change in electrostatic potential energy per unit charge.

$$\Delta V = \frac{\Delta U}{q}$$

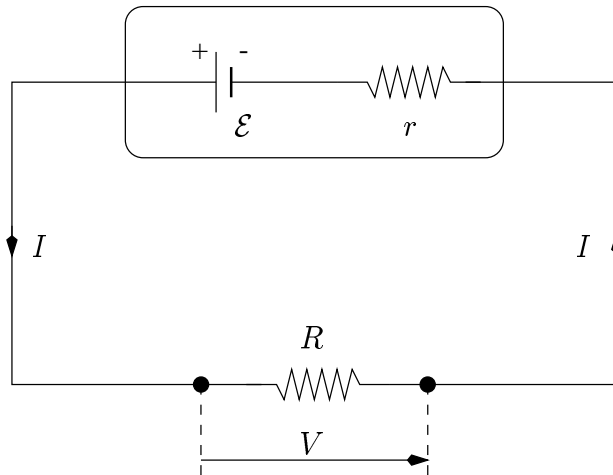
- ☞ A potential energy is associated only with a (conservative) electrostatic field (charges move at constant speed).

- ☞ The SI unit of the potential difference is the volt ($V \equiv J/C$).

Rm: $1 \text{ eV} = 1.602 \times 10^{-19} \text{ J}$

- ☞ Ex: $\mathcal{E} = I(r + R)$ and $V = RI \rightarrow V = \mathcal{E} \frac{R}{r + R}$

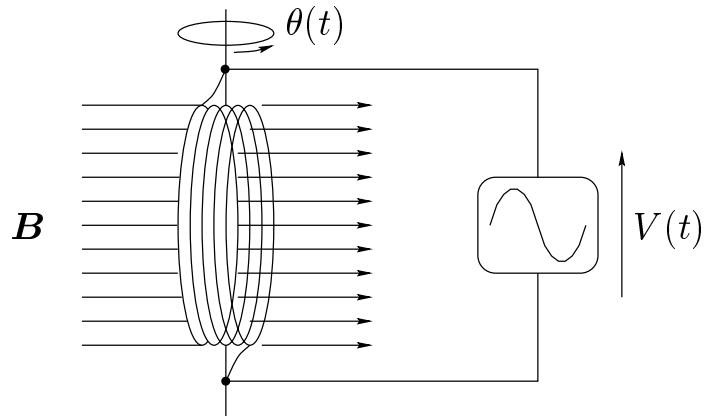
A.N.: $r = 400 \Omega$, $R = 2 \text{ M}\Omega \rightarrow V = (1 - 2 \times 10^{-4}) \mathcal{E}$



$$\Delta V_{A \rightarrow B} = \int_A^B \mathbf{E} \cdot d\mathbf{l}$$

Motion in a steady-state magnetic field

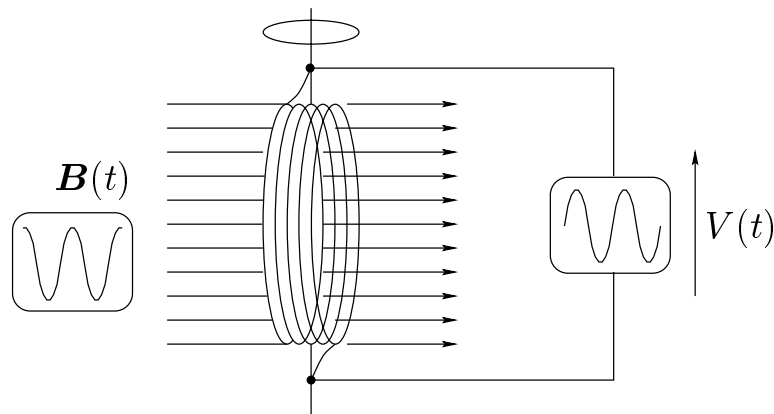
$$\theta(t) = \omega t \quad ; \quad B$$



$$\Phi(t) = SB \cos(\omega t) \quad \text{and} \quad \mathcal{E}(t) = \omega SB \sin(\omega t)$$

Motionless in a time-dependent magnetic field

$$\theta = 0 \quad ; \quad B(t) = B \cos(\omega_0 t + \phi_0)$$



$$\Phi(t) = SB \cos(\omega_0 t + \phi_0) \quad \text{and} \quad \mathcal{E}(t) = \omega_0 SB \sin(\omega_0 t + \phi_0)$$

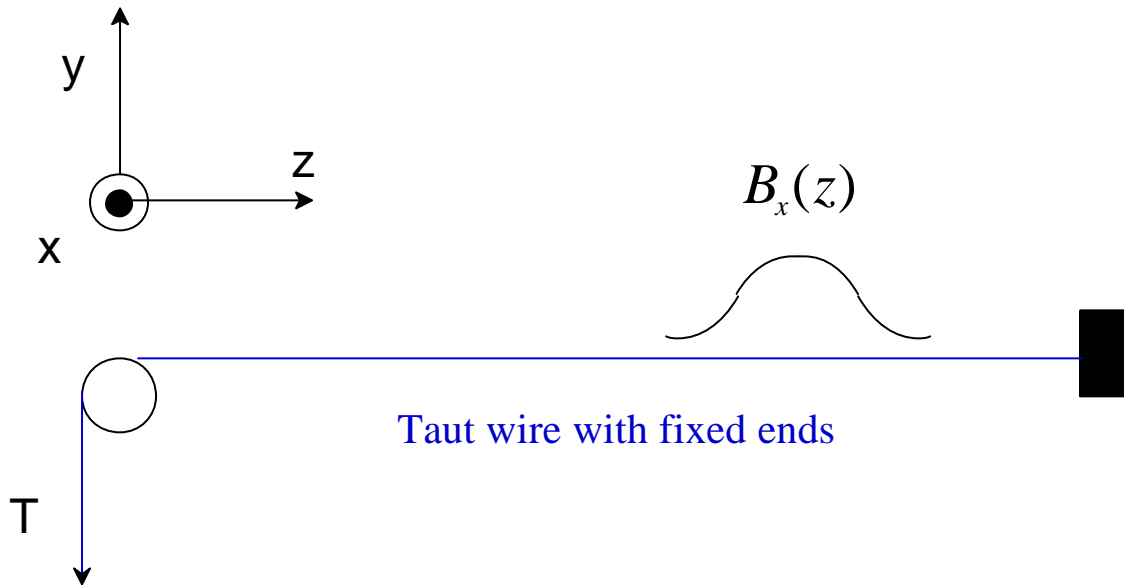
The Magnetic Center Finding using Vibrating Wire Technique

IMMW 1999, BNL
Sept 21 1999

Alexander Temnykh,
LNS, Cornell University

- Method
- Setup and instruments
- Measurements
- Conclusion

Method



$X(z, t), Y(z, t)$ – horizontal, vertical wire position

$B_x(z)$ – horizontal magnetic field

$I(t)$ - current through the wire

T – tension, g – gravity, m - specific weigh

$$X(z = 0, t) = 0; X(z = l, t) = 0$$

$Y(z = 0, t) = 0; Y(z = l, t) = 0$ - wire ends are fixed

$B_x(z = 0) = 0; B_x(z = l) = 0$ - no field at wire ends

$$I(t) = I_0 \cdot \exp(i\omega t)$$

Method

Equation for $Y(z, t)$:

$$m \frac{\partial^2 Y}{\partial t^2} = T \frac{\partial^2 Y}{\partial z^2} - g \frac{\partial Y}{\partial t} - mg + B_x(z)I(t) \quad (1)$$

Let's find solution for $Y(z, t)$ in form :

$$Y(z, t) = Y_s(z) + Y_d(z, t); \text{ static + dynamic/vibration}$$

For static part, $Y_s(z)$, we have :

$$T \frac{\partial^2 Y_s(z)}{\partial z^2} - mg = 0; \text{ with solution } Y_s(z) = \frac{mg}{2T} z(z - l)$$

$B_x(z)$ may be rewritten as :

$$B_x(z) = \sum_0^n B_{x,n} \cdot \sin\left(\frac{pn}{l} z\right), \quad (2)$$

$$\text{where : } B_{x,n} = \frac{n}{l} \int_0^l dz B_x(z) \cdot \sin\left(\frac{pn}{l} z\right)$$

Solution for vibrating part, $Y_d(x, t)$, may be find in form :

$$Y_d(x, t) = \sum_n Y_n \cdot \sin\left(\frac{pn}{l} z\right) \cdot \exp(i\omega t); \quad (3)$$

Y_n - amplitudes of wire vibration modes

Method

Composing (1), (2) and (3) one can write:

$$\sum_{n=1}^{\infty} (\mathbf{w}^2 - \mathbf{w}_n^2 + i\mathbf{g}\mathbf{w}) \cdot Y_n \cdot \sin\left(\frac{n\mathbf{p}}{l}z\right) = \sum_{n=1}^{\infty} \frac{I_0 B_{x,n}}{\mathbf{m}} \cdot \sin\left(\frac{n\mathbf{p}}{l}z\right) \quad (4)$$

where: $\mathbf{w}_n = 2\mathbf{p} \cdot f_n$; $f_n = \frac{n}{2l} \sqrt{\frac{T}{\mu}}$

Note: $Y_s(z) = \frac{\mathbf{m}\mathbf{g}}{2T} z(z-l) = \frac{\mathbf{g}}{8f_1^2} \cdot \frac{z}{l} \left(\frac{z}{l} - 1\right)$;

Maximum wire displacement (sag) will be :

$$Y_s(z = l/2) = \frac{\mathbf{g}}{32f_1^2},$$

where f_1 is the first mode frequency

From (4) we have: $Y_n = \frac{I_0 B_{x,n}}{\mathbf{m}} \cdot \frac{1}{(\mathbf{w}^2 - \mathbf{w}_n^2 + i\mathbf{g}\mathbf{w})}$

If $\mathbf{w} \approx \mathbf{w}_n$, i.e., the frequency of driving current close to the one of wire vibrating modes, then

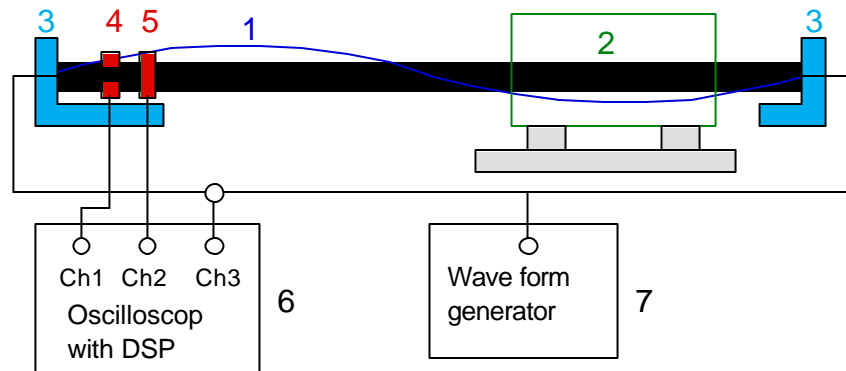
$$Y(z, t) \approx Y_n \sin\left(\frac{\mathbf{p}n}{l}z\right) \cdot \exp(i\mathbf{w}t) = \frac{I_0 B_{x,n}}{\mathbf{m}} \cdot \frac{\sin\left(\frac{\mathbf{p}n}{l}z\right)}{(\mathbf{w}^2 - \mathbf{w}_n^2 + i\mathbf{g}\mathbf{w})} \cdot \exp(i\mathbf{w}t)$$

Let z_0 be the location of wire position sensor,

Φ is the measured parameters,

$$\Phi = \frac{1}{t} \int_0^t Y(z_0, t) \cdot I(t) \cdot dt = \frac{I_0^2 B_{x,n}}{2\mathbf{m}} \cdot \sin\left(\frac{\mathbf{p}n}{l}z_0\right) \cdot \frac{\mathbf{w} - \mathbf{w}_n}{4\mathbf{w}(\mathbf{w} - \mathbf{w}_n) + \mathbf{w}\mathbf{g}^2}$$

Setup and Instruments



1 - 0.100 mm diameter copper-beryllium wire,
2.5m length

2 - SC quadrupole magnet prototype

0.65m length. 1A of maximum current and
0.04 T/m maximum gradient at room
temperature

3 - horizontal / vertical movable stages

4,5 - horizontal / vertical wire position sensors,

6 - Oscilloscope TDS 430

7 - Wave form generator

Setup and Instruments

In measurement $n = 2$ vibration mode has been used.

$$\Phi = \frac{1}{t} \int_0^t Y(z_0, t) \cdot I(t) \cdot dt = \frac{I_0^2 B_{x,2}}{2m} \cdot \sin\left(\frac{2p}{l} z_0\right) \cdot \frac{1}{4wdw};$$

$dw = (w - w_n)$; $|dw| \gg g$ assumed.

$$B_{x,2} = \frac{n}{l} \int_0^l dz \left(B^{bg}_x \cdot \sin\left(\frac{2p}{l} z\right) + B^{mg}_x(z) \cdot \sin\left(\frac{2p}{l} z\right) \right) \approx$$

$$\approx \frac{n}{l} \int_0^l dz B^{mg}_x(z) \cdot \sin\left(\frac{2p}{l} z\right) \approx 2 \frac{Gl_m}{l} \cdot dy;$$

G - gradient, l_m - magnet length, dy - vertical center offset.

Finally :

$$\Phi = \frac{I_0^2 l_m}{4ml} \cdot \sin\left(\frac{2p}{l} z_0\right) \cdot \frac{G}{wdw} \cdot dy;$$

To exclude the background complitly, deferential effect, $d\Phi$, between $+G$ and $-G$ was measured.

$$d\Phi = \frac{I_0^2 l_m}{2ml} \cdot \sin\left(\frac{2p}{l} z_0\right) \cdot \frac{|G|}{wdw} \cdot dy;$$

Measurements

The first vibrating mode frequency : $f_1 = 36.6 \text{ Hz}$; \Rightarrow

$$\Rightarrow Y_{\max}(z = l/2) = 0.229 \text{ mm}$$

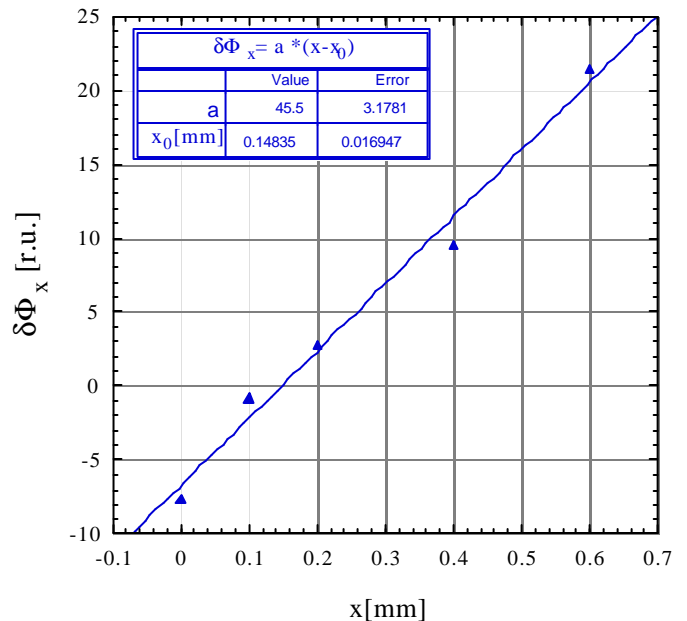
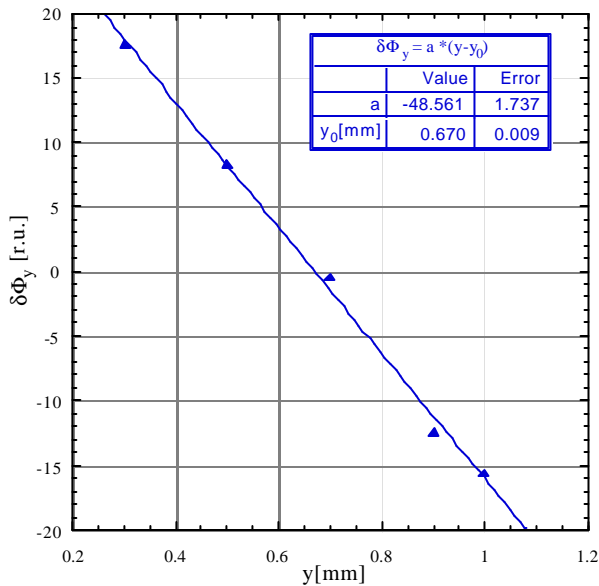
The second mode frequency : $f_2 = 73.1 \pm 0.1 \text{ Hz}$

To reduce noise in measured parameter, $d\Phi$, the driving current frequency was settled to 71.5 Hz , i.e., 1.5 Hz lower than f_2 .

Wire current amplitude $\sim 0.46 \text{ A}$.

Current through the magnet $\pm 1 \text{ A}$, $G = \pm 0.040 \text{ T/m}$.

Differential effect versus wire position in vertical and in horizontal plane.



Magnetic center position :

$$y_0 = 0.148 \pm 0.017 \text{ mm} ; \quad x_0 = 0.670 \pm 0.009 \text{ mm}$$

Conclusion

Sensitivity :

$$\begin{aligned} \Delta Hl &= Gl_m \cdot dx \approx 0.040[T/m] \cdot 0.65m \cdot 0.017mm = \\ &= 4.3 \cdot 10^{-7}[Tm] \text{ or } 0.43 [Gcm]; \end{aligned}$$

Technique may be used for quadrupole alignment with extremely high precision.

References

- A. Temnykh, Vibrating Wire Field-Measuring Technique Preprint CBN 96-7;
<http://www.lns.cornell.edu/public/CBN/1996>
- A. Temnykh, Vibrating wire field-measuring technique. Nuclear Instruments and Methods, A 399 (1997) 185-194.
- A. Temnykh, The Magnetic Center Finding using Vibrating Wire Technique, Preprint CBN 99-22;
<http://www.lns.cornell.edu/public/CBN/1999>

A Mole for warm magnetic and optical measurements of LHC dipoles¹

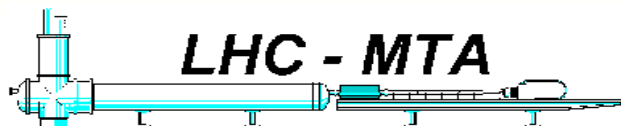
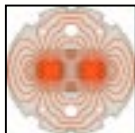
L Bottura¹, M Buzio¹, G Deferne¹, H Jansen², C Glöckner², A Köster²,
P Legrand¹, A Rijllart¹, P Sievers¹, F Villar¹

¹ CERN, European Organization for Nuclear Research - 1211 Geneva 23, Switzerland
² Fraunhofer Institut IPT, Aachen, Germany

Eleventh International Magnet Measurement Workshop
September 21 – 24, 1999
Brookhaven National Laboratory, Upton, New York, USA

Thursday, 23 Sept. 1999
Berkner B
10:50-11:20

¹Also published in the proceedings of the 16th International Conference on Magnet Technology, Ponte Vedra Beach, IL, 26 Sept– 2 Oct 1999



LHC - MTA

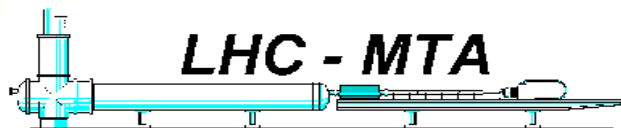
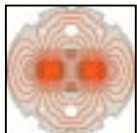
A mole for warm magnetic and optical measurements of LHC dipoles
IMMW XI, Brookhaven National Laboratory, 21–24 Sept. 1999
marco.buzio@cern.ch



A Mole for Warm Magnetic and Optical Measurements of LHC Dipoles

- ◆ Introduction
- ◆ Mechanical layout
- ◆ *VR Demo¹*
- ◆ Magnetic performance
- ◆ Optical performance
- ◆ Conclusions

¹ <http://home.cern.ch/m/mtauser/www/applications/mole/virtualmole.wrl>



LHC - MTA

A mole for warm magnetic and optical measurements of LHC dipoles
IMMW XI, Brookhaven National Laboratory, 21–24 Sept. 1999
marco.buzio@cern.ch



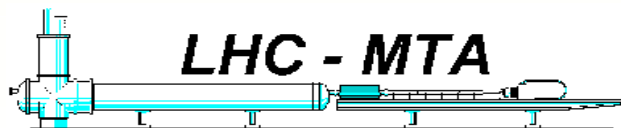
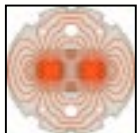
Introduction

◆ Why use a mole ?

- Purpose: measure magnetic axis
- Cold measurements done for max. efficiency with 15 m long coil shaft, obstructing line-of-sight to the coil center \Rightarrow **travelling probe is needed**
- Additional duties: warm field quality of all dipoles, cold field of samples

◆ Requirements for series measurements

- Coil center position: precision better than **0.1 mm**
- Warm measurements: \varnothing 50 mm, $B \leq 25\text{mT}$
- Rugged, quick and simple to setup and operate
- As many off-the-shelf components as possible

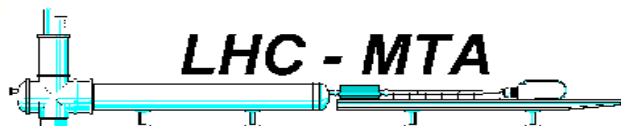
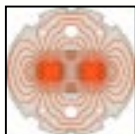
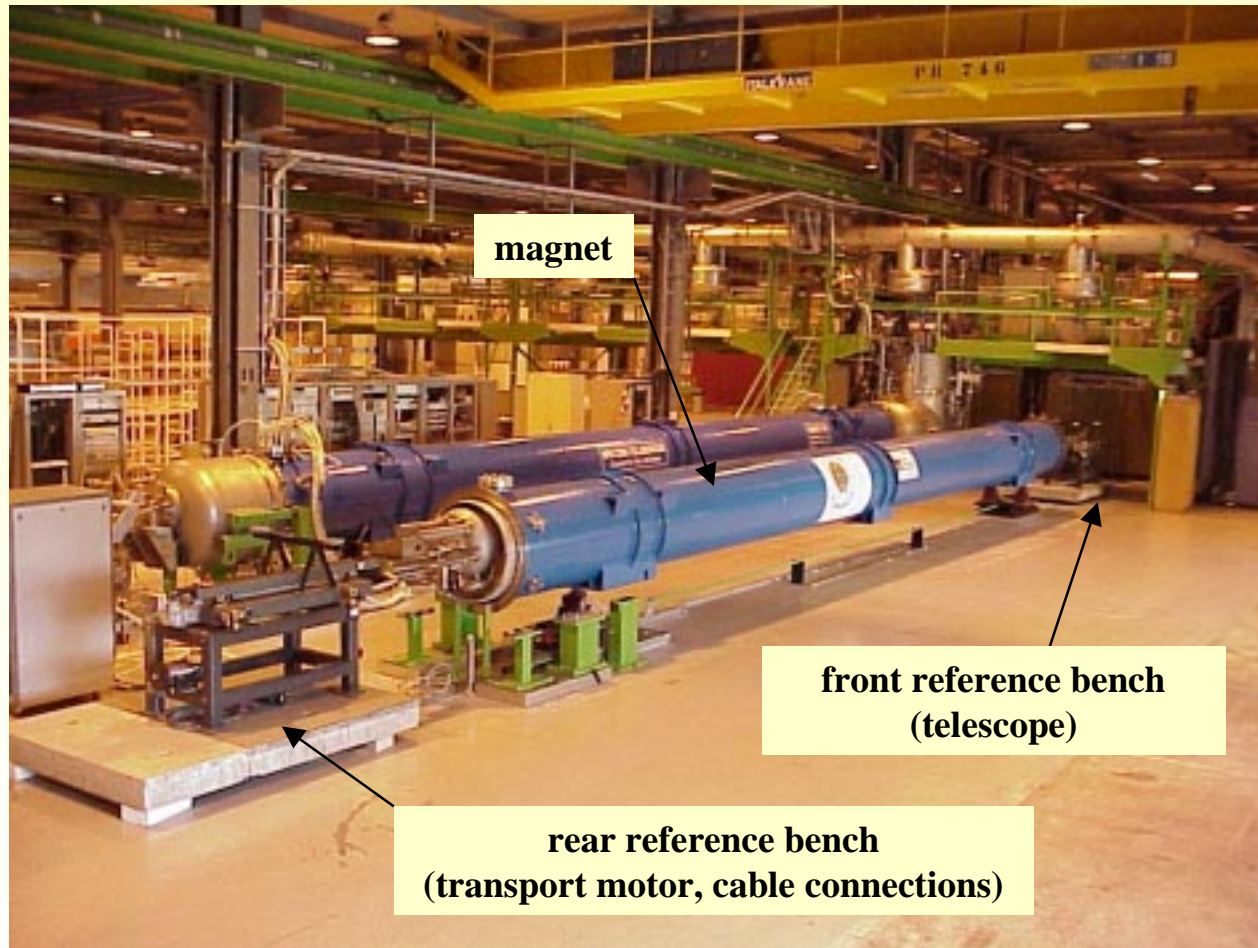


LHC - MTA

A mole for warm magnetic and optical measurements of LHC dipoles
IMMW XI, Brookhaven National Laboratory, 21–24 Sept. 1999
marco.buzio@cern.ch



Mole test bench overview

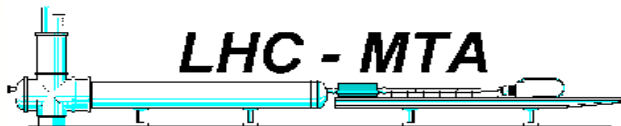
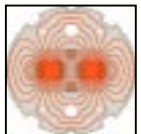
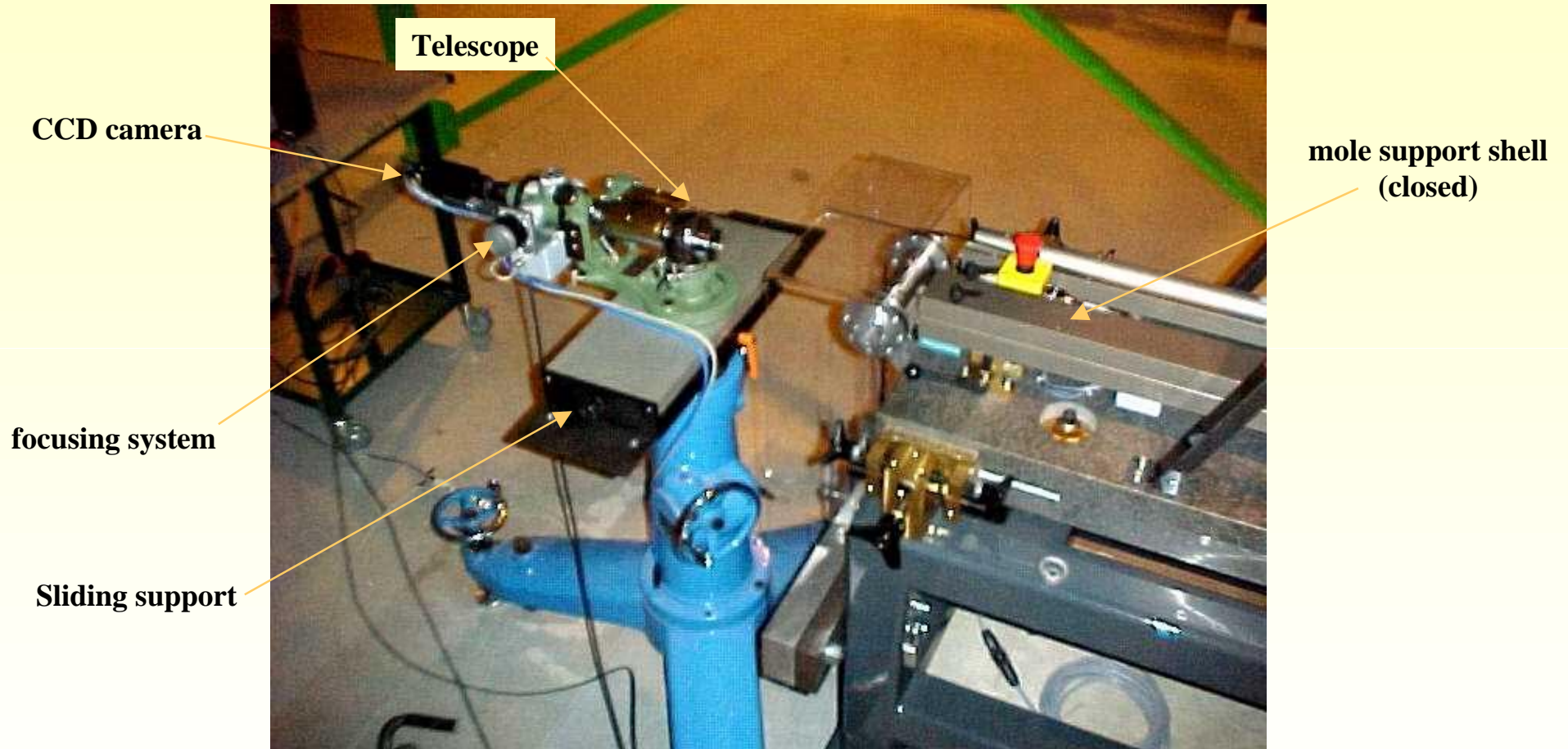


LHC - MTA

A mole for warm magnetic and optical measurements of LHC dipoles
IMMW XI, Brookhaven National Laboratory, 21-24 Sept. 1999
marco.buzio@cern.ch



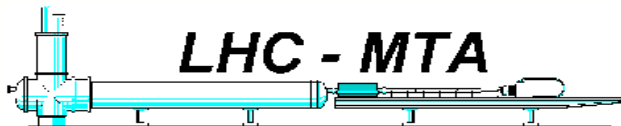
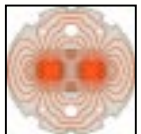
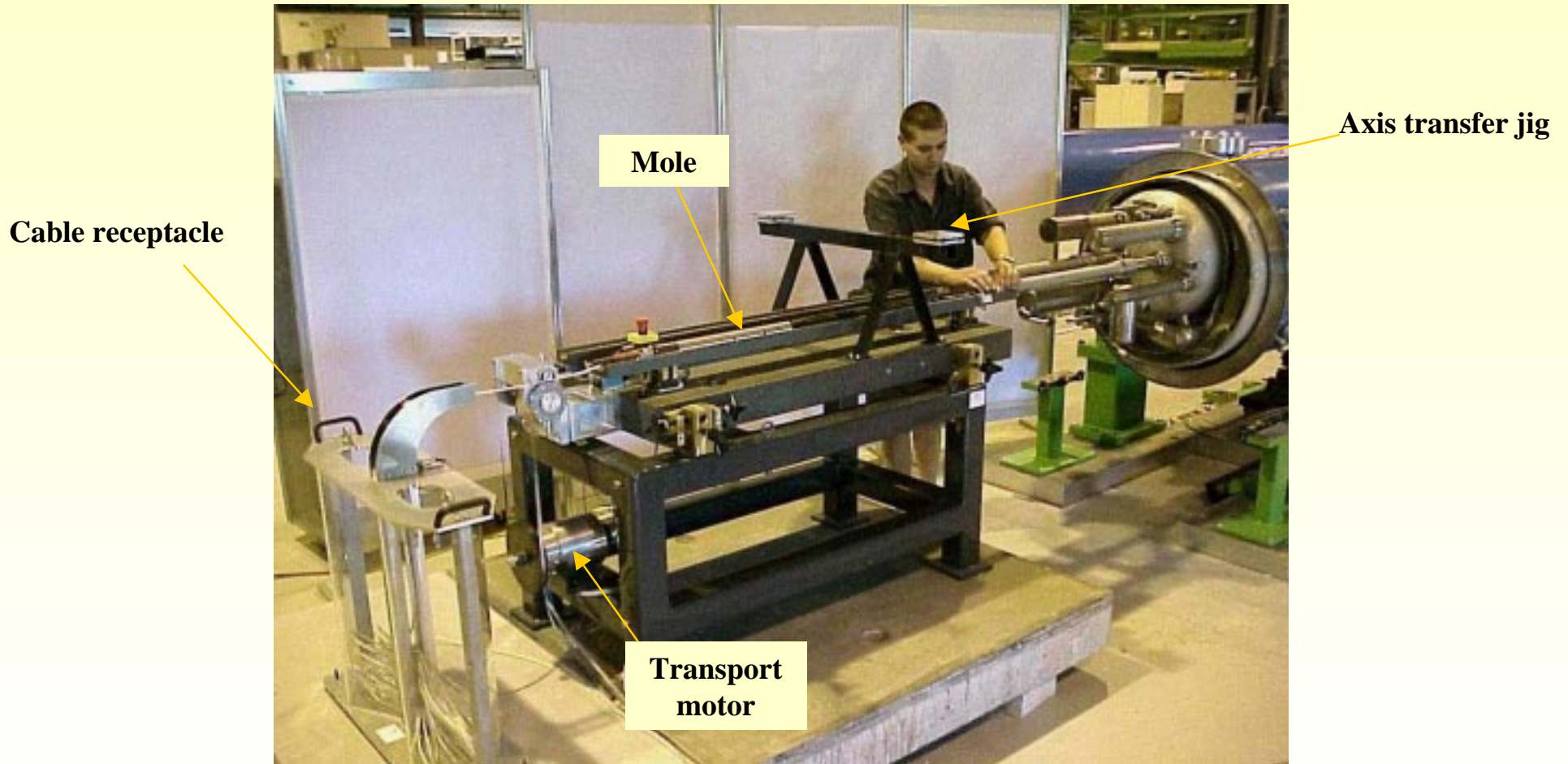
Front reference bench



A mole for warm magnetic and optical measurements of LHC dipoles
IMMW XI, Brookhaven National Laboratory, 21-24 Sept. 1999
marco.buzio@cern.ch



Rear reference bench

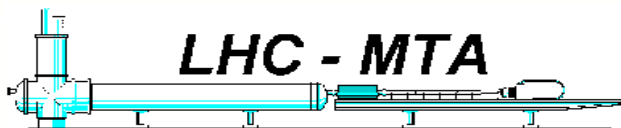
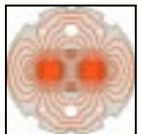
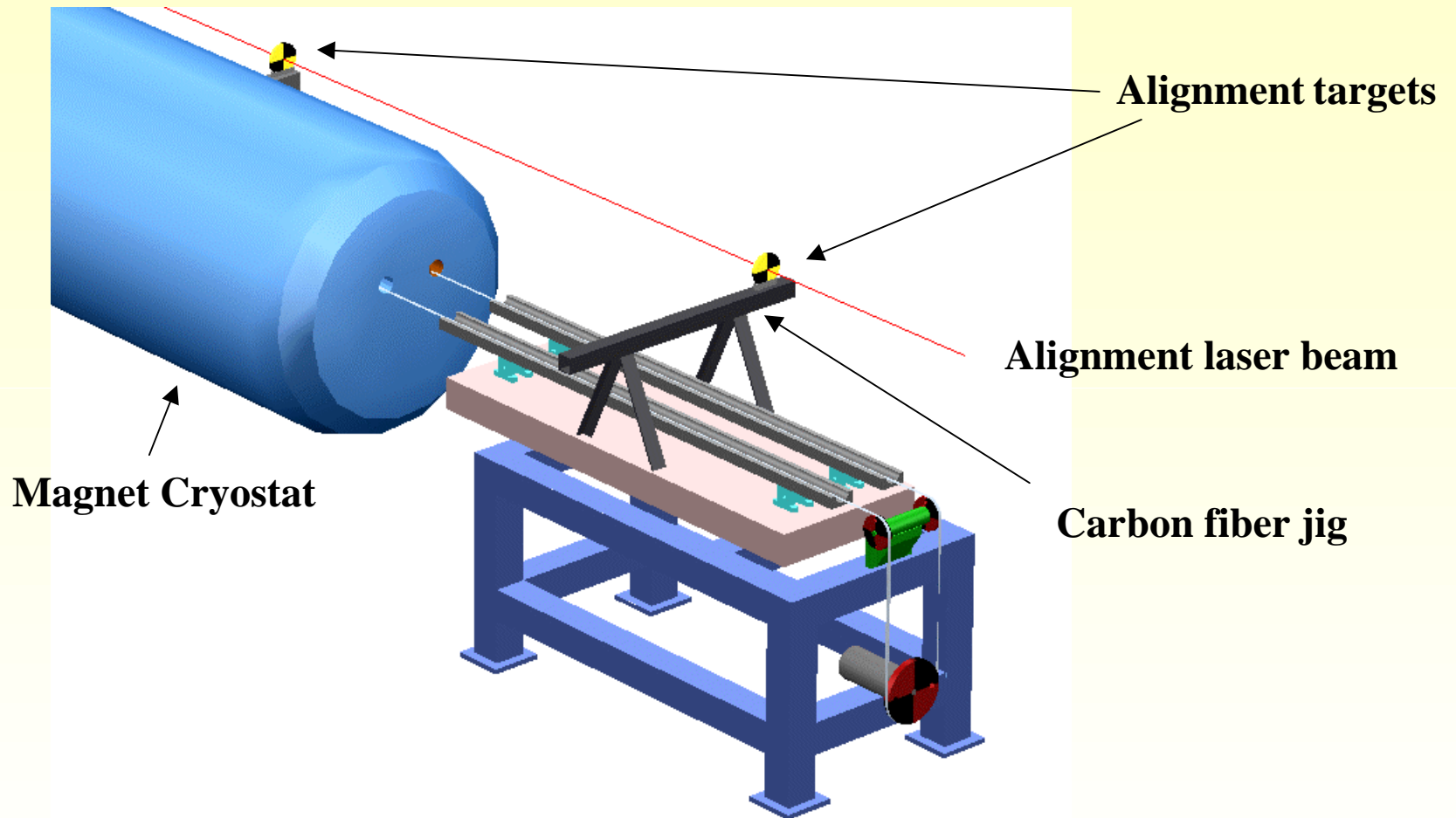


LHC - MTA

A mole for warm magnetic and optical measurements of LHC dipoles
IMMW XI, Brookhaven National Laboratory, 21-24 Sept. 1999
marco.buzio@cern.ch



Reference Table

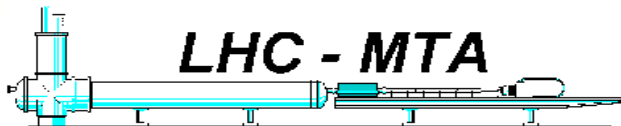
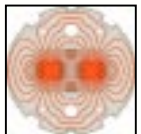
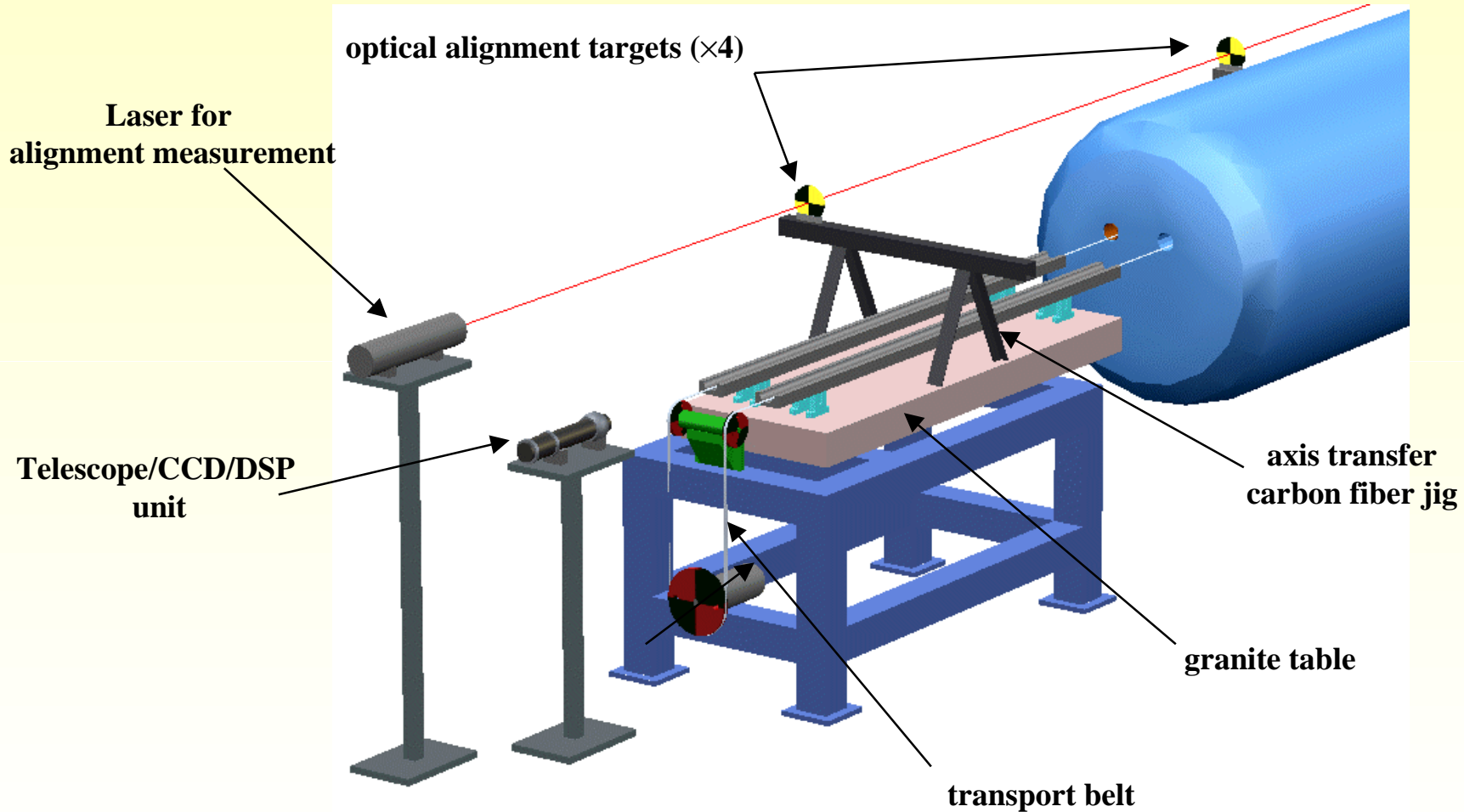


LHC - MTA

A mole for warm magnetic and optical measurements of LHC dipoles
IMMW XI, Brookhaven National Laboratory, 21-24 Sept. 1999
marco.buzio@cern.ch



Front reference bench



LHC - MTA

A mole for warm magnetic and optical measurements of LHC dipoles
IMMW XI, Brookhaven National Laboratory, 21-24 Sept. 1999
marco.buzio@cern.ch



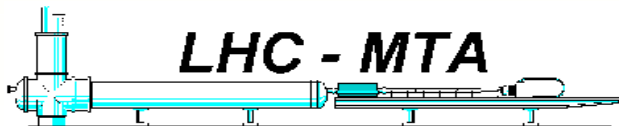
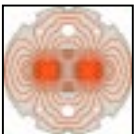
Status

◆ Warm Mole

- First unit accepted and under commissioning
- Two more units to come, will perform warm test of all LHC dipoles
- Can be readily adapted to warm quadrupole tests

◆ Cold Mole

- Order started, last design details now being finalized
- Will perform cold tests for a sample populations of LHC dipoles to get warm-cold axis correlation
- Further units may be slightly modified for cold quadrupole tests



LHC - MTA

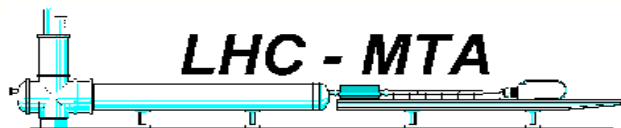
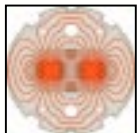
A mole for warm magnetic and optical measurements of LHC dipoles
IMMW XI, Brookhaven National Laboratory, 21-24 Sept. 1999
marco.buzio@cern.ch



Mechanical layout

◆ Main features

- three 750 mm long radial coils
- coil drive: Shinsei travelling-wave ultrasonic piezo motor
- 4096 CPR Heidenhein angular encoder
- On-board feedback auto-leveling system
- Spring-loaded roller system
- Motorized traction belt drive
- Two granite benches to establish reference positions
- LED+lens system to create virtual light-spot in the coil centre
- Telescope + CCD camera + DSP to measure light-spot position
- All functions remotely controlled via RS232
- Auxiliary optical system to transfer axis to magnet fiducials

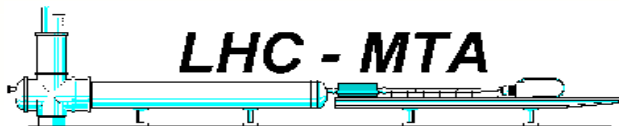
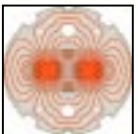
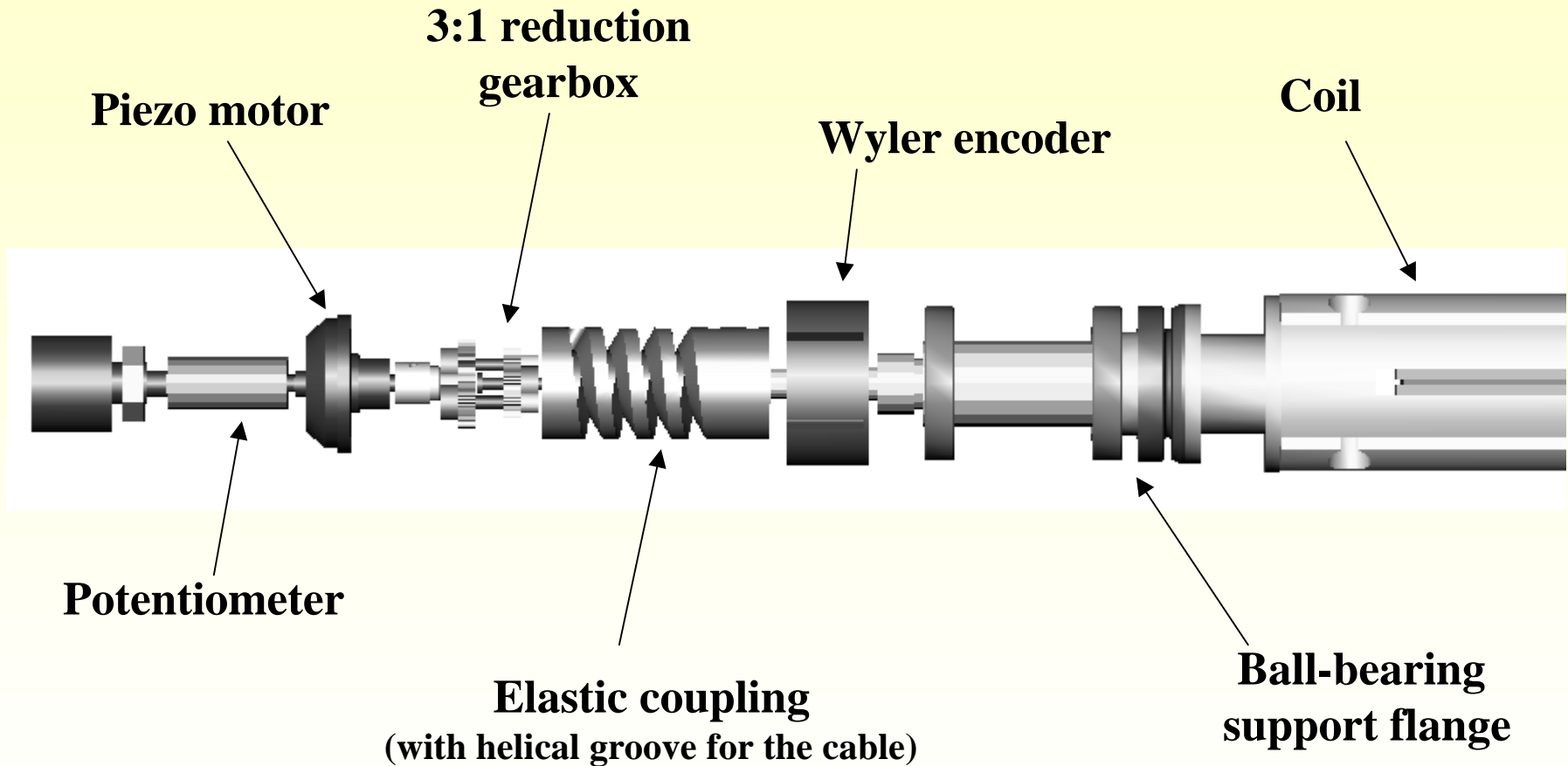


LHC - MTA

A mole for warm magnetic and optical measurements of LHC dipoles
IMMW XI, Brookhaven National Laboratory, 21-24 Sept. 1999
marco.buzio@cern.ch



Main components



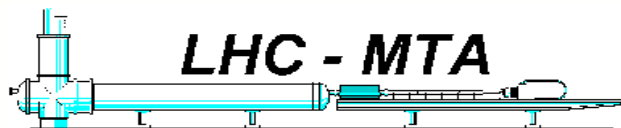
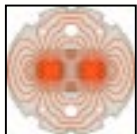
LHC - MTA

A mole for warm magnetic and optical measurements of LHC dipoles
IMMW XI, Brookhaven National Laboratory, 21-24 Sept. 1999
marco.buzio@cern.ch



Longitudinal transport

- closed-loop pre-tensioned Inconel transport belt
- feedback-controlled DC motor drive
- referencing given by optical barriers at both ends of the magnet (self-calibration at the end of each trip)
- max. velocity about **1 m/s**
- precision of positioning better than **0.5 mm**
- mole must be switched manually between apertures

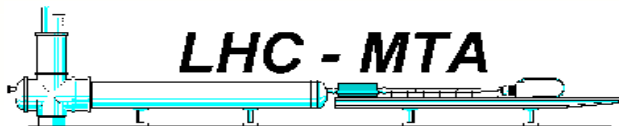
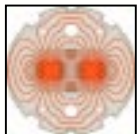
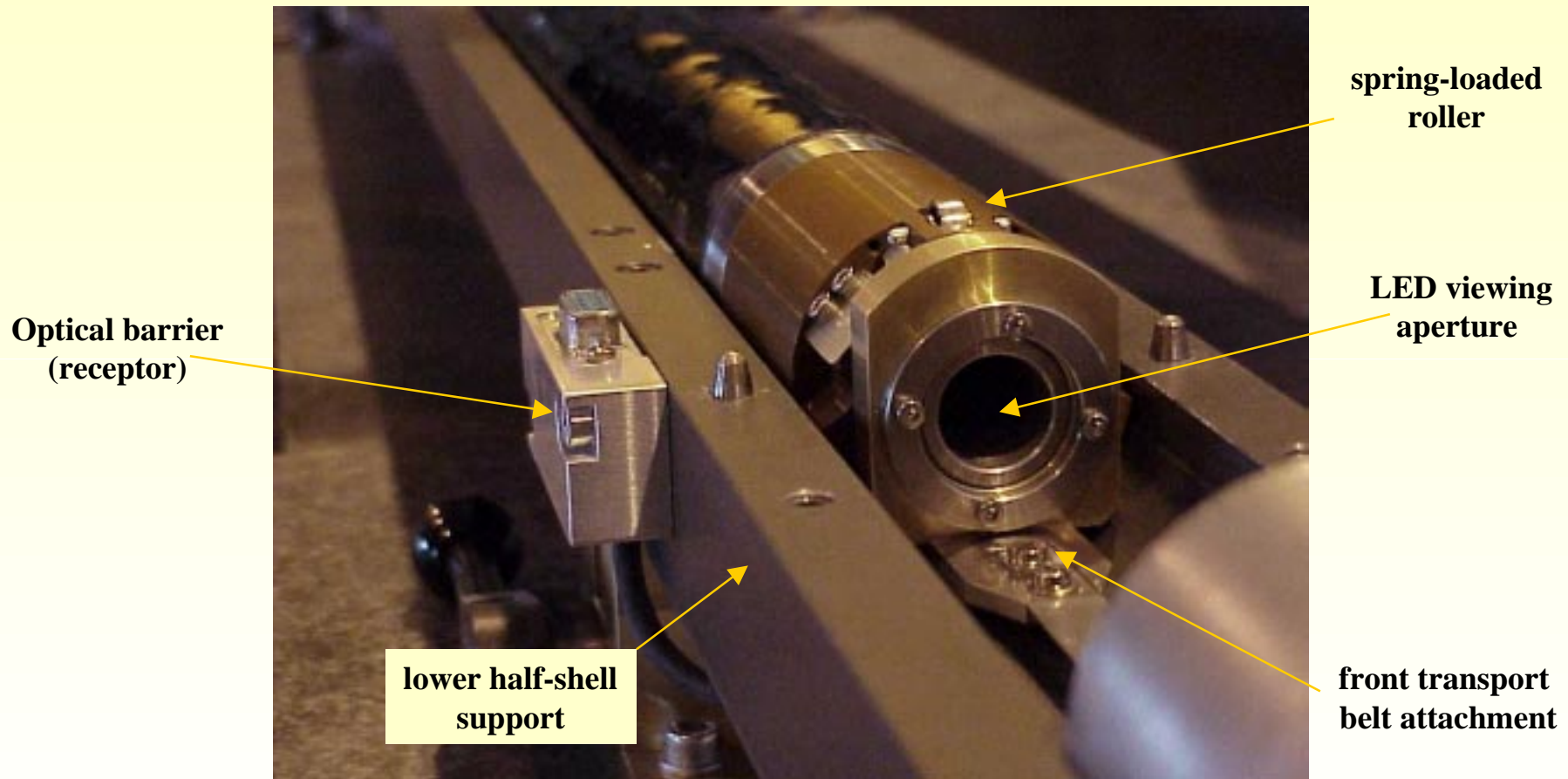


LHC - MTA

A mole for warm magnetic and optical measurements of LHC dipoles
IMMW XI, Brookhaven National Laboratory, 21-24 Sept. 1999
marco.buzio@cern.ch



Longitudinal reference position

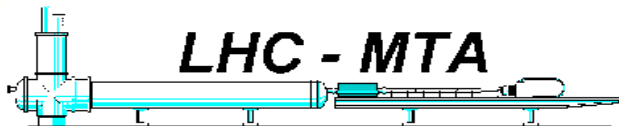
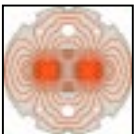


A mole for warm magnetic and optical measurements of LHC dipoles
IMMW XI, Brookhaven National Laboratory, 21-24 Sept. 1999
marco.buzio@cern.ch



Safety

- interlock system: mole will stop if covers are removed, transport cable gets tangled, transport motor drains overcurrent
- reduced velocity close to the edges
- longitudinal position cross-checked with two independent measurements (angular encoder + linear potentiometer)



LHC - MTA

A mole for warm magnetic and optical measurements of LHC dipoles
IMMW XI, Brookhaven National Laboratory, 21-24 Sept. 1999
marco.buzio@cern.ch



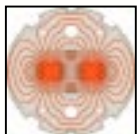
Autoleveling

◆ Why autoleveling ?

- imperfections of beam pipe/rollers \Rightarrow **rotation of container during travel**
- observed rotation up to **$2\sim 3^\circ/\text{m}$**
- transport belt & cable may be twisted
- coil must be level prior to measurement

◆ How does it work ?

- DC motor engaged in container to rotate coil+encoder+piezo motor
- feedback system using wide-range level meter
- precision achieved better than **4 mrad**
- time needed less than **5 s**
- autoleveling done at the end of each longitudinal movement

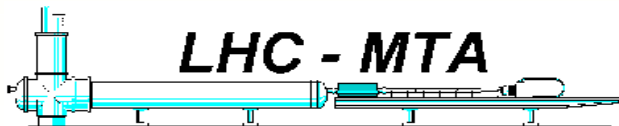
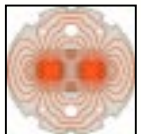
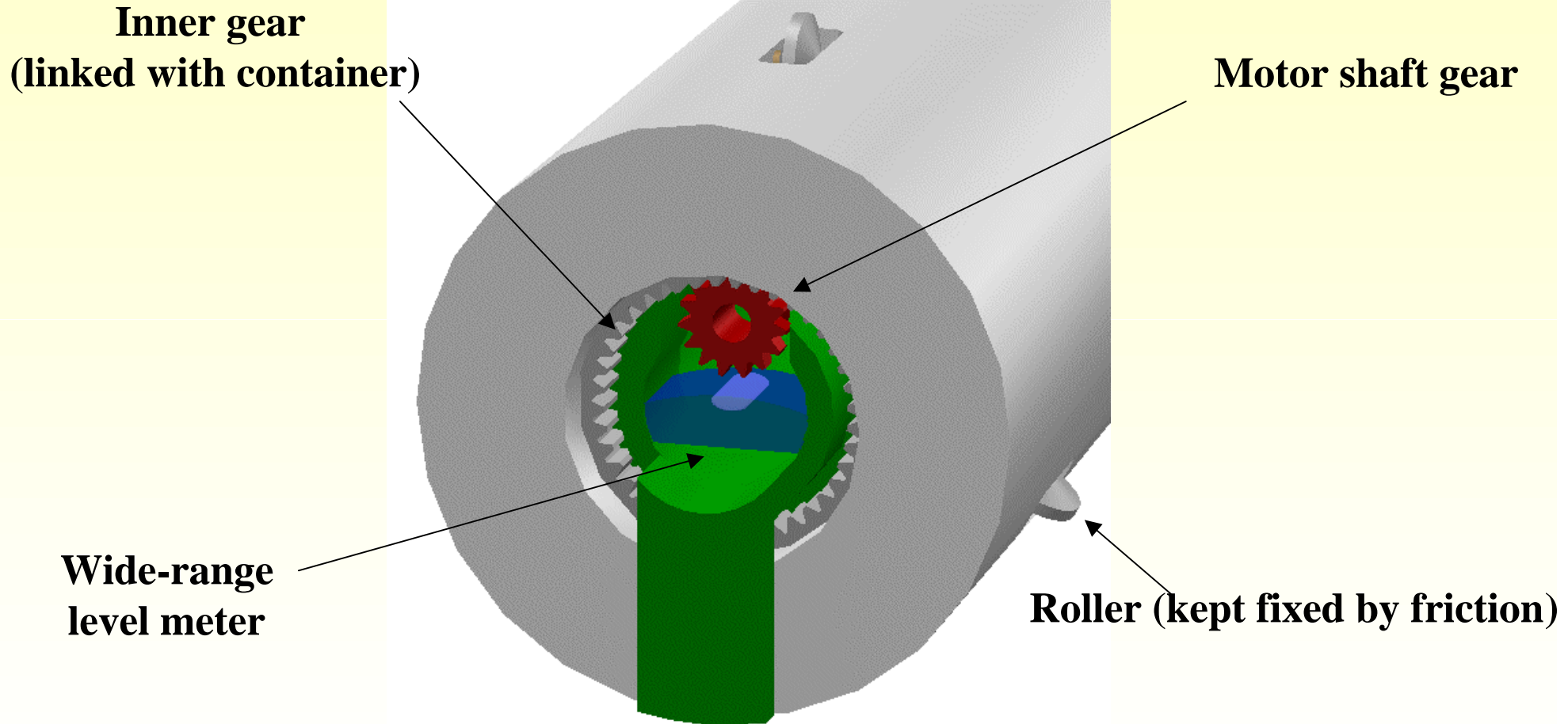


LHC - MTA

A mole for warm magnetic and optical measurements of LHC dipoles
IMMW XI, Brookhaven National Laboratory, 21-24 Sept. 1999
marco.buzio@cern.ch



Auto-leveling mechanism

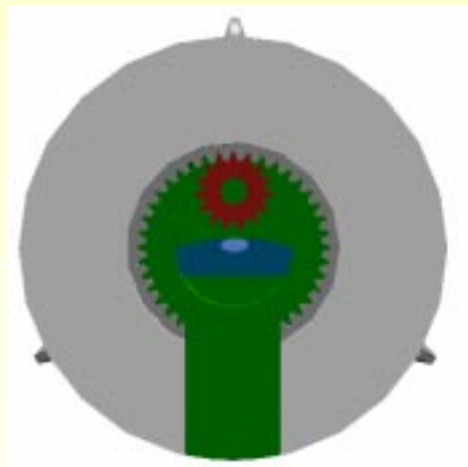


LHC - MTA

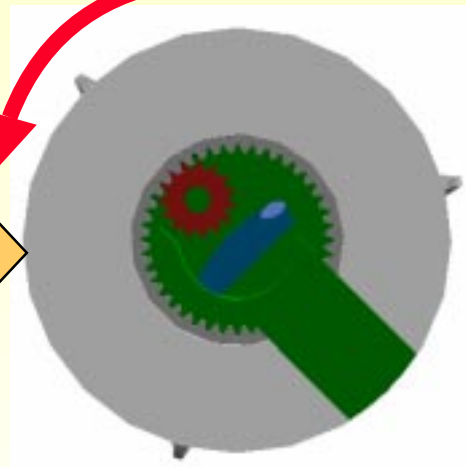
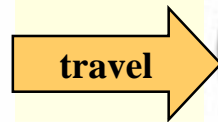
A mole for warm magnetic and optical measurements of LHC dipoles
IMMW XI, Brookhaven National Laboratory, 21-24 Sept. 1999
marco.buzio@cern.ch



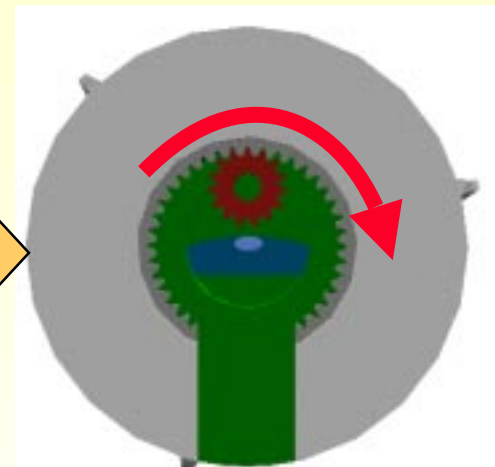
Auto-leveling mechanism



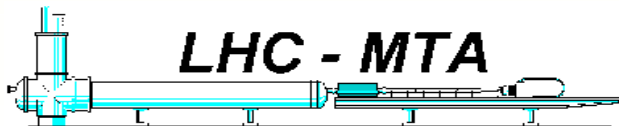
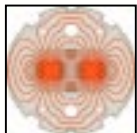
Start



End of travelling



Final configuration



LHC - MTA

A mole for warm magnetic and optical measurements of LHC dipoles
IMMW XI, Brookhaven National Laboratory, 21-24 Sept. 1999
marco.buzio@cern.ch



Optical measurement

◆ Telescope

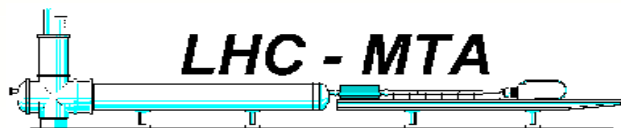
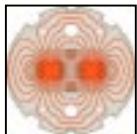
- accurately leveled and aligned wrt magnet
- mounted on rails to serve both apertures

◆ CCD camera

- 752×582 pixel, 6.00×4.96 mm size
- self-aligned to telescope via reference marks

◆ DSP image processor

- threshold filtering + center of gravity calculation
- measurements internally averaged over multiple takes
- software calibration map

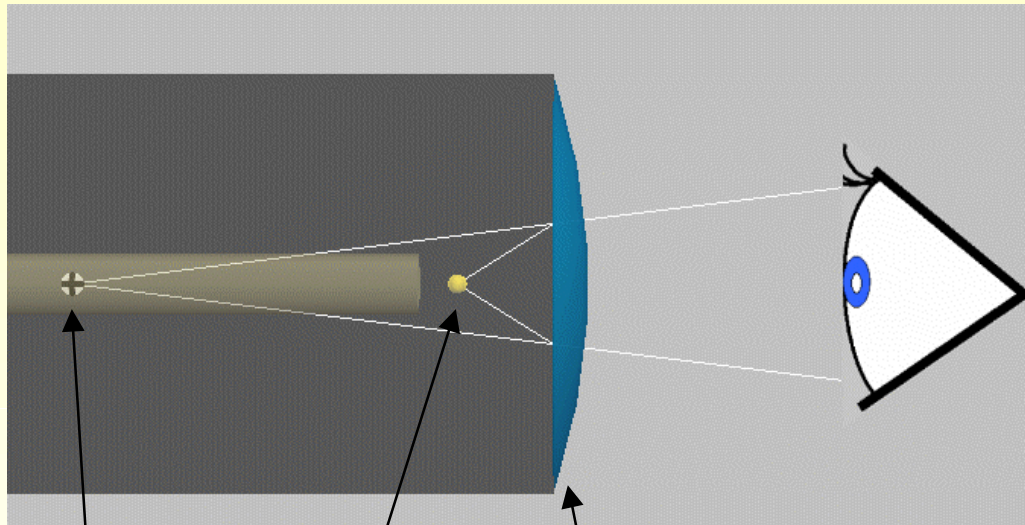


LHC - MTA

A mole for warm magnetic and optical measurements of LHC dipoles
IMMW XI, Brookhaven National Laboratory, 21–24 Sept. 1999
marco.buzio@cern.ch



Virtual lightspot

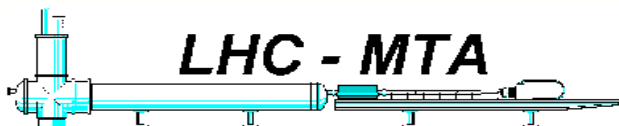
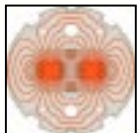
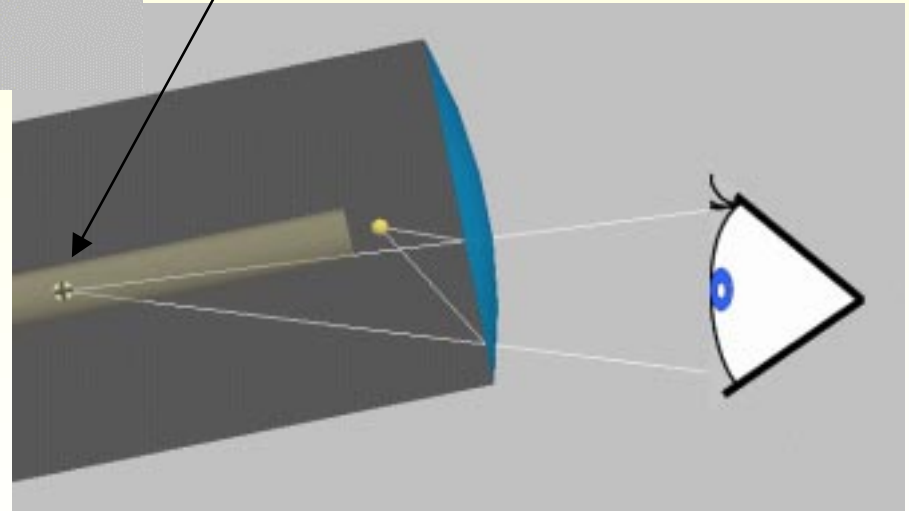


the virtual image remains in the coil center even when the mole rotates

LED

Magnifying lens

Virtual lightspot



LHC - MTA

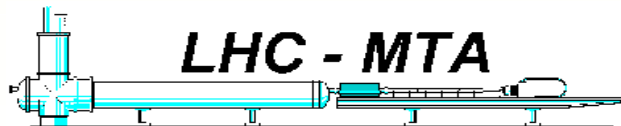
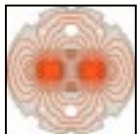
A mole for warm magnetic and optical measurements of LHC dipoles
IMMW XI, Brookhaven National Laboratory, 21-24 Sept. 1999
marco.buzio@cern.ch



Optical measurement

◆ Performance

- 4 mm × 14 mm × 20 m range
- total error ≤ **60** μm
- measurement time ≤ **4** s at closest range



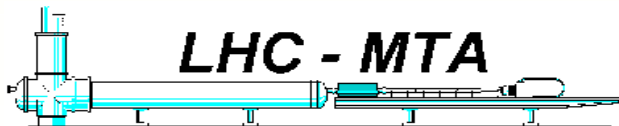
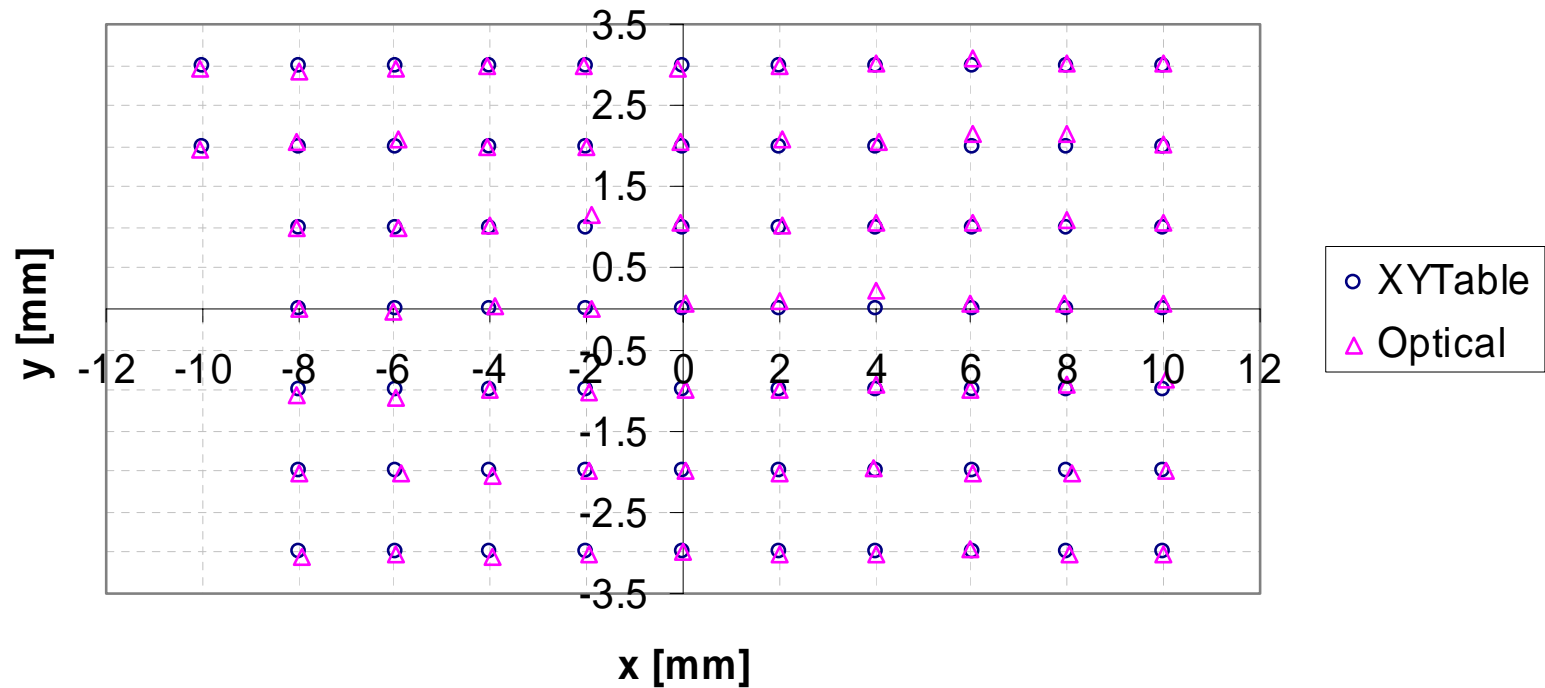
LHC - MTA

A mole for warm magnetic and optical measurements of LHC dipoles
IMMW XI, Brookhaven National Laboratory, 21–24 Sept. 1999
marco.buzio@cern.ch



Optical system calibration

Mole XY calibration check (z=20m)



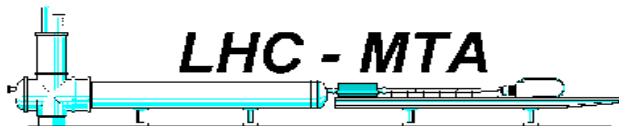
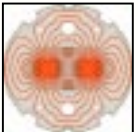
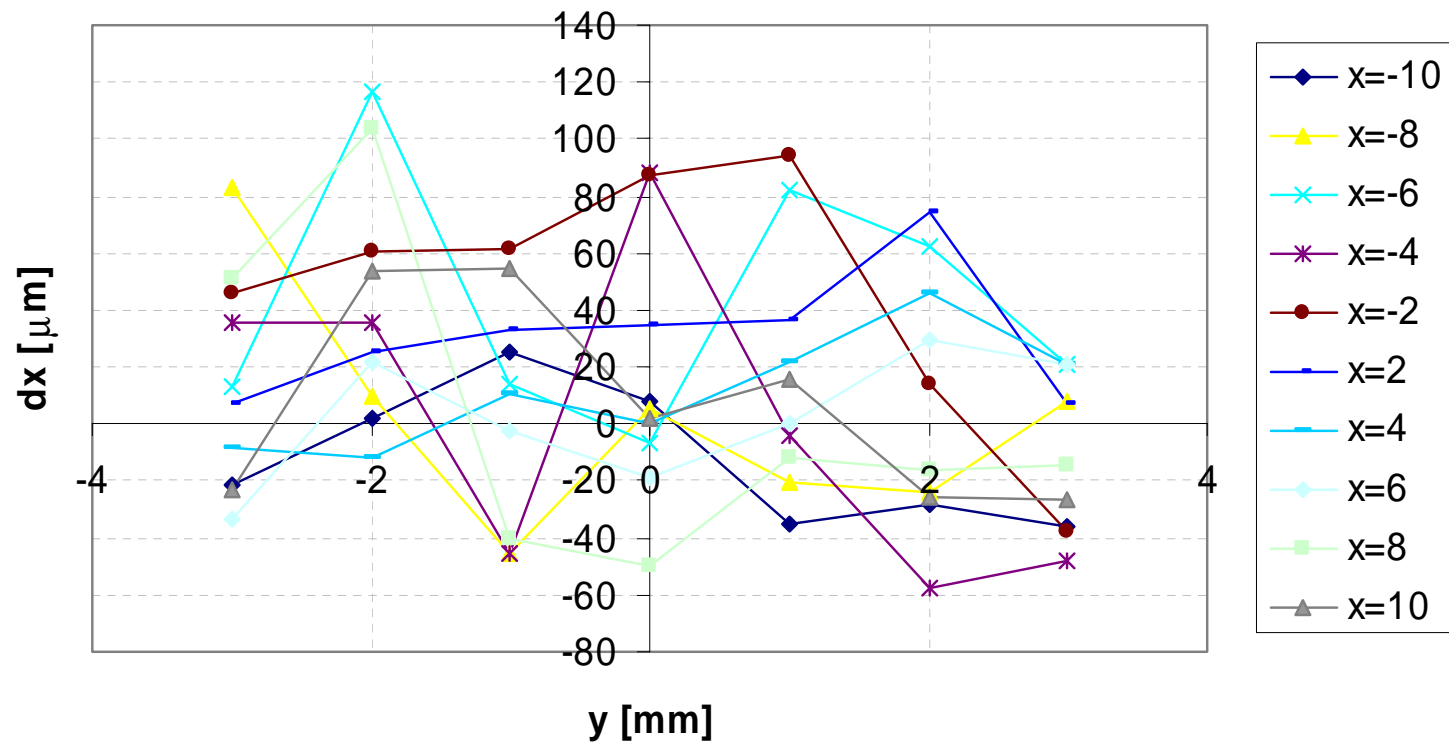
LHC - MTA

A mole for warm magnetic and optical measurements of LHC dipoles
IMMW XI, Brookhaven National Laboratory, 21-24 Sept. 1999
marco.buzio@cern.ch



Optical system calibration

Measured X Error vs. y position (z=20 m) (zoomed)

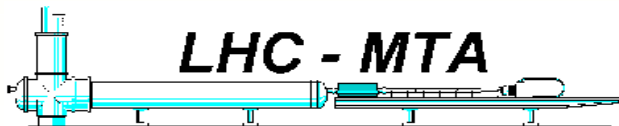
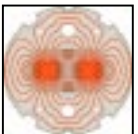
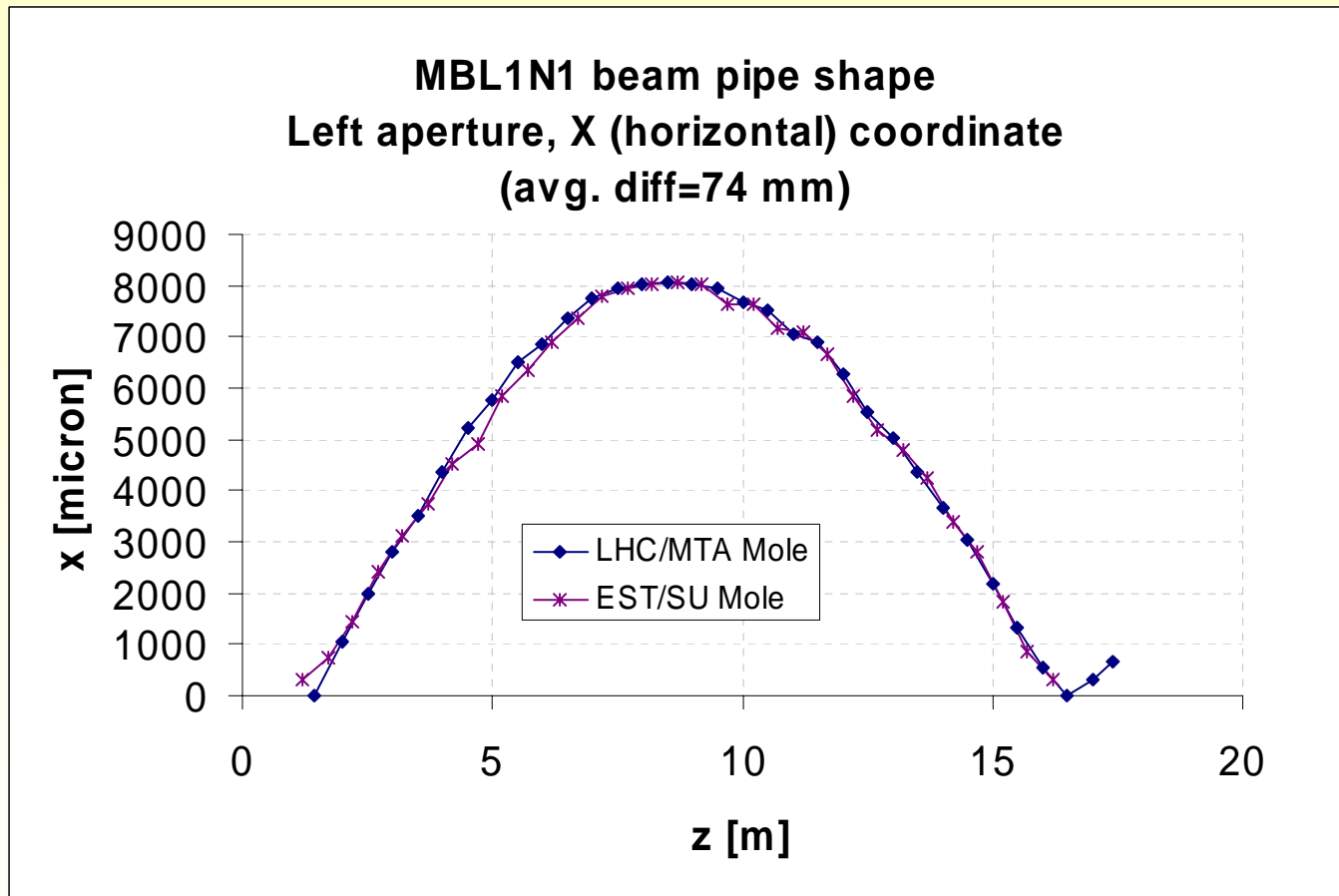


LHC - MTA

A mole for warm magnetic and optical measurements of LHC dipoles
IMMW XI, Brookhaven National Laboratory, 21-24 Sept. 1999
marco.buzio@cern.ch



Example: optical measurement



LHC - MTA

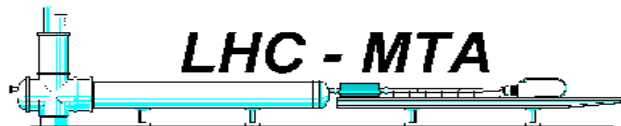
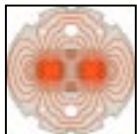
A mole for warm magnetic and optical measurements of LHC dipoles
IMMW XI, Brookhaven National Laboratory, 21-24 Sept. 1999
marco.buzio@cern.ch



Focusing system

◆ How does it work

- no autofocus needed
- longitudinal position sent to the camera at the end of each movement
- focusing motor follows a software calibration table
- total error if out-of-focus $\leq 1 \mu\text{m}/\text{mm}$



LHC - MTA

A mole for warm magnetic and optical measurements of LHC dipoles
IMMW XI, Brookhaven National Laboratory, 21-24 Sept. 1999
marco.buzio@cern.ch



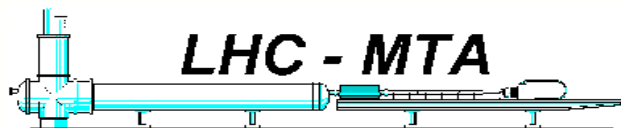
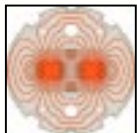
Magnetic performance

◆ Harmonic Coils

- $\text{Ø}41 \times 750$ mm fiberglass/epoxy coil support
- 3 radial coils with 400 turns, 3.4 m^2 area
- 1 coil for main dipole, 1 for dipole compensation + 1 spare

◆ System precision

- Main dipole: better than 10^{-4}
- Dipole angle: better than **0.2 mrad**
- Multipoles: generally better than $2 \cdot 10^{-6}$ relative to B_1
- bucking factor ≈ 2000



LHC - MTA

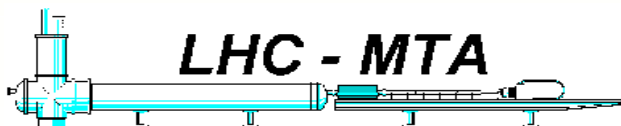
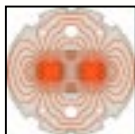
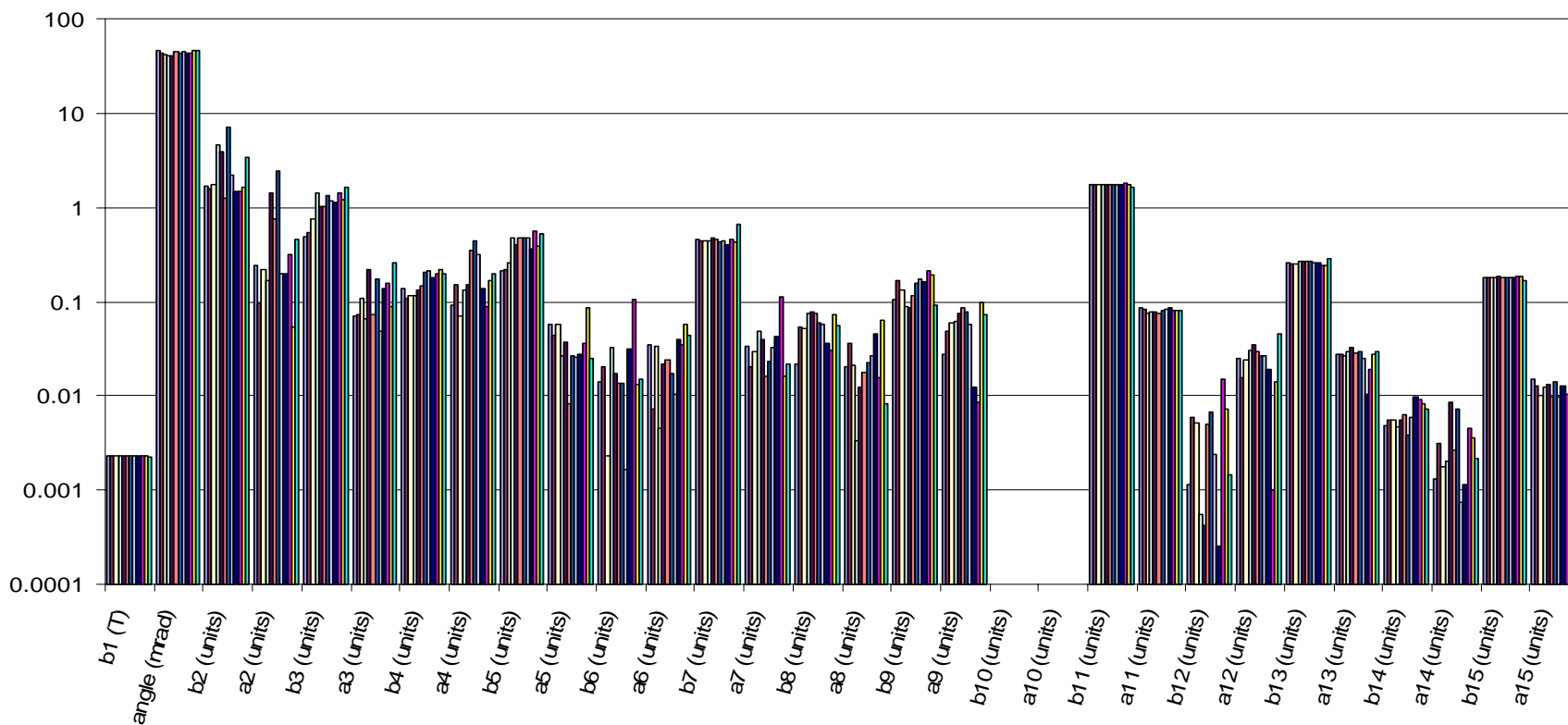
A mole for warm magnetic and optical measurements of LHC dipoles
IMMW XI, Brookhaven National Laboratory, 21–24 Sept. 1999
marco.buzio@cern.ch



Example: multipoles

Field harmonics in Ap. 1 of MBL1N1 @ I=30A

linearly corrected for feed down - all units @ 17 mm

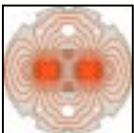
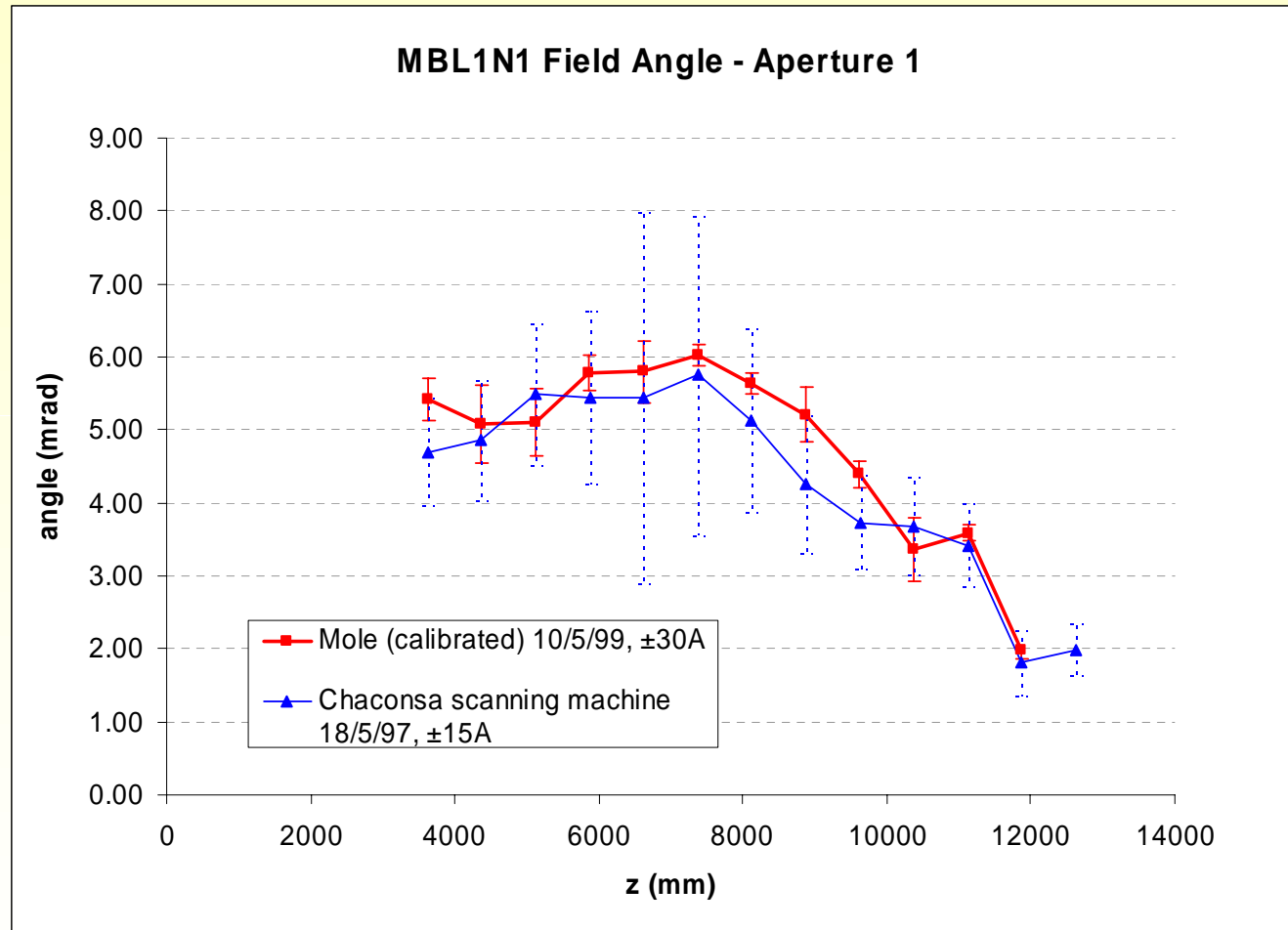


LHC - MTA

A mole for warm magnetic and optical measurements of LHC dipoles
IMMW XI, Brookhaven National Laboratory, 21-24 Sept. 1999
marco.buzio@cern.ch



Example: calibrated dipole angle



LHC - MTA

A mole for warm magnetic and optical measurements of LHC dipoles
IMMW XI, Brookhaven National Laboratory, 21-24 Sept. 1999
marco.buzio@cern.ch



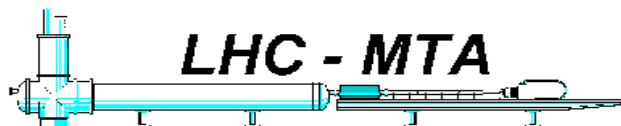
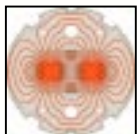
Axis Transfer

◆ Why transfer the magnetic axis ?

- harmonics, and hence magnetic axis, are measured in the coil reference frame
- the center of the coil is measured in the telescope reference frame
- the magnetic axis is needed in the reference frame of the magnet fiducials

◆ How the transfer will be done

- the granite tables establish two reference positions per aperture, vertically and laterally reproducible within **20 μm**
- reference positions are measured by the telescope
- relative position of magnet fiducials and granite tables is measured by means of an auxiliary laser system
- relative position of coil center wrt magnet fiducials can thus be computed

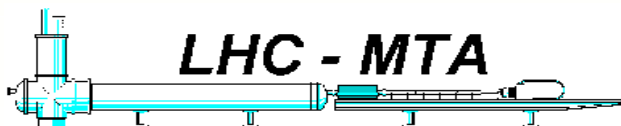
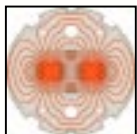
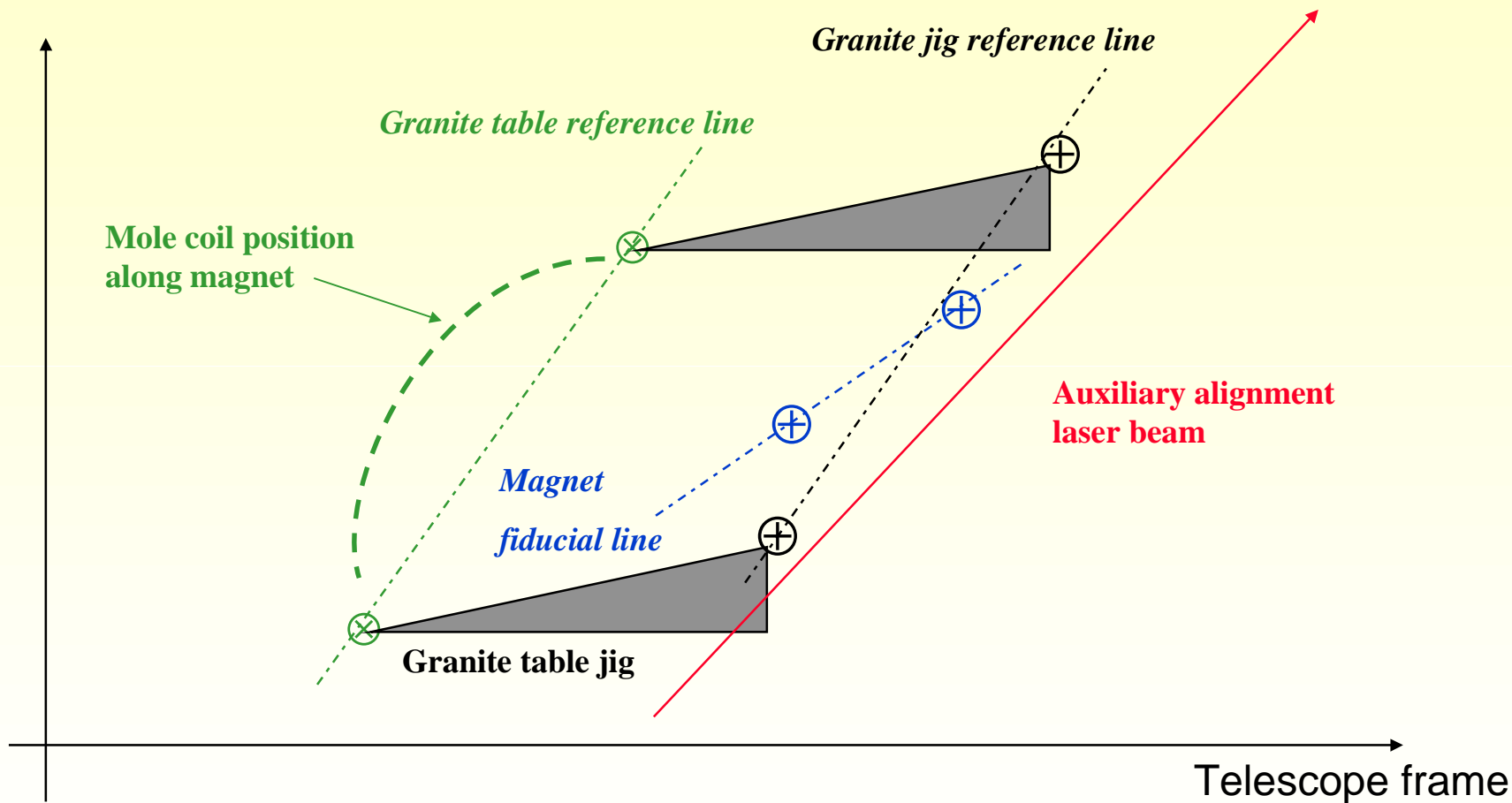


LHC - MTA

A mole for warm magnetic and optical measurements of LHC dipoles
IMMW XI, Brookhaven National Laboratory, 21-24 Sept. 1999
marco.buzio@cern.ch



Axis Transfer

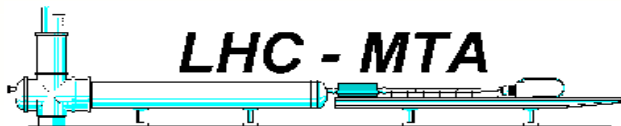
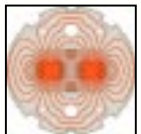
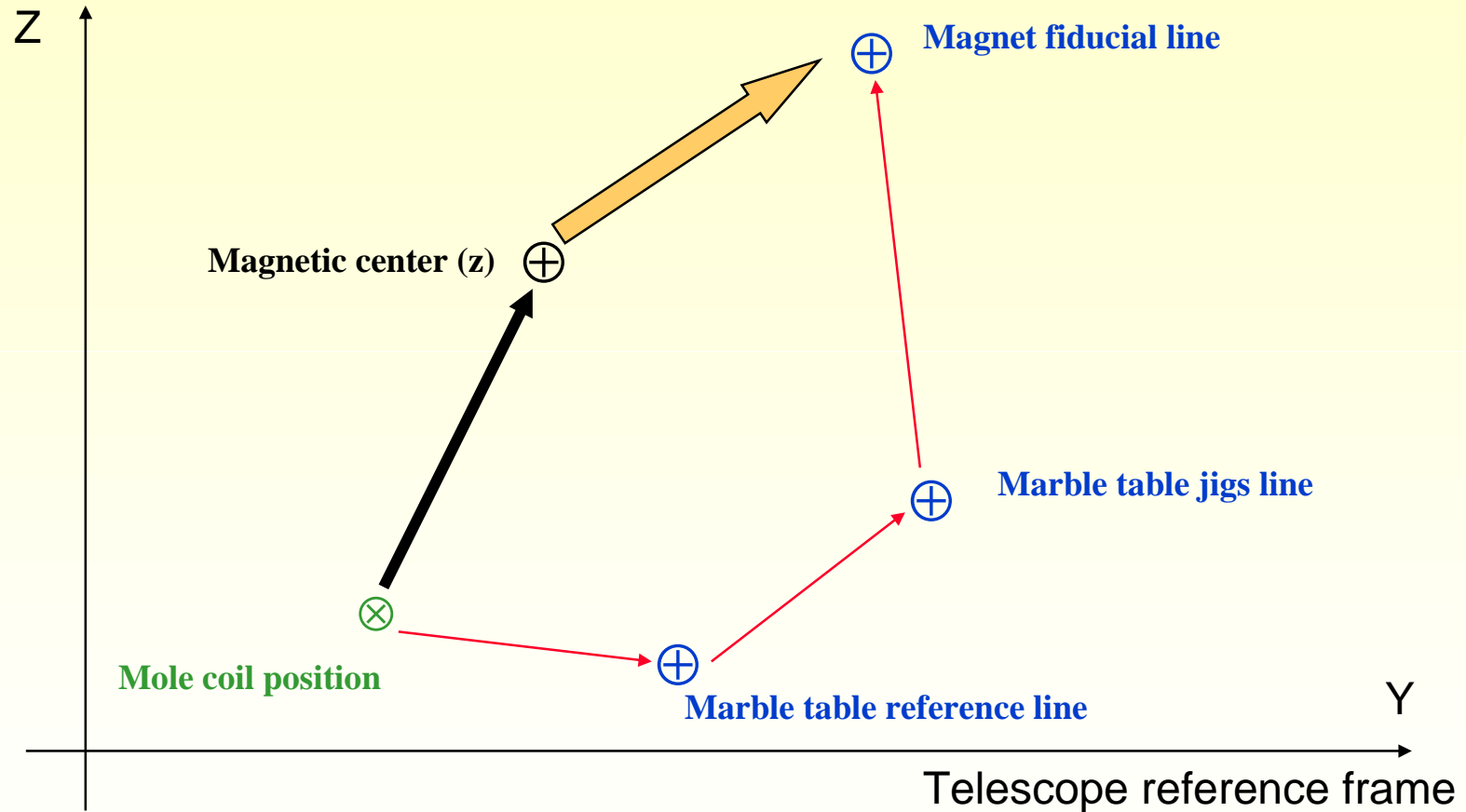


LHC - MTA

A mole for warm magnetic and optical measurements of LHC dipoles
IMMW XI, Brookhaven National Laboratory, 21-24 Sept. 1999
marco.buzio@cern.ch



Axis Transfer



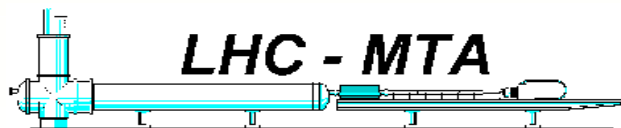
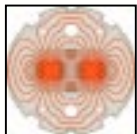
LHC - MTA

A mole for warm magnetic and optical measurements of LHC dipoles
IMMW XI, Brookhaven National Laboratory, 21-24 Sept. 1999
marco.buzio@cern.ch



Problems encountered

- ◆ **Unsteady velocity of piezo-motor, getting worse with motor heating**
- ◆ **Micro cables and connectors delicate and difficult to handle**
- ◆ **Fine alignment of the lens**
- ◆ **Image distortion due to thermal gradients in the magnet**



LHC - MTA

A mole for warm magnetic and optical measurements of LHC dipoles
IMMW XI, Brookhaven National Laboratory, 21-24 Sept. 1999
marco.buzio@cern.ch



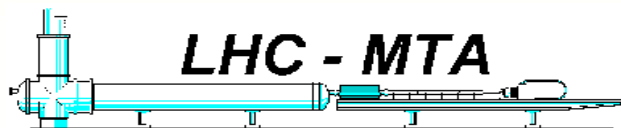
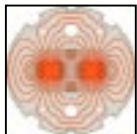
Piezo motor rotation speed

◆ Rotation speed quality

- encoder detects low-frequency rotation speed oscillations up to $\pm 8\%$
- oscillation amplitude gets larger as motor heats up
- oscillations interfere with measured harmonics (errors in b_2 up to **0.5 units** observed)

◆ Improvements under way

- optimization of stiffness and damping of the coil/motor link to minimize response
- fine tuning of motor speed map $\omega(t)$ to minimize excitation
- enhanced motor cooling
- automatic off-line filtering of spurious harmonics

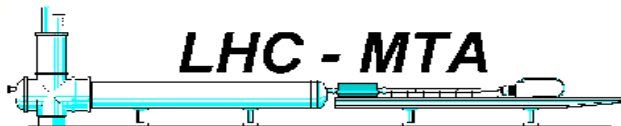
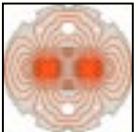
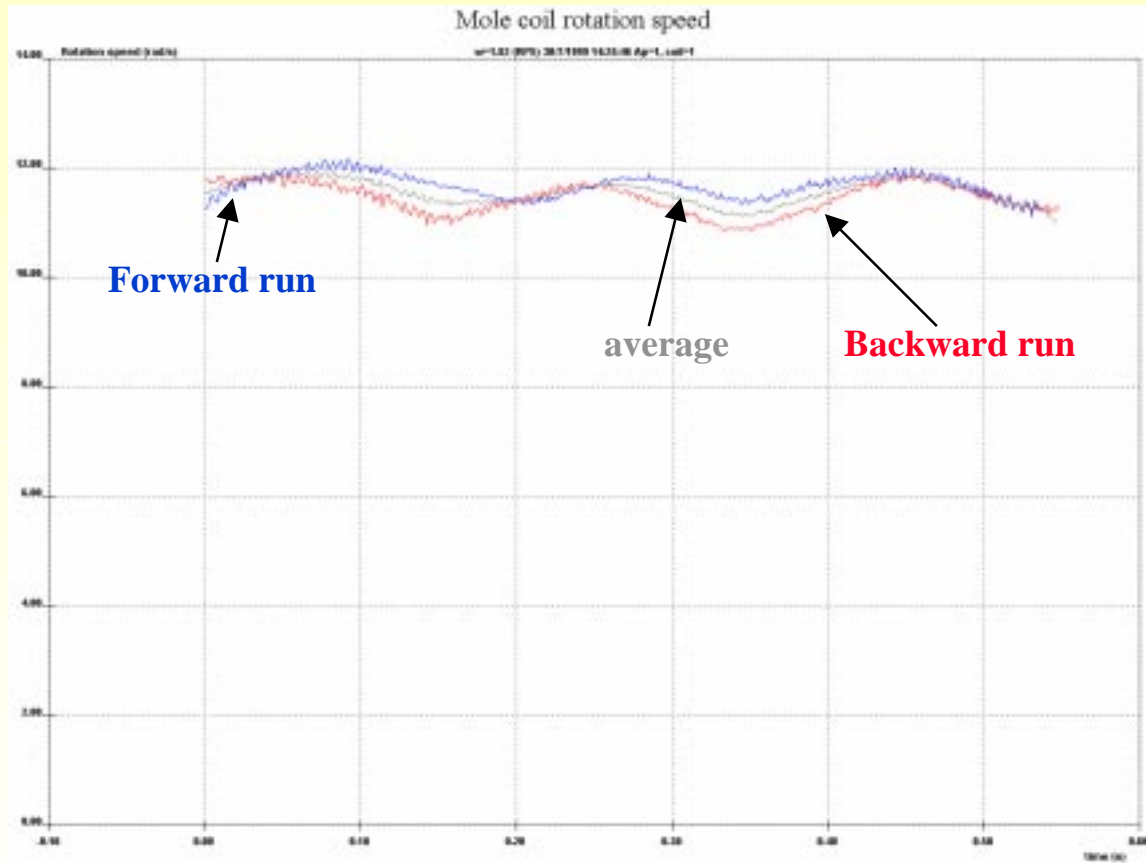


LHC - MTA

A mole for warm magnetic and optical measurements of LHC dipoles
IMMW XI, Brookhaven National Laboratory, 21-24 Sept. 1999
marco.buzio@cern.ch



Piezo motor rotation quality

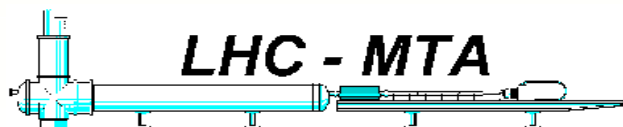
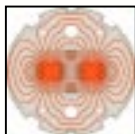
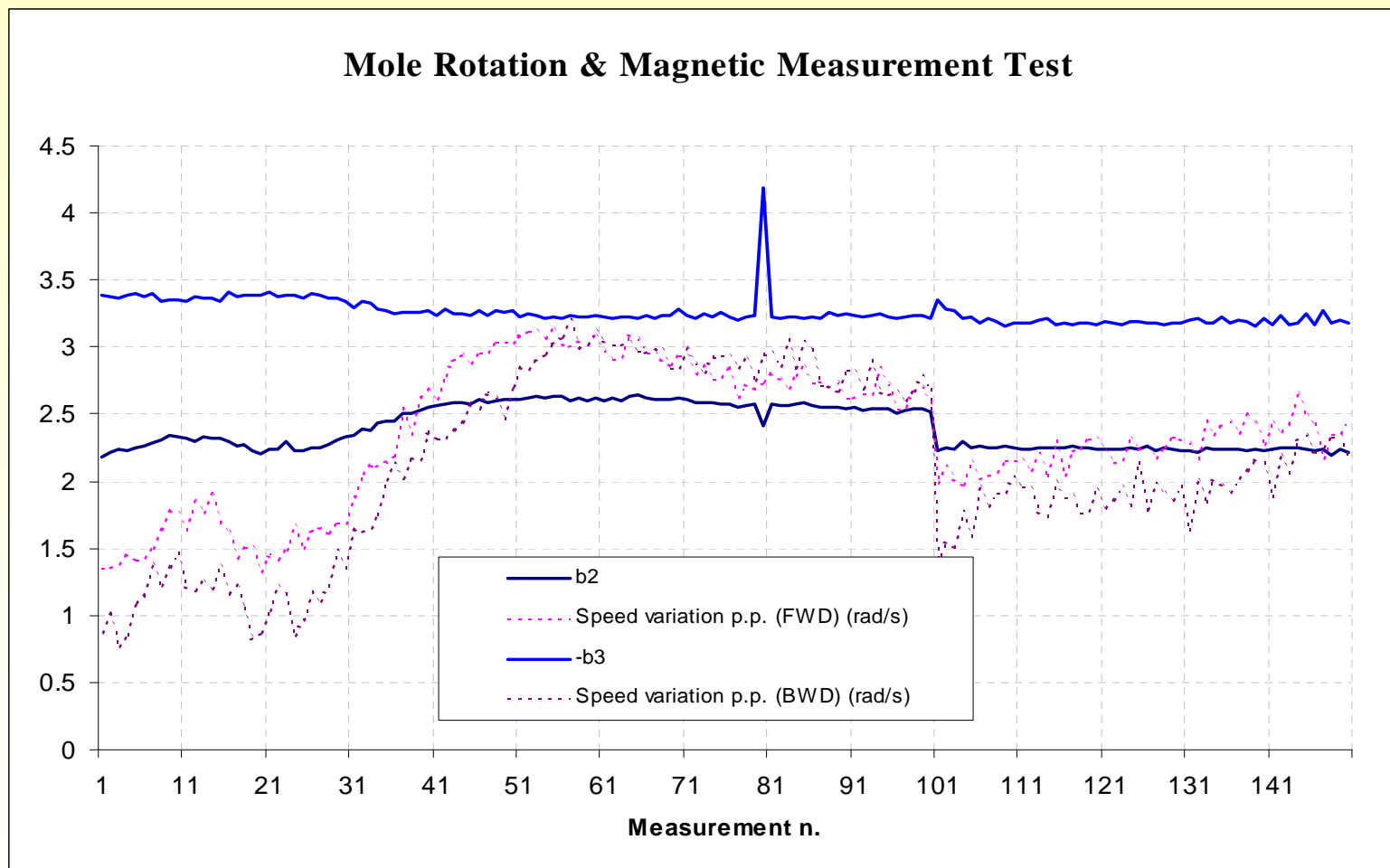


LHC - MTA

A mole for warm magnetic and optical measurements of LHC dipoles
IMMW XI, Brookhaven National Laboratory, 21-24 Sept. 1999
marco.buzio@cern.ch



Piezo motor rotation quality

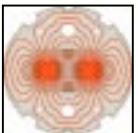
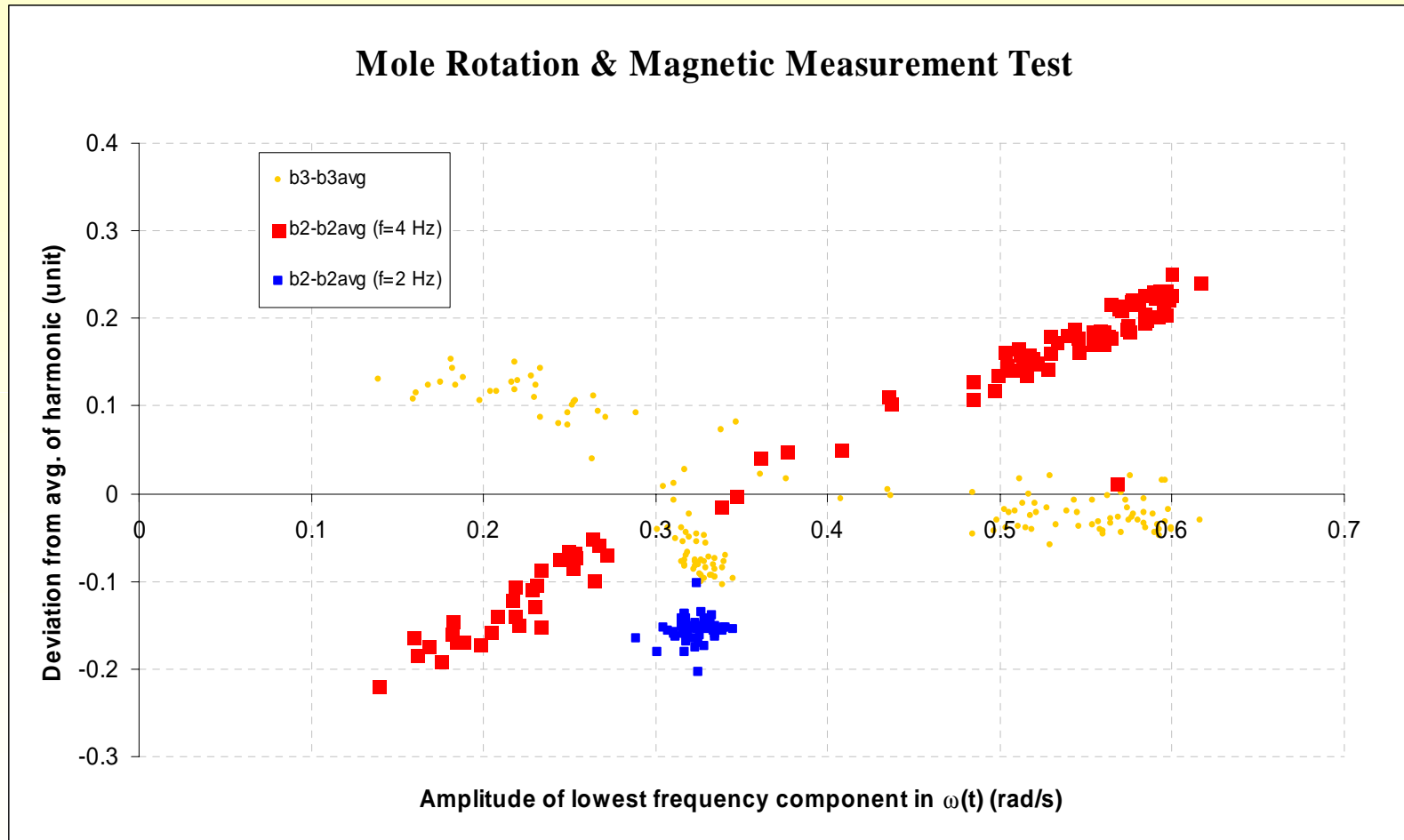


LHC - MTA

A mole for warm magnetic and optical measurements of LHC dipoles
IMMW XI, Brookhaven National Laboratory, 21-24 Sept. 1999
marco.buzio@cern.ch



Piezo motor rotation quality



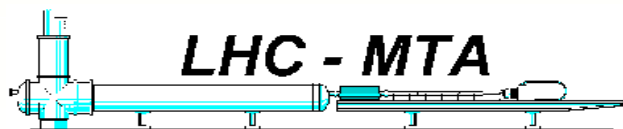
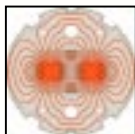
LHC - MTA

A mole for warm magnetic and optical measurements of LHC dipoles
IMMW XI, Brookhaven National Laboratory, 21-24 Sept. 1999
marco.buzio@cern.ch



Conclusions

- ◆ **Magnetic and optical performance generally exceeding specifications**
- ◆ **Well suited for industrial-type test environment**
- ◆ **Test bed for further technological improvements (piezo-motor, remote encoders, etc.)**
- ◆ **Software integration under way**
- ◆ **Minor improvements under way: smoother velocity control, better optics alignment**



LHC - MTA

A mole for warm magnetic and optical measurements of LHC dipoles
IMMW XI, Brookhaven National Laboratory, 21-24 Sept. 1999
marco.buzio@cern.ch



Pulsed Wire System
for Magnetic Measurements at SLAC

G. MORITZ

GSI/SLAC

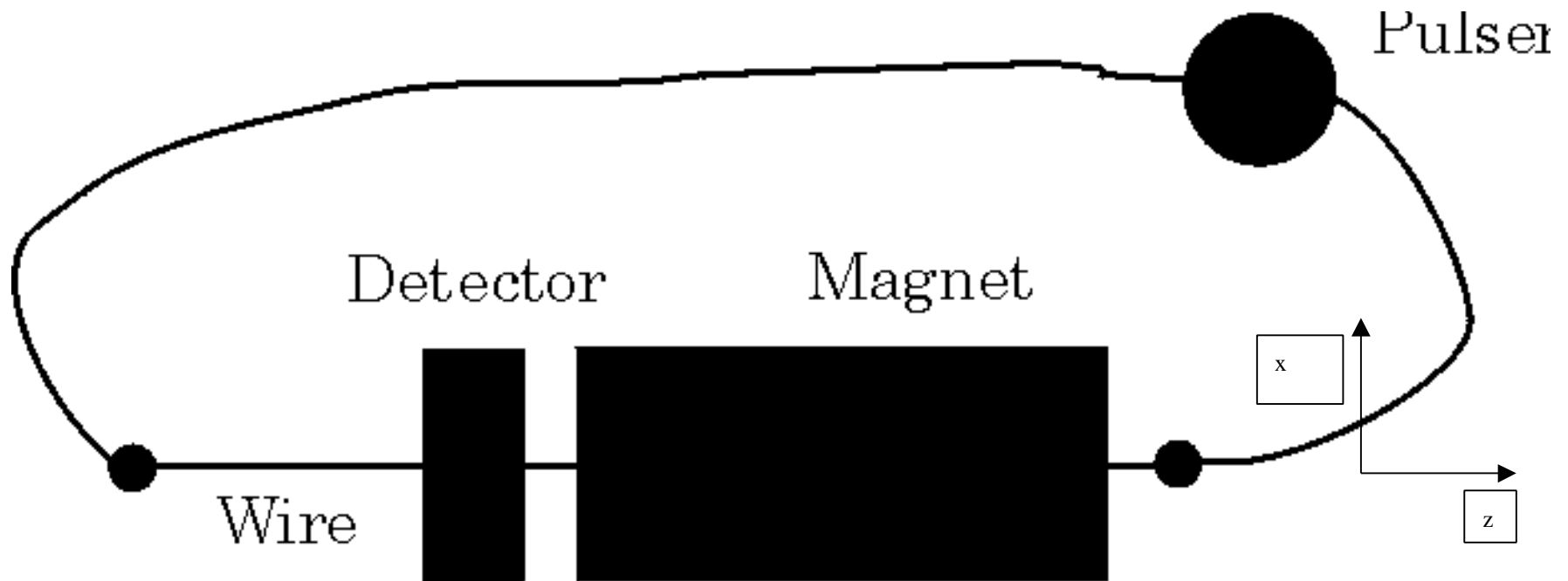
IMMW XI

BNL

9/21/99- 9/24/99

Principles of the 'Pulsed Wire' System

Schematic view of the bench



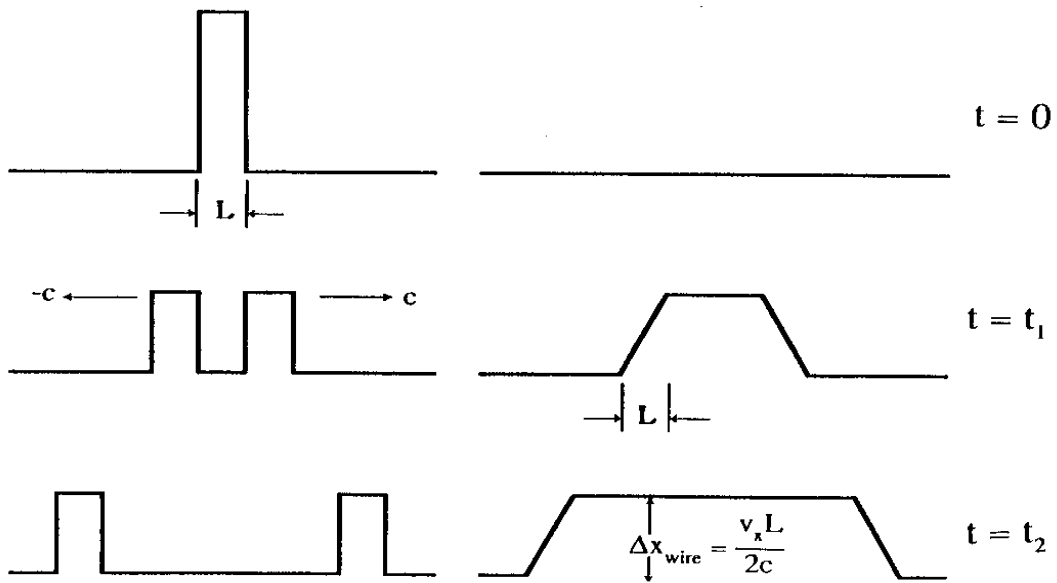
impulse approximation:

$$\mathbf{r} * v_x = I * B * \Delta t$$

Wire Velocity and Displacement Profiles

Transverse
Velocity
 $v_x(z)$ versus z

Transverse
Displacement
 $x(z)$ versus z



Longitudinal velocity

$$c = \sqrt{T/\rho}$$

typically 200-300 m/sec.

Transverse displacement of the wire:

$$x = 1 / (2 c \rho) * I \Delta t * \int B(z) dz$$

$$z = ct$$

where

I = current [A]

Δt = pulse length [sec]

B = magnetic induction [T]

ρ = wire linear mass density [kg/m]

T = tension of the wire [N].

Important conclusions:

1. The pulse length Δt has to be short so that the impulse approximation is not violated; i.e. the displacement during Δt must be small in comparison to the final displacement. This gives the condition

$$v \Delta t \ll v L_m / 2 c \quad \text{or}$$

$$\Delta t \ll L_m / 2 c,$$

where v is the transverse speed and L_m [m] is the magnet length. Typically for our applications Δt is between 1 and 100 μsec with $c=300$ m/sec.

2. To resolve magnetic field structures separated by a distance Δz , the following relation has to be fulfilled:

$$\Delta t < \Delta z / c$$

Then the two separated structures do not overlap. For $\Delta z = 1$ cm and $c = 280$ m/sec we obtain $\Delta t = 35$ μsec .

3. Typical displacement number

For $I = 10$ Amps, $\rho = 3.7\text{E-}5$ kg/m (75 μm wire), $\Delta t = 100$ μsec , $T = 3$ N, $c = 285$ m/sec we obtain a displacement of 47 μm for an integrated field of 0.01 Tm.

Advantages of the ‘Pulsed Wire’ Method

- The bench is simple and cheap.
- It can be used in very small bores.
- One gets the local and integral transverse field component at the same time, if the pulse length is sufficiently small.
- The method is fast; it can be used ‘online’, allowing for an easy alignment of the magnet for example.

Main Limits

The Wire's Sag S

Near the yield point we have

$$S = \rho g L^2 / 8 T$$

where L [m] is the wire length and g the acceleration of gravity.

With the numbers above and a typical wire length of 0.5 m we get $S = 4 \mu\text{m}$. This can be corrected for.

Dispersion

The stiffness of the wire causes the different wavelengths within a wave to travel at different velocities. The short wavelengths have a higher velocity than the longer wavelengths and thus arrive earlier at the detector. The speed depends on the wavelength. This effect is called dispersion.

A detailed analysis is given in [1] R.W. Warren, Nuclear Instruments and Methods in Physics Research, A272 (1988), 257 – 263.

$$c = c_0 [1 + (a\pi^2/8) * M/F * d^2/W^2]$$

where

- c_0 [m/sec] is the velocity without stiffness
- M [N/m² or Pa] is the elastic modulus of the wire
- a is a constant near unity
- d [m] is the diameter of the wire
- W [m] is the wavelength
- F [N/m²] is the tension in the wire per unit area

The problem is not severe if the shortest wavelength of interest is shifted forward on the wave by a distance significantly less than its own wavelength. The effect becomes visible only after a certain travel distance of the wave. This leads to a limit of the wire/ magnet length:

$$L < 8W^3F / (\pi^2 a M d^2)$$

With W=8 mm, T=3 N, M= 130 GPa, d= 75 μm we obtain a value of 39 cm. The typical length of the permanent magnet stack is 13 cm.

Applications ('zero'-method)

- First/Second Field Integral of a wiggler/undulator
- Measurement of transverse field components
- Finding the axis of quadrupoles/solenoids
- Comparison of magnets

Typical requirements:

	$\int B dl$	Wavelength [mm]
First Field Integral (LBNL ALS Insertion Device)	100 Gauss cm	50
Klystron permanent magnet stack (SLAC)	1 Gauss cm	7.9



The Bench

Wire

We used CuBe – wire with diameters of 3, 4 and 6 mils, 75, 100 and 150 μm respectively. Wire tension: 7 N

Detector (measures horizontal/vertical displacement)

The detector measures the mechanical displacements of the wire in both transversal directions. Each channel is equipped with a diode laser, a photodiode to detect the laser light, and a rectangular slit to keep the stray light out. The diode output is amplified by a wide bandwidth amplifier.

Diode Amplifier

Melles Griot, Wide Bandwidth Amplifier 13 AMP 007
Ranges/Bandwidth: 200 μA /1000 KHz, 20 μA /300 KHz
Output: -4 V to + 4 V (unterminated)

The Diode

Melles Griot, Silicon Photodiodes,

Responsivity: 0.45 Amps/Watt at 830 nm
Active Area [mm^2]: 10/30

The Laser

Melles Griot, 0.9 mW Visible Diode Laser, Wavelength 670 nm, Nominal Beam Size 1.0 mm x 1.5mm,

The Slit

Melles Griot, Precision Air Slit, 3mm x 25 μm , 3mm x 50 μm , 3mm x 100 μm ,

High Voltage Pulser

Compliance voltage: 1000 V

Max. current: 100 A

Rise/Fall time: $< 0.2 \mu\text{sec}$

Rep. Frequency: $> 0.5 \text{ Hz}$

Data Acquisition

Digital Voltmeter HP3458A

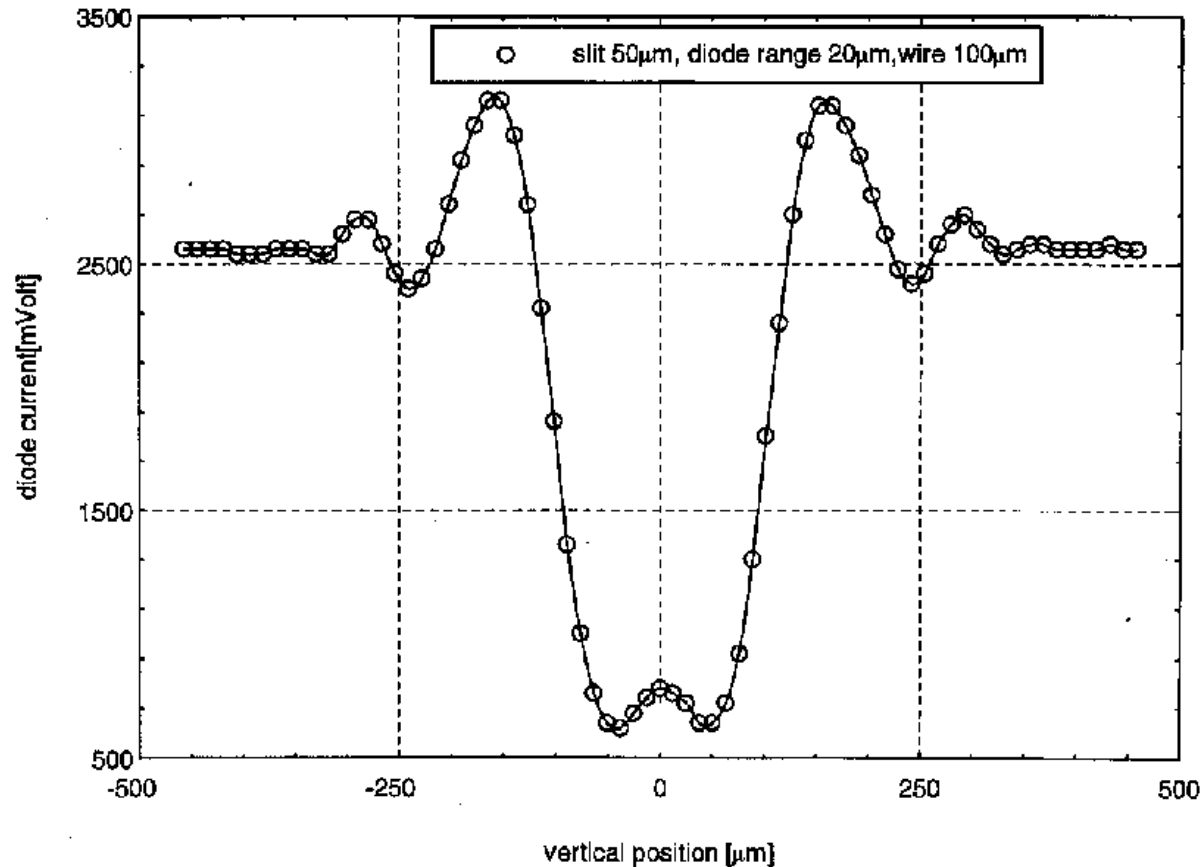
The highest possible sample rate is 0.1 MS/sec, corresponding to a time resolution of 10 μsec .

With an aperture of 1.4 μsec it still has a resolution of 16 bits.

Tektronix Digital Scope TDS 684B

This is a four channel scope with a bandwidth of 1 GHz and a sample rate of up to 5 GS/sec.

Detector Calibration Curve (produced by moving the wire over the slit)

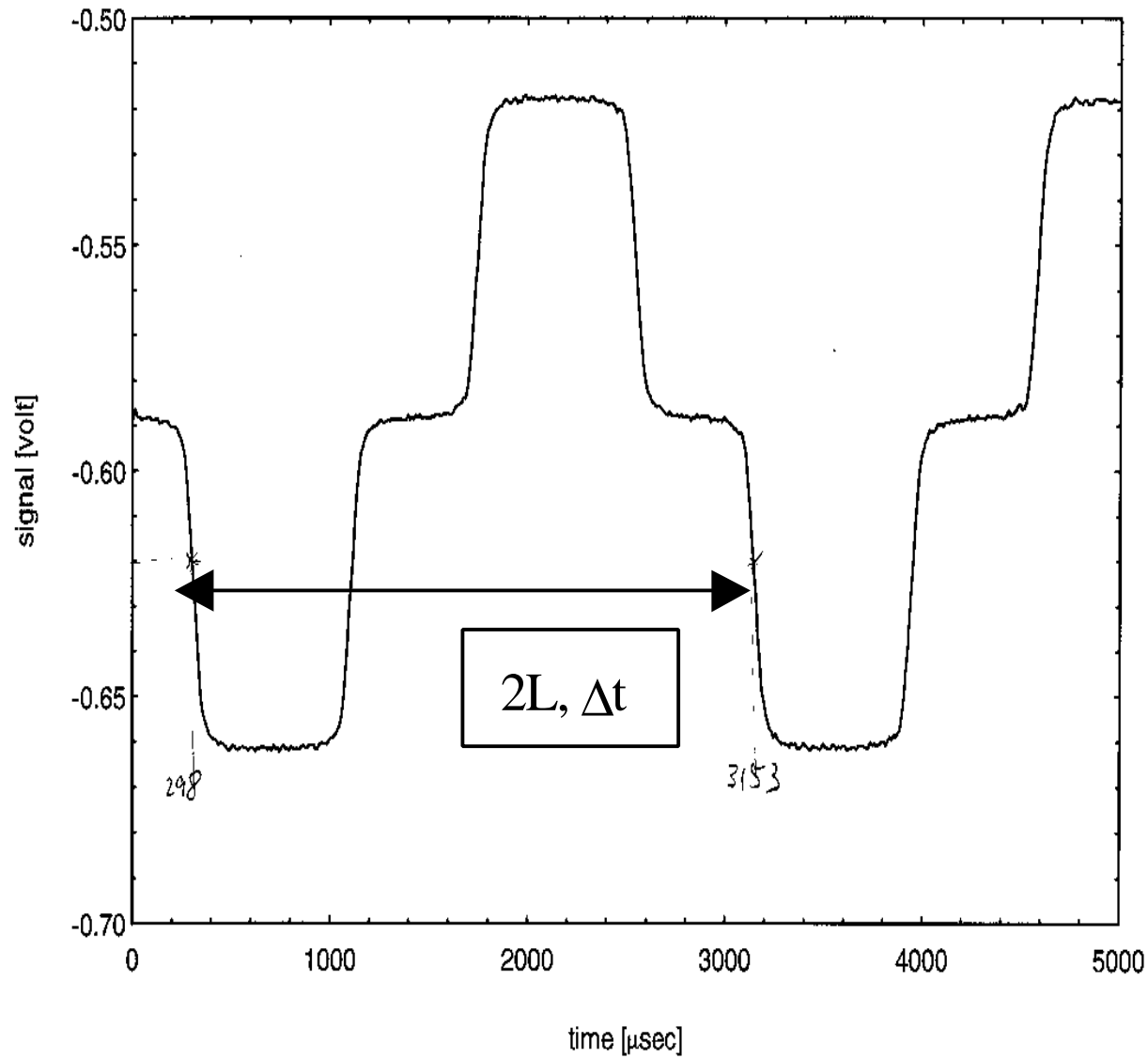


Nonlinear slope

Typical av. sensitivity:
35 mV/ μm

Useful range : 1500
mV or 50 μm
respectively.

Typical noise: 1 mV
RMS



Determination of
the longitudinal
velocity c :

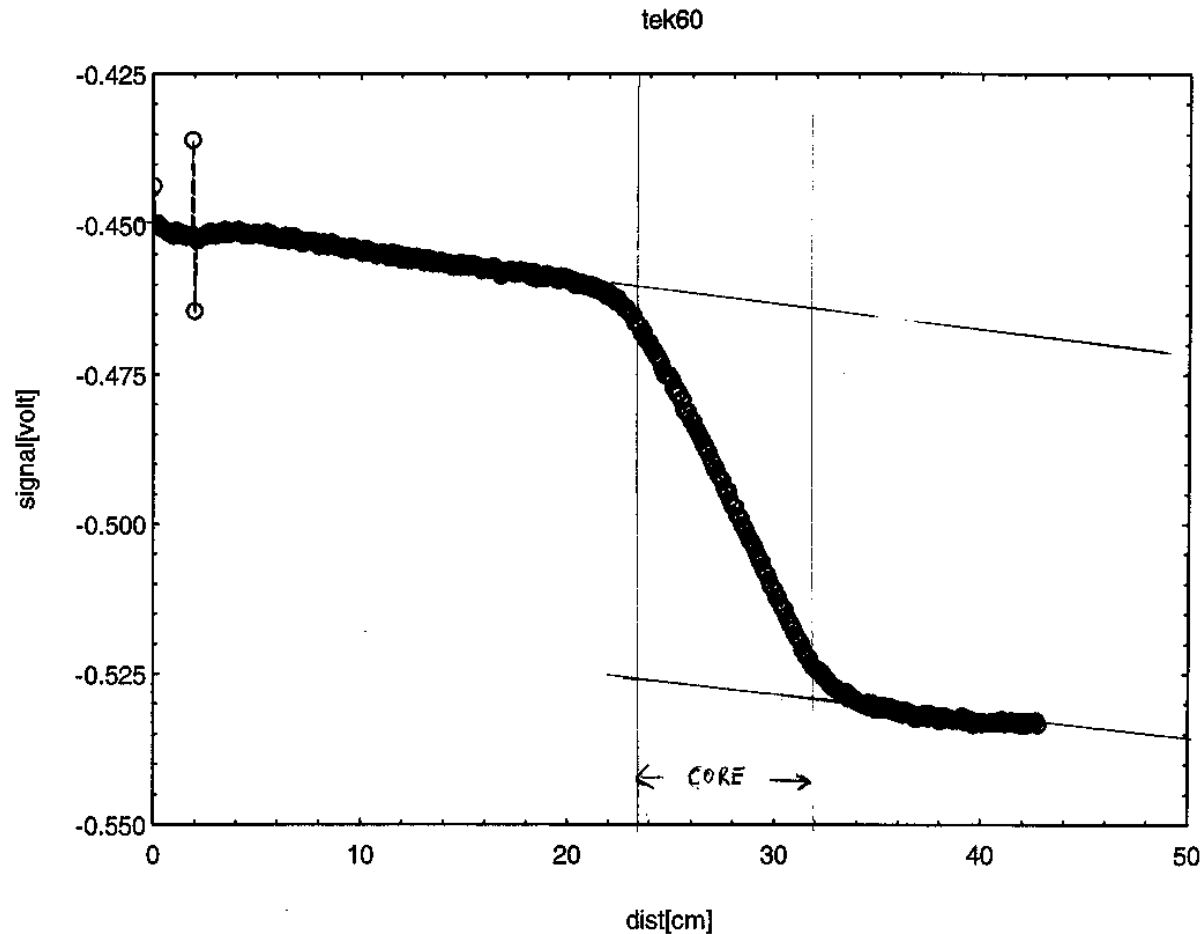
$$c = 2L / \Delta t$$

Calibration
Constant:

$$C [\text{Volt/Asec/Tm}]$$

(Determined with
permanent magnet)

Application: Alignment of a quadrupole

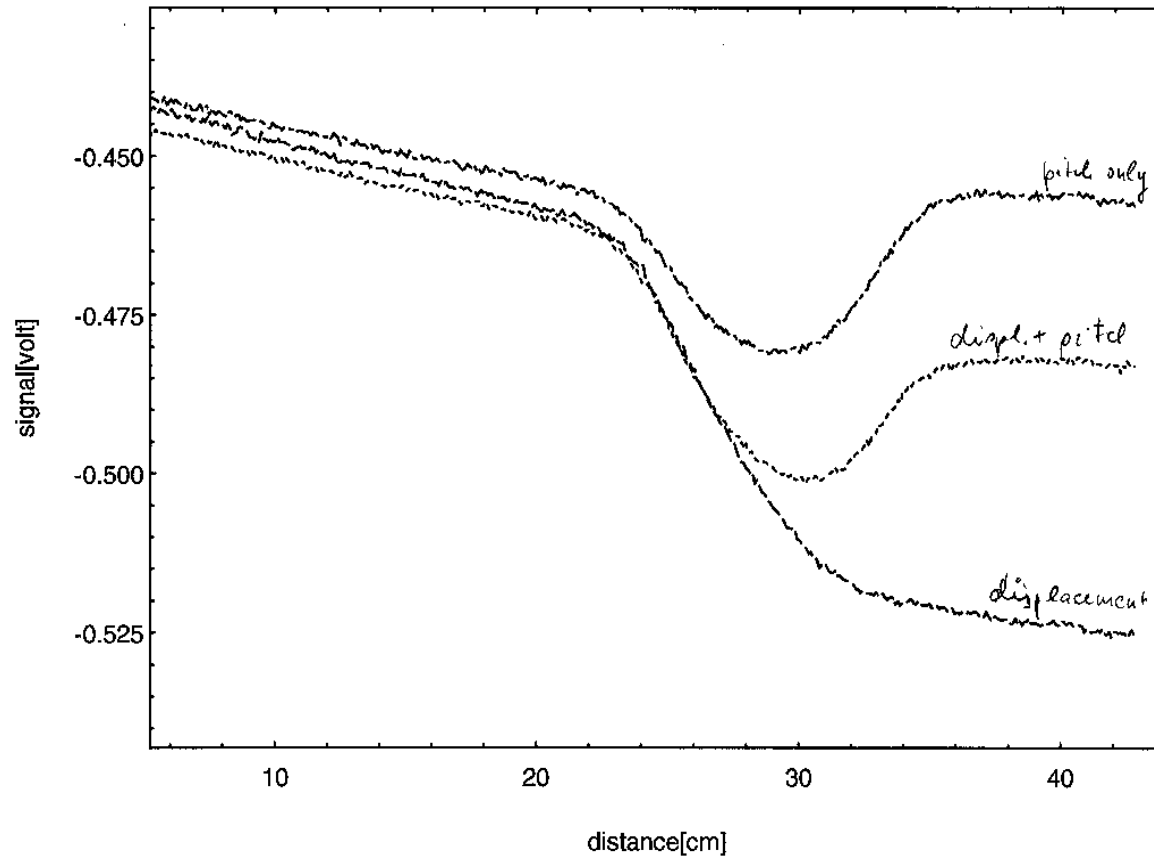


Integral horizontal
field component
(the wire not
centered)

(slope outside of the
magnet due to the
earth field)

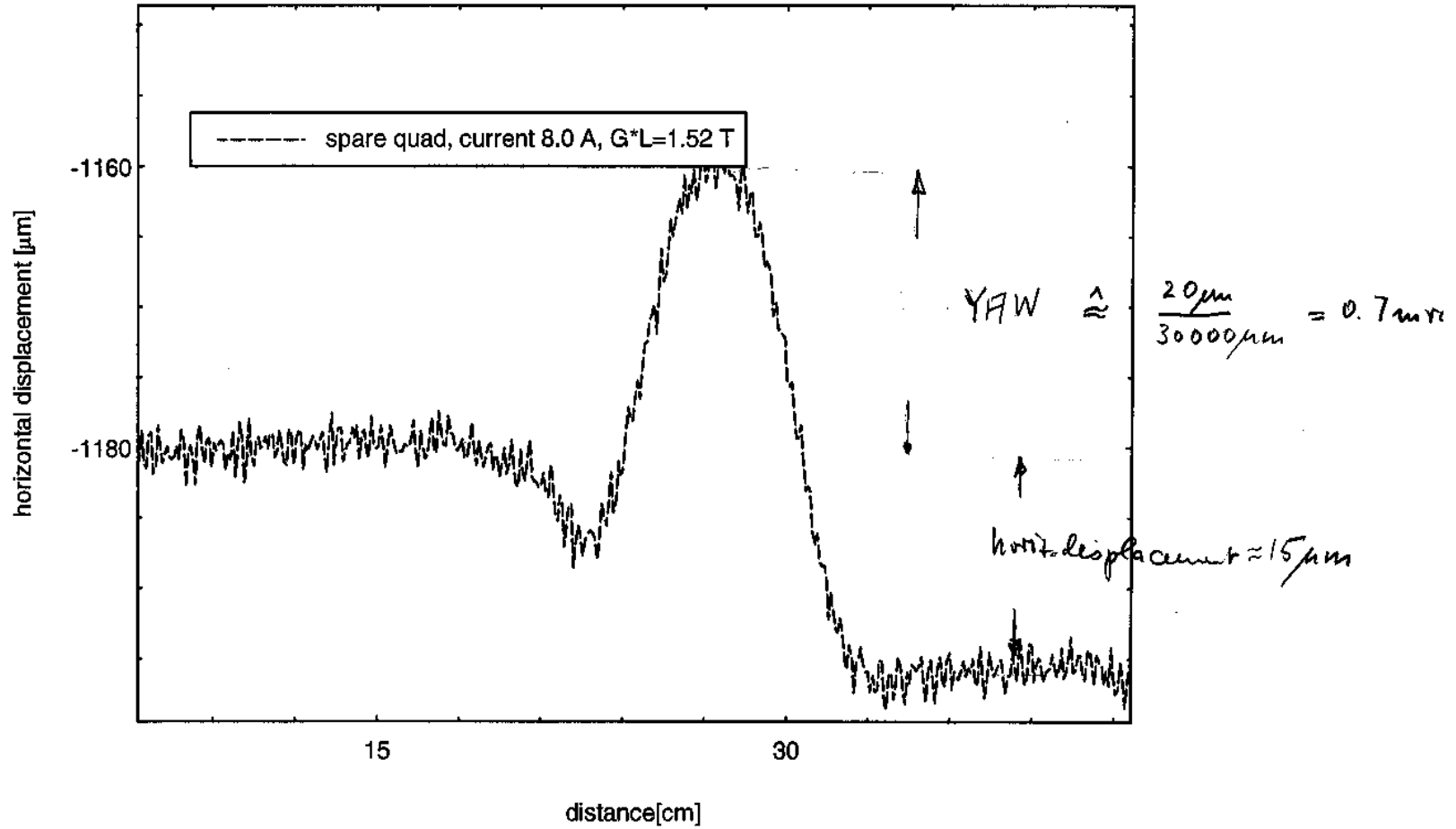
long. distance
 $z = c * t$

tek66-68, hor. field, vert. displacement and pitch



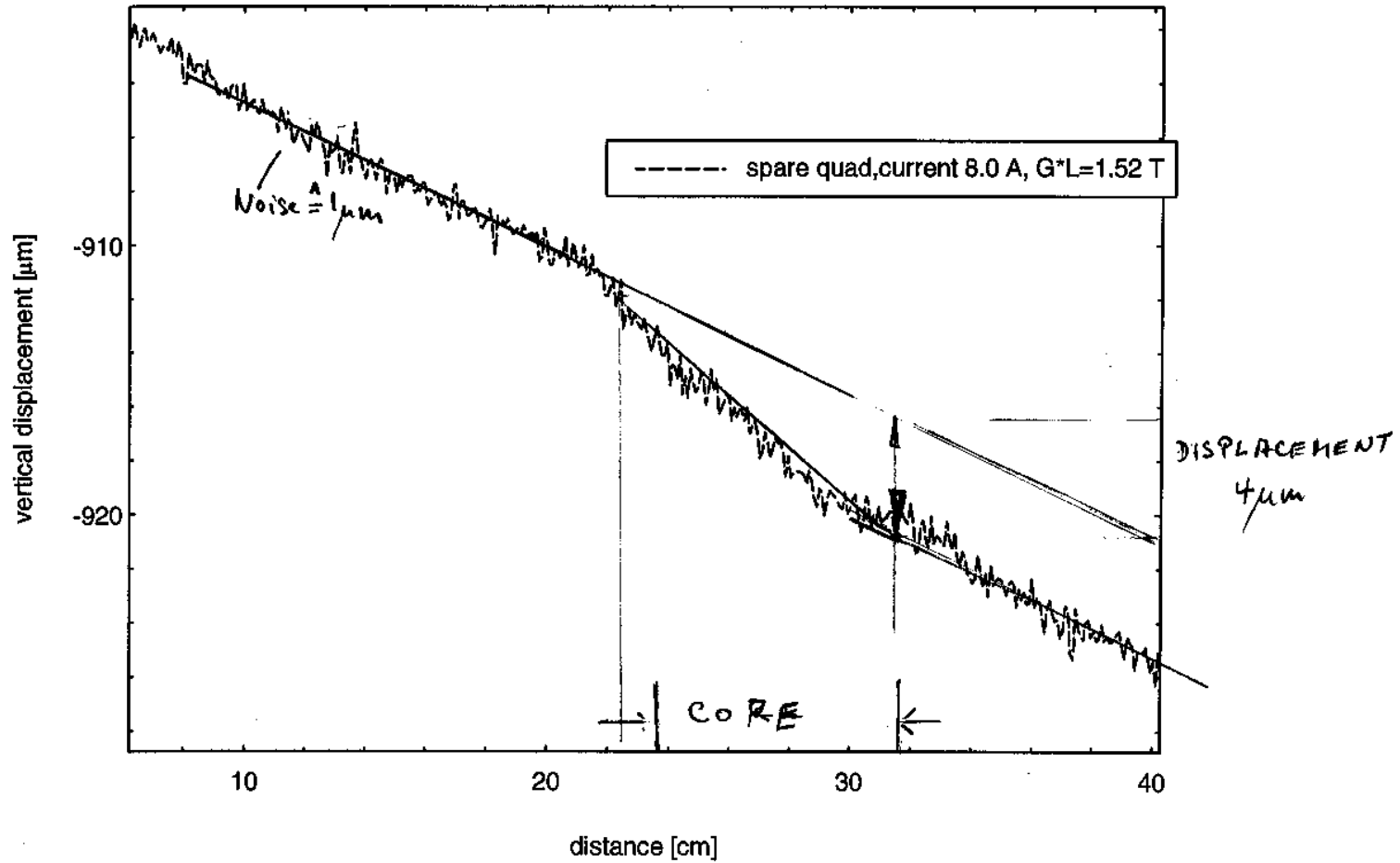
Integral horizontal field at different wire positions (including pitch)

horizontal alignment(displacent/yaw) tek70



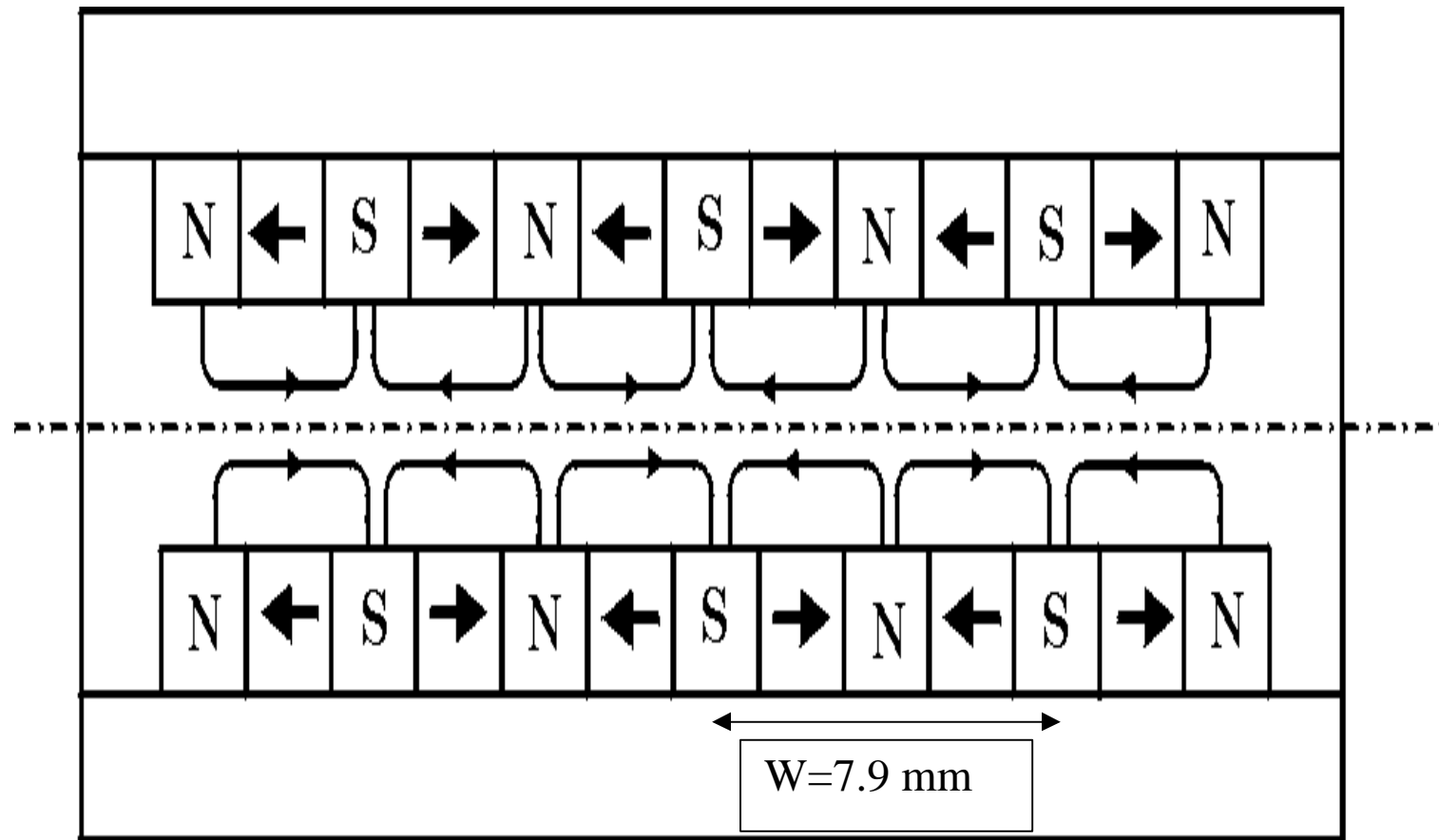
Residual horizontal displacement after alignment (including yaw)

vertical alignment (displacement/pitch) tek71

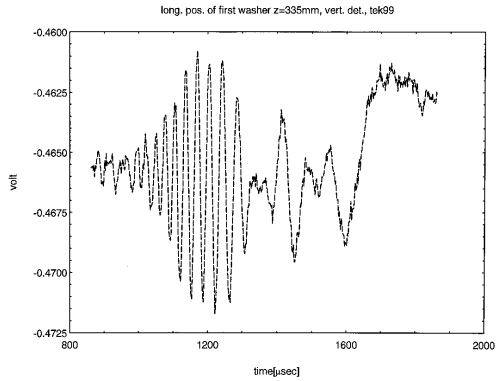


Residual vertical displacement after alignment

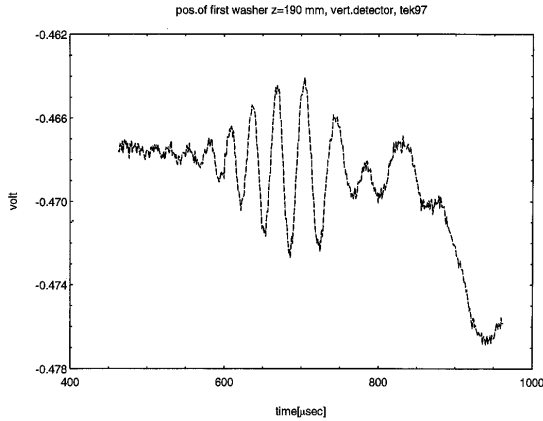
Application: Permanent magnet stack



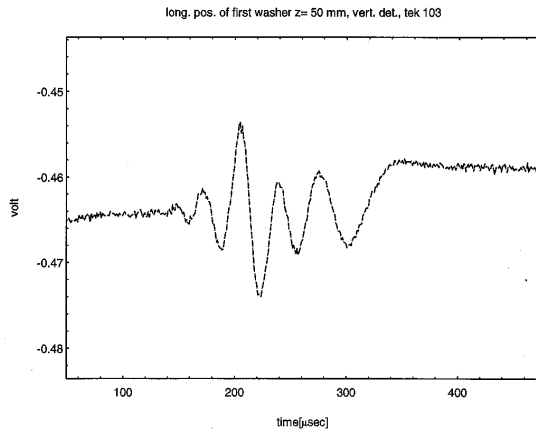
Schematic view of the permanent magnet stack



Signal at a longitudinal distance of 335 mm



Signal at a longitudinal distance of 190 mm

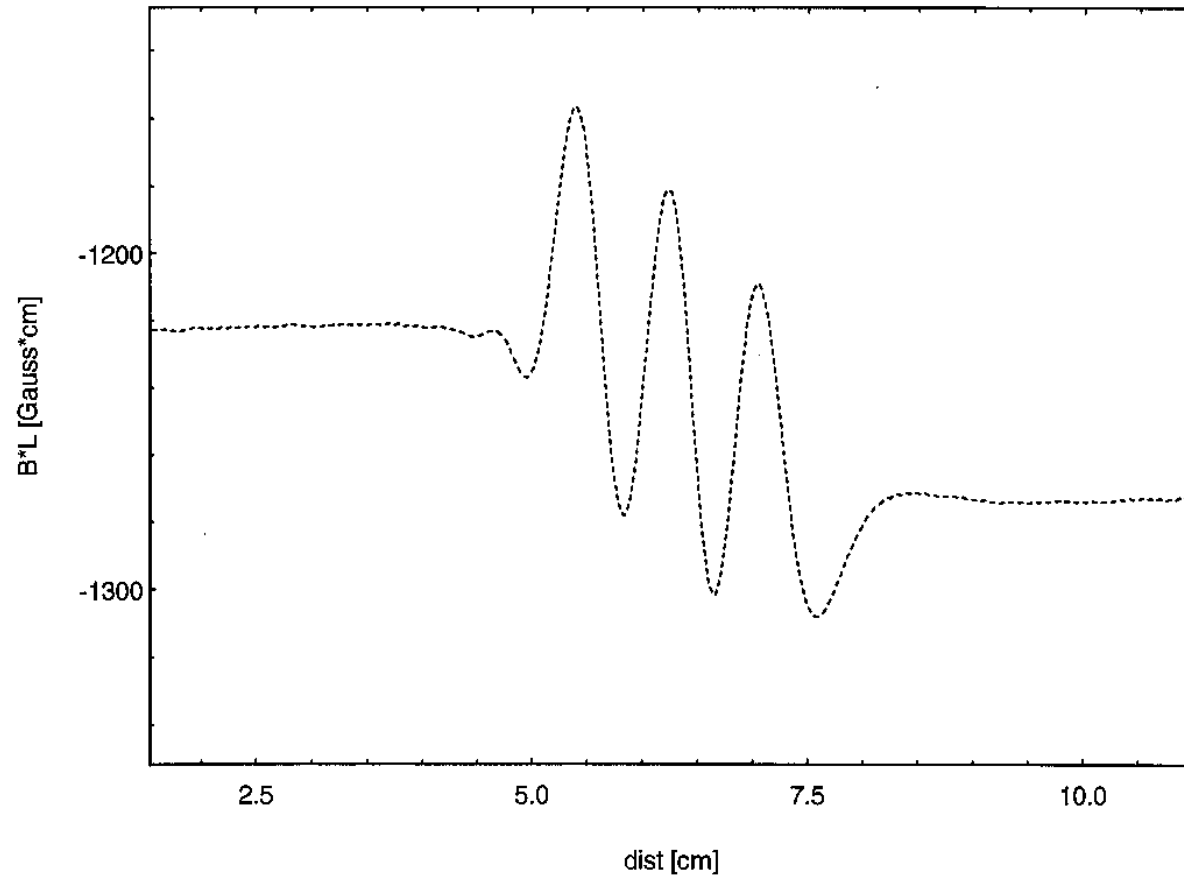


Signal at a minimum distance of 50 mm

Dispersion effects
 $(\propto d^2)$:
 Shorter wavelength
 travel faster

Wire diameter d:
 150 μm

hor. det., tek113, wire not centered

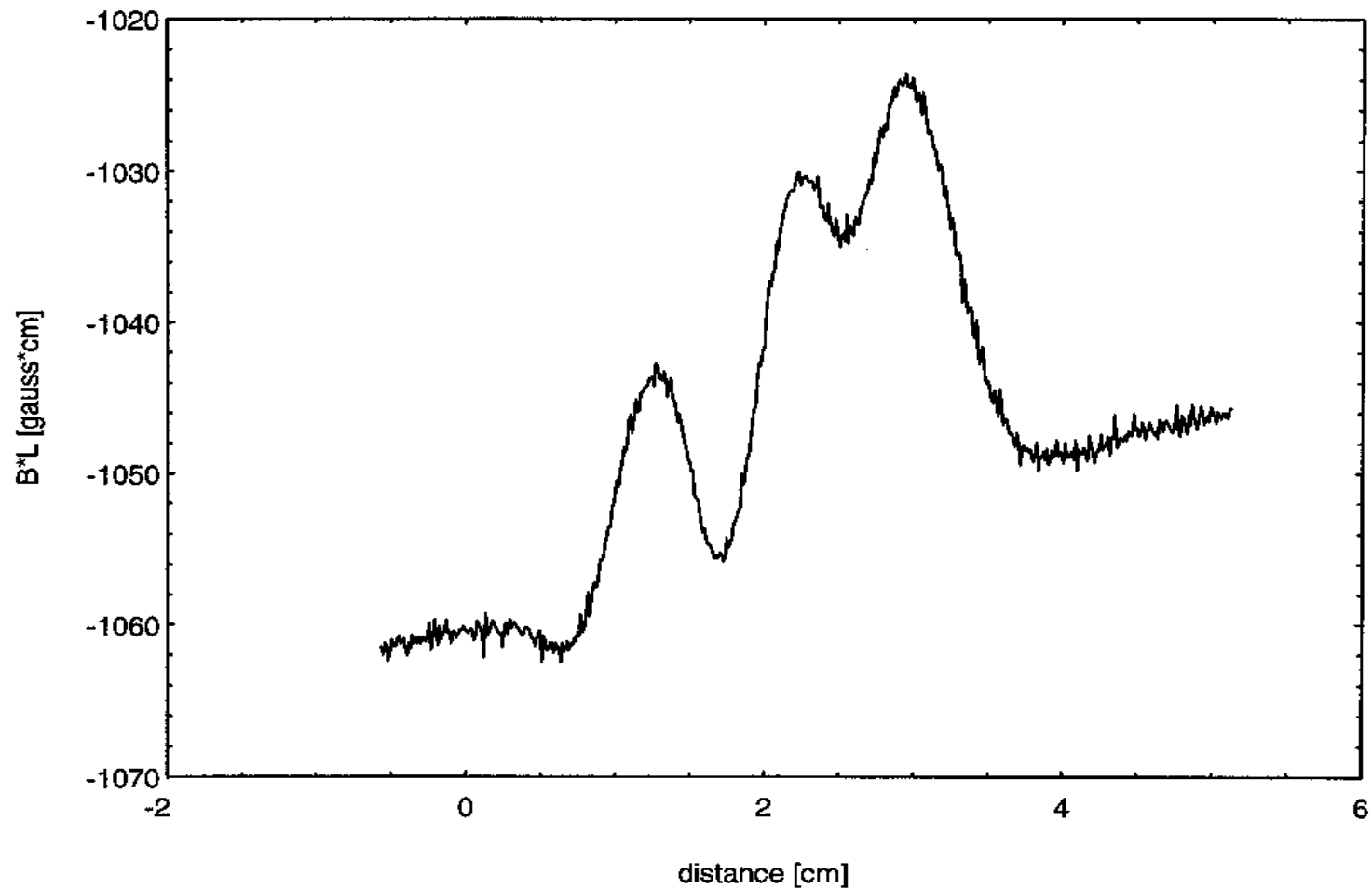


without dispersion :

Wire diameter
reduced: 75 μm

Integral vertical field of the permanent magnet stack

Residual integral field strength (horizontal component) after alignment



Summary

A 'pulsed wire system' for magnetic measurements has been built and successfully tested with several applications. The most demanding design goal of a vertical resolution of 1 Gauss*cm together with a longitudinal resolution of 3 mm has been reached.

Acknowledgement

I would like to thank all members of the Magnetic Measurement Group at SLAC, especially Zack Wolf, for their support and many helpful discussions. Special thanks to Doug Mc Cormick for lending me the oscilloscope, to Foster Thompson for the technical support and to Robert Ruland, who made my stay at SLAC possible.

Bibliography

- [1] R.W. Warren, Nuclear Instruments and Methods in Physics Research, A272 (1988), 257 – 263.
- [2] C. M. Fortgang, 6th International Magnetic Measurement Workshop, Lawrence Berkeley Laboratory, (1989)
- [3] D. W. Preston and R.W. Warren, Nuclear Instruments and Methods, A 318 (1992), 794-797.
- [4] C. M. Fortgang et al., LINAC Conference Albuquerque, (1990).
- [5] O. Shahal, R. Rohatgi, Nuclear Instruments and Methods, A285 (1989) 299-302.
- [6] S.M. Wallas et al., Nuclear Instruments and Methods, A 331, (1993) 759-762.
- [7] C.M. Fortgang, R.W. Warren, Nuclear Instruments and Methods, A 341, (1994) 436-439.

An AC field static system for measuring the magnetic axis of LHC superconducting magnets in warm condition

Abstract

The choice of a 3D-laser tracker for controlling several delicate operations during the fabrication process of the LHC magnets gave us the idea of using a single mole to measure simultaneously the centre axis of the cold bore tube and the magnetic axis of the magnet. This mole houses, at the same cross-section point, four tangential coils for detecting the magnetic axis, a corner cube for detecting the centre of the mole and a mechanical system for centring the mole inside the cold bore tube. Here we describe the principle, the equipment and preliminary results related especially to the measurement of the magnetic axis.

Introduction

The LHC machine is very sensitive to magnet misalignment and special attention has been paid to buying or developing dedicated instruments. Most such magnets are superconducting, hidden inside cryostats when they are finished, so very precise control of their geometry is necessary during production. A measurement accuracy of within 0.1mm must be guaranteed. A first major decision has been to buy 3D-laser tracker devices to facilitate certain very delicate operations in the magnet fabrication process. Taking advantage of the possibilities given by these devices, a mole has been designed to measure the axis of the cold bore tubes of the magnets. This operation is particularly important for dipole magnets which are 15m long and bent with a 10mm sagitta. The idea was launched to incorporate in such a mole a capacity to measure the magnetic axis at the same time.

The two geometry parameters of the magnetic field are the magnetic axis position, expressed in mm, and the field direction, expressed in mrad. Both can be determined from magnetic measurements. For the field direction, gravity sensor and encoder allow for an accuracy better than 0.1mrad, while for the magnetic axis, a complicated system is required to extrapolate the measurement to the fiducials. The following system is mainly dedicated to the measurement of the position of the magnetic axis but can also give the field direction, with a limited accuracy of 1mrad.

Design criteria

First of all this mole should be easy to use. It should be as simple as possible: no motor, no encoder. As explained in another presentation of J. Garcia at this Workshop, it has a pendulum function to stay vertical. Nevertheless a gravity sensor is integrated to take into account the remaining deviation from the vertical. Other functions have been added to centre the mole automatically and to measure on two diameters, the average cold bore tube diameter and any possible circularity defect of the tube.

Another important aspect of the design is that this operation must not introduce any heating of the air inside the tube, so that the laser beam trajectory is in no way disturbed, so the excitation current to produce the field must be very small. The solution adopted was to use tangential search coils in an AC field and measure their induced voltage with a synchronous detection method. Tangential coils placed at the largest radius give the greatest sensitivity and synchronous detection can make out very small signals even in a very noisy

environment. Fabrication of such search coils and design of synchronous detection electronic circuits is now well advanced at CERN.

The idea of this system was first applied to measure quadrupole magnet axe so that the choice of a four coil system was natural. In design, the positioning tolerance of the coils inside the mole is less than 0.05mm but still graeter accuracy can be obtained from dedicated calibrations.

After some calculations, it was deduced that the system can also be used to measure the magnetic axis of other multipole field magnets, such as sextupoles, octupoles and decapoles. Such magnets are widely used in the LHC machine as corrector magnets, either inside the dipole cold mass spool pieces or inside the short straight sections (SSS) cold mass on each end of the quadrupole magnets.

Another important application of this system is the 15m long dipole magnets. Obviously a dipole field has no centre, but the coils producing this field have a mechanical centre and the “permitted” components coming from the discretisation of the coil blocks have this centre as their axis. A way of creating this centre is to excite the two poles of the dipole in opposition instead of in series turning the dipole field in a skew quadrupole field together with some other components, the so-called “Quadrupole Configured Dipole” (QCD).

The equipment

The search coils

These four coils are 100mm long and 10mm in width, and have 600 turns made from a $32\mu\text{m}$ copper wire. With a 0.6m^2 surface area, the sensitivity is excellent. A sorting of 4 over 25 coils gives a difference in surface area and a parallelism better than 1/1000. To increase the sensitivity of the mole still further, the centre of the windings is on a radius of 22.5mm for a cold bore tube of 25mm radius. As the mole diameter is 47mm, the coils winding centres are only 1mm inside the mole.

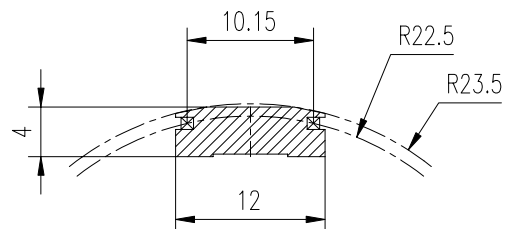


Fig. 1 Cross-section of a search coil

The coil assembly

The four coils are mounted on a non-metallic tube to avoid any induced current. Their final positioning accuracy is well within 0.05mm, radially and azimuthally. The four coil voltages are measured individually. The coil assembly orientation can be changed with respect to the pendulum part of the mole in four precise azimuthal positions, to allow measurement of the different type of magnets. A gravity sensor measures the direction of the pendulum portion of the mole with an accuracy better than 0.5mrad

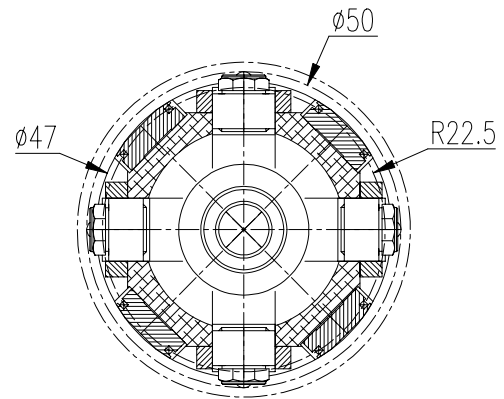


Fig.2 Cross-section of the coil assembly



Fig.3 One of the search coils and its mounting in the mole

The electronics

The AC excitation current comes from a KEPCO bipolar power supply. The synchronous detection circuit is based on the AD630 integrated circuit. The greatest efficiency is obtained at a frequency of 25Hz, half of the main frequency, because the rejection is at its greatest. This frequency is made by a sine generator driven by a quartz oscillator and is therefore very stable. Fig.4 shows the 25Hz signals of the excitation current and the corresponding voltage induced in the search coils. The LHC lattice quadrupole has a $220 \text{ T}\cdot\text{m}^{-1}$ field gradient at a nominal current of about 12000A. The magnetic warm measurement is made at about 12A, i.e. three orders of magnitude lower. The synchronous detection technique makes it still possible to measure three orders of magnitude below. At such a level, the heat input is absolutely negligible

Table 1. The sensitivity of the system at 10^{-4} to 10^{-6} of the LHC quad maximum field

Coil voltage (mV)	Field at $r = 17\text{mm}$ (T)	Stability (mm)
37	$3\cdot 10^{-4}$	< 0.001
3.7	$3\cdot 10^{-5}$	0.002
0.37	$3\cdot 10^{-6}$	0.01

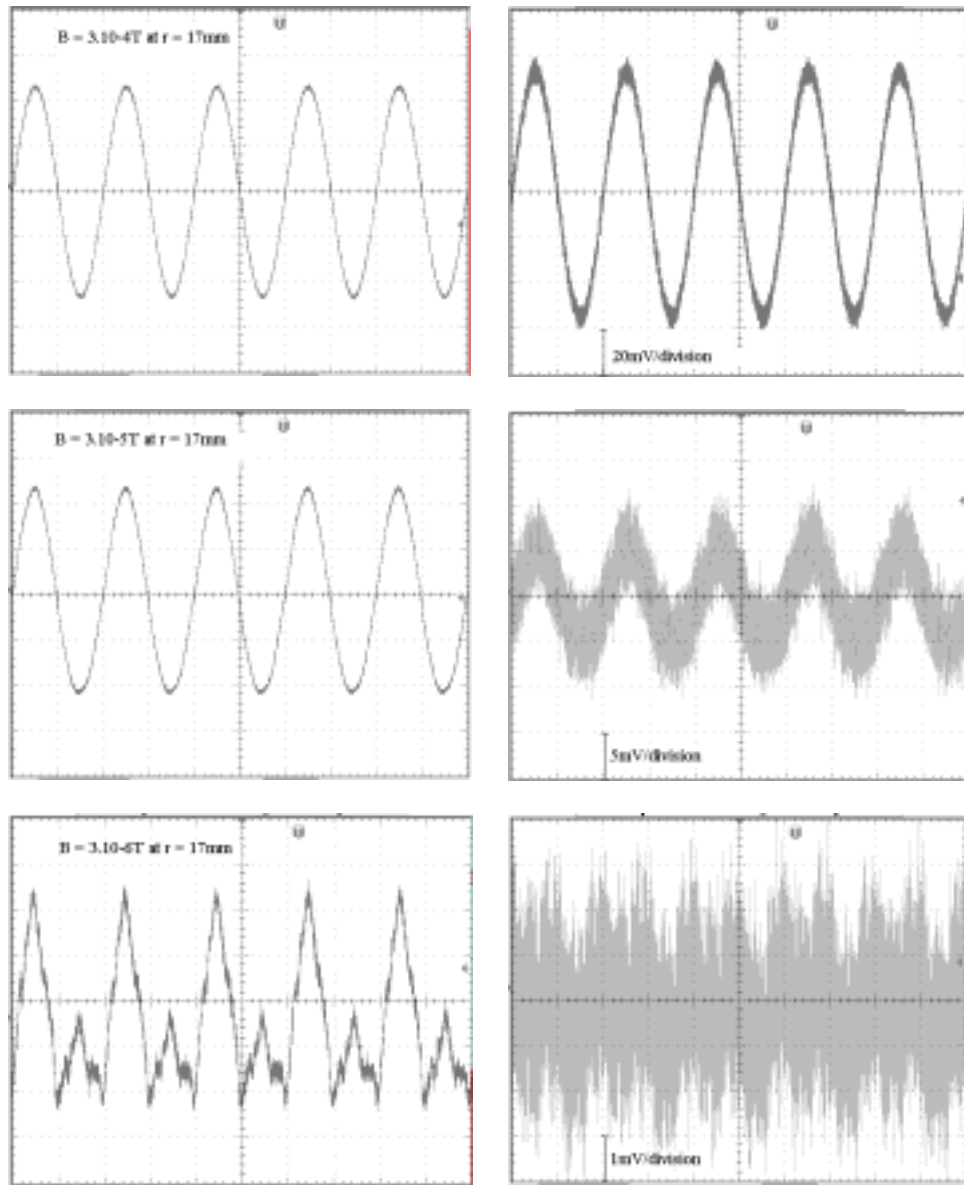


Fig.4

AC field

Coil voltage

Principle of the magnetic axis measurement in a quadrupole field

When the four coils are perfectly centred in the quad, the flux linked in each coil is exactly identical. As soon as an excentration is applied, differences appear and are proportional to this excentration according to Eq.1 and Eq.2. In these equations $\theta = \pi/4$, and $\delta\theta$ is the orientation error around θ . $\delta\theta$ is due to the limited efficiency of the pendulum effect of the mole. It is measured by a gravity sensor and introduced in the calculation, thereby cancelling most of the crosstalk it induces between δx and δy . The residual crosstalk has been calculated for angular errors of $\pm 100\text{mrad}$ and excentrations up to $\pm 2\text{mm}$ and found to be smaller than 0.01mm .

$$\delta x = k_{2N} \cdot \frac{(1 - \delta\theta^2) \cdot (-V1 - V2 + V3 + V4) - \delta\theta \cdot (V1 - V2 - V3 + V4)}{V1 - V2 + V3 - V4} \cdot \cos(2 \cdot \delta\theta) \quad (1)$$

$$\delta y = k_{2N} \cdot \frac{(1 - \delta\theta^2) \cdot (-V1 + V2 + V3 - V4) - \delta\theta \cdot (V1 + V2 - V3 - V4)}{V1 - V2 + V3 - V4} \cdot \cos(2 \cdot \delta\theta) \quad (2)$$

k_{2N} is a coefficient that is dependant on the probe dimensions. Such a coefficient is different for other types of magnets. The measurement is independent of the excitation current level and frequency.

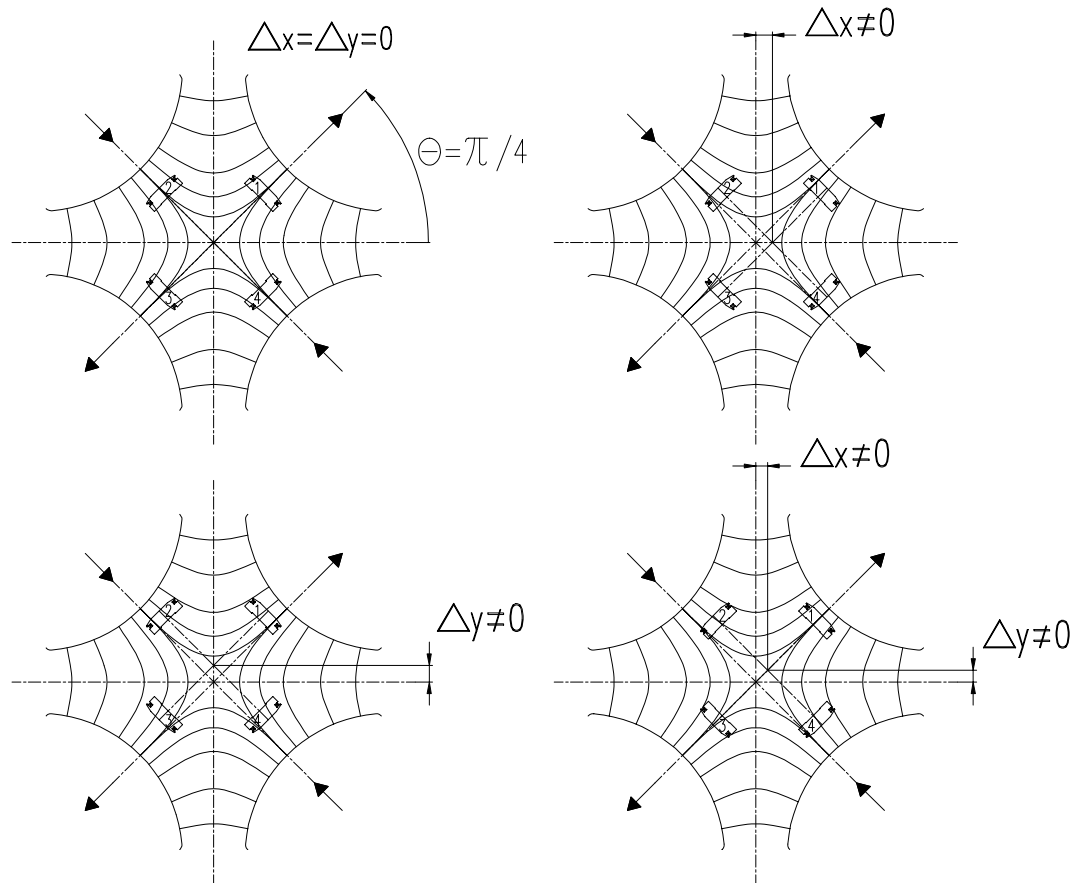


Fig.5 A schematic view of different excentration options

Principle of the measurement of other magnets

By modifying the initial orientation of the probe, it is possible to measure the axis excentration in some other magnets. An application has been studied for most of the magnets used in the LHC machine.

As in the above explanations for normal quadrupoles (B2), a simultaneous measurement of δx and δy can be also made with skew quadrupoles (A2) and normal octupoles (B4). But for normal sextupoles (B3) and normal decapoles (B5), two measurements have to be made on different orientations for δx and δy . A compensation for crosstalk and mis-orientation is proposed.

Measurements with a single probe orientation

Fig. Shows the orientation of the probe for measuring A2, B2 and B4 magnets. In case of a dipole magnet (B1), if the connection point between the two poles is accessible, two identical power supplies exciting these poles in opposition, create mostly a skew quadrupole field (QCD). In each specific case this field contains other harmonics which can be taken into account when they are known to improve measurement.

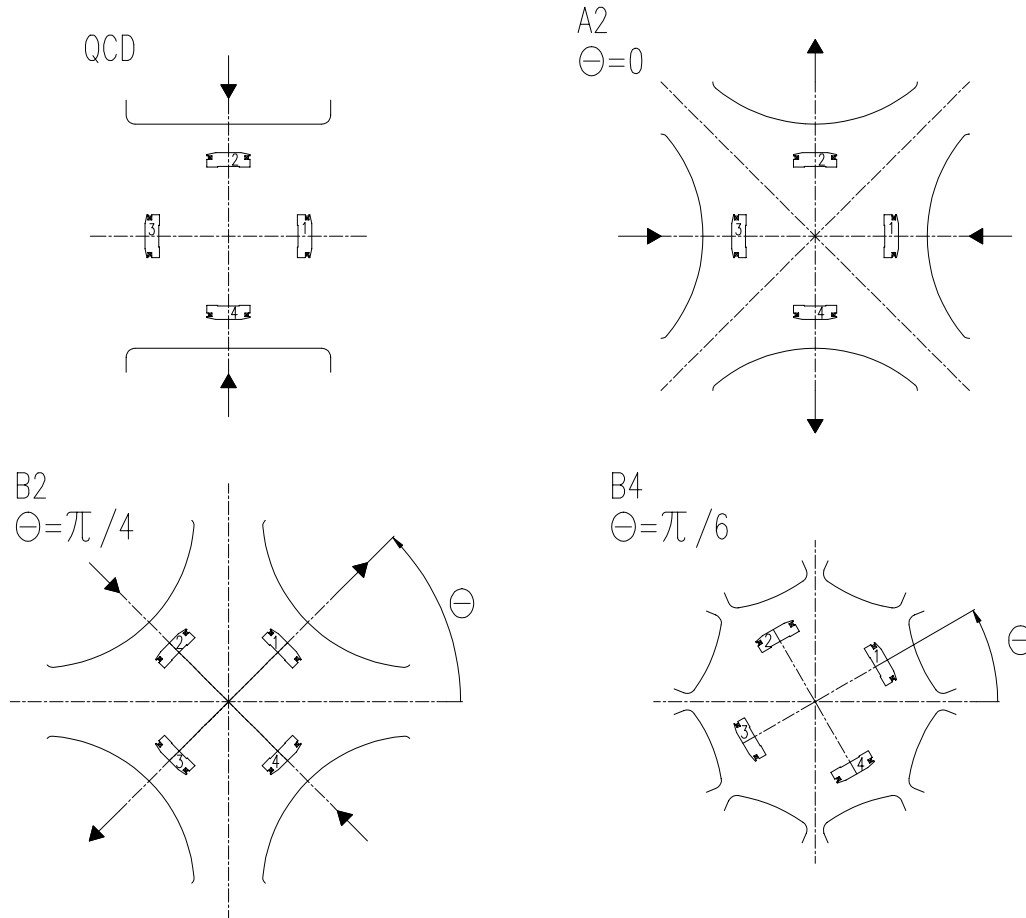


Fig.6 Orientation of the search coil assembly for measuring A2, B2 and B4 magnets

Skew quadrupole magnet (A2)

In a skew quadrupole magnet, the probe orientation is $\theta = 0$

$$\delta x = k_{2s} \cdot \frac{(1 - \delta\theta^2) \cdot (-V1 + V3) - \delta\theta \cdot (V2 - V4)}{V1 - V2 + V3 - V4} \cdot \cos(2 \cdot \delta\theta) \quad (3)$$

$$\delta y = k_{2s} \cdot \frac{(1 - \delta\theta^2) \cdot (V2 + V4) - \delta\theta \cdot (V1 - V3)}{V1 - V2 + V3 - V4} \cdot \cos(2 \cdot \delta\theta) \quad (4)$$

Normal octupole magnet (B4)

In a normal octupole magnet, the probe orientation is $\theta = \pi/6$

$$\delta x = k_{4N} \cdot \frac{(1 - 4 \cdot \delta\theta^2) \cdot (V1 - V3) - 3 \cdot \delta\theta \cdot (V2 - V4)}{V1 + V2 + V3 + V4} \cdot \cos\left(\frac{\pi}{6} + 4 \cdot \delta\theta\right) \quad (5)$$

$$\delta y = k_{4N} \cdot \frac{(1 - 4 \cdot \delta\theta^2) \cdot (V2 - V4) + 3 \cdot \delta\theta \cdot (V1 - V3)}{V1 + V2 + V3 + V4} \cdot \cos\left(\frac{\pi}{6} + 4 \cdot \delta\theta\right) \quad (6)$$

Quadrupole configured dipole magnet (QCD)

In QCD, the probe orientation is that of the skew quadrupole, i.e. $\theta = 0$. An application has been made to the case of the LHC dipole magnet with the last 6 block version. A 1A excitation current would give about $2.1 \cdot 10^{-4}$ T @ 17mm. A current ten times smaller should still be sufficient. The best configuration is that of the two coils in their common yoke and excited in series. Then the calculated harmonics, in units @ 17mm is:

$$a1 = 24.1 \quad a3 = -1.4 \quad a4 = 248.5 \quad a6 = 11.4 \quad a8 = 0.7$$

all the others components being negligible. Due to the dyssimetry introduced by the other magnet, component a1 is not zero. This component corresponds to a systematic horizontal displacement of the QCD axis from the mechanical coil axis of 0.04mm. This is small but can be taken into account as a systematic error. For each component content specific equations can be found to suppress most of the crosstalk and mis-orientation effects.

Measurements with two probe orientations

For normal sextupole and decapole magnets, two measuring orientations are needed to measure successively δx and δy . The two measurements are combined to compensate crosstalk and mis-alignment effects.

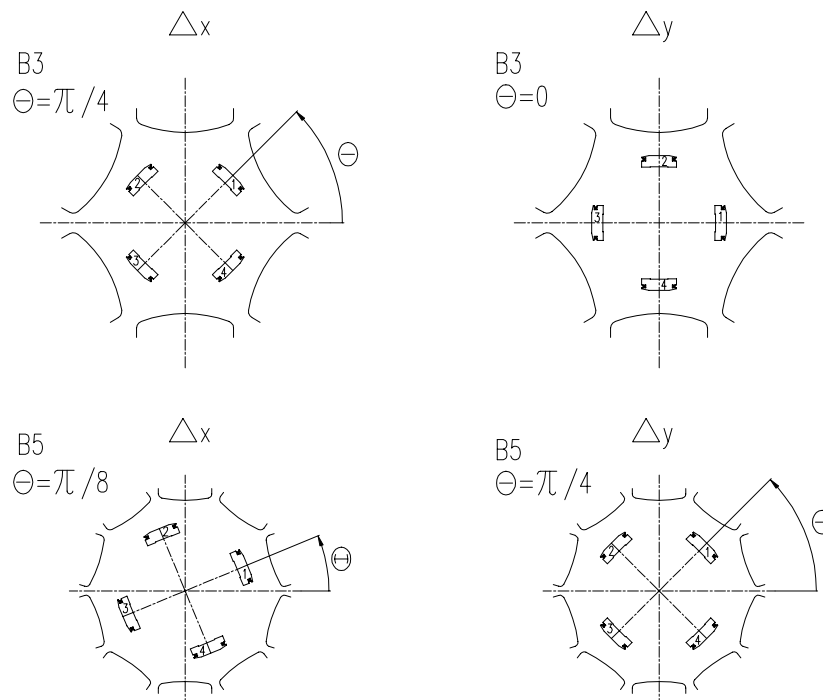


Fig.7 Orientation of the search coil assembly for measuring B3 and B5 magnets

Normal sextupole magnet (B3)

In a normal sextupole magnet, the probe orientation is $\theta = \pi/4$ for measuring δx in a first approximation

$$\delta x = k_{3Nx} \cdot \frac{(1 - 3 \cdot \delta\theta^2) \cdot (Vx1 - Vx2 + Vx3 - Vx4) - 4 \cdot \delta\theta \cdot (Vy2 + Vy4)}{Vx1 + Vx2 - Vx3 - Vx4} \cdot \cos(3 \cdot \delta\theta) \quad (7)$$

In a normal sextupole magnet, the probe orientation is $\theta = 0$ for measuring δy in a first approximation

$$\delta y = k_{3Ny} \cdot \frac{(1 - 3 \cdot \delta\theta^2) \cdot (Vy2 + Vy4) + \delta\theta \cdot (Vx1 - Vx2 + Vy3 - Vx4)}{Vy2 - Vy4} \cdot \cos(3 \cdot \delta\theta) \quad (8)$$

Vx 's correspond to the $\theta = \pi/4$ measurement and Vy 's to the $\theta = 0$ measurement

Normal decapole magnet (B5)

In a normal decapole magnet, the probe orientation is $\theta = \pi/8$ for measuring δx in a first approximation

$$\delta x = k_{5Nx} \cdot \frac{(1 - 5 \cdot \delta\theta^2 - 300 \cdot \delta\theta^4) \cdot (Vx1 + Vx3) + (0.005 + 3.8 \cdot \delta\theta) \cdot (Vy2 + Vy4)}{Vx1 - Vx3} \cdot \cos\left(\frac{\pi}{8} + 5 \cdot \delta\theta\right) \quad (9)$$

In a normal decapole magnet, the probe orientation is $\theta = \pi/4$ for measuring δy in a first approximation

$$\delta y = k_{5Ny} \cdot \frac{(1 - 5 \cdot \delta\theta^2 - 300 \cdot \delta\theta^4) \cdot (Vy2 + Vy4) - (0.005 - 3.8 \cdot \delta\theta) \cdot (Vx1 + Vx3)}{Vy1 + Vy2 - Vy3 - Vy4} \cdot \cos(5 \cdot \delta\theta) \quad (10)$$

Vx 's correspond to the $\theta = \pi/8$ measurement and Vy 's to the $\theta = \pi/4$ measurement

Preliminary tests

Preliminary tests to check the performance of this probe have been done in a small quadrupole magnet. The probe is static and the magnet is moved

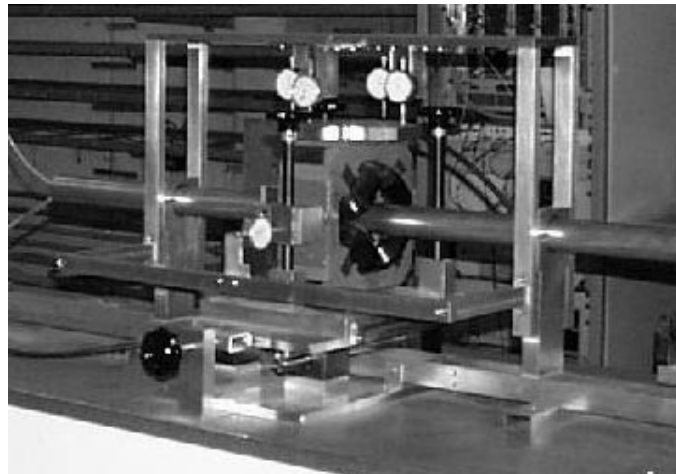


Fig.8 The bench for the tests and calibration of the geometric mole

Excentrations of the small quad have been done by moving the magnet along the x and y axis and the two lines at 45° over ±1mm. The non-linearity errors are within ±0.01mm which are also the limit of measurement precision

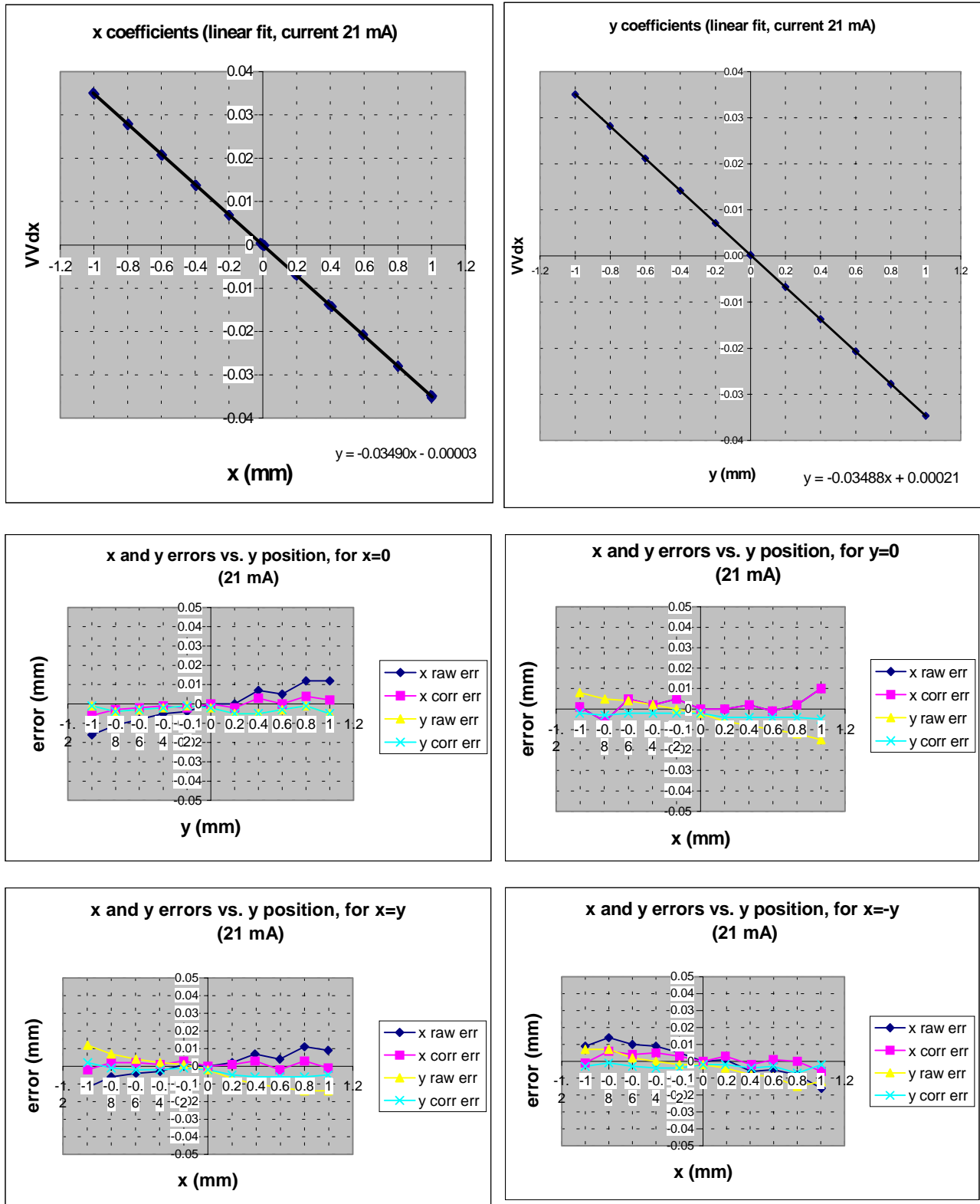


Fig.9 Results of the measurements in a quadrupole magnet



Development of a measurement system for the magnetic field geometry of LHC magnets



◆ Introduction

◆ Measuring system

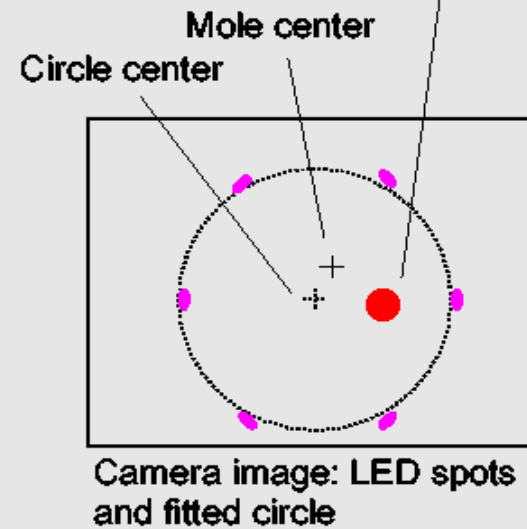
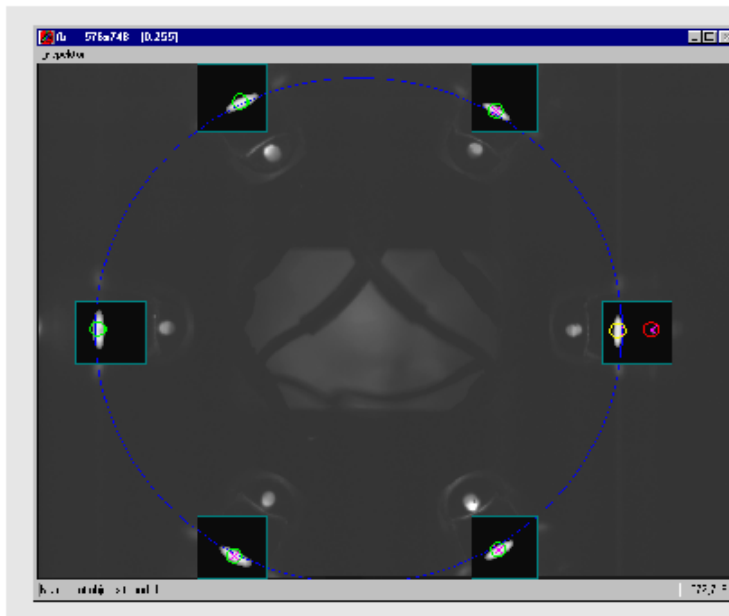
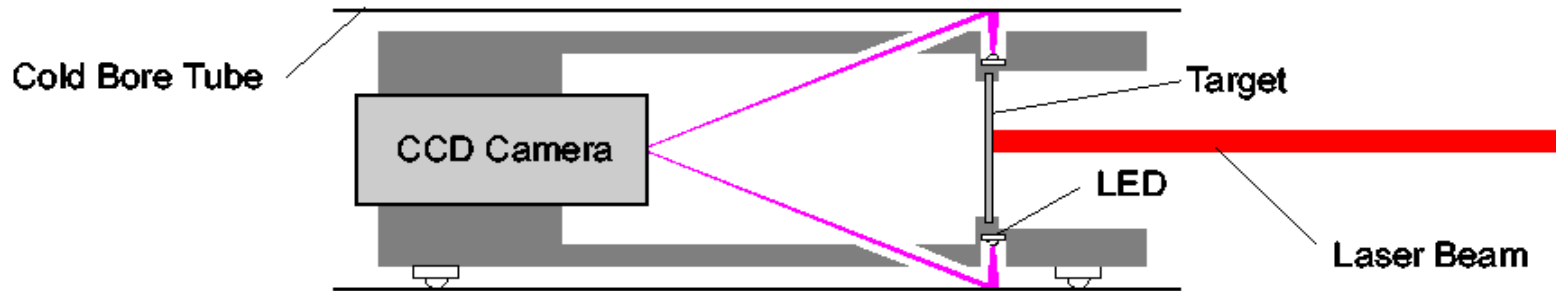
- Geometric mole description and performances
- Global mole description and performances
- Alternative technique

◆ Conclusion



Measure methods

Geometric mole (Version 2)



Christian Rathjen EST/ESI



Optical system components

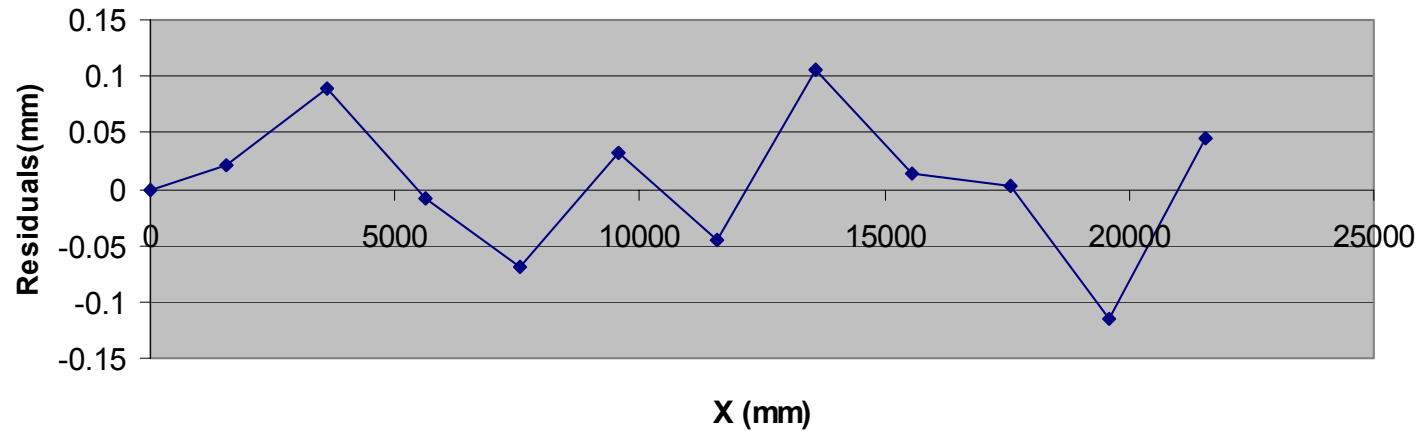


- ◆ Laser diode
- ◆ optical fibre
- ◆ Diffuser
- ◆ Collimating lenses
- ◆ CCD camera

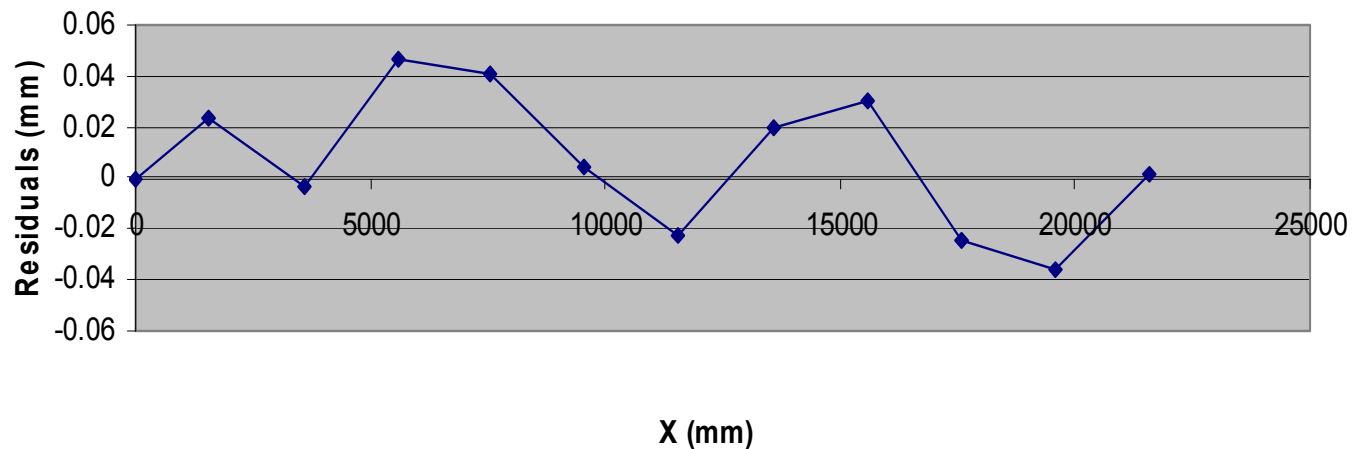


Geometric mole performance

Horizontal Residuals Plot ($\sigma=60 \mu\text{m}$)



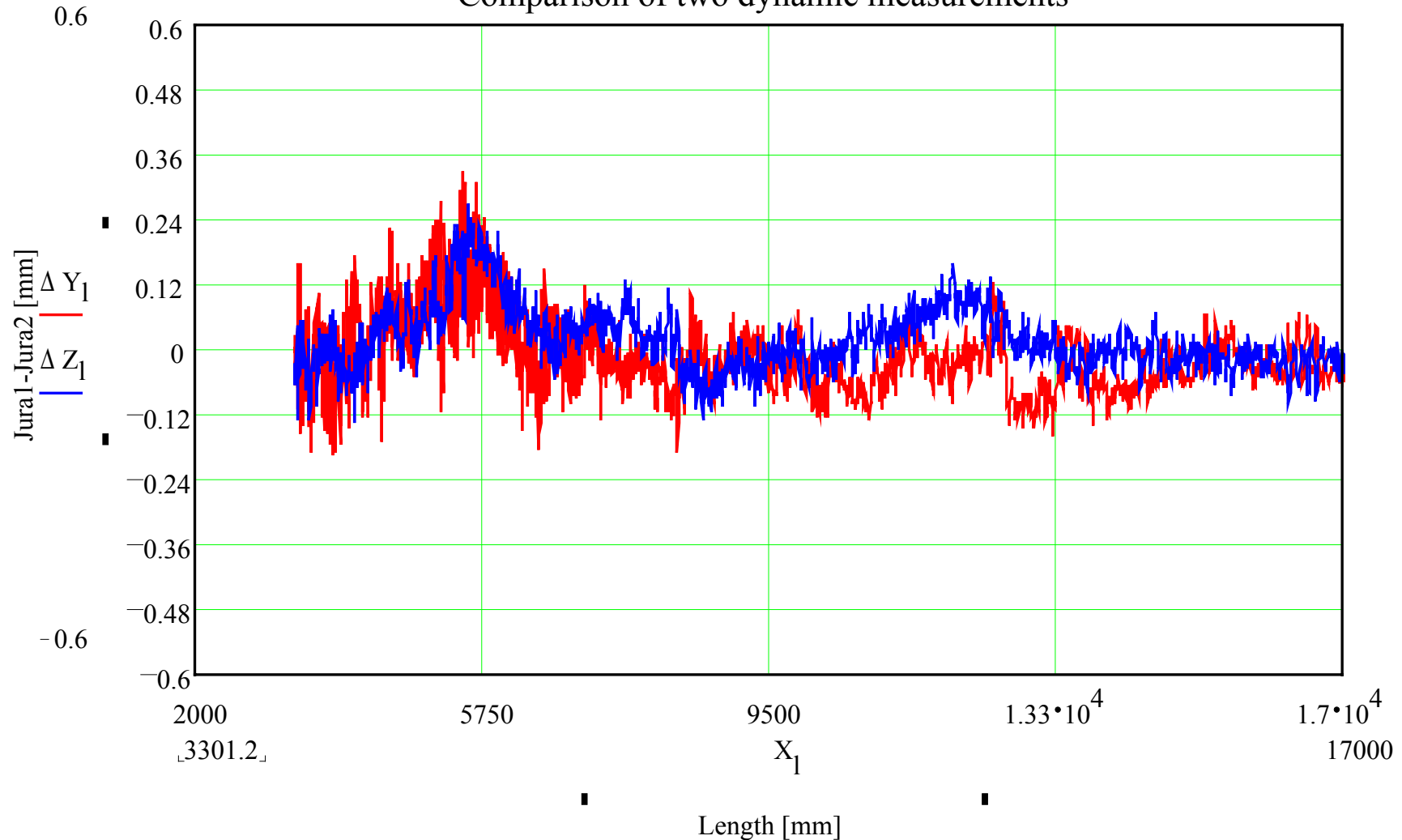
Vertical Residuals Plot ($\sigma=30 \mu\text{m}$)





Getting the mole centre position

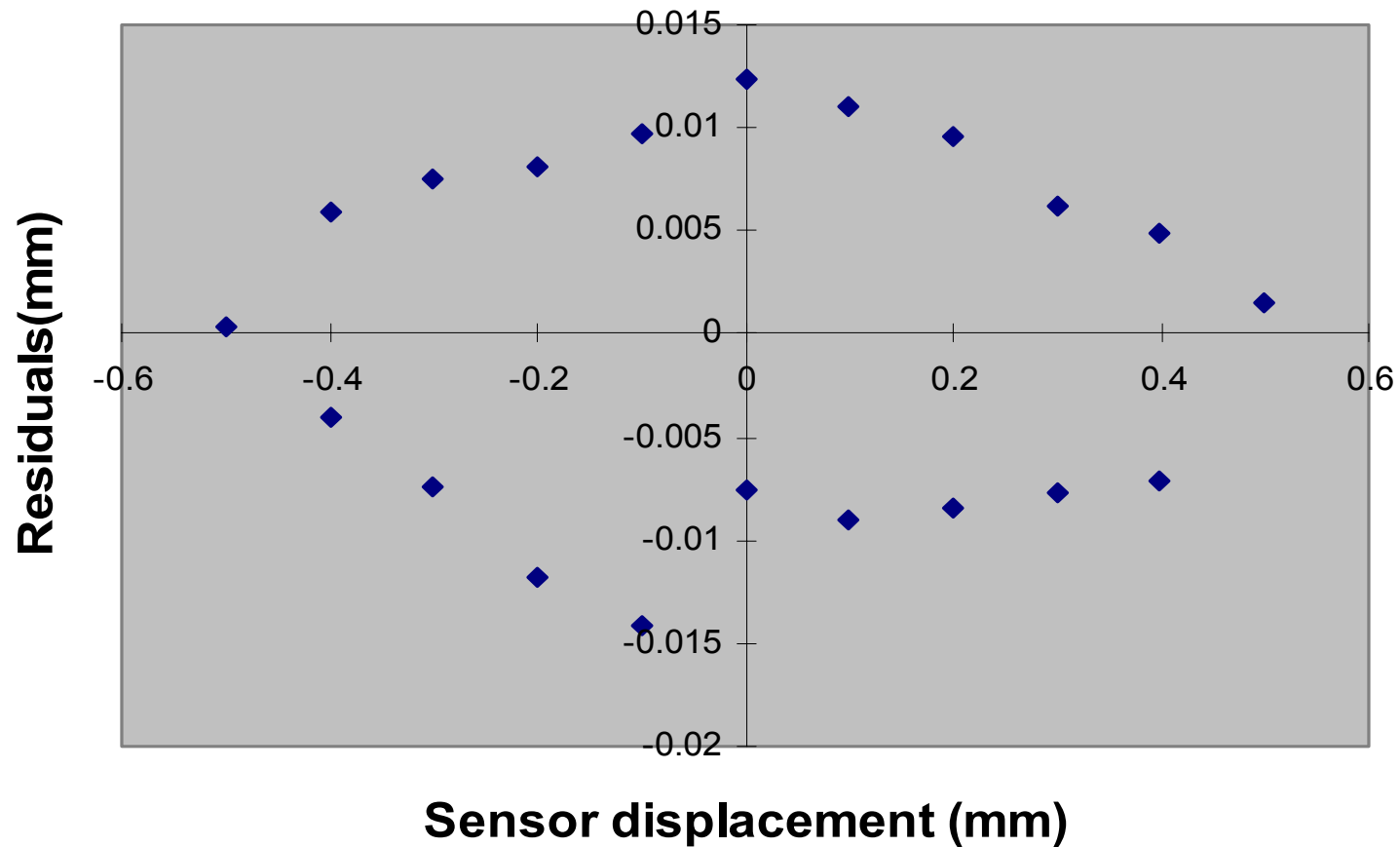
Comparison of two dynamic measurements





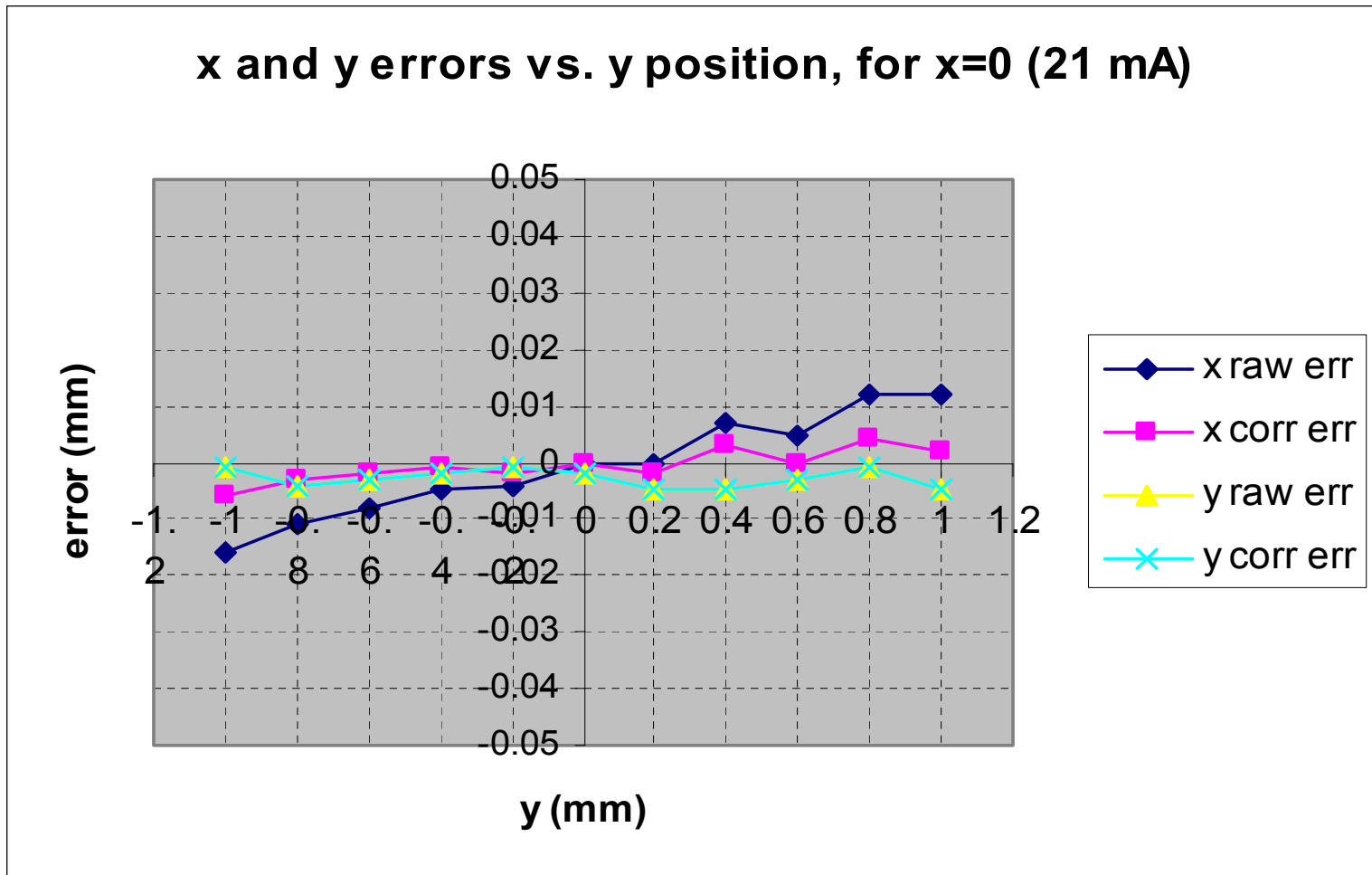
Measure of the cold bore diameter

Calibration Residuals Plot



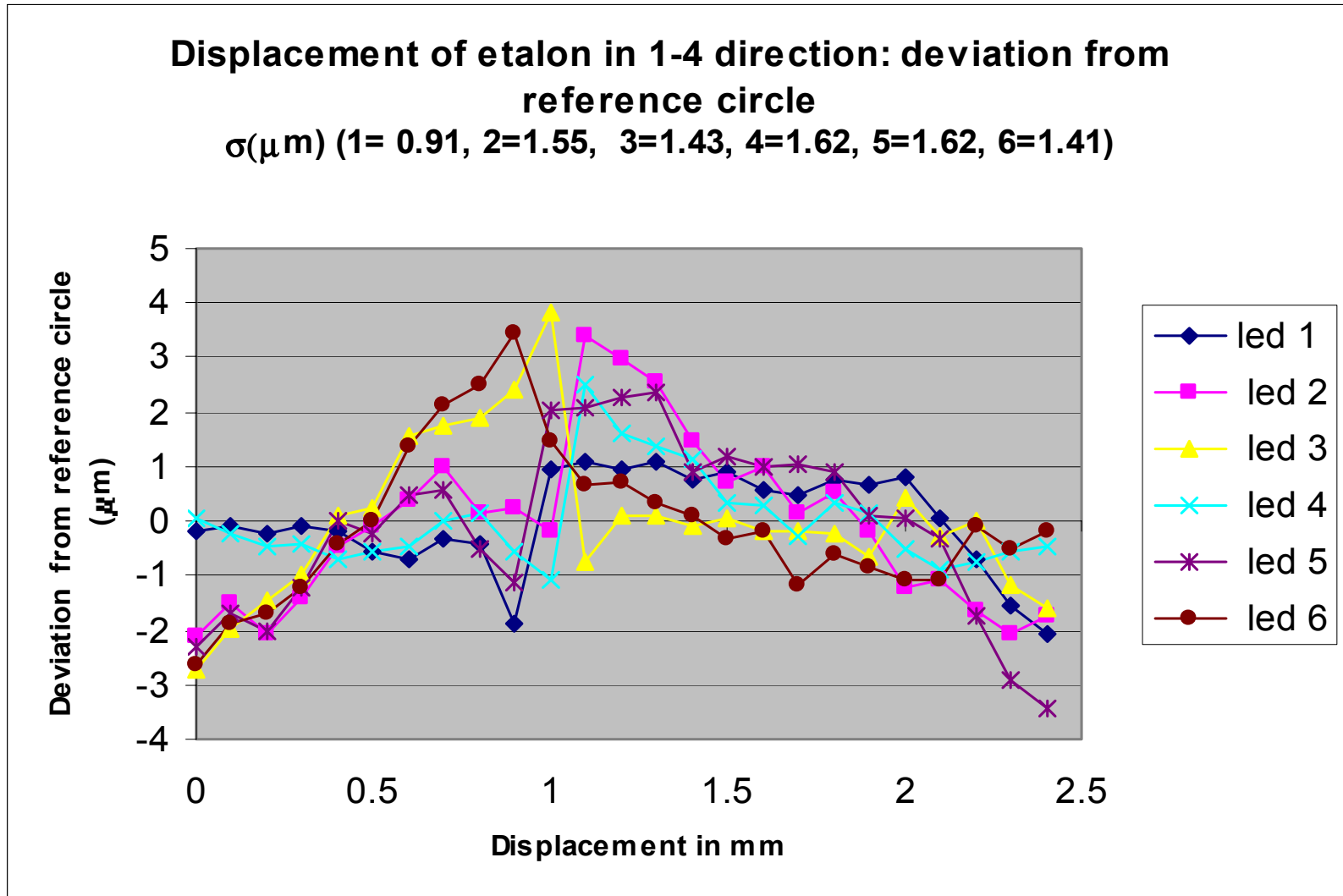


Measure of the magnetic field geometry





LED's calibration results

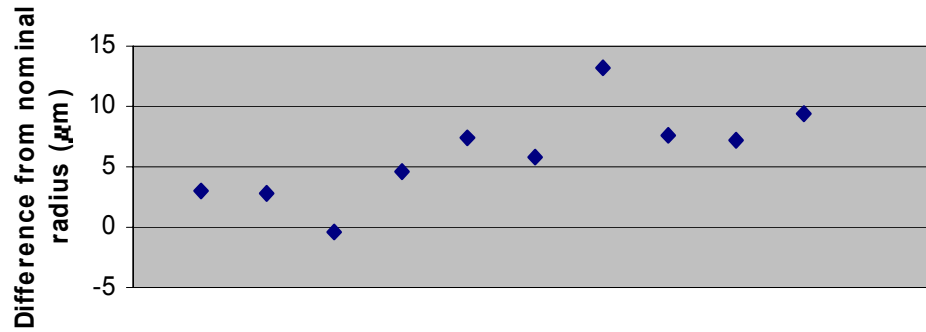




LED's diameter measurements results

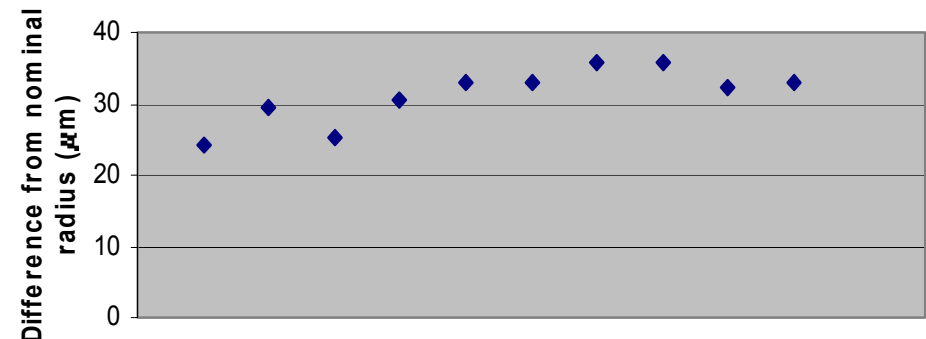
Etalon tube. Nominal radius 25 mm

measured radius 25.002 mm
stdv 0.004 mm



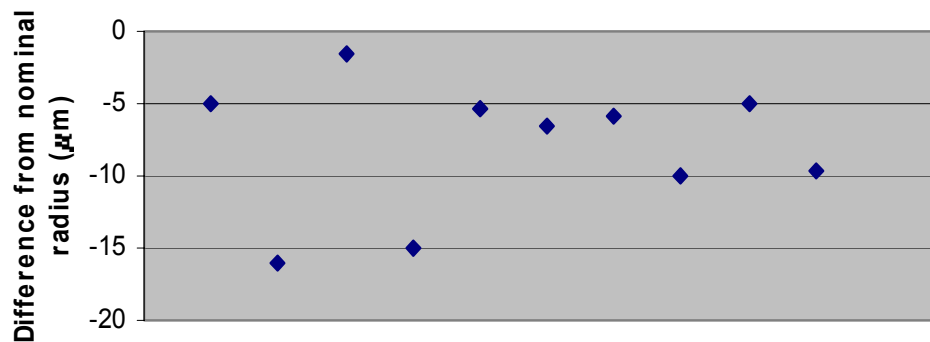
Etalon tube. Nominal radius 24.5 mm

measured radius 24.526 mm
stdv 0.012 mm



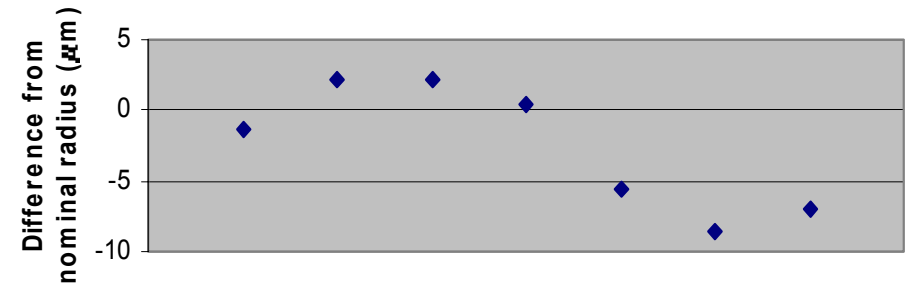
Etalon tube . Nominal radius 25.5 mm

measured radius 25.490 mm
stdv 0.006 mm



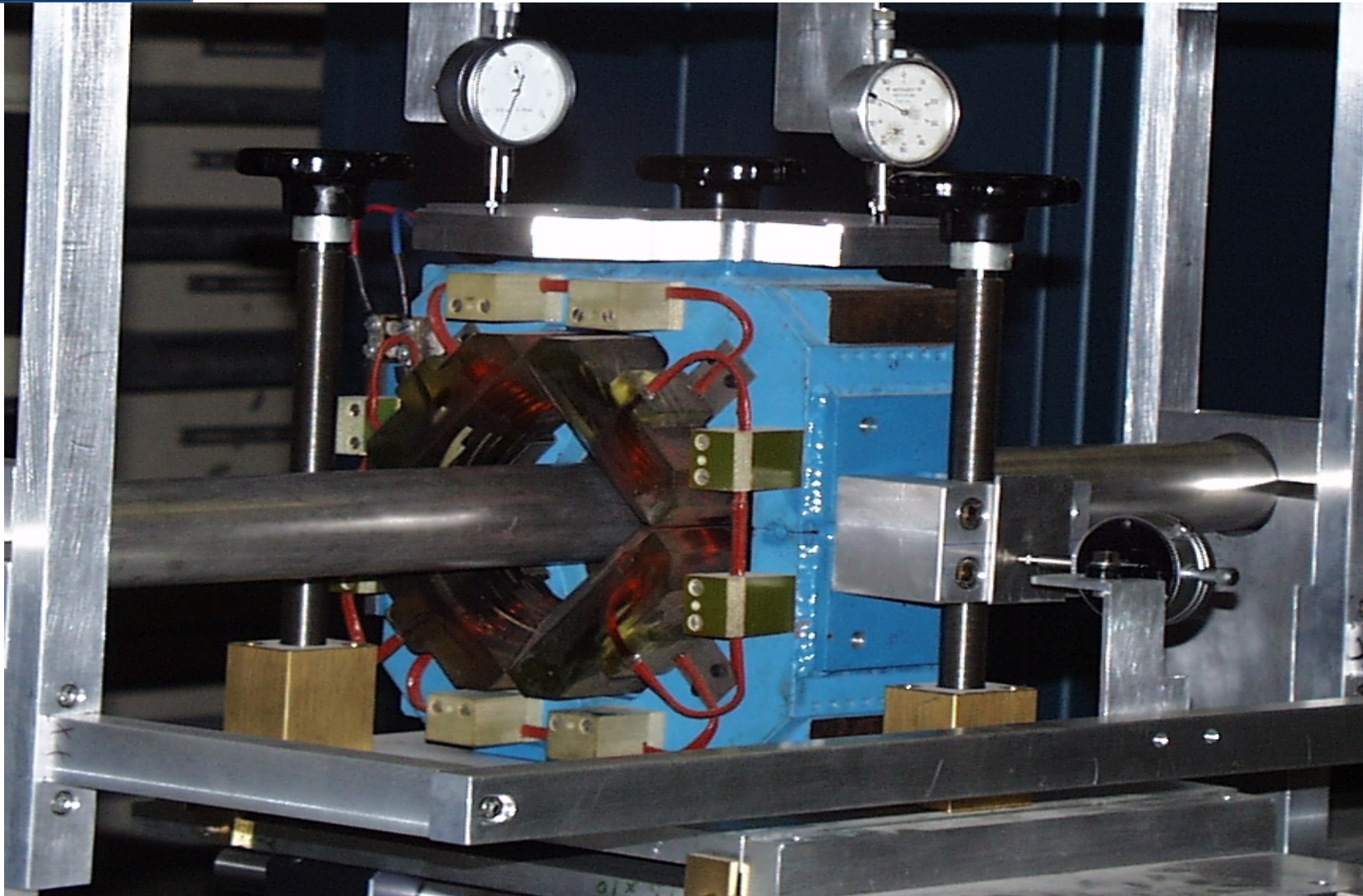
LHC tube. Nominal radius= 25.076 mm

measured radius= 25.073 mm
stdv= 0.005 mm



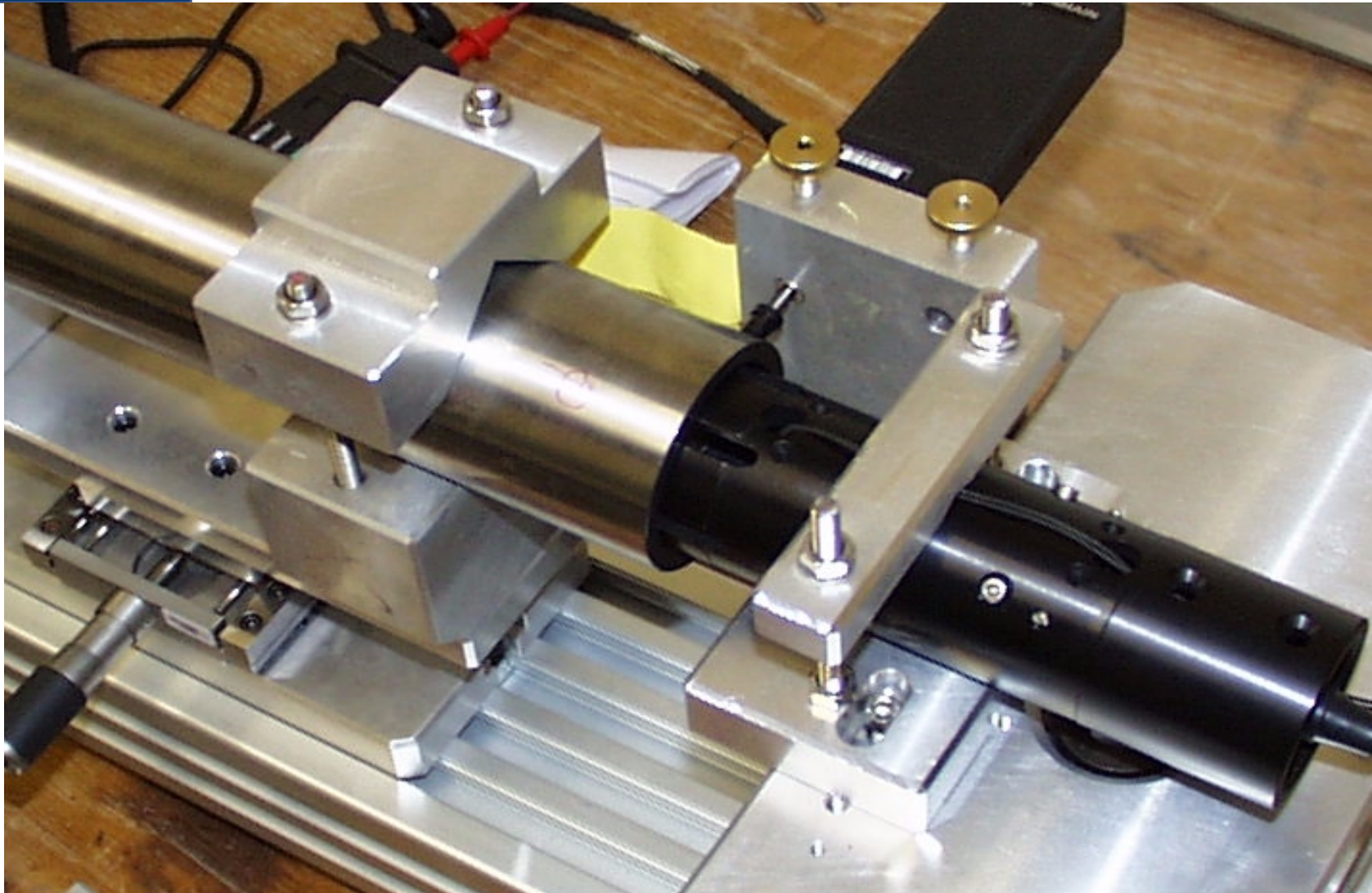


Global mole test set-up for Quadrupole





LED's calibration set-up





Biaxial calibration bench (1)



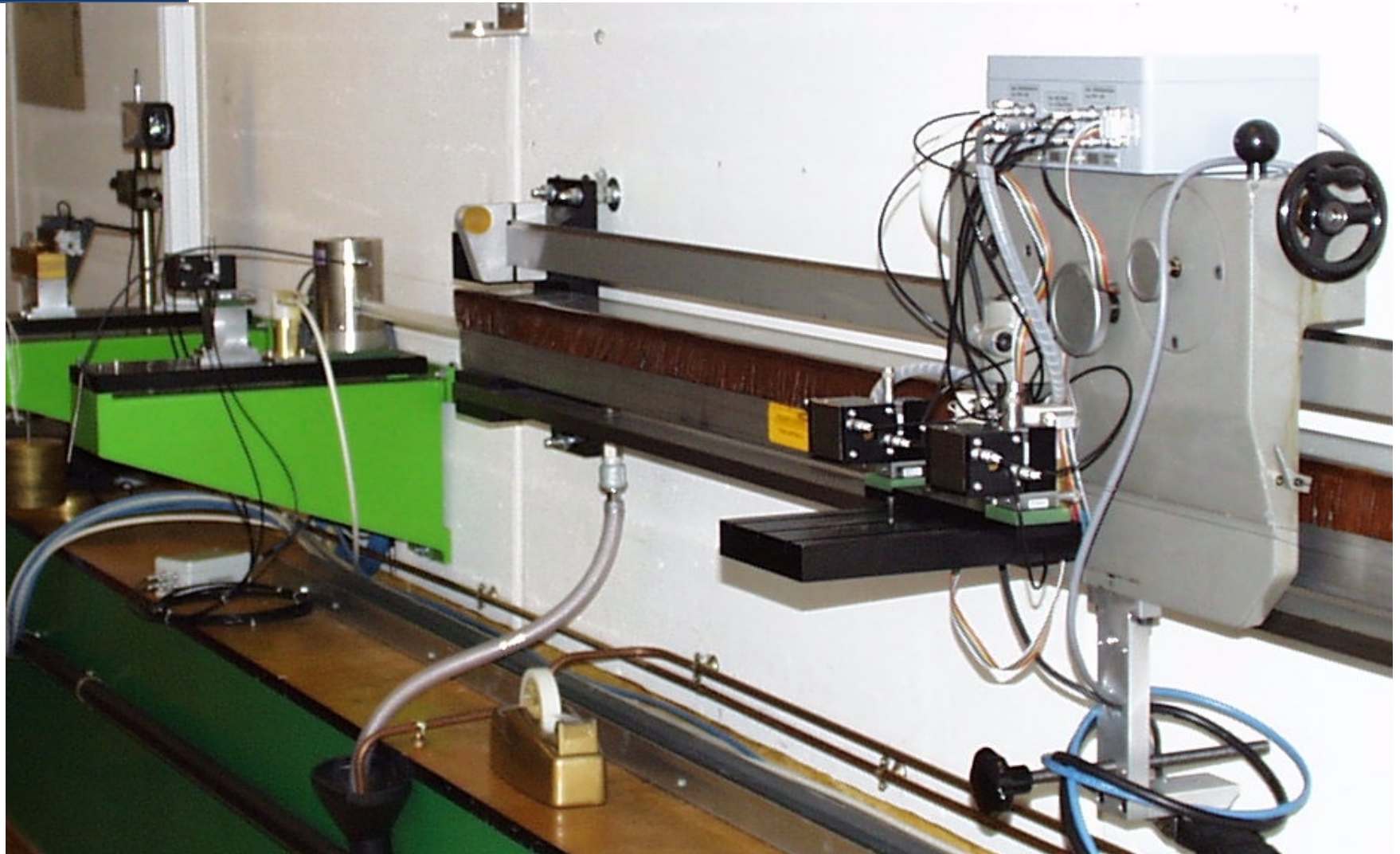
21/9/99

Prepared by J.Garcia

Nice



Biaxial calibration bench (2)



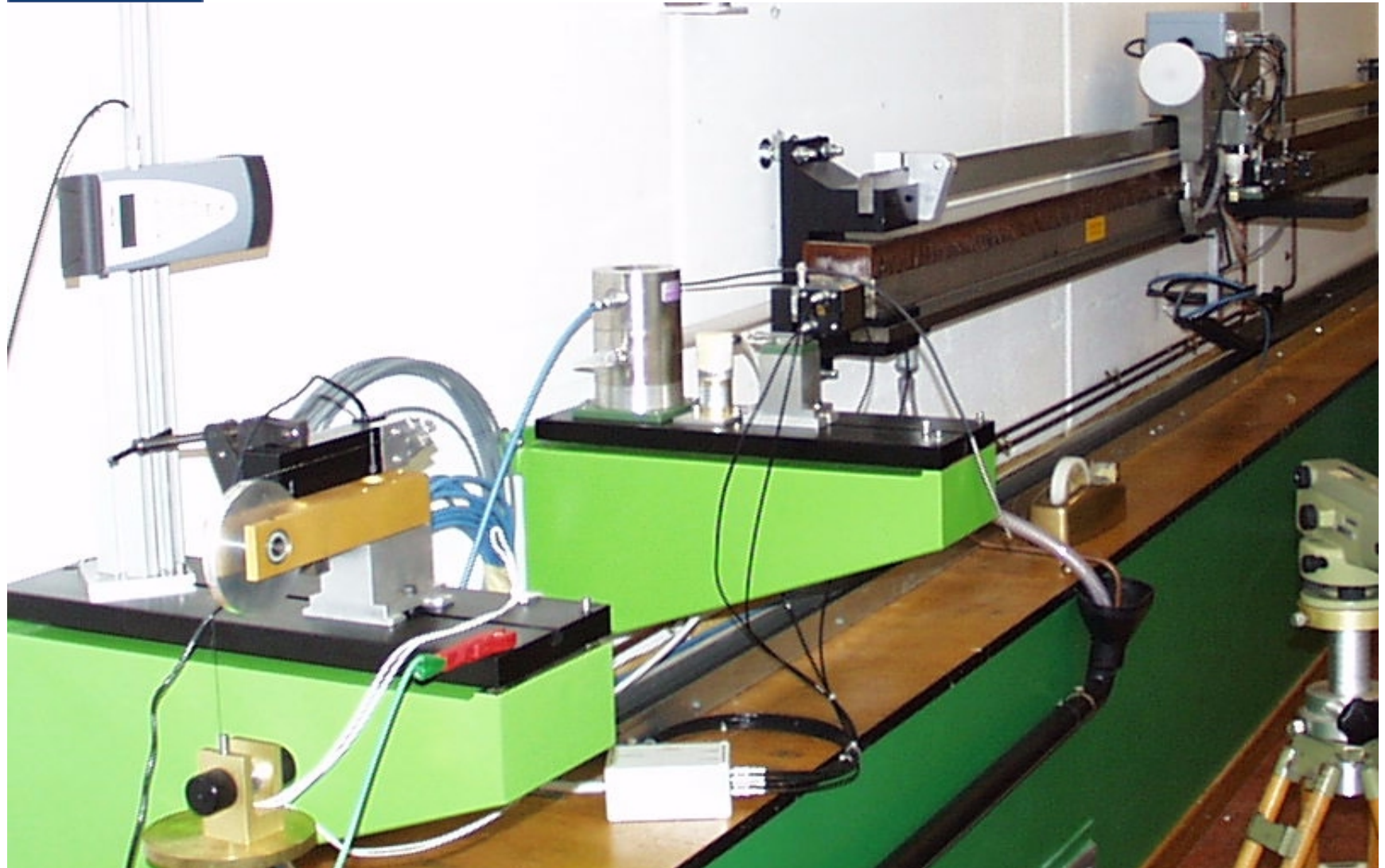
21/9/99

Prepared by J.Garcia

Nice



Biaxial calibration bench (3)



21/9/99

Prepared by J.Garcia

Nice



Geometric mole (1)



21/9/99

Prepared by J.Garcia

Nice



Geometric mole (2)



21/9/99

Prepared by J.Garcia

Nice



Geometric mole (3)





Global mole (1)





Global mole (2)



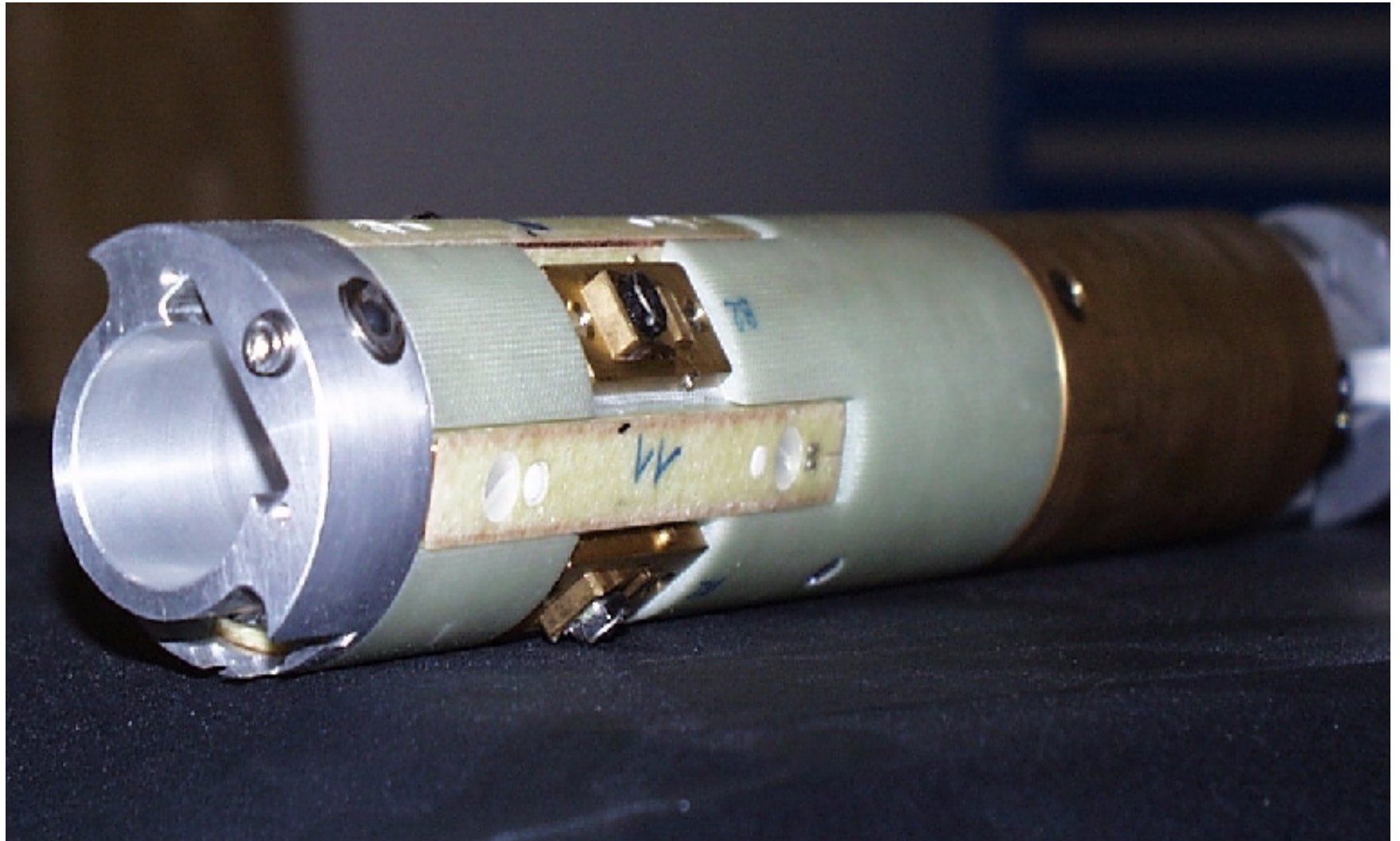
21/9/99

Prepared by J.Garcia

Nice



Global mole (3)



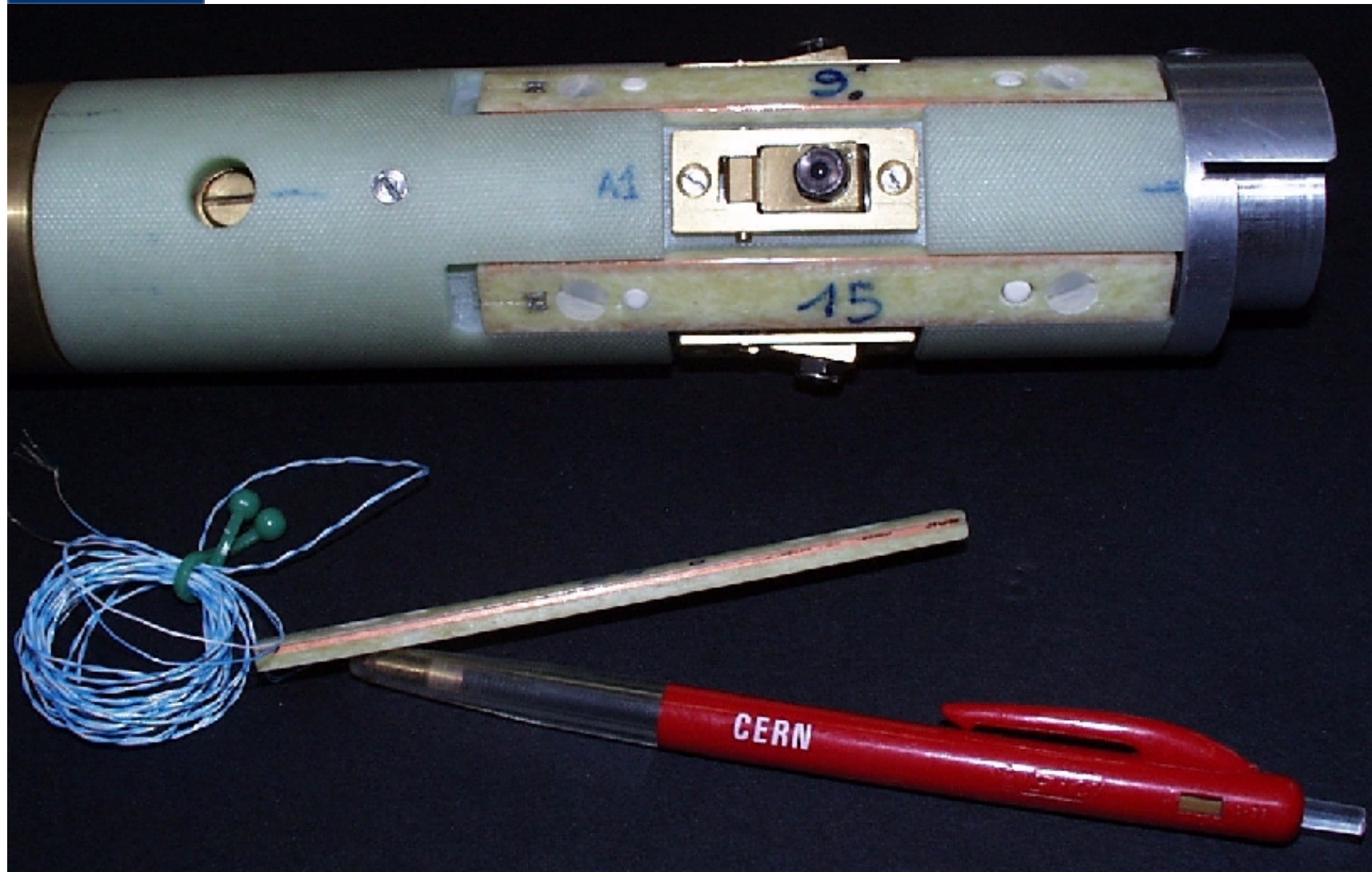
21/9/99

Prepared by J.Garcia

Nice



Global mole (4)



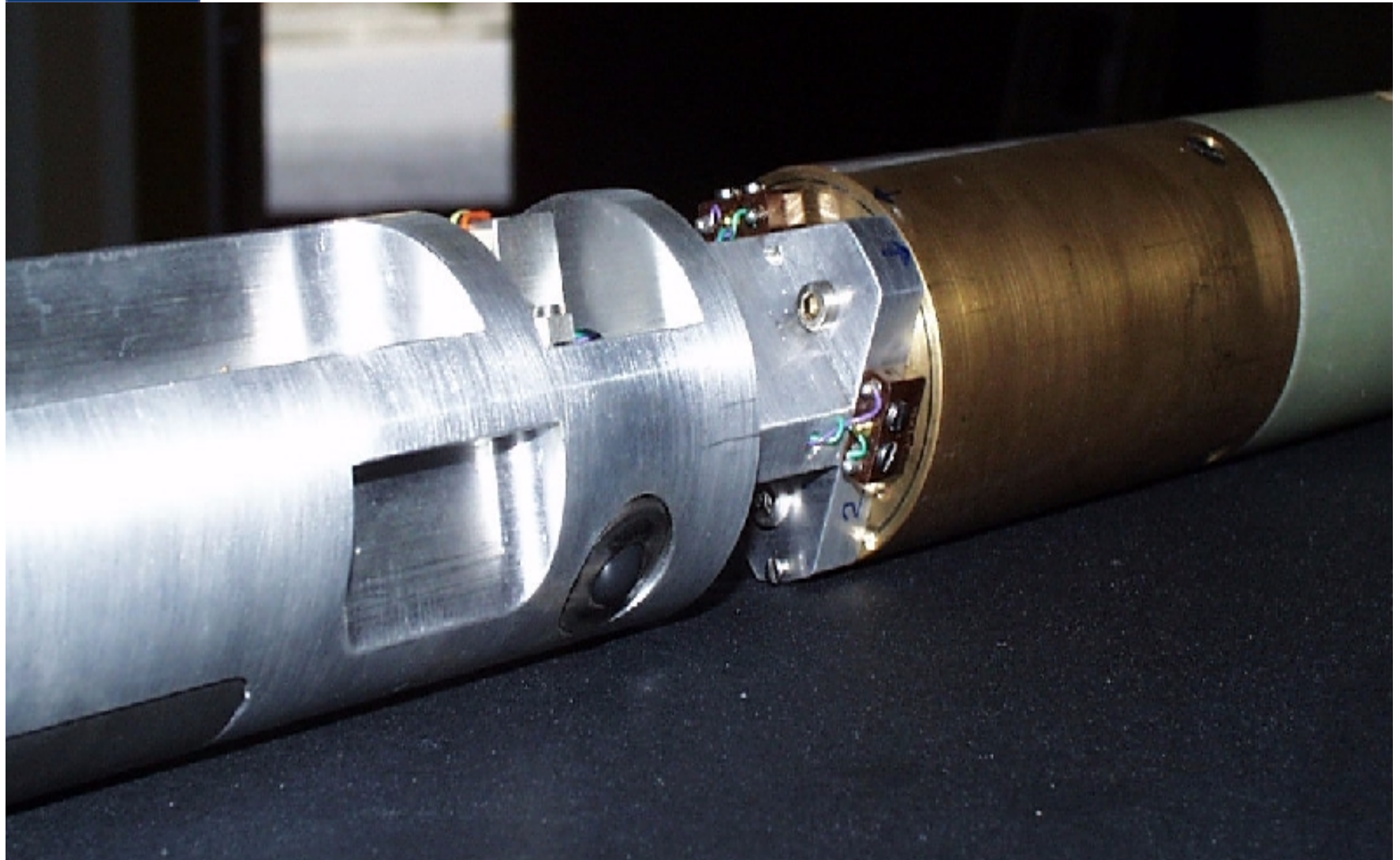
21/9/99

Prepared by J.Garcia

Nice

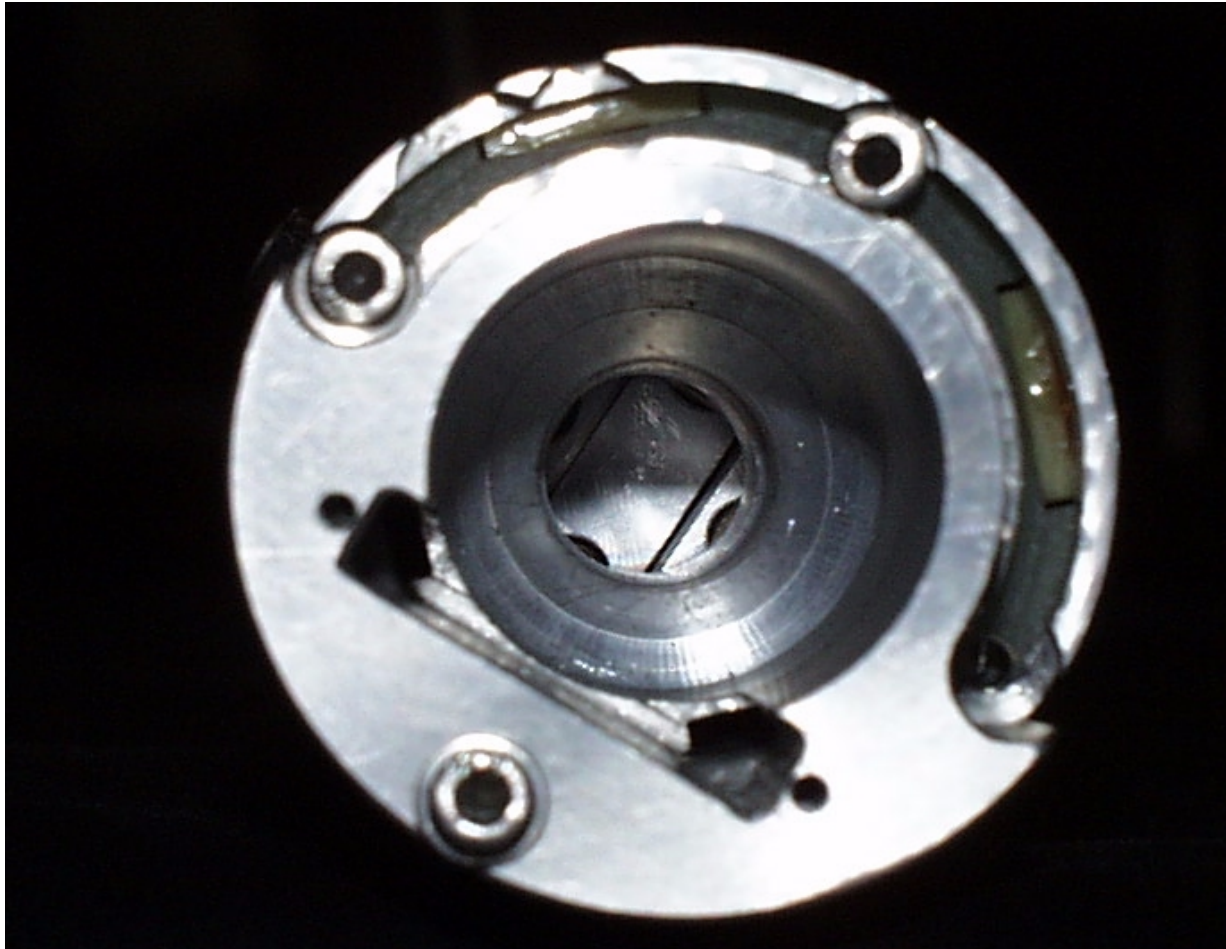


Global mole (5)





Global mole (6)



21/9/99

Prepared by J.Garcia

Nice

Development of a measurement system for the magnetic field geometry of LHC magnets

by Juan García

Abstract

In the context of the LHC superconducting dipoles production it is foreseen to perform acceptance tests, including field measurements of the collared coils assembly to estimate, at an early production stage, the possible significant deviations from the expected multipole component value of these magnets. A sensitive measuring probe and efficient data acquisition are the consequence of a low magnetisation current necessary to limit the coils heating. The knowledge of the magnetic field geometry is very important, especially for multipole magnets. In order to get this information two systems have been conceived. First, a mole miming the magnetic one but equipped only with position sensors laser beam as reference line, target and CCD camera) to complement the magnetic measurement. A second system equipped with magnetic sensors (4 static tangential coils and AC excitation current for the magnet) and position sensors (3D-laser tracker and light reflector) allow the detection of the magnetic field axis and the cold bore axis. Another capability of this system is to work for several field configurations ($n=1, 2, 3, 4$ and 5). This conference contribution describes these two systems and gives the preliminary performance results.

1. Introduction

In the context of the tests of LHC magnets to be perform in the near future, at warm and at the firm premises, instruments to perform these tasks were launched several years ago. Following the development of a magnetic measurement mole (REF) with a principle of a low field level (warm measurements) a geometric mole was designed to complement the magnetic measurement. The idea is to measure the position where the centre of the search coils set of the magnetic mole was when it has done its measurement. So their support feet are miming the magnetic mole ones. The measuring point is situated at the centre of the magnetic coils, and the steps along the tube where it measures are the same as those done previously with the magnetic mole. So the objective is to find the Y-Z co-ordinates of the centre of the coils at every measurement point, X-axis being the cold bore axis.

The technique used is based on a laser beam, which represents a reference straight line aligned onto the cold bore axis and a target plus a CCD camera embarked inside the mole. The position of the laser spot image onto target can be measured with image processing of CCD signal.

A second device with a more ambitious goal has been designed. It has been triggered by the demonstration of a laser tracker (3-D measuring system) with 10 ppm accuracy. It allows a very precise detection of a mechanically well-defined point in space, materialised by a laser reflector (corner cube) fixed at the centre of the mole which travels inside the cold bore tube. Moreover, it has a support system which can centre the mole inside the cold bore and even allows to make two independent measurements of cold bore diameter.

The most important feature of this mole is its capability to measure the centre and direction of the magnetic field. It is done by a set of 4 tangential coils centred on the corner cube reflector. Being fixed the mole at some predefined X position then the magnet to be measured is feed with alternate current. The alternate magnetic field created induces a voltage in the 4 search coils. Analysing these signals is possible to find the magnetic field centre.

It has also the possibility to rotate the detector head in order to get the best orientation of the coils in function of the magnet type to measure. So it has certain universality of use against magnet type (dipole, quadrupole, séxtupole, octupole and décapole).

2. Measuring system

2.1. *Description of "geometric" mole*

It consists of several cylindrical modules interconnected (**fig. 9**) and we can distinguish two main parts. One controls the positioning of the mole inside the cold bore and takes care of the aligning of its Z-axis with gravity. The second one is responsible for the optical measurement of the mole position.

2.1.1. Mole positioning system

In order to measure the position, first one has to fix the mole position and then control the rotation of the mole around its axis. For the first task, once the mole is in the right X co-ordinate, a break is activated, blocking a part of the mole against the cold bore. This avoids a movement of the mole along X-axis. To orient the mole, both ends are provided with two ballast pieces that function as pendulum; is a kind of passive orientation. In addition the mole is equipped with a very small motor, which makes the mole turning around its longitudinal axis until the angle with respect to gravity is lower than 0.5 mrd. A Labview™ program controls the motor guided by the readout of an inclinometer mounted onto the mole. At that moment one is ready to measure the position of the mole with respect to the laser beam line.

2.1.2. Geometry measurement technique

Once the mole is in measuring position the method used to get the coordinates of its centre is quite simple. It is based on the well-known idea of using a laser beam as a straight-line reference (**fig. 1**). So, a diode laser mounted on a special support is feeding a light guide (optical fibre) with at its end is connected a collimating lens device (**fig 2**). This device is aligned in such a way that the light can cover the region of interest. Inside the mole the detector of this light is composed of a target (diffuser) which produces a circular spot as a projection of the laser beam. This spot is detected by a very small (17 mm diameter) CCD camera. A frame grabber acquires the image, and an image-processing program (Heurisko™) makes the analysis. First it filters the background and noise and then evaluates the centre of the spot with a very good resolution (pixel size ~ 90 µm).

So, relatively to this the laser beam line as reference, the position of the opto-electronics device is determined. The device (CCD chip) is itself in contact with the mole. By calibration, the centre of the chip and its co-ordinate axis can be found. We can get then the coordinates (Y-Z) of spot centre. Knowing these centre coordinates along the cold bore length, a fit can be done to estimate its shape in 3-D.

2.1.3. Performance

The main features of this optical system are:

1. Measuring range 25 mm x 20 mm x 20000 mm.
2. Excellent linear behaviour.
3. System noise (without averaging) 2 µm and below.
4. Lateral accuracy better than 0.1% full-scale output for a full field calibration, 0.01% in a range of 1 mm (should also be achievable for the whole measuring range if a calibration device with 1 µm is available).
5. No warm up effects (fibre light guide helps). Measurements can be done immediately after power on.

Noise due to air fluctuations can be reduced significantly when laser and camera are in a tube. In this case the noise doesn't increase significantly with the distance.

The motor has been tested with its control program, and it is able to keep the mole oriented with gravity within ±0.5 mrd. It takes only one or two iterations (about 1 minute) to get in best position.

The main test has been done in a special biaxial (X-Z axis) test bench. It uses high precision capacitive sensors and inclinometers. The vertical reference line is made by a hydrostatic levelling ($\sigma = 2 \mu\text{m}$), and the horizontal one by a stretched wire ($\sigma = 5 \mu\text{m}$). The body camera module (target and CCD camera) is mounted on a chariot which is displaced on to a rail in steps of 2 m (X position measured with a manual distancemeter with 1 mm precision). The position in space of the target centre is measured with our system, and compared with the one get from the test bench. Making the hypothesis that the laser gives a straight line, but not perfectly parallel to the axis of the bench, the residuals from the comparison are obtained.

We can see the results of these tests on the graphs for both Y-Z co-ordinates (**fig. 3**). The residuals plot for the vertical co-ordinate ($\sigma=30 \mu\text{m}$) is better than the horizontal ($\sigma=60 \mu\text{m}$). This can be due to a wrong behaviour of the sensors used for this axis (stretched wire capacitive sensor). As well

known from laser propagation behaviour, vertical axis is more critical (ambient temperature gradient). Vertical co-ordinate is measured by hydrostatic level. So we can believe that both co-ordinates could be better than 30 μm .

2.2. Description of "global" mole

A second system called global mole (**fig. 10**) has been designed with the aim of measuring in one go the geometry of the magnetic field and the cold bore with respect to an external reference system, with the help of a laser tracker. The mole has a centre defined mechanically around which are placed with very good precision the three main sensors:

1. 4 tangential coils,
2. 4 diameter measuring legs
3. the corner cube reflector with its centre in that point

We keep the mole oriented vertically by a ballasting system. It consists of Tungsten piece at the bottom of the mole which avoids it turns too much. Moreover it is equipped with a good levelmeter in order to measure any deviation from vertical, which is used in the calculation needed for the magnetic sensors.

2.2.1. Getting the mole "centre" position

To get the position of the mole in space (external reference) a laser tracker is used. A laser tracker is a portable 3D measuring system, having a precision better than 10 ppm (at 2σ). It sends a laser beam onto a small corner cube reflector that is placed at the point to measure. The head, source of the beam, is then oriented until the laser is get back on the detector. The angles of this orientation and the distance measured by interferometry are then the three polar coordinates.

In our application, the corner cube is a cylindrical prism that is inserted in the axis of the mole, and its centre is placed at the median plane of the 4 tangential coils. So measuring this point, we know where the centre of the mole is.

2.2.2. Measure of cold bore diameter

Two pairs of mobile legs allow the centring of the mole inside the cold bore. They follow two radius of the mole at the same median plane as for the reflector. They can be retracted, by a compressed air system, to freely move along the cold bore to change position. Otherwise, during measurement they are in close contact with the cold bore wall. These legs are connected with two linear sensors by a mechanism that transforms the radial displacement in a longitudinal one. Each pair of legs gives then a diameter measurement at the cold bore tube cross section.

So, with this device we can know the centre and diameter of the cold bore at test point related to the external (laser tracker) reference system.

2.2.3. Measure of magnetic field geometry

The magnetic system of the mole is composed of 4 tangential coils placed in square vertices, and separated 45 degrees from the diameter measuring legs. They are centred around the mole centre, and are 10 cm long, running along the mole axis direction. The whole head can be turned around the mole axis to get best performance for different types of magnets (dipole, quadrupole, sextupole, octupole, and decapole) [3].

Powering the magnet with alternate low frequency (25 Hz) small current (20 mA) and reading synchronously the induced currents in the coils we can measure the centre of the magnetic field. In the special case of a dipole (no centre) each pole can be powered differently and we obtain a skew quadrupole. Relating the three sensors results, the position of the field centre can be expressed in the external reference system, or with respect to the cold bore centre.

2.2.4. Performance

For this system the three main sensors have been tested.

1. Repeatability of the position measurement through a cold bore with the Laser Tracker. The mole was equipped with a corner cube reflector, and introduced in a test 17 m long cold bore. It has

been displaced manually in a continuous mode through the tube and the laser tracker was measuring 1000 times per second its position. Then a mean integrating over 10 mm was obtained from these positions. One must say but the system was thought for static measurements but nevertheless the test gives an idea of the precision one can get. The plot (**fig. 4**) illustrates this result. The repeatability, even in these conditions, is better than 0.1 mm for both coordinates.

2. Calibration of the two diameter measurement sensors. A calibration of this device has been performed taking special care of the symmetry around the mole centre of every pair of legs. A calibration set-up has been realised to check this with a good precision. The residuals of this calibration are shown in the plot (**fig. 5**) for one sensor. There are several residuals per point because measurements are repeated in forward and backward direction, and there is some mechanic play. Nevertheless is better than 15 μm .
3. Coils calibration on a Quadrupole magnet over ± 1 mm (X-Y). The mole was inserted in a short piece of cold bore. The whole set was introduced in the air gap centre of a quadrupole and then fixed in a support. Exciting the magnet with a small alternate current the induced currents in the coils were synchronously read out. A grid of X-Y positions covering ± 1 mm was fill. Expected displacements are only a few tenths of a mm. An example of the residuals is shown in the plot (**fig. 6**), residuals are better than 10 μm .

2.3. *Alternative technique*

2.3.1. LED's technique

To measure the cold bore diameter and its centre a new technique has been developed (**fig. 1**). On the laser target support a set of 6 LED's have been added each on one-hexagon vertex. LED's light is shining in radial direction on to the cold bore inner surface producing six bright spots. These light spots are visible from the CCD camera through six longitudinal holes made in the camera body module. The position of these spots is measured, and using a triangulation method one can estimate the position of six cold bore's inner circle points. Fitting these points to a circle we can get the cold bore centre and the estimated diameter at that particular section. Before doing that one has to make the appropriate calibration. So, applying the method to several calibrated tubes we can get the different parameters of this technique.

This method doesn't disturb the measurement of the mole position with a laser reference technique as one can see in the same picture; the laser spot is well separated from the six LED's ones. Combining the two optical methods the cold bore tube shape can then be measured in a purely optical way. The advantage of this approach is that a precise mechanical guidance and calibration of the camera centre are not necessary any more. It is planned to try this method in the global mole to be able to work even when a laser tracker is not available.

2.3.2. Performance

A calibration has been made with a 50-mm diameter calibrated tube (about 2-micron accuracy). From this calibration a set of parameters has been obtained. Using this parameters to measure two other tubes of the same characteristics but of a 51 and 49-mm diameter one can obtain the residuals from the nominal values. It has been checked the stability of the results turning the tubes around their axis, and even inclining the tube axis with respect to the camera body module axis. So we can check the fitted centre position and diameter. Finally a real test was done on a piece of a cold bore with quite different reflectivity. Its diameter and shape was previously carefully measured.

In the plots the results of this tests are shown. In the first set of plots (**fig. 7**) we see the deviations of every LED signal from the fitted circle, when displacing the tube horizontally up to 2.5 mm. They are smaller than 5 μm , and even better for the LED's aligned with the movement direction. In the second set of plots the results of the diameter measurement is shown. As mention above calibration was done on the 25-mm radius tube. Ten diameter measurements have been done turning the object tube around its axis an arbitrary angle. The residuals shown in the plot (**fig. 8**) have a standard deviation of 4 μm . Going to 1 mm smaller and bigger calibrated tubes, the σ is 12 and 6 μm

respectively but there is a small offset. If then one measures a sample of LHC tube, the σ is 5 μm without any offset.

3. Conclusion

Several techniques to help in the measurement of the magnetic field geometry of the LHC magnets have been implemented in two moles. The results are quite promising. The techniques are robust and easy to use. They take advantage of the optical methods where mechanical contact is minimised. Some more tests, on real magnet conditions, are still to be performed and they are planned to be done soon.

4. References

- [1] J. Billan, "Ambient Temperature Field Measuring System for LHC Superconducting Dipoles", CERN AT-95-21, LHC Note 332
- [2] Christian Rathjen, "Optical method to align and measure long structures", Technical Note CERN EST-ESI/99-10
- [3] J. Billan, "An AC field static system for measuring the magnetic axis of LHC superconducting magnets in warm condition", Paper presented at this conference IMMXXI.

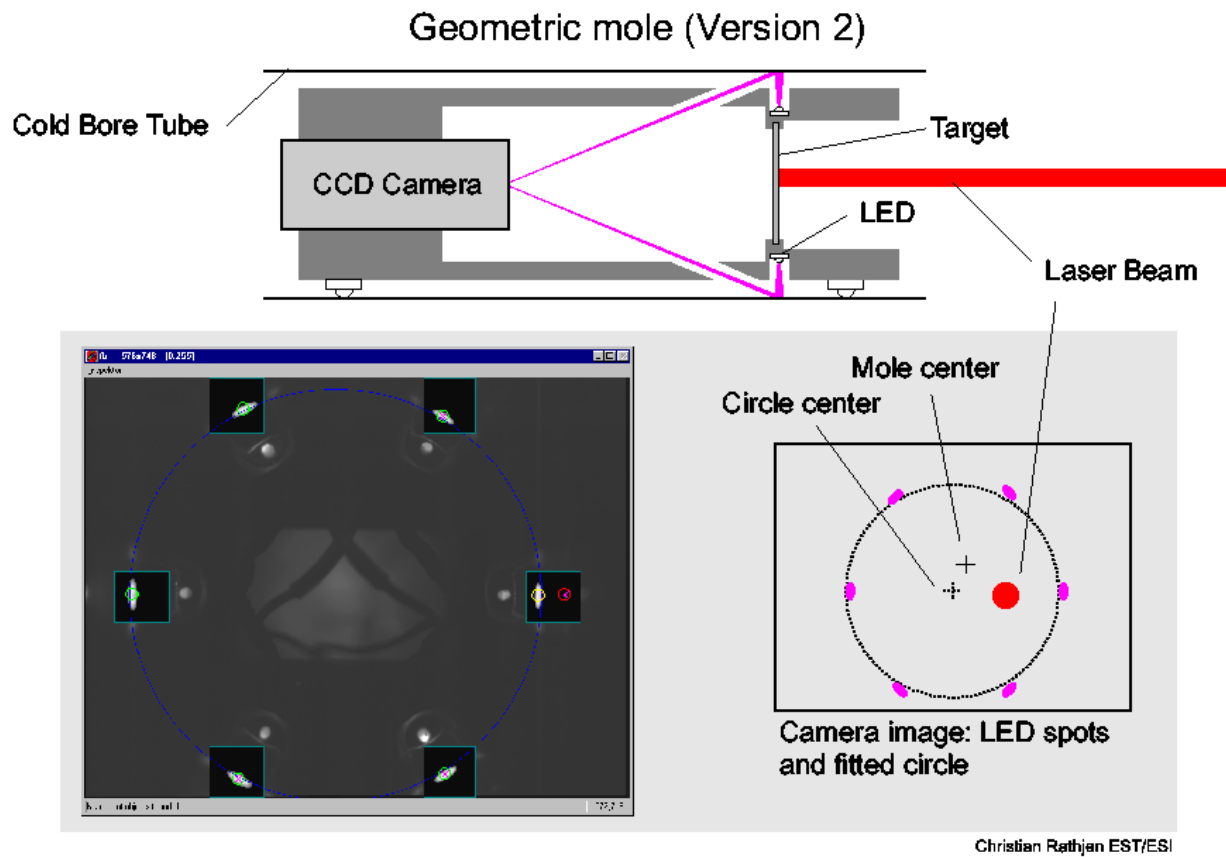
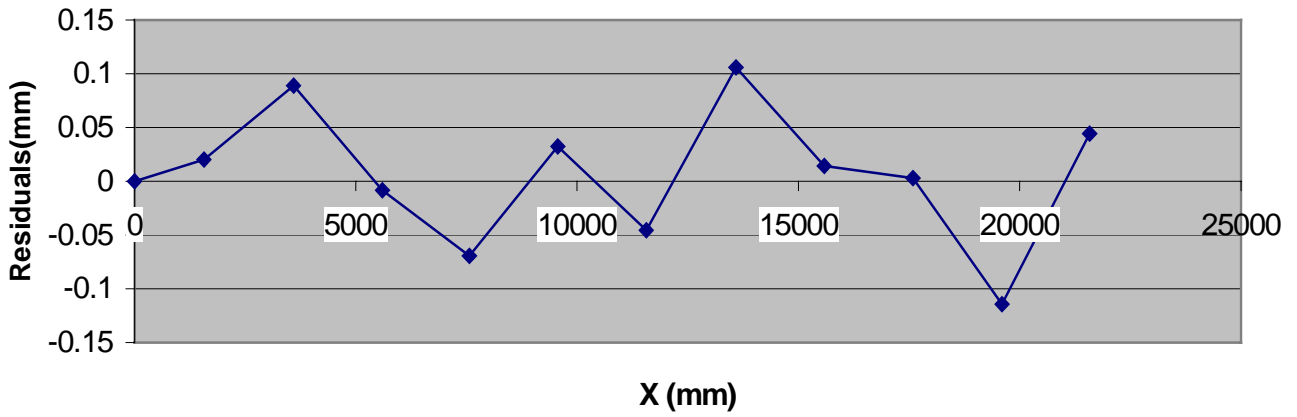


Figure 1 Method of measurement for a cold bore using Laser beam as a straight-line and LED's to find the cold bore shape and LED's for diameter estimation.



Figure 2 Components of the optical device: Laser diode, optical fibre, and collimating lenses, beam diffuser and miniature CCD camera.

Horizontal Residuals Plot ($\sigma=60 \mu\text{m}$)



Vertical Residuals Plot ($\sigma=30 \mu\text{m}$)

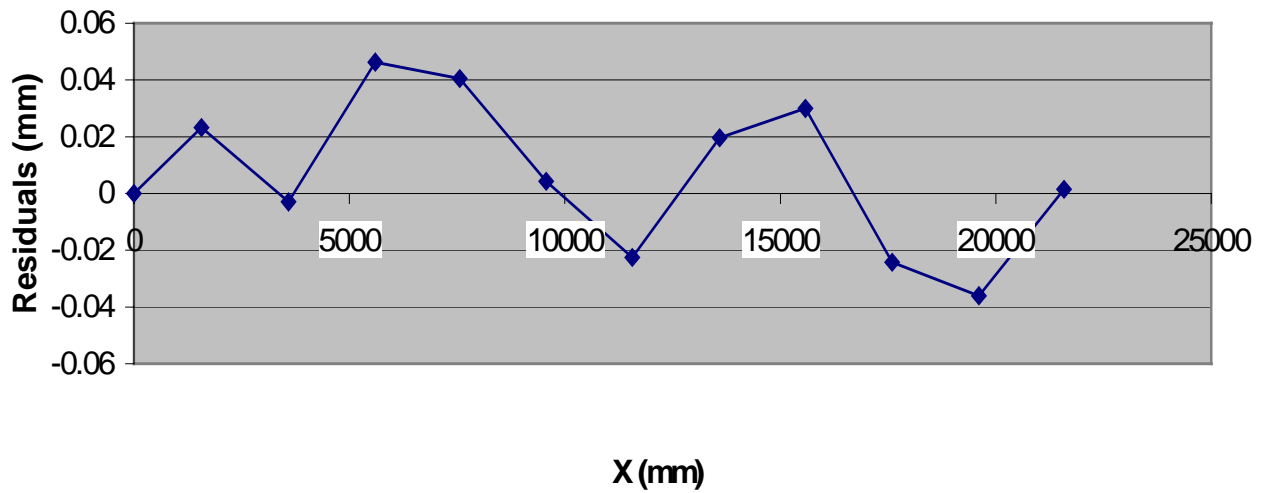


Figure 3 Results of the biaxial calibration test bench for the geometric mole. Linear fit is made with the differences between mole and test bench results for the two transverse coordinates.

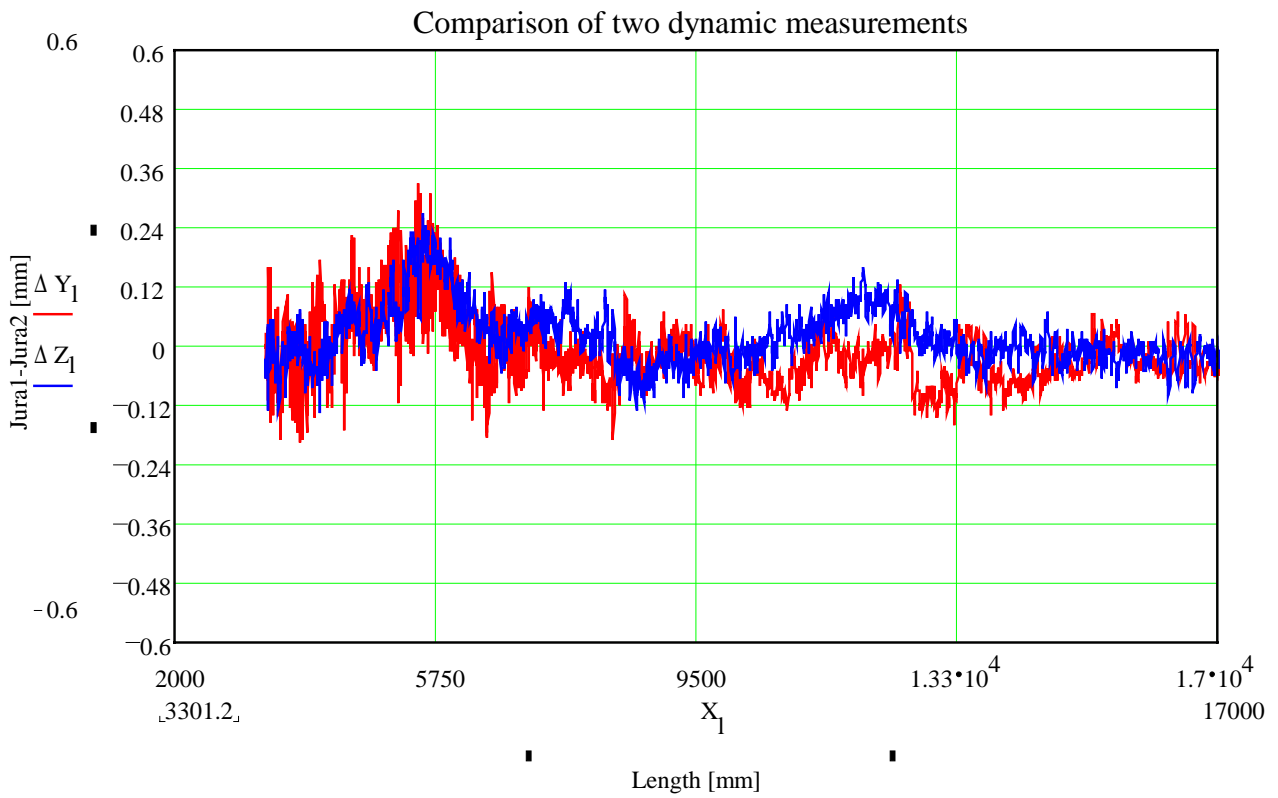


Figure 4 Comparison of two measurements with a Laser Tracker on a 15 m long cold bore tube.

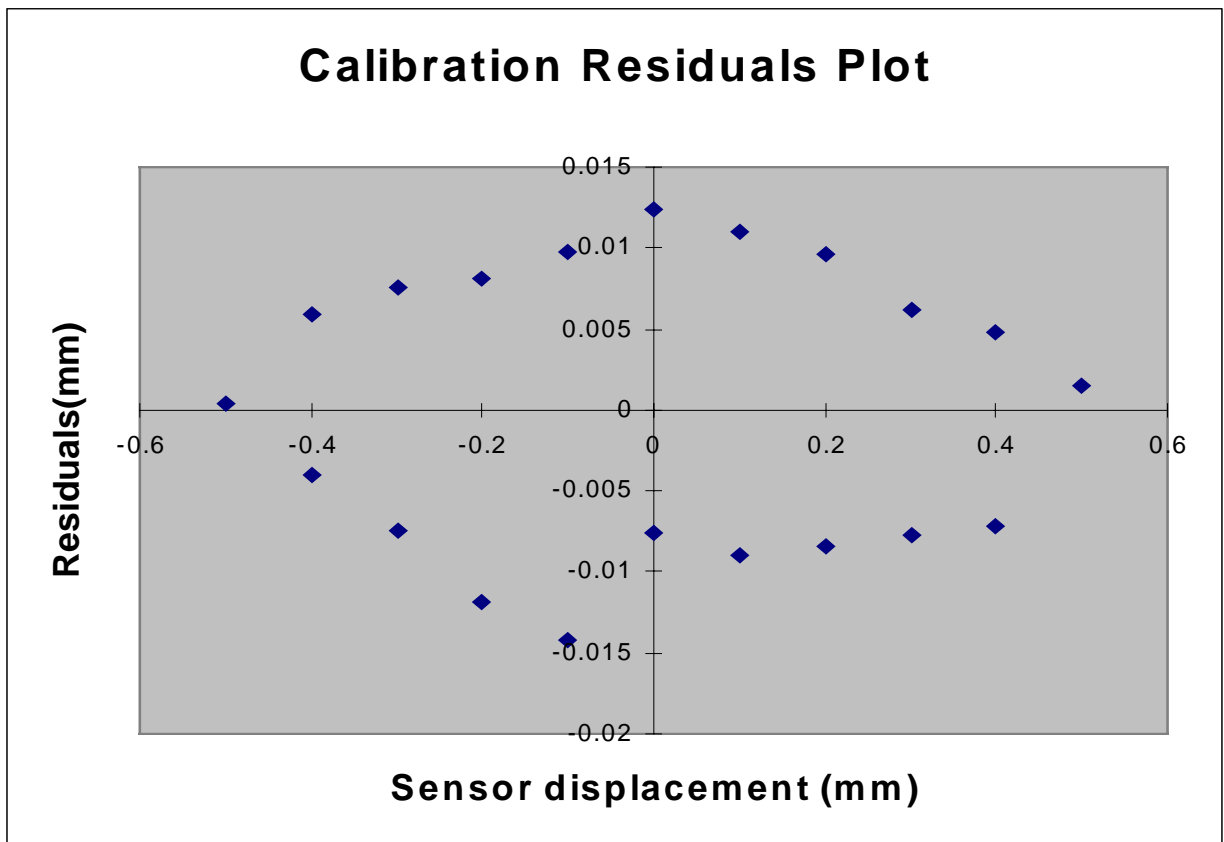


Figure 5 Calibration residuals of mechanic sensor to measure diameter's tube

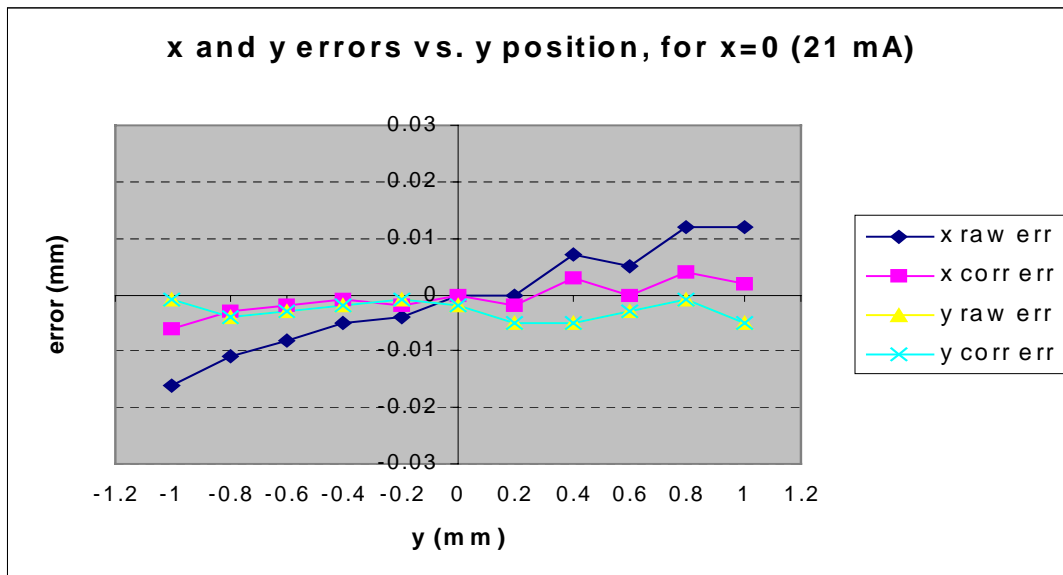


Figure 6 Calibration residuals from magnetic sensor in a quadrupole test bench

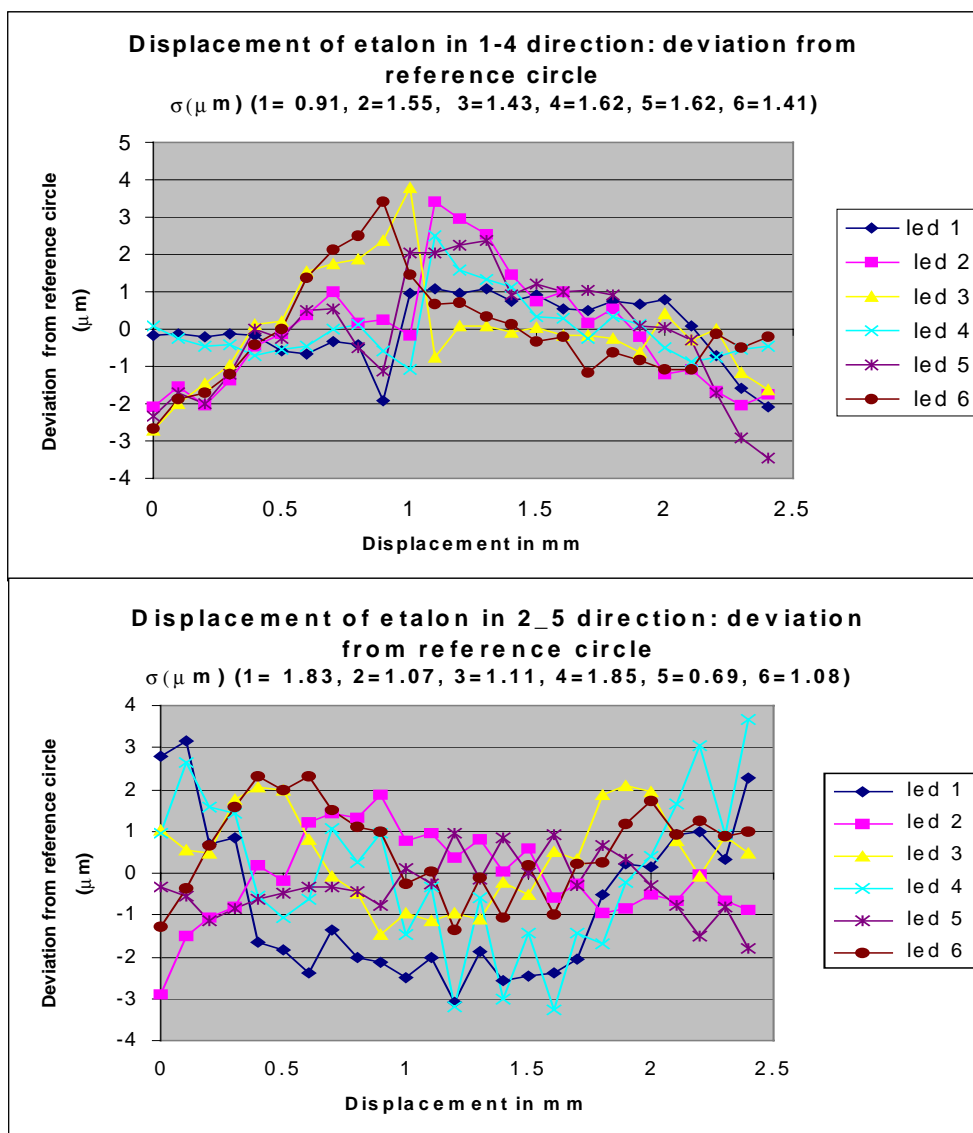


Figure 7 Calibration residuals from LED's technique in a 50 mm diameter.

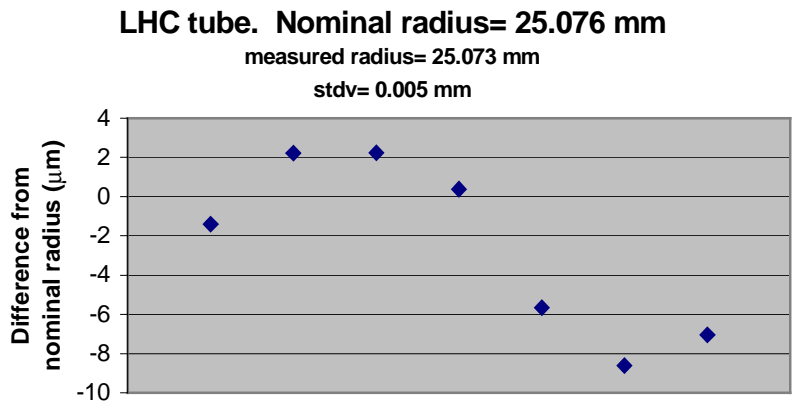
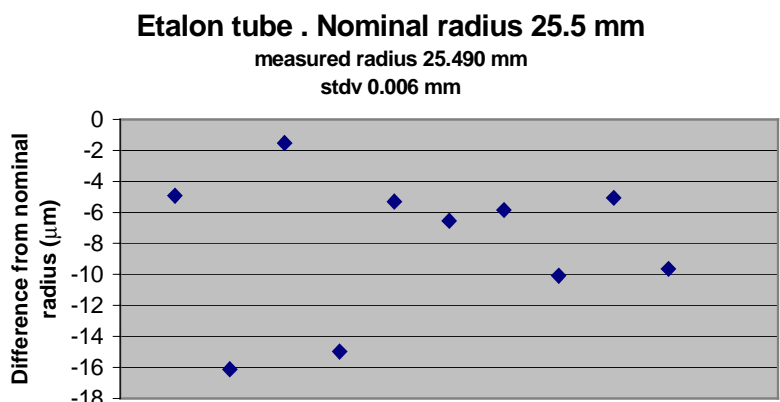
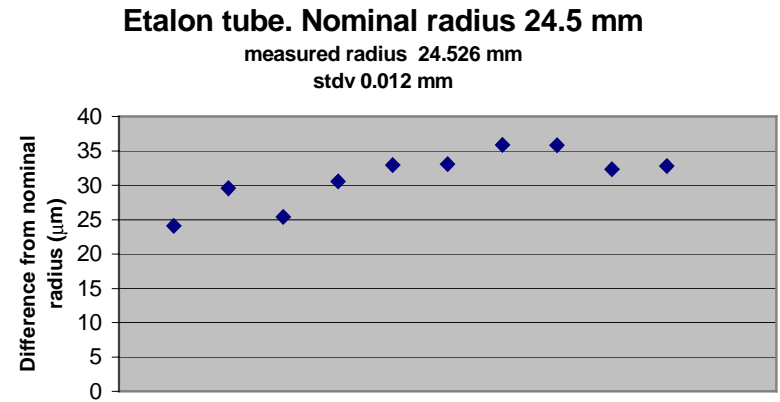
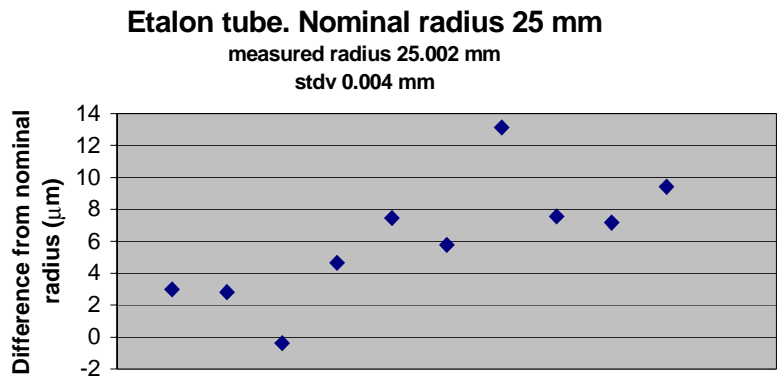


Figure 8 Results from diameter measurements for three calibrated tubes and one sample of LHC cold bore.

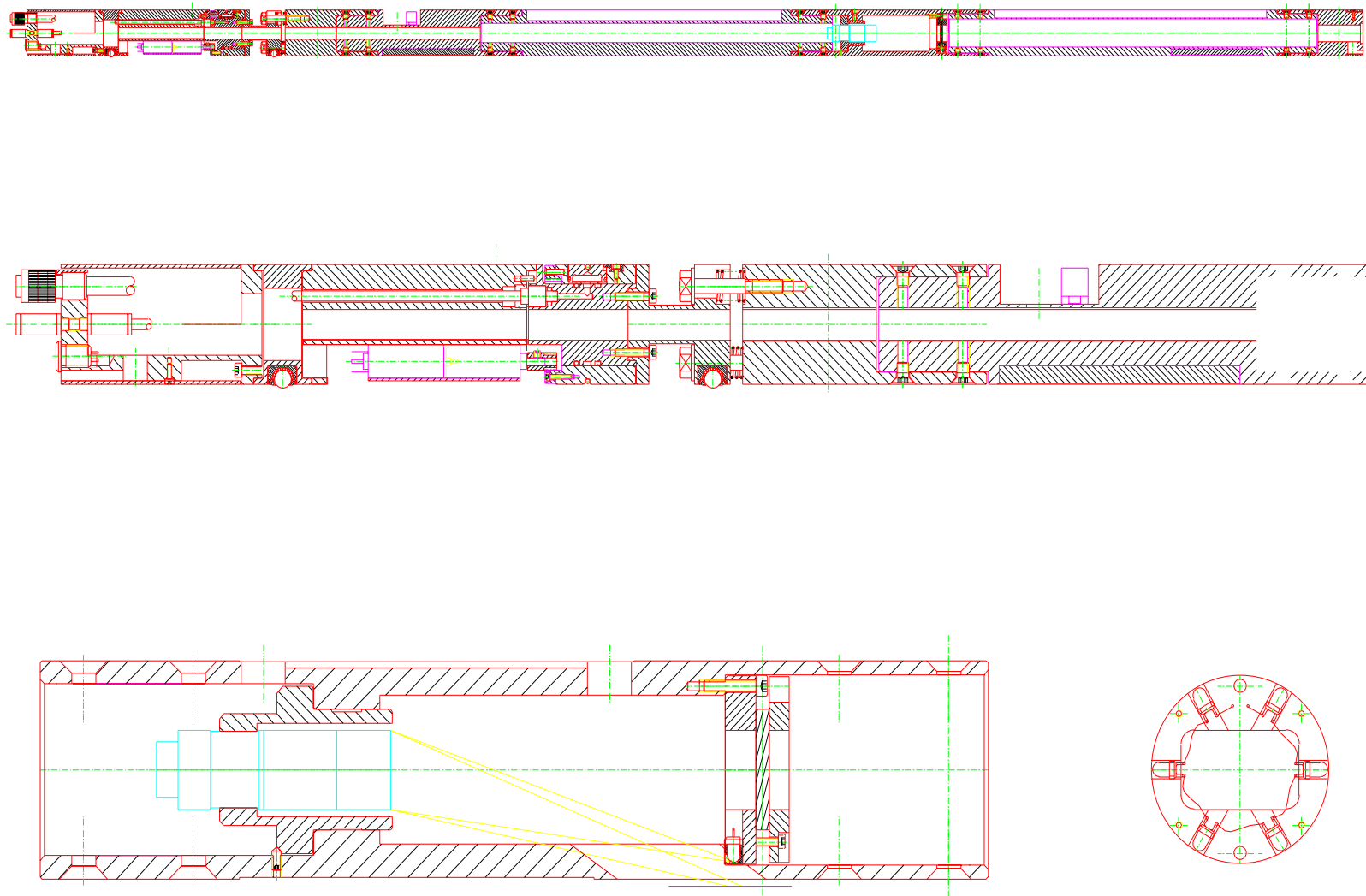


Figure 9 Geometric mole drawing with LED's technique

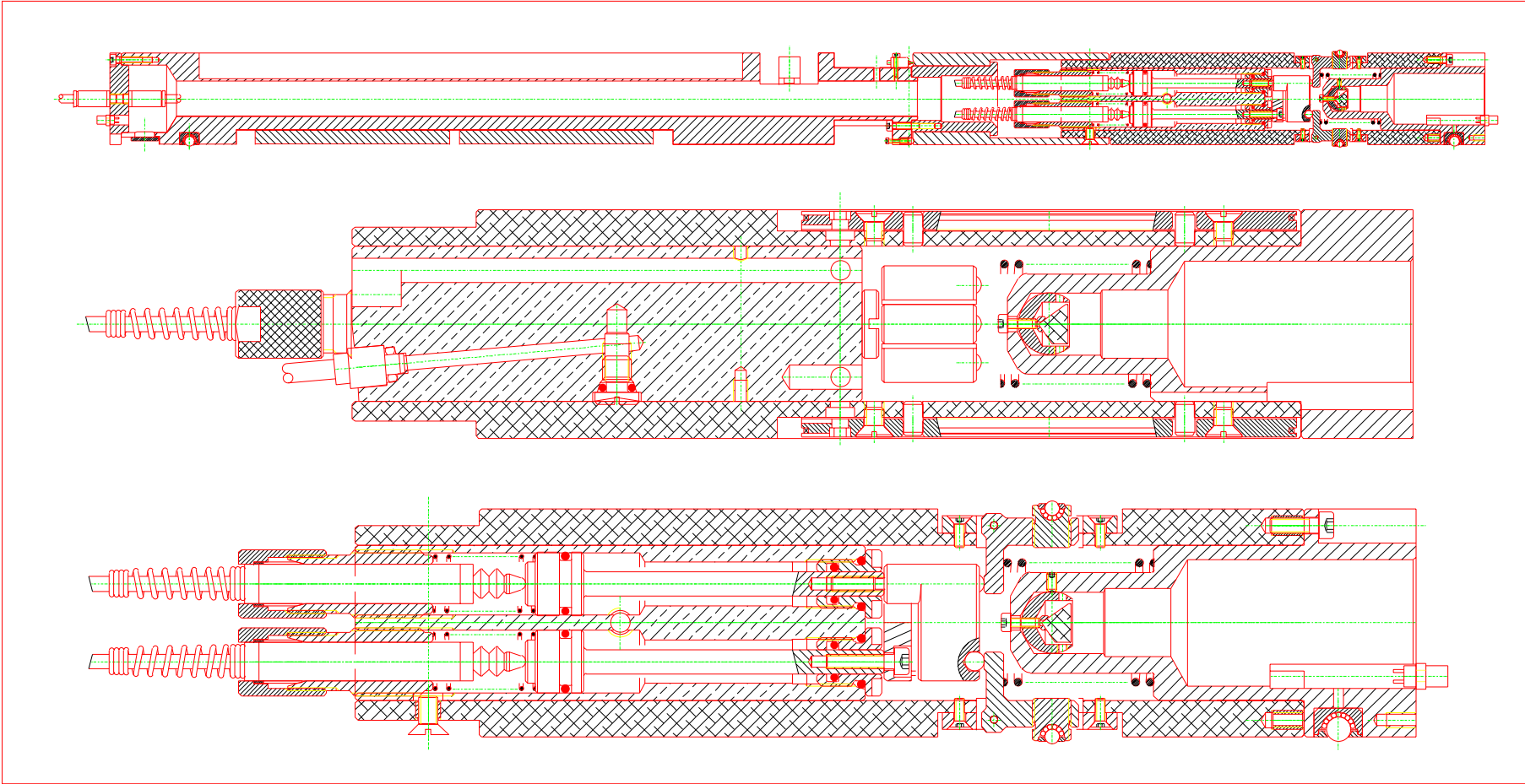


Figure 10 Global mole drawing

A New Challenge in Magnetic Axis Transfer

Corinne EVESQUE
Magnetic Measurement Laboratory (LMM)
CEA Saclay - DSM/IN2P3 - F.91191 Gif-sur-Yvette

IMMW11
Brookhaven National Laboratory
September 21 - 24, 1999

EVE01

To contact us :

By post :

Laboratoire de Mesures Magnétiques du CEA-CNRS
DAPNIA - SEA - Bâtiment 701
CEA SACLAY
F - 91191 GIF-SUR-YVETTE

Phone number : 331.69.08.90.02

Fax number : 331.69.35.14.06

email : cevesque@cea.fr

Aim of the drill

	Before Y2K	After Y2K
Precision	$\leq 100 \mu\text{m}$	$\leq 30 \mu\text{m}$
Delay	hours	minutes
Manpower	qualified	unqualified
Money		ALAP

Highly automated

IMMW11

The purpose is to set precise fiducial marks which represent the real magnetic axis of a magnet. This leads to :

- a transfer of the axis outside the magnet
- an accessed reference target setting
 - for the installation of the magnet in the accelerator
 - for monitoring an automatic process of alignment.

Specifications have changed a lot in recent years :

- tolerances are tighter and tighter,
- means are lower and lower.

So, new challenges have been created for designers and their computer skills.

Customers

■ 1997 : 3rd generation light sources (SOLEIL)

Magnetic axis transfer : $\pm 30 \mu\text{m}$ - 1 quad

G = 20 T/m
 $\Phi = 66 \text{ mm}$ and L = 0.32 m or 0.46 m
H = 600 mm or 300 mm

■ 1999 : high intensity proton injector (IPHI)

Magnetic axis transfer : $\pm 15 \mu\text{m}$ - 54 quads

G = 80 T/m
 $\Phi = 13 \text{ mm}$ and L = 6 m
H = 300 mm

IMMW11

We can notice that magnetic axis transfer tolerances are only one part of the purpose.

With these two French customers, we can point out that dimensions are not the same.

- Gradient G has increased by a factor of 4.
- the ratio aperture - length has gone down.

Furthermore, only one quad was to align at the same time for SOLEIL (160 total quads for storage ring). They are 54 for IPHI.

SUMMARY of the talk

- ✓ Transfer process description
- ✓ Classical AH benches
- ✓ R&D topics (SOLEIL)
- ✓ New requirements (IPHI)

IMMW11

First, I would like to analyze the complete process transfer and to compare two magnetic measurement methods well suited for quad magnets.

To achieve the desired tolerances, I will make a study of each error. First for classical benches (DANFYSIK), then for the Super-Bench studied for SOLEIL, and for the bench required for IPHI.

I will conclude with a discussion about the new technical challenges, mainly about the operating mode of wire as magnetic sensor.

Transfer process

④ Sockets adjusting

With respect to the measured magnetic axis

③ Transfer to H

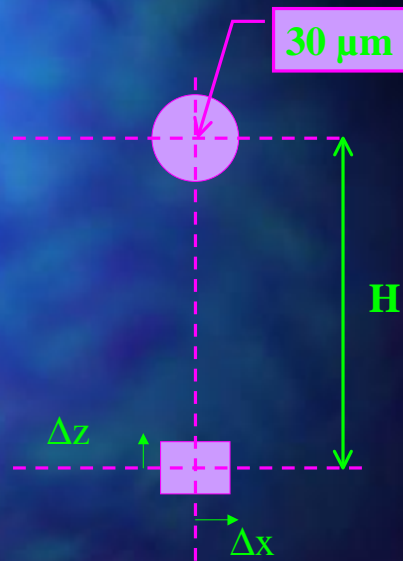
Mechanical transfer support (TS)

② Magnet centering

Mechanical canceling of Δx , Δz

① Magnetic axis seeking

Magnetic measurement of Δx , Δz



IMMW11

Magnetic measurement laboratory task includes four steps involving both

- sensor designs
- mechanical adjustments.

This transfer process links the magnetic axis to external fiducial marks. Then, surveyors have to insure magnet installation and monitoring.

Magnetic measurement methods

Rotating coil (A.H)

Stretched wire



For large aperture quad, we are used to **the rotating coil method** :

- a bundle of windings rotates on a mechanically stable cylinder. The induced voltages are sampled thanks to precise angles. The offsets of the magnetic center are determined with the magnitudes of the dipole field.

The **stretched wire method** seems well suited for measurements of small aperture with high gradient.

- a light wire is stretched and tensioned between two points. It moves in either the vertical plane or horizontal plane, with a step width called d. We generate two loops of voltage having opposite polarity. We assume that the gradient is a constant during wire displacement. The relationship between the magnetic center and induced voltage shows that we have to zero the signal.

Both methods require an up-to-date integrator, having good enough resolution to measure small voltages when measuring large voltages.

Magnetic measurement bench

■ A vertical plane :



IMMW11

The main purpose of a magnetic measurement bench is to define a very precise vertical plane including :

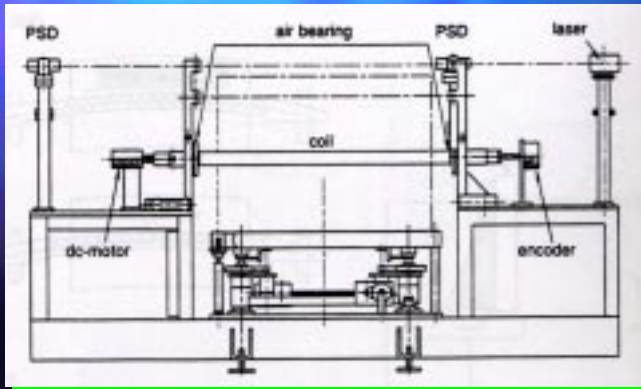
- measurement axis depicted by the coil,
- reference (transferred) axis depicted by a laser

beam.

Classical benches :

Magnetic axis transfer : < 100 μm

■ DANFYSIK system side view



- Four heads
 - 2 for reference axis
 - 2 for coil axis
- +
1 transfer support
- Magnet centering system

IMMW11

DANFYSIK benches are made of :

➔ four heads :

- two of them, located above the magnet, determine the reference axis

- two other twin heads determine the measurement (or sensor) axis. They can receive, one after the other, a mechanical transfer support in order to transfer this axis to the top of the magnet.

➔ One automatic magnet centering system. The magnet can move around three axis with motors and air cushions.

Furthermore, these benches are designed for only one type of magnet : transfer height, aperture diameter, magnet length are chosen when purchasing.

Classical benches

Standard error analysis : $\pm 75 \mu\text{m}$

	Syst	Rand
1 Axis seeking		
Magnetic Measurement of $\Delta x, \Delta z$	probe sag ± 15	
	wire vibration ± 10	± 10
	integrator (PDI) ± 10	± 10
2 Magnet centering		
Mechanical canceling of $\Delta x, \Delta z$	Air cushion table ± 20	± 20
3 Transfer to H		
Mechanical interface	Air cushion bearings ± 5	
	Machining of T.S. ± 25	± 15
	Adjusting of T.S. ± 25	± 25
	Adjusting laser axis ± 20	± 20
4 Socket adjusting - fastening		
(Reference targets)		± 15
	Standard errors ± 30	± 45

IMMW11

This is the standard error analysis of classical benches.

As shown in a previous transparency, four steps are studied and each item is estimated with a systematic error and a random error.

Values are not DANFYSIK specifications. The data are based on our own experience, gained on the LMM home made bench (steps 3, 4 and integrator) and the ESRF - DANFYSIK bench (steps 1 and 2).

The result of our own experiments is that magnetic axis transfer (absolute values and not identity of magnets) can not be better than $75 \mu\text{m}$. Moreover, it is time and qualified manpower spending.

R&D topics - Technical requirements

Magnetic axis transfer : < 20 μm

- **Super bench**
 - included transfer height H
 - probe centering
- **CEA integrator voltmeter**
 - high resolution, high dynamic
 - no temperature drift
- **New sockets**
 - H & V adjustments separation
- **New coil design**
 - tangential windings
 - sag compensated cylinder
 - vertical windings
 - easy to use
- **Reference axis (laser)**
 - automatic spot light adjustment

IMMW11

In order to cater to the new requirements of SOLEIL, **five topics of research and developments** were undertaken during the last years.

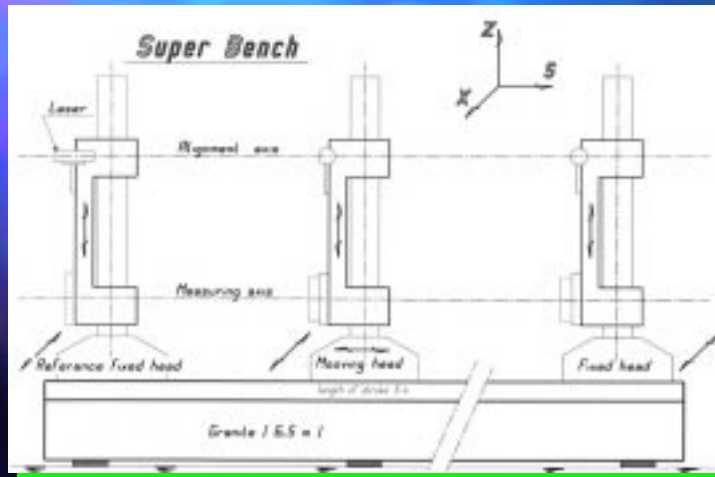
The purpose was to improve previous specification. For each topic, it leads to technical requirements.

Apart from the new sockets (designed by surveyors), we are going to have a closer look at the topics which will be useful for the IPHI bench. More information can be found in the reference [1].

On the next transparency, the standard error analysis will show that the magnetic axis transfer is expected within 20 μm .

[1] : J.BISSIRIEIX - C.EVESQUE - R.THAUVIN. Propositions techniques pour les mesures de série des dipôles, quadrupôles et hexapôles de l'anneau de stockage, du booster et de LT2 de SOLEIL. DSM/DAPNIA/SEA 99/04

Super bench side view



- Three heads :
 - 2 axis together
 - arm selection
 - internal transfer
- Probe centering :
 $\pm x, z$ displacements

IMMW11

The super-bench removes the main disadvantages of classical benches :

- the vertical plane is defined with only three heads linked to a granite girder.
- the mechanical transfer support is replaced by an internal column.
- the magnet does not move. The probe is adjusted, with the three columns, on the center of the magnet.
- all the mechanical dimensions can be adapted to a new magnet, in a few hours, according to arm selection.

Starting from specification, this bench was subcontracted to the manufacturer MICROCONTROLE-NEWPORT. The cost is cheaper than the DANFYSIK bench.

Integrator specifications

■ METROLAB PDI 5025

- V/F Conversion
- G64 Standard (1980)
- input voltage ± 5 V
- integration ≥ 1 ms
- Resolution $2 \cdot 10^{-8}$ V.s
- Reproducibility $0,95 \cdot 10^{-3}$
- Factory calibration
- Temperature sensibility

■ CEA patent

- A/D Conversion
- PXI Standard (1997)
- input voltage ± 10 V
- integration $\geq 0,1$ ms
- Resolution $3 \cdot 10^{-11}$ V.s
- Reproducibility 10^{-5}
- Internal calibration
- Specifications guaranteed
20 to 40 °C

IMMW11

In 1999, the CEA has patented a new integrator device including :

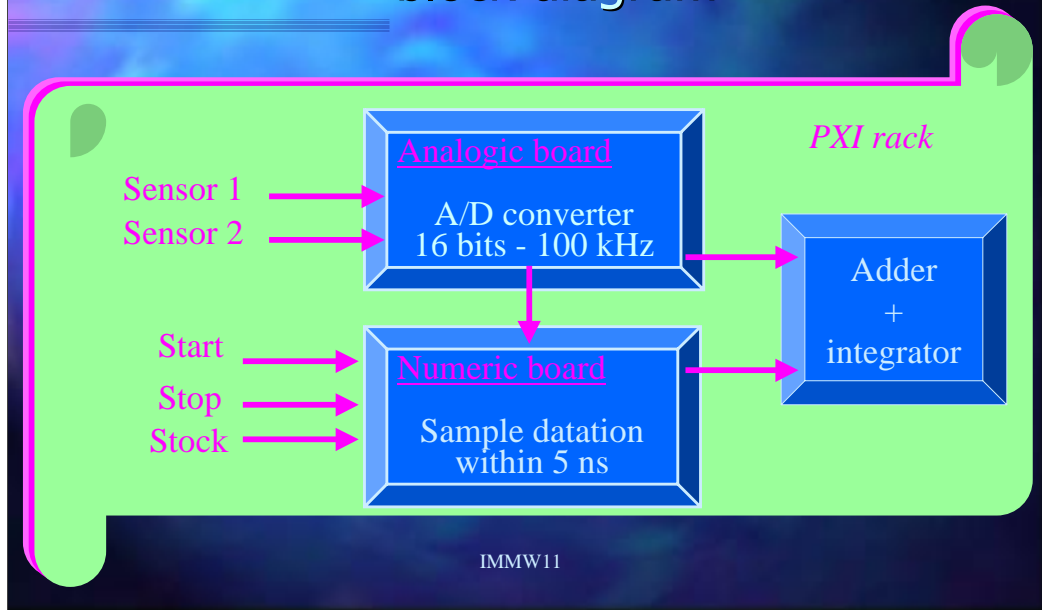
- a new integration process
- a selection of up to date electronic components.
- improved specification (100 times)
-

This study was conducted with SUPELEC (a leading French school of electricity).

This device is now under test and the first results are encouraging.

CEA is looking for an industrial partnership.

New integrator - CEA patent block diagram



The CEA integrator is made of two boards included in a PXI rack. An internal computer monitors everything and makes the calculations.

Reference axis : laser adjustment



Test stand

Laser head
with monitoring equipment
+ socket with target

Stability over 1 hour

$\sigma_{\text{temperature}} < 0.2 \text{ } ^\circ\text{C}$

Length	Signal	
	Magnitude	σ
m	μm	μm
0.390	0.5	0.10
1.725	1.0	0.15

IMMW11

Reference axis adjustment according to laser drift and laboratory disrupts (temperature, vibrations, ...) is an important item.

A piece of equipment (LAE500) was purchased from MICROCONTROLE-NEWPORT. Some attempts have been realized in ideal conditions. An automatic process has been defined.

At present, we can report that a reference axis did not move within $1 \mu\text{m}$ over 1 hour in ideal conditions. A tolerance of $2 \mu\text{m}$ seems a good value for magnetic measurement laboratory conditions.

Super-bench (SOLEIL)

Standard error analysis : $\pm 17 \mu\text{m}$

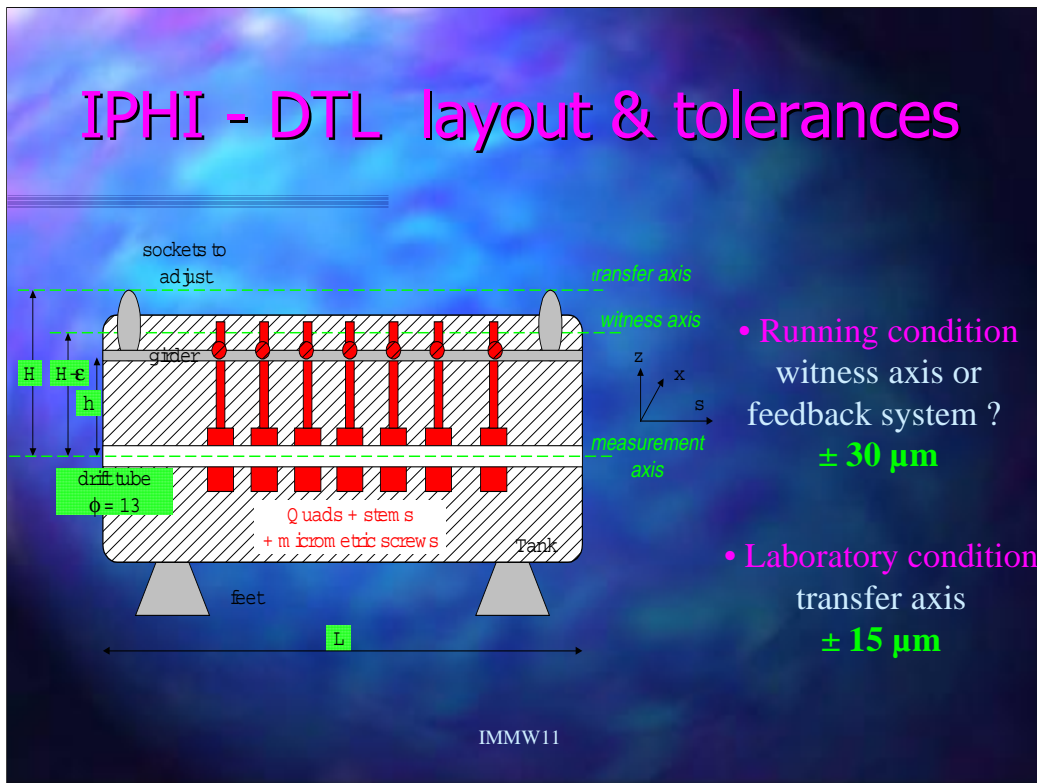
	S	R	S	R
1 Axis seeking Magnetic Measurement of $\Delta x, \Delta z$	Probe sag	± 15	± 10	± 6
	Wire vibration		± 10	± 0
	CEA integrator			± 0
2 Magnet centering Mechanical canceling of $\Delta x, \Delta z$		± 20		± 10
	Magnet position Probe centering			± 1
3 Transfer to H Mechanical interface		± 5	± 15	
	Adjusting laser axis		± 25 ± 20	± 2
4 Socket adjusting - fastening (Reference targets)			± 15	± 1
	Standard errors	± 30	± 45	$\pm 6 \pm 11$

IMMW11

This is the standard error analysis of the Super-bench for SOLEIL measurements. The values of classical benches are given for comparison.

The result is that magnetic axis transfer should be better than $20 \mu\text{m}$.

IPHI - DTL layout & tolerances



The DTL layout has three axis.

Measurement axis and transfer (reference) axis have the same arrangement, as previously discussed. Except, 54 quads have to be aligned in respect to two sockets. Moreover, the magnet centering is obtained with a stem adjustable thanks to micrometry screws.

The third axis is the witness axis. It will be equipped with capacitive sensors fixed on the girder. Their data will be recorded during magnetic measurements : they will be reference values. During running condition (Temperature, RF, vacuum, ...) these data should be stable within $\pm 30 \mu\text{m}$. We assume that witness axis and magnetic axis move together. A test plan should be conducted to determine the necessity of implementing a feedback system.

As a result, this involves, in laboratory conditions, making a transfer axis within $\pm 15 \mu\text{m}$.

Required bench (IPHI)

Standard error analysis : $\pm 15 \mu\text{m}$

	S	R	S	R	S	R	
1 Axis seeking Magnetic Measurement of $\Delta x, \Delta z$	wire disrupts	± 15			± 6		± 5
	CEA integrator	± 10			± 0		± 0
	step width	± 10					$\pm 1 \pm 1$
2 Magnet centering Mechanical canceling of $\Delta x, \Delta z$	screw resolution	± 20			± 10		± 10
	report height, fastening				± 1		± 10
3 Transfer to H Mechanical interface	Adjusting laser axis	± 5 ± 25	± 15 ± 25		± 2		± 2
		± 15			± 1		± 1
4 Socket adjusting - fastening (Reference targets)	Standard error	± 30	± 45		± 6	± 1	$\pm 1 \pm 15$

IMMW11

Now, let us consider the standard error analysis of the required bench. The result must be $\pm 15 \mu\text{m}$.

Previous choices of steps 4, 3 and integrator should be renewed.

The mechanical engineer in charge of the DTL design gives an estimation of tolerances of the step 2. Some studies are still in progress.

Only a few microns are left for step 1. Our ability to make this transfer axis depends both on the wire (choice and operating mode), and on absolute displacements of x, z stages.

Technical challenges :

Magnetic axis transfer : 15 μm

- *Absolute step measurements < 1 μm over 5 mm width*
- *Wire straightness < 5 μm over 7 m long*
 - sag = f (length) calibration curve
 - high precision sag measurement setup
 - tension and temperature free getting
 - operating mode : vibrations, diameter inhomogeneity, thermoelectric voltage ...
 - wire choice

IMMW11

It is obvious that the wire must be perfectly straight and parallel to the transfer axis. This means, with the same position for each quad.

The wire deflection can not be avoided over 7 m long.

To simulate the wire straightness one calibration curve is needed. It will give a sag correction versus the longitudinal position of a quad. Therefore, a sag measurement setup has to be performed. Furthermore, two parameters should be under control during magnetic measurements. Indeed, random errors could appear and must be avoided :

- Sag depends on tension
- Length depends on temperature.

To get free of these parameters, a control has to be implemented. It could be a process of sag and temperature monitoring. Another possibility to overcome this problem, could also be to cancel it by a mechanical design.

Other parameters can also disturb the measurements. An operating mode, established from experience, should be able to resolve these difficulties.

Another point, is the absolute measurement of step width. Commercial available stages (25PP1 of MICROCONTROLE) give a precision lower than 1 μm .

Which wire do we choose ?

	Wire characteristics		IPHI Application			Wire control	
	Yield point (Kg/mm ²)	Density (Kg/dm ³)	Sag (μm) <small>sag = L² $\frac{\rho}{8T}$</small>	Tension (kg) <small>Tension = $\rho \cdot \text{length} \cdot \text{section}$</small>	Length Expansion <small>μm per °C</small>	Tension (g)	Temp (°C)
Cu	32	8.6	1640	1.005	119	1	0.01
CuBe	146	8.25	346	4.587	125	27	0.01
Tungsten	55	19.3	2140	1.728	31.5	2	0.05
Carbon fiber	300	1.6	43	9.425	1.75	335	1
Aluminum Alloy	48	2.8	355	1.508	175	8	0.01

IMMW11

The wire choice may occur among a few materials but we have to weigh the advantages and drawbacks of each of them.

The sag depends only on the ratio density - Yield point. **CuBe** and **Aluminum alloy** give the same result. The best material is carbon fiber.

The tension applied to the wire depends on the product of Yield point and wire section. It will determine the choice of stages. **Aluminum alloy** is a rather good choice. **Carbon fiber** is the worst.

Temperature effect on the length is very strong with **CuBe** and **Aluminum alloy**, but very low with **Carbon fiber**.

In addition, resistivity inhomogeneity (**Carbon fiber**) or paramagnetic properties (**Tungsten**) must be taken into account.

In conclusion, Aluminum alloy seems to be the best choice.



Currently, we have been asked to make a proposition for a test bench

I look forward to gathering your recommendations according to your knowledge and experience.